1-1-2004

Olefin polymerization from single site catalysts confined within porous media.

Rajeswarmi M. Kasi
University of Massachusetts Amherst

OLEFIN POLYMERIZATION FROM SINGLE SITE CATALYSTS CONFINED WITHIN POROUS MEDIA

A Dissertation Presented

by

RAJESWARI M. KASI

Submitted to the Graduate School of the
University of Massachusetts, Amherst in partial fulfillment
of the requirements for the degree of

DOCTOR OF PHILOSOPHY

September 2004

Polymer Science and Engineering

OLEFIN POLYMERIZATION FROM SINGLE SITE CATALYSTS CONFINED WITHIN POROUS MEDIA

A Dissertation Presented

by

Rajeswari M. Kasi

Approved as to style and content by:

E. Bryan Coughlin, Chair

Thomas J. McCarthy, Member

D. Venkataraman, Member

Sandra L. Burkett, Member

Shaw Ling Hsu, Head
Department of Polymer Science and Engineering

ACKNOWLEDGEMENTS

I would like to profusely express my appreciation to my advisor Prof. Bryan Coughlin for his encouragement and guidance over the past four years. I especially remember Bryan's explicit instructions while he demonstrated mundane tasks like changing a nitrogen tank or controlling the steering wheel of a car, glad to be have been the source of amusement to him during this learning process! Prof. Sandra Burkett and Prof. D. Venkataraman have been role models to whom I have looked-up to for guidance. We have collaborated with Sandi Burkett in a number of projects, and I would like to thank her for helping me to grasp the complexity of mesoporous silica. I appreciate Prof. Tom McCarthy's input in addressing some of the research problems and for serving on my thesis committee. I would also like to thank Professors Greg Tew and Todd Emrick for their time and insightful comments during the process of postdoctoral applications.

Special thanks go to Dr. Charles Dickinson for teaching me the fundamentals of NMR (solutions and solids), Dr. Alan Waddon for providing greater knowledge of semicrystalline polymers, Dr. Stephen Eyles for schooling me in air-sensitive Mass Spectroscopy and in maintaining the temperamental high temperature GPC and Dr. Greg Dabkowski for all the elemental analyses data reported in this thesis.

It would be very difficult to imagine going through graduate school without the help and advice of the past and present Coughlin group members. I want to thank Lei Zheng, who although was physically absent from B666, did

turn up sporadically to offer a sympathetic ear to my problems. I especially appreciate all the help and timely suggestions that Greg Constable and Ramon Gonzalez have given me; and I could not have done any lab work had it not been for their expertise! I want to remind Greg that there is a fair chance that he might be wrong about the effect of the triple sixes on graduation prospects. I am appreciative of the contributions from Anne Forcum and Jeanette Craymer, who have worked with me in a couple of projects.

Outside the lab, there are several people whose friendship has been very important; Margarita Herrera, Irene Tsai, Pushkala Krishnamurthy and Vishak Venkataraman have tried very hard to get me to develop some sense of fashion! I am only sorry that it was a wasted effort. I have known Push for over eight years and have to thank her for putting up with me as a roommate and for the all the home cooked food that I have consumed over the last four years. I will dearly miss spending time with Irene, Push, Vishak and Jay, Monday morning deliberations with Greg and Ramon, chance corridor encounters and discussions with Margarita, Manuel Garcia, Sian, Taehung Kim and Habib Skaff. Inspite of having spent inordinate amount of time staring at the ceiling, I have managed to bag memories, fresh water and a moose in your company!

The PSE volleyball team has had a consistent losing streak while I had been its co-captain, hopefully the team will proceed beyond the initial play-off games to win the "just fun league" one of these days. Angelo, you did a much better job at captaining and coaching the team.

I want to thank Prof. Damodharan Iyengar for having given me the idea of coming to PSE-UMASS for doctoral studies and for his interest and input in my education.

Amma and Appa, you have always given me the courage and the moral support to venture-out; without your encouragement and enthusiasm this journey could have never been completed.

ABSTRACT

OLEFIN POLYMERIZATION FROM SINGLE SITE CATALYSTS

CONFINED WITHIN POROUS MEDIA

SEPTEMBER 2004

RAJESWARI M. KASI

B.Sc., UNIVERSITY OF MADRAS

M.Sc., INDIAN INSTITUTE OF TECHNOLOGY, MADRAS, INDIA

Ph.D., UNIVERSITY OF MASSACHUSETTS, AMHERST

Directed by: Professor E. Bryan Coughlin

Single Site Catalysts (SSCs) have been utilized for olefin polymerization.. Altering the metal-ligand architecture in the SSCs, polyolefin properties can be enhanced in a rational manner. This influence of the ligands in the SSC on the property of polyolefins prepared can be referred to as the primary ligand influence. Extending this understanding and subsequent control of the metal-ligand framework to the interaction of SSCs within organic and inorganic supports is vital for the synthesis of polyolefins with tailored properties. The motivation behind this thesis was to explore the support influence on the reactivity of the SSC tethered to a support matrix during ethylene homo and copolymerization. In order to address this question of the support influence on the final polyolefin properties, synthetic routes to covalently bind SSCs on different matrices have been explored. The second part of the thesis will deal with homo and copolymerization of ethylene and α-olefin and the material property evaluation of the polymers. The physical characteristics of the

polyolefin synthesized from the supported SSC should be altered due to the perturbation of the support environment. Hence, the study of the thermal transitions and morphological properties of the polyolefin produced has been used to assess the influence of the support on the metal-ligand reactivity.

Two distinct supported SSCs have been used to prepare branched polyethylenes. Branched polyethylenes can be prepared by either copolymerization (ethylene and α-olefin) or oligomerization/copolymerization processes (ethylene and *in situ* generated α-olefin). Synthetic routes to prepare precursor catalysts to Constrained Geometry Catalysts (CGCs) by silyl elimination chemistry have been developed (Chapter 2). Efficient synthetic protocols to assemble CGCs on aminomethylpolysytrene matrices (Chapter 3) and amine-functionalized mesoporous silica (Chapter 4) are also reported. These supported catalysts, with appropriate cocatalysts have been used to prepare ethylene homo and copolymers, the polymer thermal properties and microstructures were analyzed by various analytical techniques. Branched polyethylenes (LLDPE) can be prepared by copolymerization chemistry. It has been observed is that the influence of the support is seen in the production of lower crystalline forms of high density polyethylene (HDPE, 20-50 % crystalline), while homogeneous polymerization of analogous soluble CGCs afford HDPE of higher percent crystallinity (greater than 60 % crystalline). High-density polyethylene with crystallinity of 40-60 % can be prepared by using cocatalysts tethered to AMPS or silica in conjunction with analogous soluble, homogeneous CGCs (Chapter 6). Preparative methods to assemble piano stool

complexes on hydroxy polystyrenes have been designed. These supported catalysts in conjunction with cocatalysts act as both oligomerization and copolymerization catalysts and allow the preparation of branched polyethylenes from ethylene only feed (Chapter 7).

TABLE OF CONTENTS

LIST OF TABLES

LIST OF FIGURES

LIST OF ABBREVIATIONS

AMPS - Aminomethylpolystyrene

aPP - Atactic Polypropylene

APS – Random Copolymer of Styrene-AcetoxyStyrene

CGC - Constrained Geometry Catalysts

HDPE - High Density Polyethylene

HPS – Random Copolymer of Styrene-HydroxyStyrene

iPP - Isotactic Polypropylene

LCB - Long Chain Branches

LLDPE - Linear Low Density Polyethylene

MAO - Methylaluminoxane

PS - Polystyrene

SCB - Short Chain Branches

SEM - Scanning Electron Microscopy

sPP - Syndiotactic Polypropylene

SSC - Single Site Catalysts

WAXD - Wide Angle X-Ray Diffraction

CHAPTER 1

INTRODUCTION

1.1 Overview of Heterogeneous Ziegler-Natta Catalysis

Polyolefins form the largest class of commodity polymers sold world wide. High-pressure free radical polymerization of ethylene affords Low Density Polyethylene (LDPE). This type of polyethylene is highly branched and the alkyl branches formed include methyl, ethyl, propyl, etc. Highly linear polyethylene and polypropylenes are not accessible by a free radical polymerization mechanism.

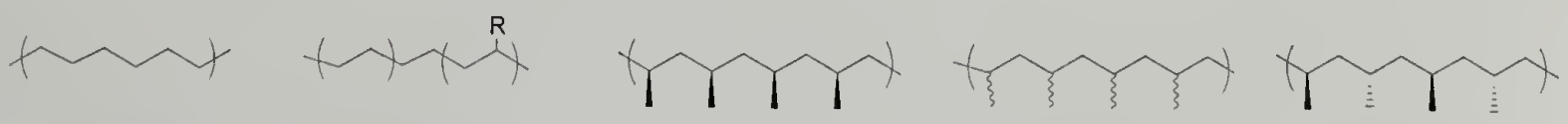

Figure 1.1 Polyolefins

Ziegler's and Natta's serendipitous discovery of metal-catalyzed olefin polymerization about 50 years ago opened up new chemistries to prepare polyolefin (linear and branched) at atmospheric pressure of the monomer. Ziegler found that the oligomerization of ethylene using alkylaluminum based catalysts was facilitated by the presence of nickel impurities in the polymerization reactor.[1] Further investigations have revealed that a variety of other transition metals in conjunction with alkyl aluminums are good catalysts for ethylene polymerization. These metal catalysts produced linear polyethylene (Figure 1.1) of a range of molecular weights and with broad molecular weight distribution. This form of highly linear polyethylene cannot be obtained by

conventional free radical polymerization of ethylene and is known as High Density Polyethylene (HDPE).

Natta and coworkers demonstrated the use of a $TiCl_4/(CH_3CH_2)_3Al$ catalyst system for the polymerization of propylene.[2] The polypropylene formed initially was heterogeneous in nature and was separated into several components using solvent fractionation. The most important component of the mixture was a white solid, which was insoluble in refluxing heptanes. This new material possessed a high melting point and was found to be highly crystalline. This form of polypropylene in which every tertiary carbon center was found to have the same configuration through out the chain is referred to as isotactic polypropylene (iPP), (Figure 1.1). Polypropylene, which is obtained from the soluble fraction has random orientation of methyl groups attached to the tertiary carbon, and is referred as atactic polypropylene (aPP), (Figure 1.1).

Investigations have revealed that there are two possible mechanisms for the polymerization of olefins using transition metal based catalysts. It is now widely accepted that the polymerization of olefins using Group IV metals occurs via the Cossee-Arlman direct olefin insertion mechanism (Figure 1.2). In this proposed mechanism there is direct insertion of olefin across the metal-carbon σ bond.[3, 4]

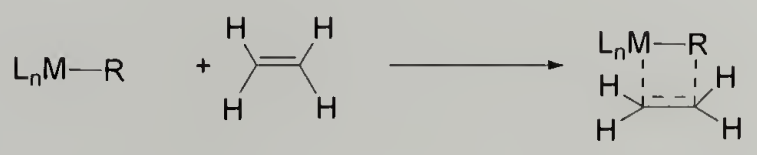

Figure 1.2 Cossee-Arlman Insertion Mechanism

During propylene polymerization, the monomer can be inserted into a metal carbon bond in either a 2,1 insertion mode (metal bound to the secondary carbon), or 1,2 insertion mode (metal bound to a primary carbon). A catalyst is said to be regiospecific when it affords polypropylene with uniform 2,1 or 1,2 insertion of the monomer units (Figure 1.3).

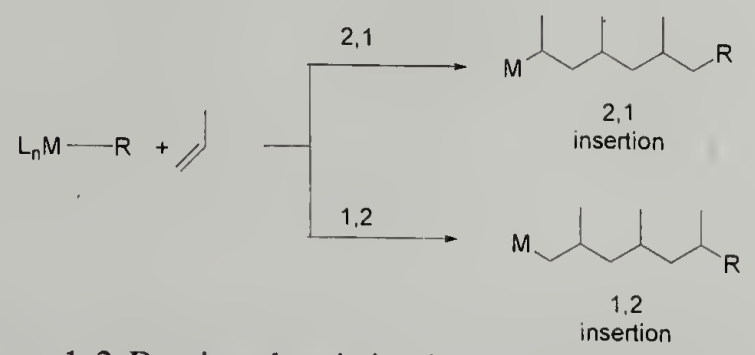

Figure 1.3 Regioselectivity in Propylene Polymerization

The other important aspect of polypropylene formation, which affords tactic polymers, is stereoselectivity. Propylene is a prochiral molecule and it is enantiotopic (*Re* or *Si* faces). When the same enantiotopic face is inserted into the metal ligand bond, the polymerization is highly stereospecific and affords isotactic polypropylene. When the *Si* or *Re* faces are inserted in an alternating manner, syndiotactic polypropylene is obtained. When *Si* and *Re* faces are inserted in a random manner, atactic polypropylene is obtained (Figure 1.4).

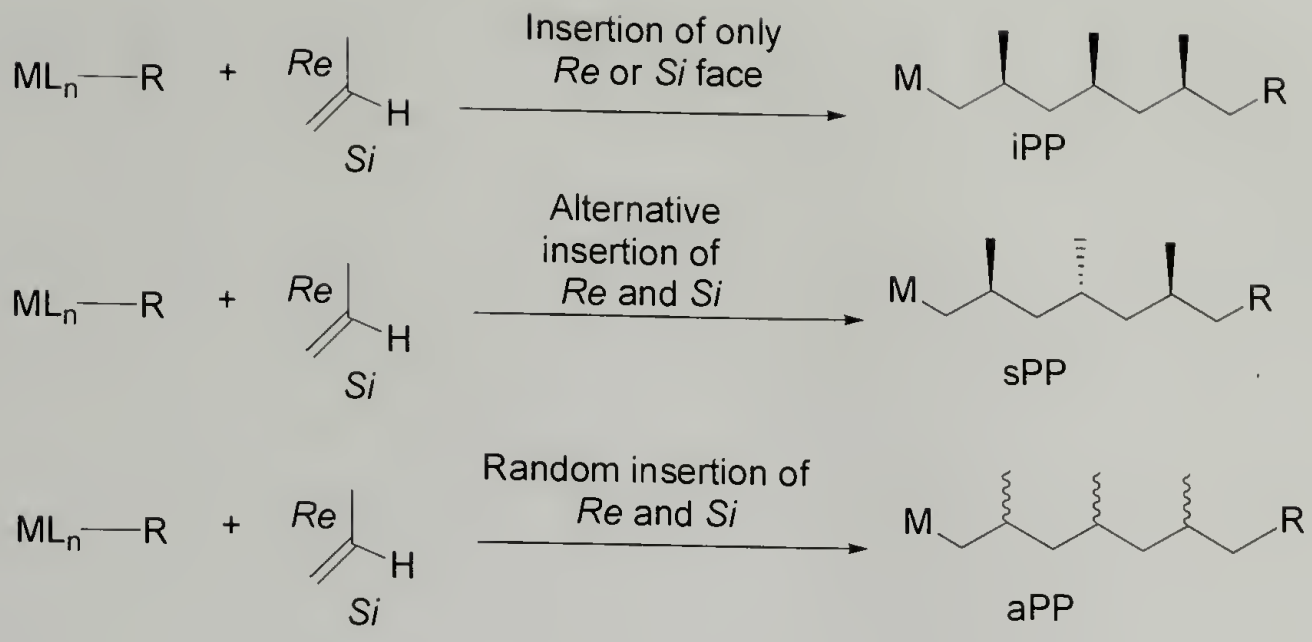

Figure 1.4 Stereoselectivity in Propylene Polymerization

The Ziegler-Natta catalysts are regiospecific, with the polypropylene synthesized from 1,2 connectivity. However, the early Ziegler-Natta catalysts were not very stereospecific, affording a mixture of isotactic and atactic components. The first generation of heterogeneous Ziegler-Natta catalyst system comprising $TiCl_4$ was activated using aluminum alkyl compounds.[5] The active metal species for olefin polymerization were believed to be a mixture of Ti(III) and Ti(II) obtained by the reduction of Ti(IV) using alkyl aluminums. These catalyst systems were multi-sited depending on the aluminum alkyl cocatalysts used. The presence of multiple active sites affords polymer with a very broad molecular weight distribution. During propylene polymerization, the nature of the titanium species formed on reaction with the alkyl aluminums affords either isotactic or atactic polypropylene. The activity of the Ziegler-Natta catalysts for the production of polypropylene was further improved by the use of additives or electron donors, such as, esters, ketones, amides, and amines.

The method of catalyst preparation influences the catalyst activity and polymer morphology. For commercial production of polyolefin, titanium chlorides are supported on matrices having high surface areas. The choice of the support, support treatment, use of donors/additives and the titanium species are very important. For commercial production of polyethylene and polypropylene; silica, alumina, or $MgCl_2$ matrices having high surface area are used as supports, with $TiCl_4$ as the titanium species, trialkyl aluminum as the activating agent, and electron donors being either ethers or amines. The copolymerization of ethylene and α-olefin with heterogeneous Ziegler-Natta catalysts affords Linear Low-Density Polyethylene (LLDPE).

There are a few problems associated with Ziegler-Natta catalysts for the production of polyolefins. The heterogeneous Ziegler-Natta catalyst has a number of active sites (multi-sited) and affords polymers with broad molecular weight distribution. A mixture of atactic and isotactic components is often formed during propylene polymerization. Syndiotactic polypropylene and other tactic polyolefins cannot be synthesized by $TiCl_4$ as the titanium species and alkyl aluminums as activating agents. In production of copolymers, little control over the comonomer distribution and chemical composition of the copolymer is achieved. The ligand environment and the reactivity of the metal centers in the heterogeneous system are ill defined. Parallel investigations into homogenous catalysts with Ziegler-Natta type transition metals have afforded catalytic species with active centers that are well characterized, and the development of soluble catalysts for olefin polymerization will be discussed in Section 1.3.

1.2 Polyolefin characterization

The semicrystalline nature of HDPE, LLDPE, and tactic PP will be discussed in this section. The materials' properties of these semicrystalline polymers that will be discussed includes their melting points (T_m), heat of fusion (ΔH_f J/g), percent crystallinity, and Wide Angle X-Ray Diffraction (WAXD) patterns of various polyolefin crystal forms. Other features of the polyolefins that will be dealt with include the microstructural analysis of the polymer by ^{13}C NMR studies.

1.2.1 High Density Polyethylene

High-density polyethylene (HDPE) was discovered by Ziegler and coworkers as mentioned in Section 1.1 and is semicrystalline in nature. HDPE has a melting point (T_m) greater than 130°C as determined by Differential Scanning Calorimetry (DSC) measurements. The heat of fusion is a measure of the enthalpy of melting of the crystalline units of HDPE and can be determined using DSC. The theoretical heat of fusion (ΔH_f) value of a single crystal of polyethylene is predicted to be 293 J/g. Calculating the percentage crystallinity of a polyethylene sample is the ratio of the experimentally observed ΔH_f to the predicted ΔH_f of a single crystal of polyethylene.[6]

HDPE has a unique X-ray diffraction pattern due to its semicrystalline nature. Diffraction peaks can be attributed to a major component with an orthorhombic unit cell and a minor component having a monoclinic unit cell. Ordinary WAXD of HDPE using Cu K(α) radiation, reveals two major diffraction peaks at $2\theta = 21.6°$ and 22.8° which correspond to d spacing values of 4.09 and 3.68 Å repectively. These peaks are attributed to (110) and (200) reflection planes in the orthorhombic unit cell. The full width at half maxima (FWHM) of the peak for the (110) or (200) plane can be used to determine the

apparent crystal thickness using Scherrer's equation. Minor diffraction peaks attributed to the (010) planes correspond to the monoclinic units cells are also observed. The chains of polyethylene are packed in a planar zigzag fashion and are comprised of 2_1 helices.

1.2.2 Linear Low-Density Polyethylene

Due to its high crystallinity, melt processing of HDPE is difficult. The flow properties of HDPE can be altered by the use of additives or by copolymerization of ethylene and α-olefins, thereby introducing short chain branches (SCB, typically ethyl, butyl, hexyl, or octyl side chains) at regular intervals in polyethylene. The presence of short branches due to copolymerization of ethylene and α-olefins changes the physical properties of polyethylene. These copolymers are referred to as Linear Low-Density Polyethylene (LLDPE). The melting point of LLDPE is considerably reduced due to the incorporation of comonomer units and there is a direct correlation between the depression in melting point of LLDPE and moles of comonomer incorporated. The percent crystallinity of LLDPE is less than that of HDPE. From ^{13}C NMR studies of LLDPE, the reactivity ratio of comonomers, the amount of comonomer incorporated, and the structural arrangement of comonomers in the copolymer have been determined.[7] From WAXD studies using Cu Kα radiation, it is observed that the intensity from diffraction peak of the monoclinic units cells is observed at $2\theta = 19.2^{\circ}$ (d=4.55 Å) in addition to the orthorhombic diffraction peak. Using Scherrer's equation, the FWHM of the peak at $2\theta = 21.6^{\circ}$ (d=4.09Å), the apparent crystal size can be determined. It has been observed that the apparent crystal size of LLDPE decreases with increased comonomer content.

1.2.3 Polypropylene

The three different forms of polypropylene, namely, isotactic (iPP), syndiotactic (sPP), and atactic polypropylene (aPP) have different thermal properties. The melting point of iPP and sPP, as determined by DSC, are greater than 160°C and 150°C, respectively. The difference in the melting behavior of the tactic polypropylene can be attributed to the difference in packing of the polymer chains in the crystalline domains of the polymer. From the X-ray diffraction pattern of tactic polypropylene, it has been determined that iPP is comprised of a monoclinic unit cell whereas sPP is comprised of an orthorhombic unit cell. As expected, atactic polypropylene does not show melting transitions due to the absence of crystalline domains.

Using ^{13}C NMR spectroscopy, the presence of tactic components in all forms of polypropylene can be determined. The chemical shift of the various carbons in a polymer chain are very sensitive to the relative stereoconfigurations of the neighbouring monomer units and the chemical shift of the methyl group is especially useful in identifying the stereoconfiguration of the propylene units. In the modified Fischer projection, the polymer backbone is represented as a horizontal line and the relative orientations of the pendant methyl groups are shown as vertical lines. The lower case letter *m* represents the meso form and *r* represents the racemo dyad between adjacent chiral methine carbon units. Each dyad is given a single letter representation, a triad is given a two-letter representation and a pentad is given a four-letter representation. The nomenclature and possible sequences for the dyads, triads and pentads are shown in Figure 1.5. From ^{13}C NMR, the three regions of the apparent 1:2:1 triplet in the triad sequences level analyses are referred to as isotactic, heterotactic, and syndiotactic triads.[8]

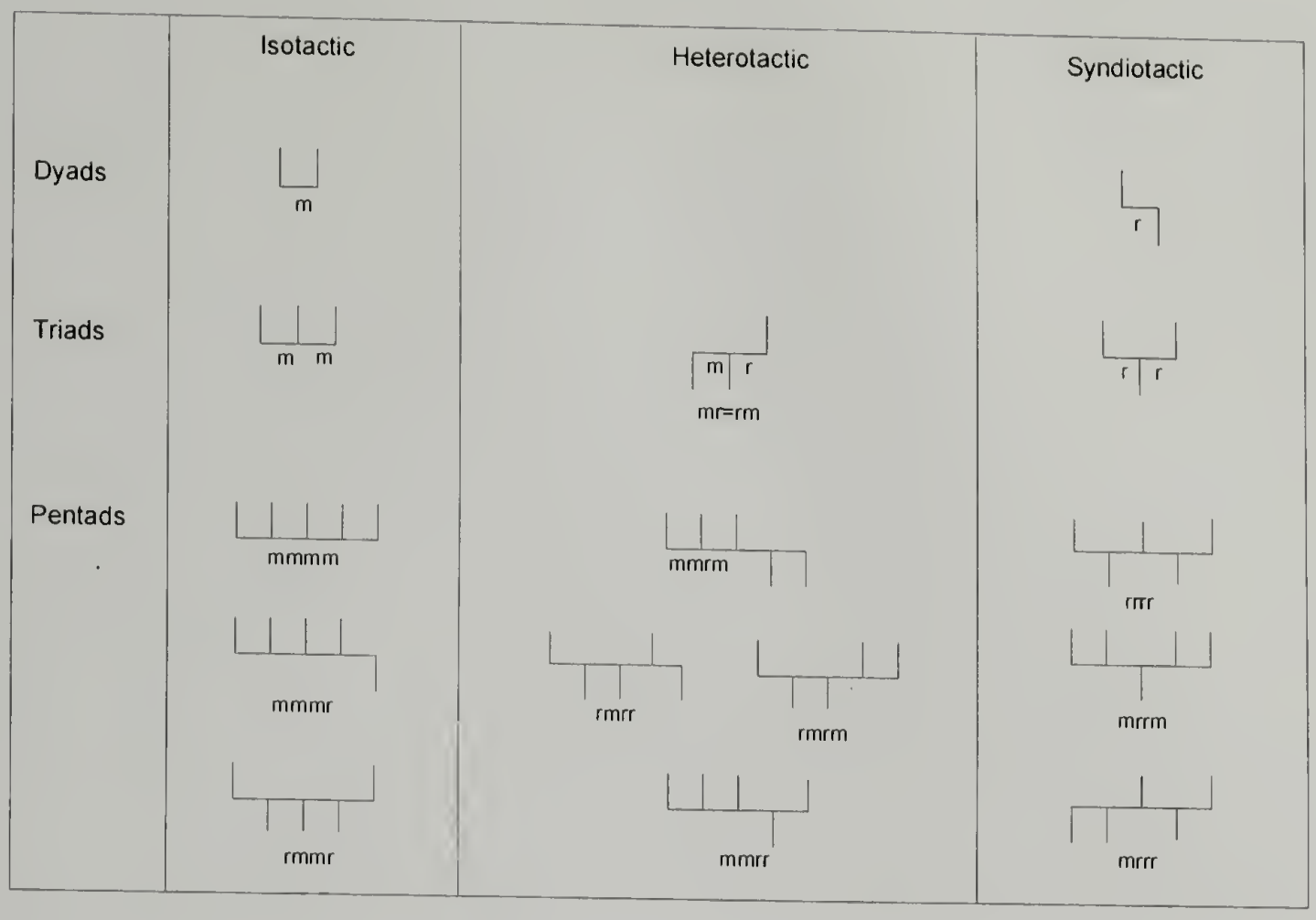

Figure 1.5 Nomenclature and Symmetry of Sequences in Polypropylenes: Dyad, Triads and Pentads

To summarize, conventional Ziegler-Natta catalysts ($TiCl_4/RAlCl_3$/support matrix) used in the industrial production of polyolefins are heterogeneous due to both the insolubility of the catalysts in the polymerizing medium as well as the multi-sited nature of the catalyst system. These catalysts are difficult to study because they give a complex mixture of polyolefins with very broad molecular weight distribution and varying microstructures. Hence, research efforts were directed towards the syntheses of soluble catalytic systems with single active sites from which polymerization occurs. These single site soluble catalysts are attractive because the structure of the active site and the kinetics of polymerization can be more readily determined.

1.3 Development of Single Site Catalysis (SSCs) and Cocatalysts for Olefin Homo and Copolymerization

Numerous efforts are being directed towards the synthesis of homogeneous Single Site Catalytic (SSCs) architectures based on group 4 metals (Ti, Zr and Hf) and the application of these for the homopolymerization and copolymerization of olefins (Figure 1.6). The first homogeneous catalyst system was reported in 1957,[9] shortly after the discovery of the heterogeneous Ziegler-Natta catalysts. This class of homogeneous catalyst system is known as the metallocenes (Cp_2TiCl_2, where Cp is the cyclopentadienyl ring) and was activated by alkyl aluminum species for olefin polymerization. These catalysts showed low activity for ethylene polymerization, propensity to decompose into inactive species, and no ability to polymerize α-olefins.

Catalyst	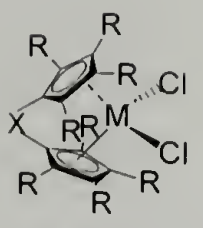 **Metallocene**	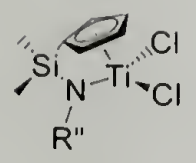 **Constrained-Geoemetry Catalysts**	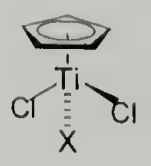 **Piano Stool Complexes**	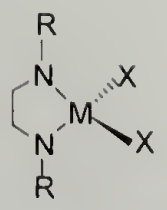 **Non-Cyclopentadienyl Catalysts systems**
	Resconi *Chem. Rev.* **2000**, 100, 1253 Waymouth *Science*,**1995**, 267, 217	Chum, *Adv. Mater.*, **2000**, 12, 23, 1759 Waymouth *Chem. Rev.*, **1998**, 98, 2587	Ishihara, *Macromolecules*, 1988, 21, 3356 Nomura *Organometallics* 1998, 17, 2152 *Macromolecules* 1998, 31, 7588, *Macromolecules* 2000, 33, 3187	Gibson *Angew. Chem. Int. Ed.* **1999**, 38, 428
Monomer(s)	**Polyolefins**			
	HDPE	HDPE	HPDE	HDPE, oligomers
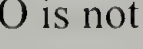	iPP/sPP Stereoblock	aPP	Not Discussed	iPP/sPP/aPP
	LLDPE Blocky comonomer incorporation	LLDPE Even comonomer distribution HT(Solution)-LCB Gas Phase (no LCB)	LLDPE · Blocky comonomer incorporation	Living Diblock copolymers, Living polymerization of α-olefins

Figure 1.6 State of the Art in Single Site Catalysts (SSCs) for Polyolefin Production

Sinn and Kaminsky's discovery of new catalytic systems based on the combination of metallocenes with hydrolyzed alkylaluminums started a new era of research in the synthesis of novel catalyst architectures.[10] The presence of partially hydrolyzed aluminum alkyls as cocatalysts for metallocenes vastly increased the catalytic activity. These partially hydrolyzed aluminum alkyls are obtained by the reaction of trimethylaluminum with an equivalent of water. This compound is referred to as methylaluminoxane (MAO) comprising [Al(O)(CH_3)] subunits. The exact structure of MAO is not known and is thought to exist in solution in a variety of linear and cyclic

oligomers. The reaction of MAO with metallocene dichlorides affords the active catalyst. The main drawback of MAO as a cocatalyst is that a large excess of the cocatalyst is required to obtain high yields of the polymer. The development of other aluminum-based and boron-based cocatalysts and their use in olefin polymerization will be discussed in Section 1.3.1.

1.3.1 Cocatalysts in Olefin Polymerization

Cocatalysts, often in the form of main group organometallic compounds, have played a very important role in the development of single site catalysts for olefin polymerization. There are several types of cocatalyst, namely alkyl aluminum, alkyl aluminoxanes, perfluoroaryl boranes, and trityl and ammonium borates (Figure 1.7). Alkyl aluminums, which include trialkylaluminums and alkylaluminum chlorides are an integral part of the classical heterogeneous Ziegler-Natta polymerization system.

Aluminoxane based cocatalysts react with SSCs in a two-step process. Firstly, the aluminoxane acts as an alkylating agent resulting in metal–alkyl bond. Secondly, acting as a Lewis acid, affording the formation of a metal–alkyl cation and an aluminate anion (Figure 1.8). This cation-anion pair can significantly influence polymerization characteristics and polymer properties.[11]

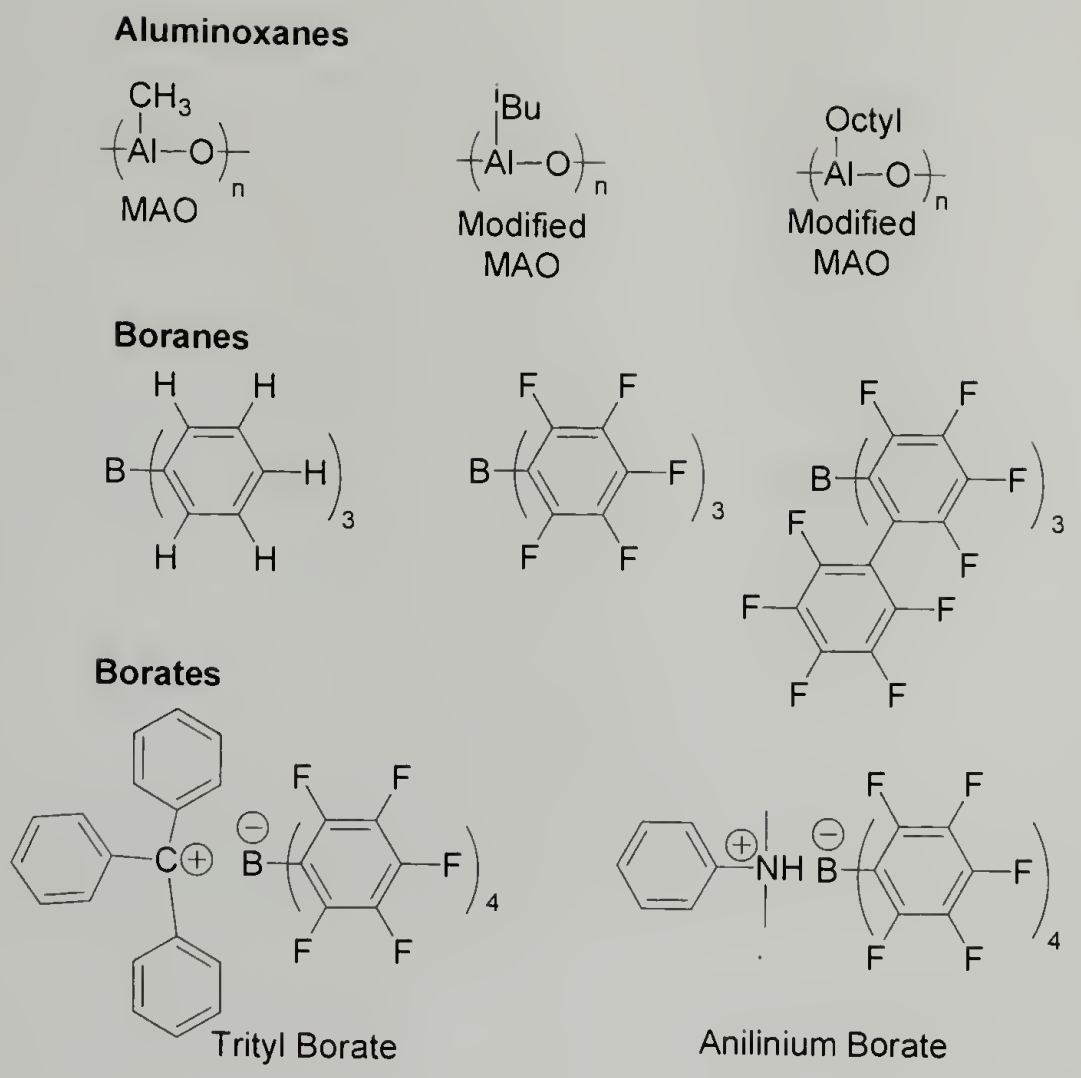

Figure 1.7 Cocatalysts Used in Polyolefin Syntheses

Alkylaluminoxanes include MAO type compounds and modified versions of MAO that exhibit higher solubility in a range of solvents. Although alkyl aluminum based cocatalysts have been widely used for olefin polymerization, there are several problems associated with these cocatalysts. Generally, high aluminum concentration is required for activation and olefin polymerization. It is difficult to study the overall activation process and the nature of the resulting species. Consequently there has been the need to develop new cocatalysts that can be used in equimolar amounts relative to the metal while also allowing characterization of the active species.

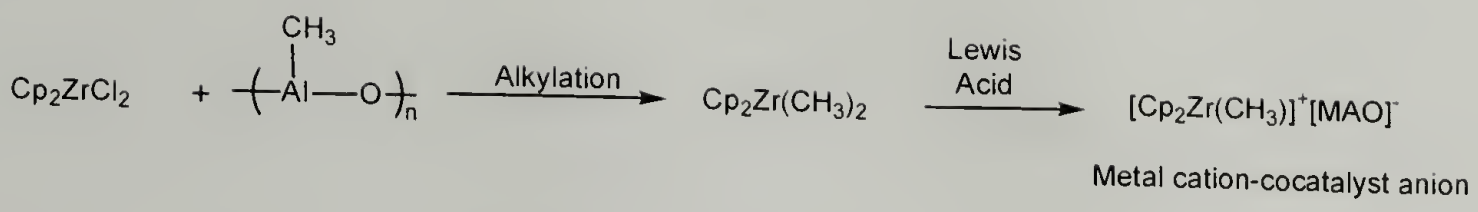

Figure 1.8 Formation of Metal Cation and Aluminate Cocatalysts Anion

Several groups have investigated the structure of the group IV metal alkyl cations and the interactions between the metal cationic metal center and the anion during polymerization.[12-14] As a result of these investigations, several new cocatalysts based on boranes and borates have been discovered (Figure 1.9). For example, reaction of $Cp_2Zr(CH_3)_2$ with highly Lewis acidic (tris(pentafluorophenyl borane)) ($B(C_6F_5)_3$) affords $[Cp_2ZrCH_3]^+[B(C_6F_5)_3CH_3]^-$ (Figure 1.9, Top). There are other synthetic strategies that makes use of non-nucleophilic counterions. For example, the use of $[(C_6H_5)N(CH_3)_2H][B(C_6F_5)_4)]$ to protonate $Cp_2Zr(CH_3)_2$, which in turn affords $[Cp_2ZrCH_3]^+[B(C_6F_5)_4]^-$, dimethylaniline and methane (Figure 1.9, Middle).[15, 16] An alternative method for generating the zirconium cation utilizes trityl borate $[(C_6H_5)_3C][B(C_6F_5)_4)]$ to abstract a methyl anion from $Cp_2Zr(CH_3)_2$ to afford $[Cp_2ZrCH_3]^+[B(C_6F_5)_4]^-$ and $(C_6H_5)_3CCH_3$ (Figure 1.9, Bottom).[17]

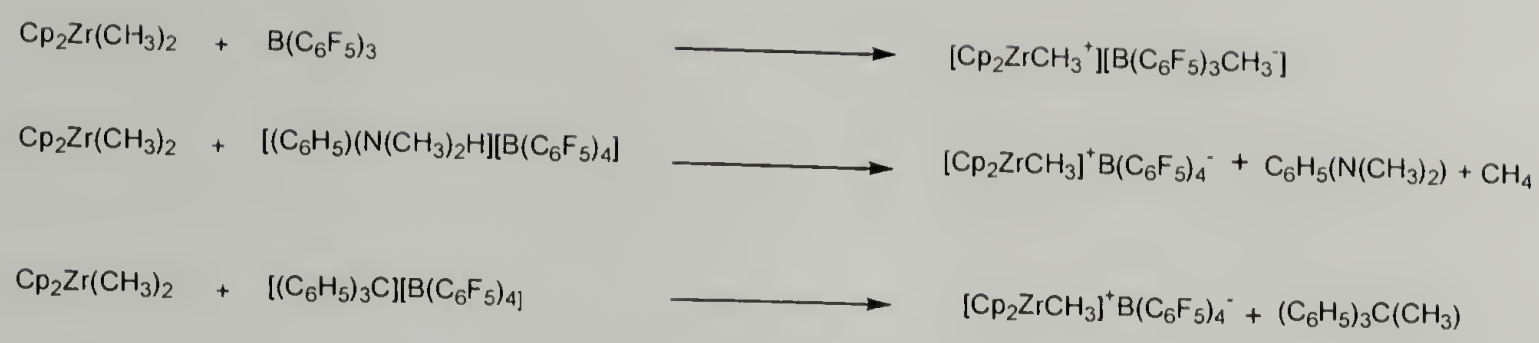

Figure 1.9 Formation of Metal Cation and Borate Coeatalyst Anions with Tris(pentafluorophenyl)borane (Top), Anilinium Borate (Middle), Trityl Borate (Bottom)

1.3.2 Metallocenes

Metalloeenes can be elassified as bridged and non-bridged metallocenes (Figure 1.10).[18,19,20] In the non-bridged metallocenes, the two eyelopentadienyl rings are not linked. Another sub-elass of non-bridged metallocenes are the oseillating-type metalloeenes used for the stereobloek polymerization of propylene. This catalyst arehiteeture has been designed to isomerize between aehiral and ehiral eoordination geometries. On the other hand, in the bridged metalloeene the two eyelopentadienyl rings are linked by a variety of groups (dimethylsilyl, isopropylidene etc). There are a few features in the design of metallocenes that are important for propylene polymerization. First, the substituents on the eyelopentadienyl ring can influence propylene polymerization aetivity. Seeondly, the presenee of stereorigid or ehiral metalloeenes allows regiospeeifie and stereospeeifie ineorporation of propylene monomer. The group symmetry of the metal eatalysts alters the stereoregularity of the polymer synthesized (Figure 1.10). [8,21,22] For instanee, using C_2 symmetrie metalloeenes, isotaetie polypropylene ean be synthesized with 1,2 regiochemistry of propylene insertion,

whereas C_s symmetric metallocenes afford syndiotactic polypropylene. Metallocenes, which oscillate between a chiral form and a non-chiral form, afford polypropylene with isotactic and atactic stereoblocks.[23] Metallocenes in conjunction with cocatalyst are known to produce HDPE from ethylene homopolymerization, while ethylene and α-olefin copolymerization affords LLDPE (Figure 1.6).

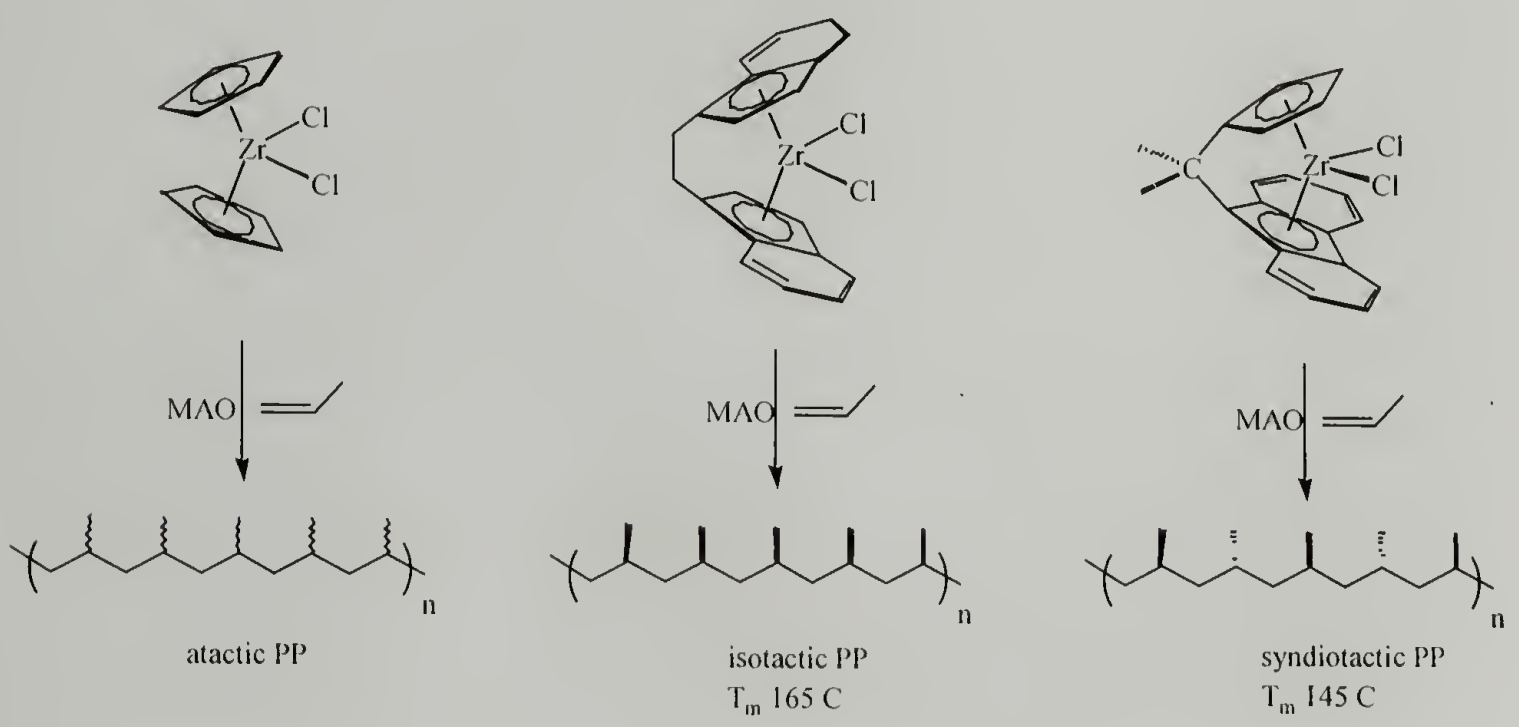

Figure 1.10 Correlations between the Structure of Metallocene and Stereoregularity of Polypropylene

1.3.3 Constrained-Geometry Catalysts

There are several examples of non-metallocene based single site catalysts systems which have been used for the polymerization of olefins. These catalyst architectures include piano-stool complexes and constrained-geometry catalysts (CGCs). The constrained geometry catalysts (CGCs, Figure 1.11) containing a

cyclopentadienyl ring and an amido ligand linked together with a dimethylsilyl unit.[24] The constrained-geometry catalysts systems were developed based on model single component scandium based systems.[25-28] These catalysts are alternatives to the well known Brintzinger and Kaminsky bridged metallocenes.

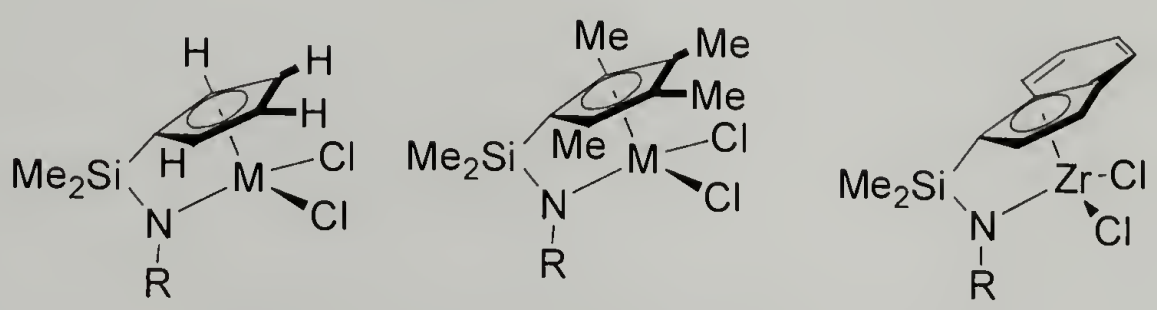

Figure 1.11 Constrained Geometry Catalysts

CGCs in combination with a cocatalyst afford linear high-density polyethylene (HDPE) with a range of molecular weight and a PDI of 2. A termination mechanism in polyethylene production is hydride elimination from the β-methylene carbon attached to the metal center. This results in the formation of metal-hydride cation in conjunction with cocatalyst anion and oligopolyethylene (M_w = 500-5000 g/mol) with a vinyl end-group (macromer). Through the use of appropriate cocatalysts and reaction conditions, the metal hydride cationic complex copolymerizes ethylene and the macromer formed *in situ* affording polyethylenes that contain a few long chain branches (LCBs) (Figure 1.12). The presence of long chain branches improves the melt flow properties of polyethylene making it easier to process and has been determined by rheological measurements.[29] The CGCs are able to very efficiently polymerize α-olefins. The copolymerization of ethylene and α-olefins using activated CGCs affords LLDPE with random incorporation of the α-

olefin in the copolymer. On the other hand, during propylene polymerization, CGCs afford atactic polypropylene with enriched syndiotactic components (Figure 1.6).[24,29,30]

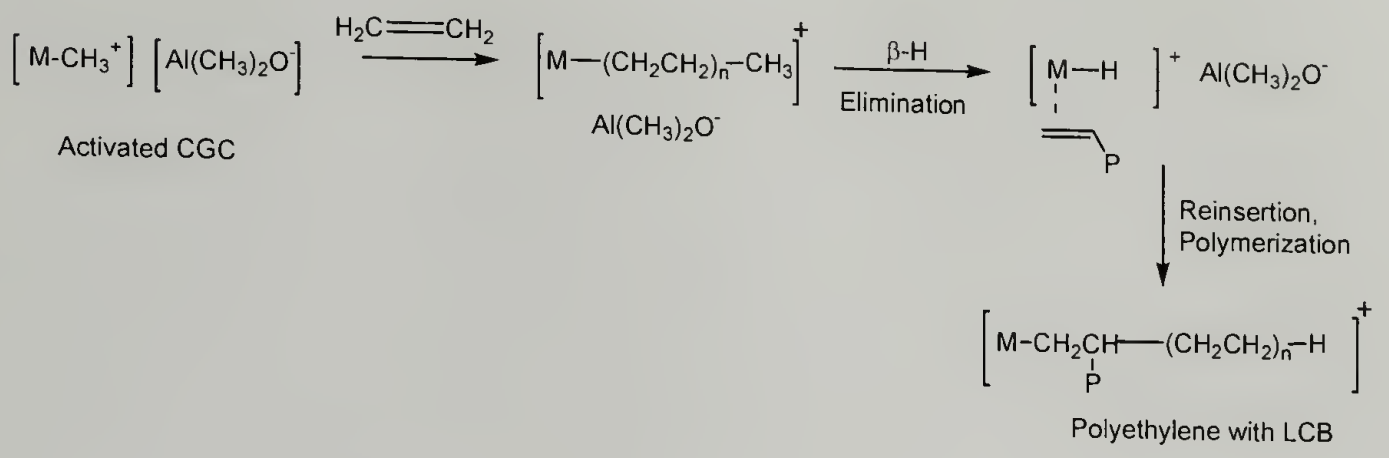

Figure 1.12 Synthesis of High Density Polyethylene (HDPE) with Long Chain Branches (LCBs)

1.3.4 Piano Stool Complexes

Titanium based piano stool complexes ($Cp'TiX_3$, Figure 1.13) have been synthesized by the reaction of trimethylsilylcyclopentadienyl analogs with titanium tetrachloride with the subsequent elimination of trimethylchlorosilane.[31-33] Treatment of $CpTiCl_3$ with phenol or aromatic amines affords modified piano stool complexes containing an aryloxy or amido moiety.[34,35]

Homopolymerization of styrene using activated piano stool affords syndiotactic polystyrene. On the other hand, the modified piano stool complexes containing aryloxy or amido groups when activated by cocatalysts affords ethylene–styrene (Interpolymers) and ethylene –α-olefin copolymers (LLDPE) with fairly good activity and comonomer incorporation (Figure 1.6).[36]

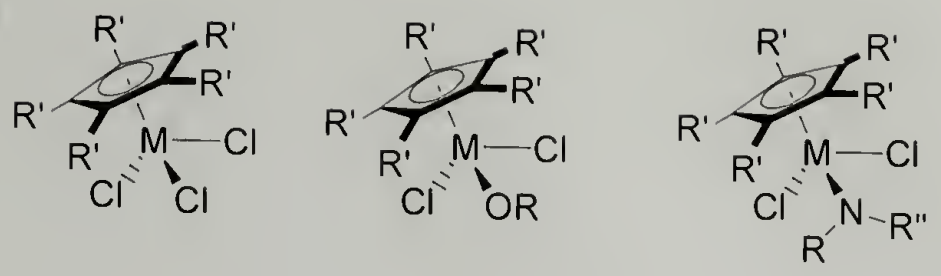

Figure 1.13 Piano Stool Complexexes

1.3.5 Non-cyclopentadienyl Based Group IV Catalysts

There has been increasing interest in the synthesis of non-Cp type ligand architectures for the synthesis of catalysts that can be used for the polymerization of olefins.[37, 38] These complexes include the diamide ligand, β-diketiminate ligands, iminopyrrolides and related five membered chelate species, amide ligands forming three membered chelates, salicylaldiminato and bis(phenoxy) ligands (Figure 1.14).

These catalysts on activation with MAO or alkylaluminum/borates in the presence ethylene monomer afford HDPE of a range of molecular weights. Not as much is known about propylene polymerization using the non-Cp type ligand framework. Using non-Cp based group IV metal catalysts, living polymerization of α-olefins has been reported, as well as block copolymers of ethylene and α-olefins (Figure 1.6). [39-42]

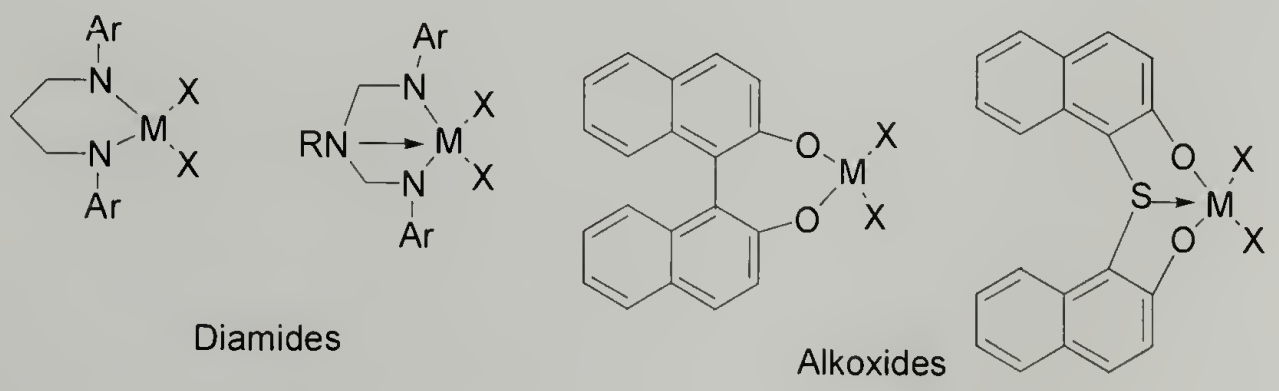

Figure 1.14 Non-Cyclopentadienyl based Group IV Metal Catalysts

1.4 Comparison between SSCs and Heterogeneous Ziegler-Natta Catalysts

In a homogeneous SSC, the ligand/metal combination influences the ability of the catalysts to produce polyolefins of a range of molecular weights, polydispersity indices (PDI), chemical composition and alters the polymerization kinetics. Ligand control is best demonstrated by propylene polymerization, for which catalysts have been designed to produce isotactic, syndiotactic, hemiisotactic, and atactic stereostructures with a high degree of stereospecificity. As with the initial heterogeneous Ziegler-Natta catalysts, the activity and the reactivity of the catalysts with different monomers can be altered by the use of an external donor. These heterogeneous catalysts afford polymers with broad molecular weight distribution, non-uniform comonomer incorporation.

Despite numerous advantages, there are still some disadvantages in using homogeneous SSCs for the large-scale production of polyolefins. Firstly, polyolefins synthesized using SSCs have lower bulk density than polymers synthesized using Ziegler-Natta catalysts. Secondly, there is some difficulty in controlling polymer morphology with soluble homogeneous catalysts. Polymerization of olefins using soluble SSCs in a polymerization reactor affords polyolefins that are often insoluble in the polymerization solvent. The formed polyolefin spreads over the walls of the reactor, resulting in no control in the morphology of the polymer. This is referred to as "reactor fouling".

Polymerization of gaseous olefins is performed in conjunction with the metal catalysts/cocatalysts. There are two major polymerization modes: solution and slurry polymerization. Polymerization of olefins using homogeneous SSCs involves the use of a soluble SSC in conjunction with a cocatalyst in a hydrocarbon solvent in a polymerization reactor. The reactor is pressurized with the monomer, and the

polymerization proceeds by a Cossee-Arlman mechanism with enchainment of the monomer to afford the polymer. As the polymer is formed, it does not remain soluble in the solvent and precipitates out of solution. During the process of precipitation of the polymer, primary and secondary crystallization forces come into play. The crystallization forces allow the polymer to adopt a more stable conformation. When heterogeneous Ziegler-Natta catalysts are used for polymerization of olefins in conjunction with cocatalysts in a hydrocarbon solvent, the active sites are not soluble in the reaction solvent. The active sites are said to be slurried in the hydrocarbon solvent. Polymerization occurs when the catalyst /cocatalyst are pressurized with the monomer, followed by the diffusion of the monomer to the active sites. Once again, the polyolefin formed precipitates out of solution as soon as it reaches a critical molecular weight. Crystallization of the polyolefin can now be affected by a number of factors, which include the type of catalyst/cocatalyst used and the support used to heterogenize the catalysts.

To summarize, homogeneous SSCs can be used in a solution polymerization mode affording polymers with controlled comonomer incorporation, high activity, regioregularity and stereoregularity, although without control over morphology and bulk density of the polymer. On the other hand, heterogeneous catalysts (Ziegler-Natta) used for olefin polymerization afford polymers of good particle size, controlled particle morphology and bulk density, but the presence of numerous active sites leads to polymer with non-uniform comonomer distribution and composition and broad PDI.

1.5 Supported Single Site Catalysts (SSCs)

There is a significant commercial drive to combine the inherent advantages of SSC catalysts (high activity, control over monomer reactivity and polymer structure control) with the attributes of supported catalyst technology (such as morphology control, high bulk density control, and low reactor fouling). The bulk density of polyolefin synthesized from metallocene-supported systems is expected to be lower than the polyolefins synthesized from traditional Ziegler-Natta systems.[43] For instance, metallocenes in conjunction with borate cocatalysts have been supported on crosslinked polystyrenes and used for olefin (ethylene and 1-hexene) copolymerization. As seen from SEM and optical micrographs, the resulting polyolefin has grown about thousand-fold compared to the starting material and the overall morphology of the support matrices is replicated in the product.[44,45]

More importantly, the support should be regarded as a part of the ligand–metal environment. Hence, chemical and structural changes to the support should, and will, affect the overall performance of the SSC bound to the support. This influence of the support on the activity or productivity of the covalently attached or adsorbed SSC can be referred to as the support influence or the "secondary sphere of influence". The challenge in the field of supported single site catalysts is to design well-defined homogeneous catalytic site on a support material. Hence, heterogenization of the metal complex or the cocatalyst must be considered. A number of inorganic or organic materials have been used for heterogenizing SSCs. Most of the developments to date have dealt with high surface area porous materials namely silica and alumina. Organic supports that have been used include polystyrene based materials.

There are three main routes to the synthesis of heterogenized SSCs (Figure 1.15), which involve bonding the SSC to the support (Figure 1.15, Top), [46-50] chemically ligating the cocatalyst to the support (Figure 1.15, Middle), [45,51] or premixing the catalysts and cocatalyst solution before they are reacted with the support (Figure 1.16, Bottom). The top and middle equations involve the design of synthetic strategies to covalently bond or assemble the SSC framework and the cocatalyst, on the support. The first and third startegies require addition of cocatalyst for subsequent polymerization of olefins.[52, 53]

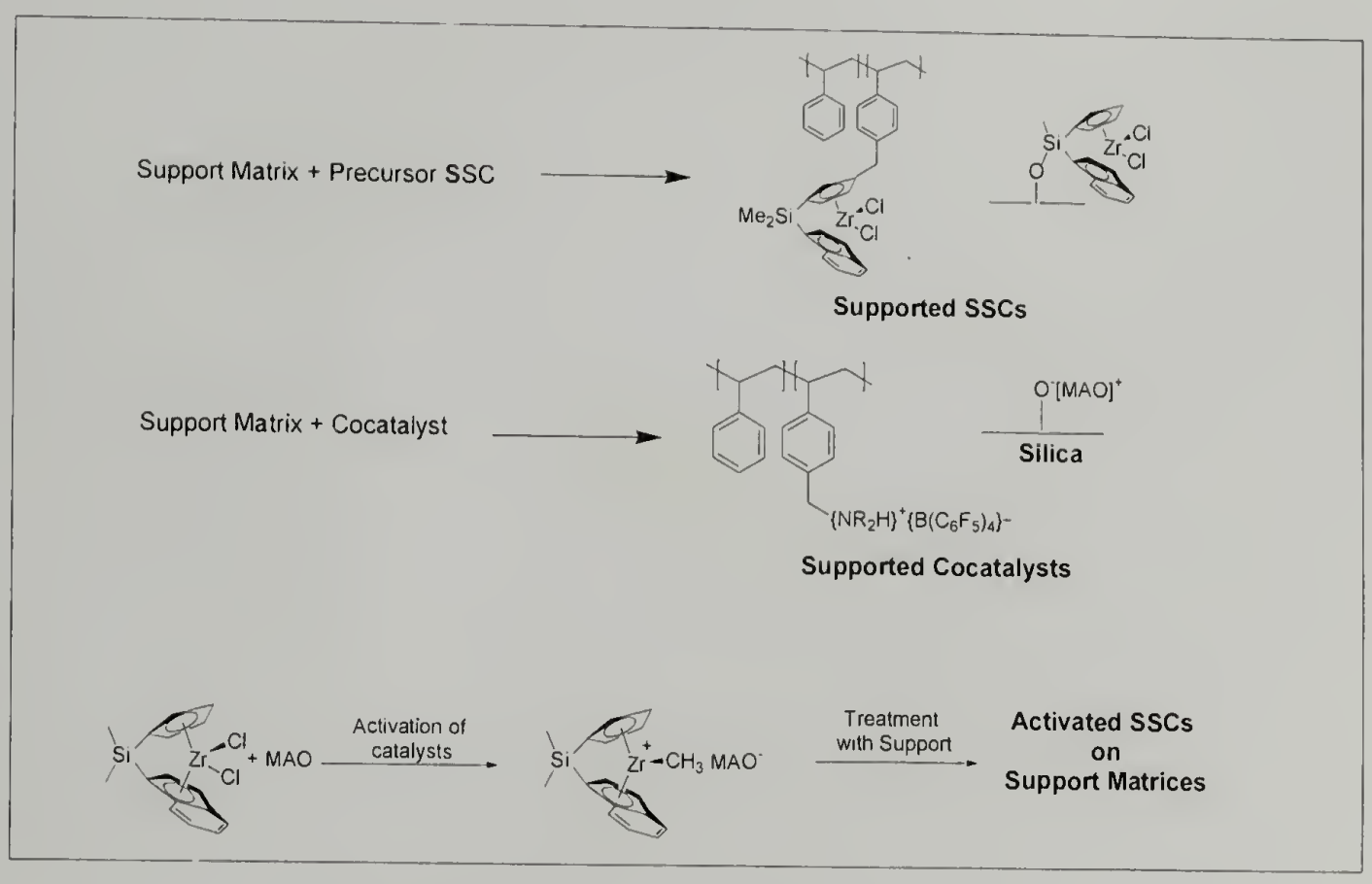

Figure 1.15 Supported Olefin Polyemerization Catalysts: Supported SSCs (Top), Supported Cocatalysts (Middle), and Activated SSCs on Support Matrices (Bottom)

It is notable that the activity of the supported SSC for olefin polymerization is about half to a tenth of the activity of the homogeneous or soluble SSC. This has been ascribed to the limited diffusion of the monomer into the pores of the support and the

presence of fewer active sites. The catalytic centers in supported SSCs may be deactivated when supported or may not be generated in the active form when treated with the cocatalysts. The molecular weight of the polymer is not affected in most cases, although in a few cases higher molecular weight polymers are obtained when a supported SSC is used. Extensive study of the effect of temperature on the propylene polymerization using homogeneous and supported-MAO shows that changes in activity, isotacticity, and polymer bulk density were lower for the supported catalysts than the soluble homogeneous SSC.

1.6 Thesis Summary

The influence of the primary ligands in homogeneous activated SSCs for the production of polyolefins (polyethylene, polypropylene, and branched polyolefins) has been well studied and documented in the literature. However, when a single site catalyst is tethered to a support matrix, the question that needs to be addressed is whether a support can influence the properties of polyolefins synthesized from the supported catalysts. This thesis focuses on SSCs tethered to different functionalized support matrices. Two different catalytic architectures have been chosen for this study, namely, titanium based CGCs and Piano Stool complexes.

Strageties for selectively assembling the constrained geometry catalysts on aminomethylpolystyrene (AMPS, Chapter 2 and 3) and amine-functionalized mesoporous silica (Chapter 4) were developed. The supported SSCs have been characterized by NMR and elemental analyses. These supported catalysts in conjunction with appropriate cocatalysts have been used for ethylene homopolymerization and copolymerization. The

polyolefins produced were analyzed for molecular weight (M_w g/mol) and polydispersity (PDI) by Gel Permeation Chromatography (GPC), melting point (T_m) and percentage crystallinity (%X= $\Delta H_{obs}/293$) by Differential Scanning Calorimetry (DSC), apparent crystal thickness by Wide Angle X-Ray Diffraction (WAXD), morphology by Scanning Electron Microscopy (SEM). Interesting correlations between the support matrix and the molecular weight, and the percent crytallinity of polyolefins synthesized from the supported catalyts were established (Chapter 5).

Synthetic routes to tether methylaluminoxanes (MAO) on aminomethylpolystyrene and non-functionalized silica were developed (Chapter 6). These supported cocatalysts in conjunction with homogeneous CGCs were used to prepare polyethylene or polypropylene. A correlation between the method of tethering the single site catalyst or cocatalyst to AMPS and the molecular weight and percent crystallinity of polyethylenes was established. The effect of supported cocatalysts on AMPS or mesoporous silica with CGCs on the properties of polypropylenes produced was studied.

The titanium based piano stool complexes were treated with a random copolymer of styrene and 4-hydroxy styrene (HPS) and afforded aryloxy complexes tethered to HPS (Chapter 7). These tethered cocatalysts with MAO as the cocatalysts afforded branched polyethylene (LLDPE) from ethylene only feed. By contrast, the homogeneous structural analogs afforded HDPE, with no branches under similar experimental conditions. This research finding is an alternative synthetic route to prepare LLDPE from ethylene feed. The influence of the support for the preparation of branched polyolefins was studied and the properties of polyolefins were studied.

CHAPTER 2

SILYL ELIMINATION CHEMISTRY TO SYNTHESIZE PRECURSOR PIANO STOOL COMPLEXES TO CONSTRAINED GEOMETRY CATALYSTS

2.1 Introduction

Numerous efforts are being directed toward the synthesis of SSCs architectures for the polymerization of ethylene and α-olefins to produce high density polyethylene, branched polyethylene as well as isotactic and syndiotactic polyolefins.[21,22,37,54] One such class of catalysts containing a cyclopentadienyl ring and an amido unit, linked with a dimethylsilyl unit are the CGCs.[24-28,55] These catalysts are alternatives to the well known Brintzinger and Kaminsky ansa-metallocenes. Due to their open nature, CGCs are able to very efficiently polymerize α-olefins. Polyolefins made using these catalysts system in homogeneous media have been studied extensively, and their properties have been evaluated.

There are several different strategies by which these catalysts have been synthesized. One of the oft-repeated synthetic routes is to synthesize $[C_5R_4HSiMe_2NHR']$, (**i**), from $(C_5R_4H)SiMe_2Cl$ and R'NHLi ,with subsequent removal of lithium chloride. The basic ligand framework of constrained geometry catalysts can be obtained by metathetical reaction of the dilithium salt of **i** with MCl_4 (M=Ti, Zr) (Figure 2.1, Method A). [25-28,56,57] This route leads to low yields of **iiiA**, which has subsequently been improved by the use of $TiCl_3(THF)_3/PbCl_2$ in the higher congeners of cyclopentadienes, whreas **iiiB** is obtained in good yield. Other preparations include amine elimination from reaction of homoleptic metal amides with **i** (Figure 2.1, Method B). [57,58,59] In this preparative method, the eliminated amine is found to coordinate to the

metal center. Reduced ethylene polymerization activity has been observed when these catalysts systems have been used, and this result could be attributed to the inefficient activation of these metal amides by the cocatalyst and presence of coordinated amines.

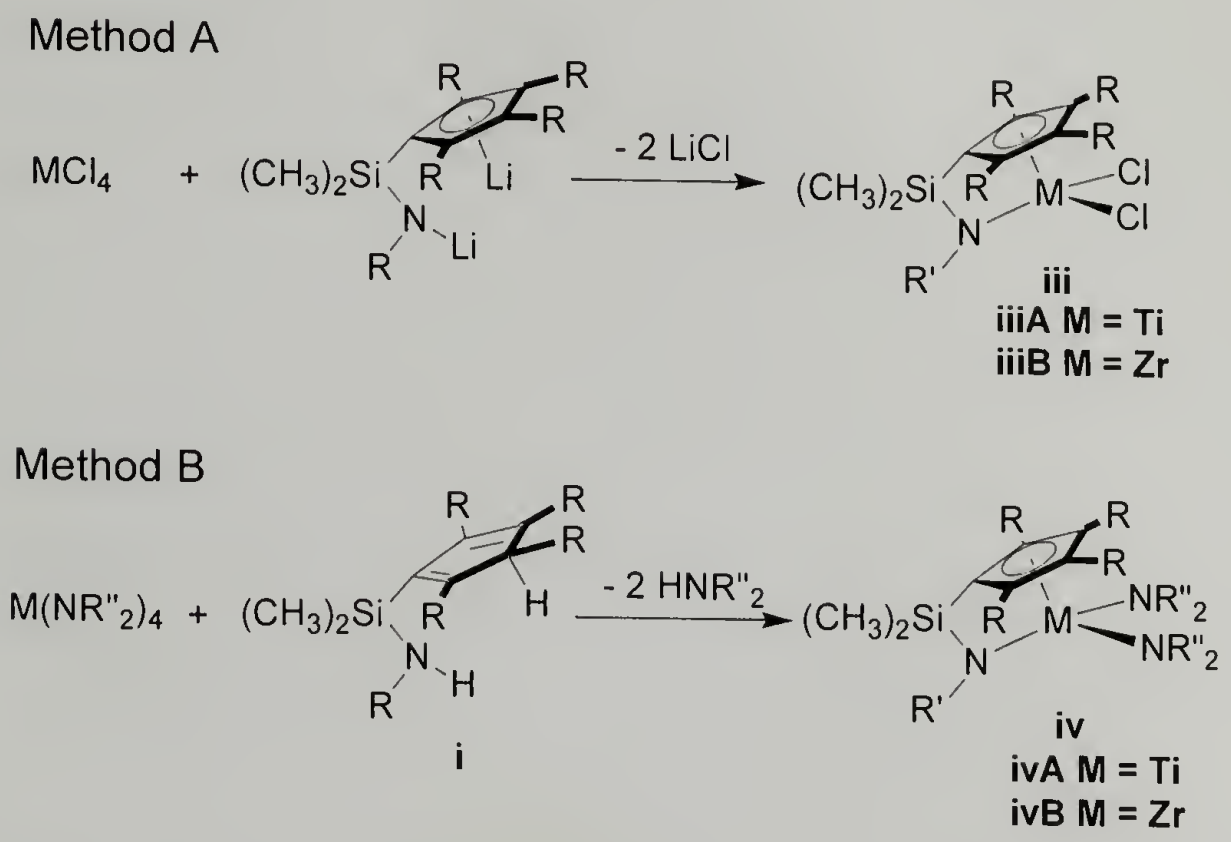

Figure 2.1 Syntheses of Constrained Geometry Catalysts by Metathetical Salt Elimination (Method A) and Amine Elimination Chemistry (Method B)

An alternative synthesis involves the formation of chlorodimethylsilyl substituted monocyclopentadienyl titanium complex **ii,** which on subsequent reaction with a primary amine yields the CGC **iii** (Figure 2.2).[60,61] To date, this approach to CGCs has been studied only in the case of the cyclopentadienyl ligand. Replacement of the hydrogen atoms of the cyclopentadienyl ring by alkyl, aryl, or fused aromatic rings has been shown to influence the steric and electronic properties of the metal center. The steric and electronic properties of the metal has a direct impact on the properties of the resulting polymer due to the structure property-relationship between the catalyst used for polymerization and the ultimate polymer properties.[62,63]

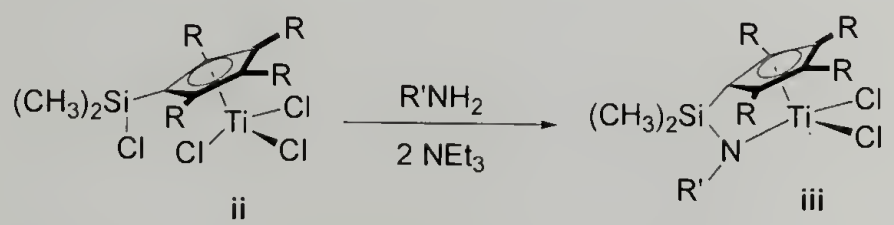

ii iii

Figure 2.2 Syntheses of Constrained Geometry Catalysts by Silyl Elimination Chemistry

In this chapter, the synthesis of trimethylsilyl (monosilyl compounds) and (chlorodimethylsilyl)trimethylsilyl (mixed silyl compounds) derivatives of tetramethylcyclopentadiene, indene and fluorene is described. Subsequent investigation of the silyl eliminations chemistries of the mixed silyl compounds with $TiCl_4$ or $ZrCl_4$ is reported. The monocyclopentadienyl titanium piano stool complexes obtained can be further used to assemble CGCs on amine-functionalized supports. The catalyst assembly protocols and the olefin polymerization studies will be discussed in Chapters 3 and 4. The properties of the polyolefins will be used as a direct measure of the influence of the

support on the metal complex during polymerization, which is the main focus of this thesis.

2.2 Experimental Section

2.2.1 Reagents and general techniques

All the reactions were performed under nitrogen in Schlenk glassware or in an inert atmosphere dry box. All solvents used were obtained from a solvent purification manifold.[64] The chlorosilanes $(CH_3)_3SiCl$ and $(CH_3)_2SiCl_2$, cyclopentadiene, tetramethylcyclopentadiene and indene were distilled from CaH_2. Methyl lithium (1.4 M in ether), $TiCl_4$, and pre-sublimed $ZrCl_4$ were obtained from Aldrich and used as received.

2.2.2 Material Characterization

^1H NMR spectra were obtained at 300 MHz using a Bruker DPX 300, ^{13}C NMR were recorded at 75 MHz using Bruker DPX 300, ^{29}Si NMR spectra were recorded at 150 MHz using an AVANCE 600 spectrometer. Mass spectral analyses were performed using JMS700 MStation (JEOL) high resolution two-sector mass spectrometer in the Electron Impact (EI) mode. GC-MS spectra were recorded using a Hewlett-Packard GC-MS system. Elemental analysis was performed using three Exeter Analytical Inc.240XA CHN analyzers.

2.2.3 Synthesis of 1-Trimethylsilylcyclopentadiene (1)

To a solution of cyclopentadiene (5.0 mL, 68 mmol) in a mixture of ether and toluene (1:4 v:v, 20 mL total), CH_3Li (5.6 mL, 70 mmol) was added dropwise and the resulting mixture was allowed to stir overnight to ensure complete deprotonation. To this solution, $(CH_3)_3SiCl$ (7.9 mL, 72 mmol) was added dropwise and the solution was stirred

for 48 hours at room temperature to ensure complete silylation. Lithium chloride was removed by filtering through celite, and the volatiles were subsequently removed *in vacuo*. Compound **1** was isolated as a pale yellow liquid (8.0 mL, 85% yield, density = 0.9 g/mL).

^{1}H NMR ($CDCl_3$): δ0-0.29 (m, 9H, $Si(CH_3)_3$, presence of isomers), 3.0-3.5 (m, 1H, ipso-*H*, presence of isomers), 5.7-6.9 (m, 4H, C_5H_4, presence of isomers).

2.2.4. Synthesis of 1-(dimethylchlorosilyl)-1-(trimethylsilyl)-cyclopentadiene (2)

To a solution of **1** (5.0 mL, 32 mmol) in a mixture of ether and toluene (1:4 v:v, 20 mL total), CH_3Li (2.6 mL, 35 mmol) was added, and the resulting solution was allowed to stir overnight to ensure complete deprotonation. To the resulting solution, $(CH_3)_2SiCl_2$ (3.87 mL, 30 mmol) was added dropwise and the mixture was allowed to stir at room temperature for 3 days. Lithium chloride was removed by filtering through celite and the solvents were removed *in vacuo*. Compound **2** was isolated as a viscous yellow liquid (6.6 mL, 90% yield, density = 0.85 g/mL).

^{1}H NMR ($CDCl_3$): δ0.0(m, 9H, $Si(CH_3)_3$, presence of isomers), δ0.3(m, 6H, $Si(CH_3)_2Cl$, presence of isomers), δ6.2–6.8(m, 4H, C_5H_4, presence of isomers)

2.2.5 Synthesis of (Chloro(dimethyl)sily)-cyclopentadienyl]titanium trichloride (3)

Compound **2** (4.0 mL, 15.6 mmol) was added dropwise to a solution of $TiCl_4$ (3.0 mL, 16.0 mmol) in 20 mL dichloromethane, and the reaction mixture was stirred at room temperature for 3 days. Volatiles were then removed *in vacuo*, and the residue was redissolved in 5 mL of dichloromethane to which 10 mL of hexane was added. Recrystallization at –30°C over a period of 2 days afforded a yellow microcrystalline solid **3** (4.1g, 85% yield).

^{1}H NMR (C_6D_6): δ0.46 (s, 6H, Si(CH_3)$_2$Cl), δ6.0 (m, 2H, C_5H_4), δ6.4(m, 2H, C_5H_4)

^{13}C NMR (C_6D_6, CPD): δ0.0 (Si(CH_3)$_2$Cl), 124.3 (C_2 of Cp), 126.3 (C_3 of Cp), C_1-Cp not located

^{29}Si NMR (Solution, C_6D_6, DEPT 45): δ -10.6 (*Si*(CH_3)$_2$Cl)

HR-MS: Calculated (m/z 311.8758), Observed (m/z 311.8743)

Elemental Analysis: Calculated $C_7H_{10}SiTiCl_4$ C (35.96)%, H (4.9%); Observed C (35.8), H (4.95)

2.2.6 Synthesis of 1-Trimethylsilyl-2,3,4,5-tetramethylcyclopentadiene (4)

To a solution of 2,3,4,5-tetramethylcyclopentadiene (5.0 mL, 44 mmol) in a mixture of ether and toluene (1:4 v:v, 20 mL total), CH_3Li (44 mmol, 3.5 mL) was added dropwise and the resulting mixture was allowed to stir overnight to ensure complete deprotonation. To this solution, $(CH_3)_3SiCl$ (4.8 mL, 44 mmol) was added dropwise and the solution was stirred for 48 hours at room temperature to ensure complete silylation. Lithium chloride was removed by filtering through celite, and the volatiles were subsequently removed *in vacuo*. Compound **4** was isolated as a pale yellow liquid (6.9 mL, 95% yield, density = 0.9 g/mL).

^{1}H NMR ($CDCl_3$): δ0.03 (s, 9 H, Si(CH_3)$_3$,), δ1.88 (s, 6 H, Cp-CH_3(α)),δ1.97 (s, 6 H, Cp-CH_3(β)), 2.75 (Cp–*H*, attached to the ipso carbon)

^{13}C NMR ($CDCl_3$, CPD): δ0.00 (Si(CH_3)$_3$), δ12.90 (Cp-CH_3(α)), δ16.20 (Cp-CH_3(β)), δ57.10 (ipso carbon-C_1), δ134.00, δ137.00 (C_2, C_3 -Cp).

Elemental Analysis: Calculated $C_8H_{14}Si$, C (74.0%), H (11.3%); Observed C (74.18), H (11.47)

2.2.7. Synthesis of 1-(dimethylchlorosilyl)-1-(trimethylsilyl)-2,3,4,5-tetramethylcyclopentadiene (5)

To a solution of **4** (5.79 mL, 30 mmol) in a mixture of ether and toluene (1:4 v:v, 20 mL total), CH_3Li (30 mmol, 2.15 mL) was added and the resulting solution was allowed to stir overnight to ensure complete deprotonation. To the resulting solution, $(CH_3)_2SiCl_2$ (3.87 mL, 30 mmoles) was added dropwise, and the mixture was allowed to stir at room temperature for 3 days. Lithium chloride was removed by filtering through celite, and the solvents were removed *in vacuo*. Compound **5** was isolated as a viscous yellow liquid (7.7 mL, 90% yield, density = 0.8 g/mL).

^{1}H NMR ($CDCl_3$) : δ0.01 (s, 9 H, Si(CH_3)$_3$), δ0.19 (s, 6 H, Si (CH_3)$_2$Cl), δ1.82 (s, 6 H, Cp-CH_3(α)) and δ2.03 (s, 6 H of Cp-CH_3(β))

^{13}C NMR ($CDCl_3$, CPD): δ-0.04 (Si(CH_3)$_3$), δ2.65 (Si(CH_3)$_2$Cl), δ11.75(Cp-CH_3(α)), δ15.44 (Cp-CH_3(β)), δ132.67 and δ139.36 (C_2, C_3-Cp), C_1-Cp not identified.

Elemental Analysis: Calculated $C_{14}H_{27}Si_2Cl$ C (58.64), H (9.4); Observed C (58.82), H (9.75)

2.2.8 Synthesis of (Chloro(dimethyl)sily)-2,3,4,5 tetramethylcyclopentadienyl] titanium trichloride (6)

Compound **5** (3.0 mL, 9.45mmol) was added dropwise to a solution of $TiCl_4$ (1.8 mL, 9.45 mmol) in 20 mL dichloromethane, and the reaction mixture was stirred at room temperature for 3 days. Volatiles were then removed *in vacuo*, and the residue was redissolved in 2 mL of dichloromethane to which 4 mL of hexane was added. Recrystallization at –30°C over a period of 5 days afforded a dark red microcrystalline solid **6** (2.83g, 83% yield).

^{1}H NMR (C_6D_6): δ0.9 (s, 6 H, Si (CH_3)$_2$Cl), δ2.38 (s, 6 H, Cp-CH_3(α)) and δ2.59 (s, 6 H, Cp-CH_3(β)).

^{13}C NMR (C_6D_6, CPD): δ5.4 (Si (CH_3)$_2$Cl), δ14.52 (Cp-CH_3(α)), δ17.89(Cp-CH_3(β)), δ143.00 and δ145.00 (C_2, C_3 -Cp), C_1-Cp not identified.

^{29}Si NMR (C_6D_6, DEPT 45): δ -5.2 (Si(CH_3)$_2$Cl)

HR-MS: Calculated (m/z 367.9385), Observed (m/z 367.9249)

Elemental Analysis: Calculated $C_{11}H_{18}SiTiCl_4$ C (35.96), H (4.9); Observed C (35.83), H (4.65)

2.2.9 Reaction of 5 with $ZrCl_4$

Compound **5** (1 mL, 3.15 mmol) was added to slurry of $ZrCl_4$ (0.733 g, 3.15 mmol) in 20 mL toluene heated in a sealed reactor for 3 days at 100°C. The solution was filtered to remove insoluble impurities, and the volatiles were removed *in vacuo* to yield an orange yellow solid. Analysis of the solid revealed the formation of two products, (1.23g; 60% **7a** and 40% **7b**).

^{1}H NMR (CD_2Cl_2) **7a**:δ0.71 (s, 6 H, Si(CH_3)$_2$Cl), δ1.95 (s, 6 H, Cp-CH_3(α)) and δ2.11 (s, 6 H, Cp-CH_3(β))

^{1}H NMR (CD_2Cl_2) **7b**: δ0.32 (s, 12H, Si(CH_3)$_2$Cl), δ1.72 (s, 12H, Cp-CH_3(α)) and δ1.83 (s, 12H, Cp-CH_3(β)).

Mass Spectrum: Calculated (m/z 409.8958 (**7a**), (m/z 588.0138 (**7b**); Observed (m/z 409.9038 (base peak in the isotope distribution of **7a**), 281.9047(M^+ of **7b**-ZrCl, 100%), 187.0095 (M^+ of **7b**-(2(Me_4Cp)$ZrCl_2$))

2.2.10 Synthesis of Trimethylsilylindene (8)

To a solution of indene (5 mL, 43 mmol) in mixture of ether and toluene (1:4 v:v, 20 mL total), CH_3Li (3.08 mL, 43 mmol) was added dropwise at room temperature, and the resulting mixture was allowed to stir overnight to ensure complete deprotonation. To the resulting solution $(CH_3)_3SiCl$ (5.47 mL, 43 mmol) was added dropwise and stirred for 2 days at room temperature. Lithium chloride was removed by filtering through celite, and the volatiles were removed *in vacuo* to yield a light yellow colored solution of **8** (6.5 mL, 90% yield).

^1H NMR ($CDCl_3$): δ-0.01-0.27 (m, 9 H, $Si(CH_3)_3$), δ3.56 (s, 1 H, C-*H*, allylic), δ6.70 (d, 1 H, C-*H* olefinic, J=6 Hz), δ6.90 (d, 1 H, C-*H* olefinic, J=6 Hz), δ7.00- 7.60 (m, 4 H, aromatic, C-*H*).

^{13}C NMR ($CDCl_3$, CPD): δ-2.09 ($Si(CH_3)_3$), δ46.9, 41.58 (C_1, isomers 1 and 2); Aromatic region (Isomer 1): δ121.30 (C_2), δ124.00 (C_3), δ136.00 ($C_{4,7}$), δ144.40 ($C_{5,6}$), δ145.80 ($C_{8,9}$), Aromatic region (Isomer 2): δ123.00 (C_2), δ125.00 (C_3), δ129.00 ($C_{4,7}$), δ144.50 ($C_{5,6}$), δ145.80 ($C_{8,9}$).

Elemental Analysis: Calculated $C_{12}H_7Si$ C (76.59), H (8.51); Observed C (76.69), H (8.61)

2.2.11 Synthesis of (Trimethylsilyl)(dimethylchlorosilyl)indene (9):

To a solution of **8** (5 mL, 26.6 mmol) in a mixture of ether and toluene (1:4 v:v, 20 mL total), CH_3Li (2.1 mL, 26.6 mmol) was added dropwise with constant stirring at room temperature. The mixture was allowed to stir overnight to ensure complete deprotonation. To this solution, $(CH_3)_2SiCl_2$ (3.4 mL, 30 mmol) was added and the solution was allowed to stir for 3 days at room temperature. Lithium chloride was

removed by filtering through celite, and the volatiles were removed *in vacuo*. Compound **9** was isolated as a yellow viscous liquid (5.5 g, 90% yield, mixture of isomers).

^{1}H NMR (CD_2Cl_2): δ0.10-0.16 (m, 9 H, $Si(CH_3)_3$), δ0.19-0.36 (m, 6 H, $Si(CH_3)_2Cl$), δ6.73-6.88 (dd, 1 H, J=1.68, 5.07Hz), δ7.09-7.16(dd, 1 H, J=1.50, 5.28), δ7.20-7.40 (m, 2 H), δ7.30-7.70 (m, 2 H)

GC/MS- Peak with the m/z of 280.00 and appropriate isotope distribution

2.2.12 Reaction of 9 with $ZrCl_4$

To a solution of **9** (5 mL, 17 mmol) in toluene taken in a reaction vessel, was $ZrCl_4$ (4.13 g, 17 mmol) was added to the mixture. The reaction vessel was sealed and heated at 100°C for 3 days with stirring. The solution was then filtered to remove insoluble impurities and the volatile components were removed *in vacuo*, leaving a red orange solid containing a mixture of **10a** (1.8g, 45% yield) and **10b** (2.2g, 55% yield) (total yield=4g).

^{1}H NMR (CD_2Cl_2): δ0.49 (s, 6 H, $Si(CH_3)_2Cl$), 10a), δ0.38 (s, 12 H, $Si(CH_3)_2Cl$, 10b), δ7.12-7.52(m, 18 H, aromatic, **10a** and **10b**).

Mass Spectrum: Calculated (m/z 403.8619 (**10a**), m/z 576.8623(**10b**)); Observed (m/z 403.8519(**10a**), 460.8612 (M^+ of **10b**-2(Me_2Si), 10%), 228.1017(M^+ of **10b**-(2(Me_2Si))$ZrCl_4$), 20%)

2.3 Results and Discussions

2.3.1 Synthesis of Mixed Silyl Congeners

The syntheses of mono and mixed silyl cyclopentadienyl analogs are shown in Figure 2.3, and the cyclopentadienyl analogs have been synthesized according to the procedure reported by Royo and coworkers.[61] Compound **1** was synthesized by the

reaction of cyclopentadienyl lithium salt with $(CH_3)_3SiCl$ at room temperature. The ^1H NMR spectrum of monosilyl compound **1** showed the presence of isomers due to 1,3-sigmatropic shift of the $Si(CH_3)_3$, with the major component being that in which the silyl group is attached at the sp^3 carbon of cyclopentadiene (Figure 2.4).[32] Deprotonation of compound **1** with CH_3Li, followed by the addition of $(CH_3)_2SiCl_2$, results in the formation of mixed silyl compound **2**, which is a very viscous liquid comprising multiple isomers (Figure 2.5), as determined from ^1H NMR. This sequence of attaching trimethylsilyl and then dimethylchlorosilyl groups to the ligand needs to be followed strictly.

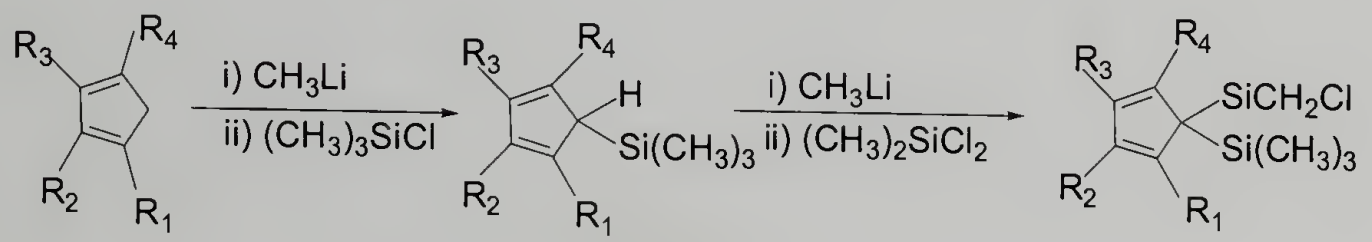

Substituents	Mono Silyl	Mixed Silyl
$R_1= R_2= R_3= R_4= H$	**1**	**2**
$R_1= R_2= R_3= R_4= CH_3$	**4**	**5**
$R_1= R_2= H$, R_3/R_4 = 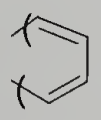	**8**	**9**

Figure 2.3 Syntheses of Mono Silyl and Mixed Silyl Compounds of Cyclopentadienes, Tetramethylcyclopentadienes, and Indenes

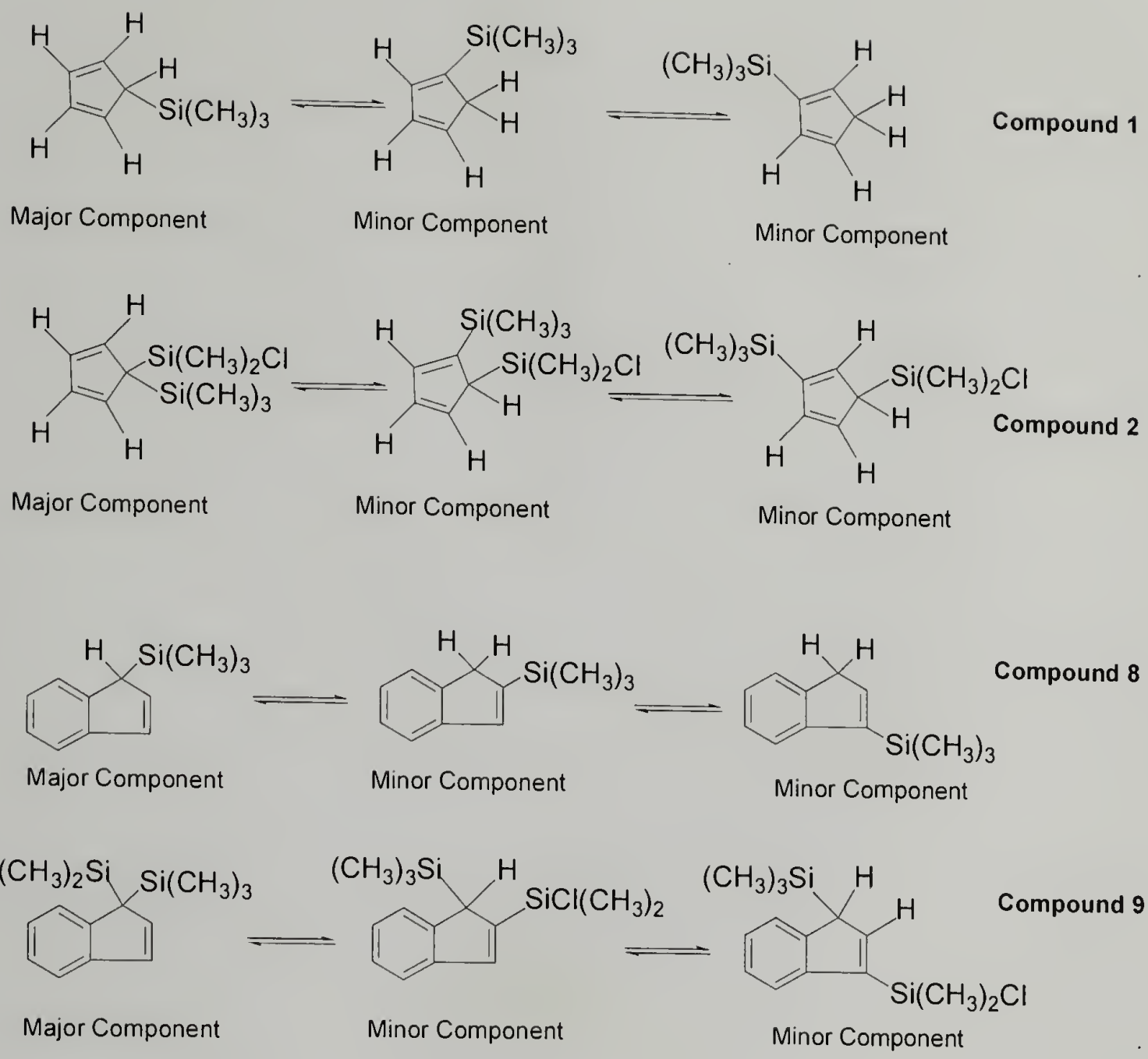

Figure 2.4 Isomers of Compounds **1**, **2**, **8**, and **9** due to Sigmatropic Shifts at Room Temperature

Similarly, monosilyl compound **4** was synthesized by the reaction of the lithium salt of tetramethylcyclopentadienyl with $(CH_3)_3SiCl$ at room temperature. The reaction proceeds cleanly and affords **4** in good yield and purity, as seen from NMR (Figure 2.5) and elemental analysis. Deprotonation of compound **4** with CH_3Li, followed by addition of $(CH_3)_2SiCl_2$, led to the formation of mixed silyl compound **5**, a slightly viscous yellow liquid in high purity, as determined from ^1H NMR (Figure 2.6) and elemental analysis.

Deprotonation of indene with CH_3Li, followed by the addition of $(CH_3)_3SiCl$, led to the formation of compound **8**. The ^1H NMR spectrum of monosilyl compound **8** showed the presence of isomers due to 1,3-silyl sigmatropic shift with the major component being that in which the silyl group is attached at the sp^3 carbon of indene (Figure 2.7, Trace A).[32] Deprotonation of compound **8** with CH_3Li, followed by the addition of $(CH_3)_2SiCl_2$, results in the formation of compound **9**, a very viscous liquid comprising multiple isomers, as determined from ^1H NMR. The possible number of isomers is even greater for the mixed silyl system **9**. At room temperature the ^1H NMR shows the major component to be the isomer with both silyl groups on the sp^3 carbon, with detectable amounts of the other possible isomers (Figure 2.7, Trace B). The ratio of the peak areas in the aliphatic region to those in the olefin/aromatic region was 15:6. Confirmation of the purity and compositional identity of **9** in all its various isomeric forms was determined using GC-MS. A peak observed at m/z of 280.00 was attributed to the mixed silyl indene **9**.

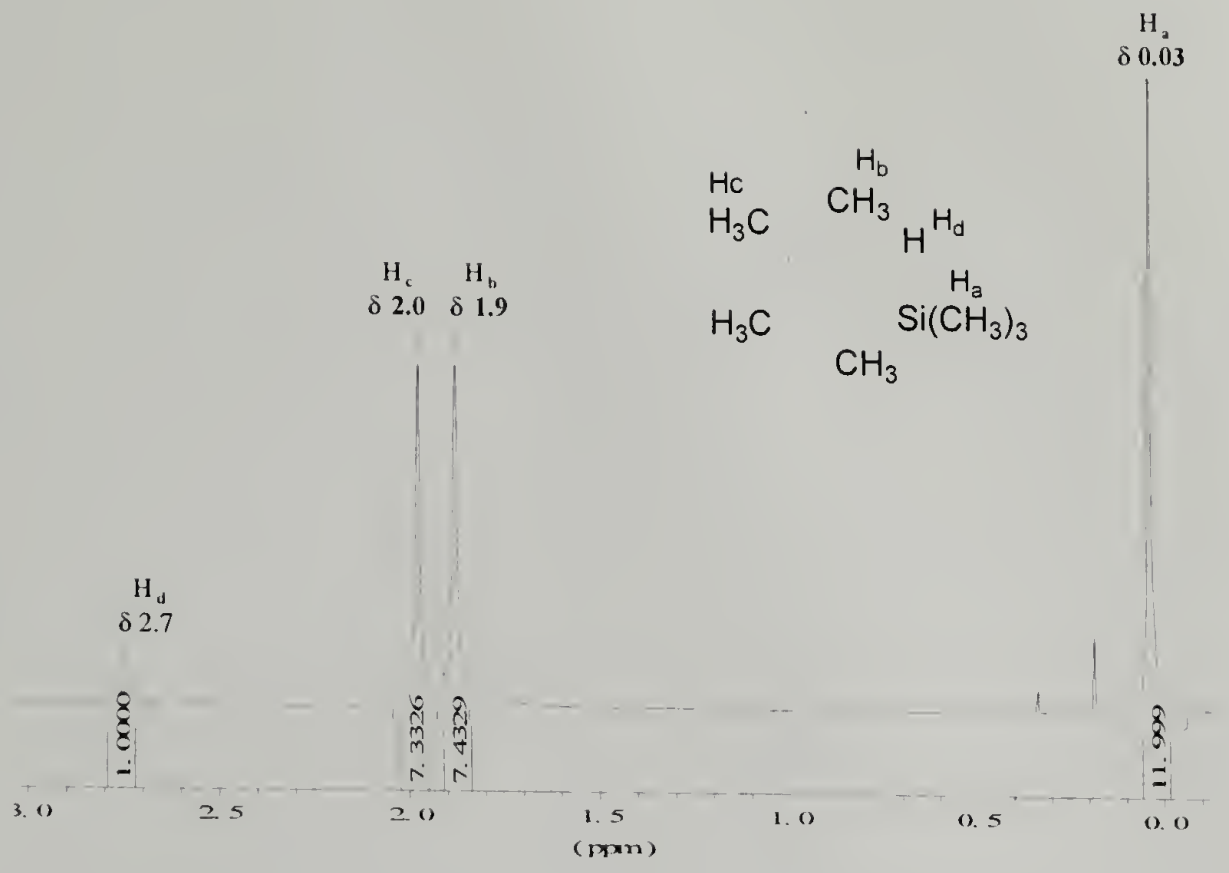

Figure 2.5 ^{1}H NMR of 1-trimethylsilyl-2,3,4,5-tetramethylcyclopentadiene (**4**) in CD_2Cl_2

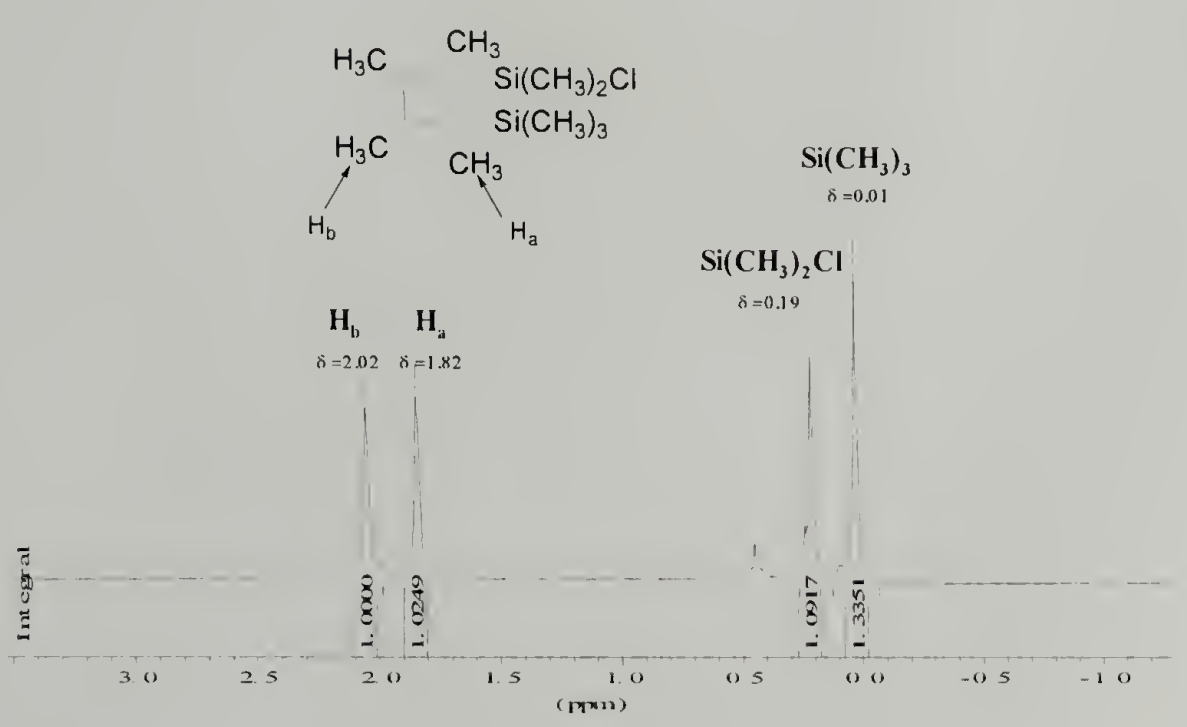

Figure 2.6 ^{1}H NMR of 1-trimethylsilyl-1'-chlorodimethylsilyl-2,3,4,5-tetramethylcyclopentadiene (**5**) in CD_2Cl_2

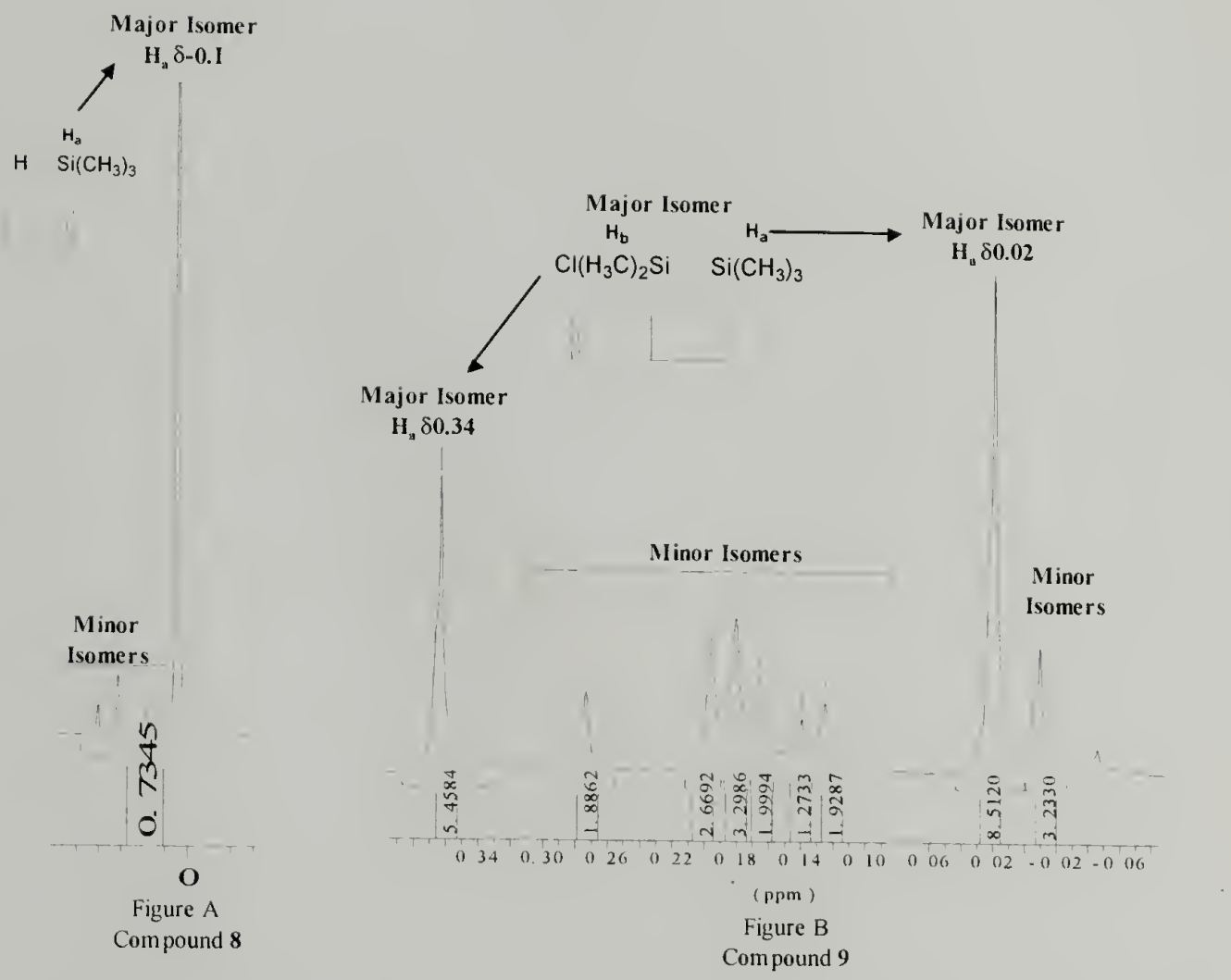

Figure A
Compound **8**

Figure B
Compound **9**

Figure 2.7 ^{1}H NMR (Solution) of Compound **8** (Trace A) and Compound **9** (Trace B): Presence of Isomers due to 1,3 Sigmatropic shifts at Room Temperature in CD_2Cl_2, $(CH_3)_xSiCl_{4-4}$ Region

2.3.2 Elimination Chemistry of Mixed Silyl Derivatives

For the silyl elimination reactions of the mixed silyl compounds **2**, **5**, or **9** using $TiCl_4$ or $ZrCl_4$, there exists the question of chemoselectivity of the chloroalkylsilane eliminated. Literature precedent for the mixed silyl cyclopentadiene $((CH_3)_3Si)(CH_3)_2SiCl))C_5H_4$ with $TiCl_4$ has demonstrated that there is chemoselective elimination of $(CH_3)_3SiCl$ and exclusive formation of **ii**.[60]

The silyl elimination reactions of **2**, on treatment with $TiCl_4$ in dichloromethane at room temperature for 3 days resulted in the exclusive formation of **3** (Figure 2.8, Top) as shown by Royo and coworkers.[60] These authors have shown that silyl elimination takes place from the major isomer, in which the silyl group is attached to the sp^3 carbon in the cyclopentadienyl moiety. ^{1}H NMR shows resonances for *H*-C_2, *H*-C_3, and $Si(CH_3)_2$, which were found in the ratio of 2:2:6 at δ0.46, δ6.0 and δ6.4 respectively (Figure 2.9). A single silicon resonance is observed in the carbon decoupled DEPT 45 ^{29}Si NMR at δ –10.6 that is attributed to ($Si(CH_3)_2Cl$) (Figure 2.10). The high-resolution mass spectrum showed the presence of molecular ion at m/z of 311.8743, which is also the base peak of **3** in the molecular ion envelope (Table 2.1).

The silyl elimination protocol was extended to the tetramethylcyclopendienyl and indenyl mixed silyl analogs. Compound **5** on treatment with $TiCl_4$ in dichloromethane at room temperature for 3 days resulted in the exclusive formation of **6** as a dark red solid in good yield (Figure 2.8, Bottom). In the ^{1}H NMR, singlet resonances for the methyl groups of $Si(CH_3)_2Cl$, ($CH_3(\alpha)$) and($CH_3(\beta)$) were found in the ratio of 1:1:1 at δ 0.90, δ 2.38 and δ 2.59, respectively (Figure 2.11). A single silicon resonance is observed in the carbon decoupled DEPT 45 ^{29}Si NMR at δ –5.2 that is attributed to ($Si(CH_3)_2Cl$) (Figure

2.12). The high-resolution mass spectrum (HRMS) showed the presence of the molecular ion at m/z of 367.9249. The purity of complex **6** was further confirmed by elemental analysis.

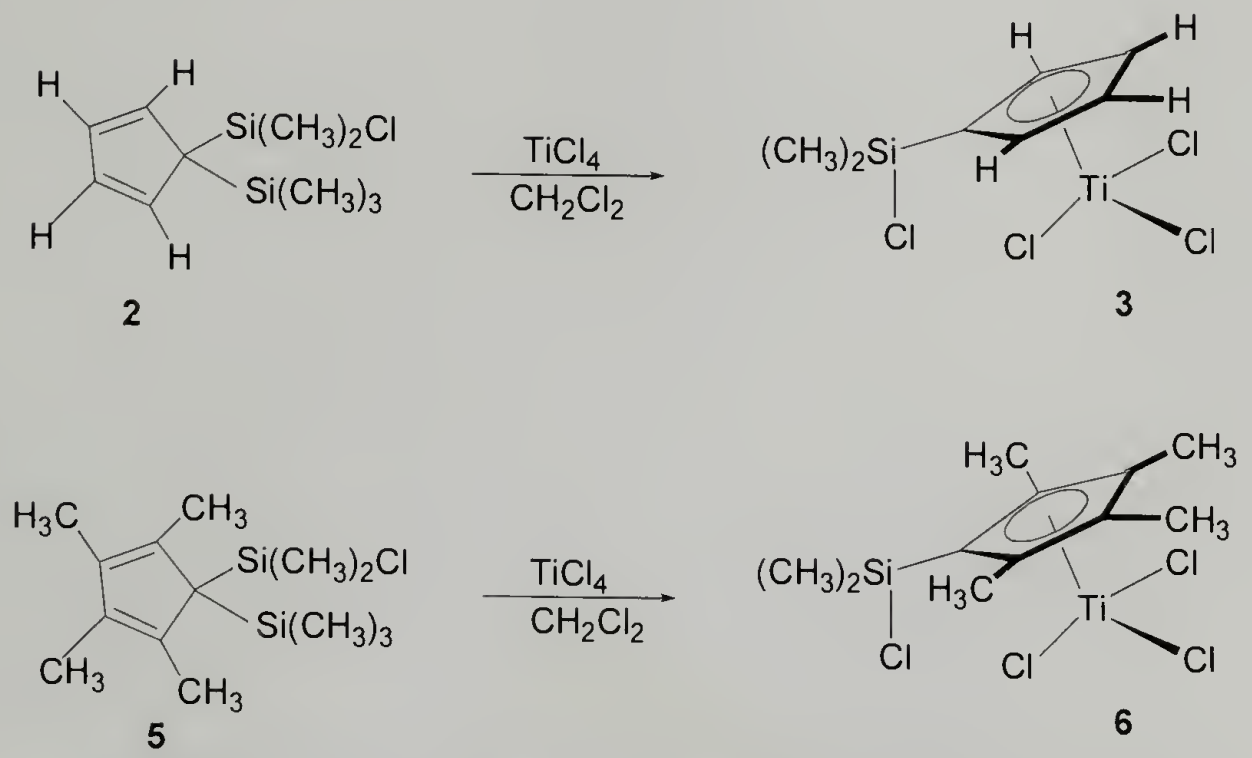

Figure 2.8 Silyl Elimination Chemistry of Mixed Silyl Cyclopentadienyl Congeners with MCl_4: Elimination from **2** with $TiCl_4$ (Top), Elimination from **5** with $TiCl_4$ (Bottom)

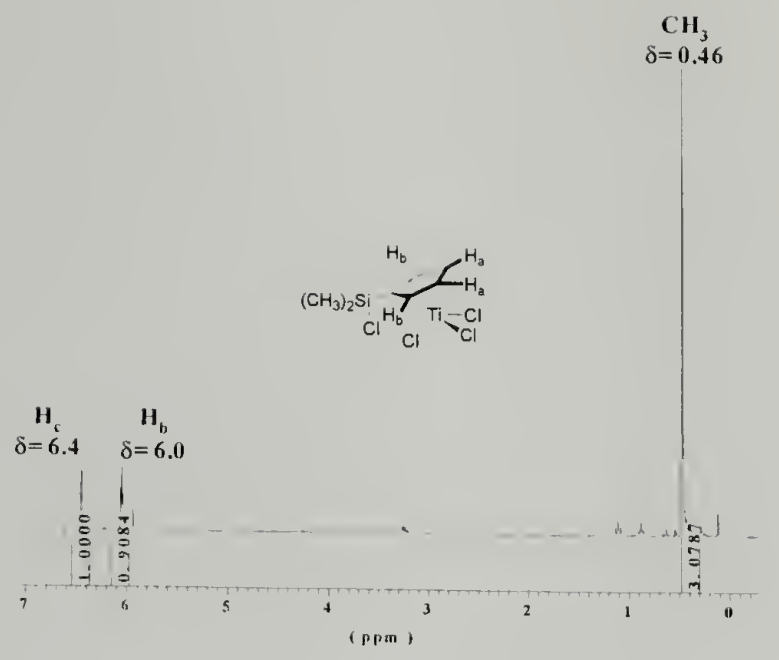

Figure 2.9 ^{1}H NMR of 1-chlorodimethylsilyl-cyclopentadienyltitanium trichloride (**3**) in CD_2Cl_2

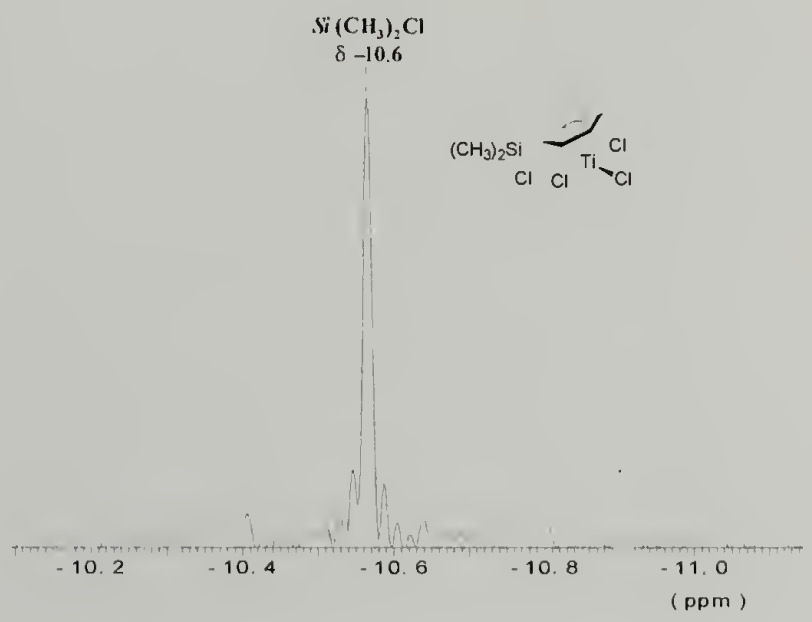

Figure 2.10 Solution ^{29}Si NMR of **3**

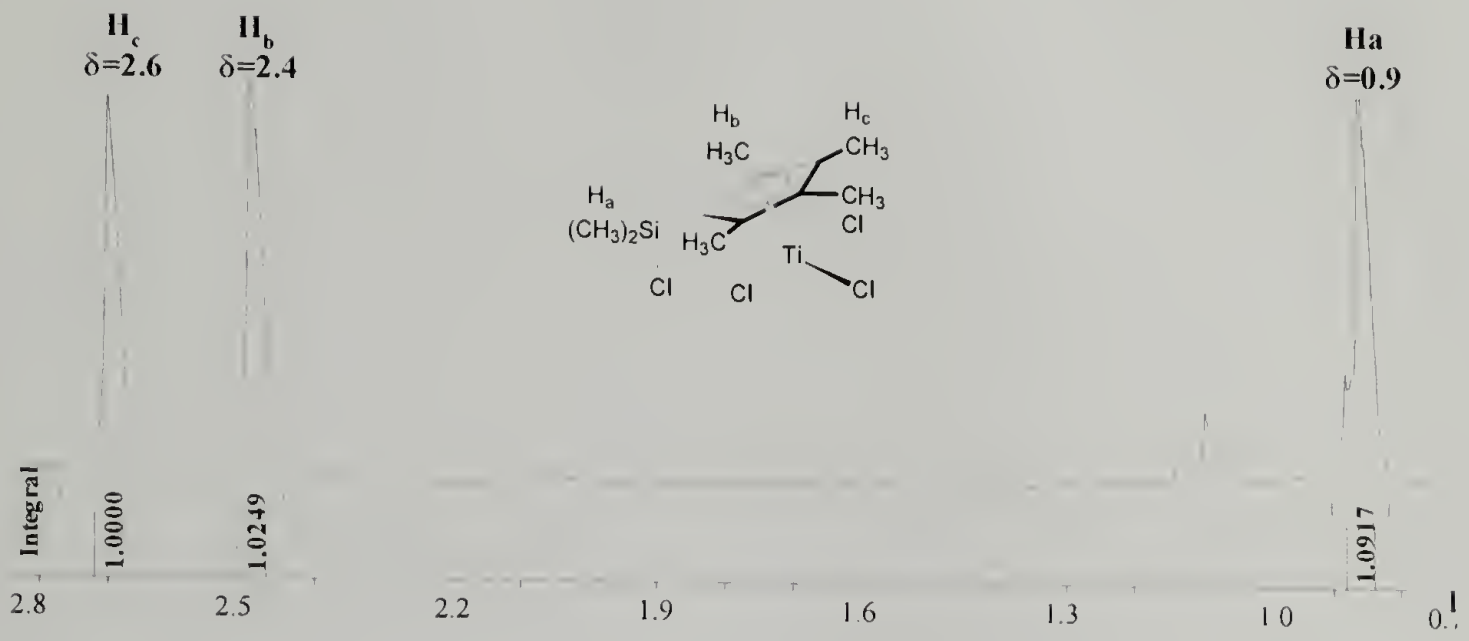

Figure 2.11 ^{1}H NMR of 6 in CD_2Cl_2

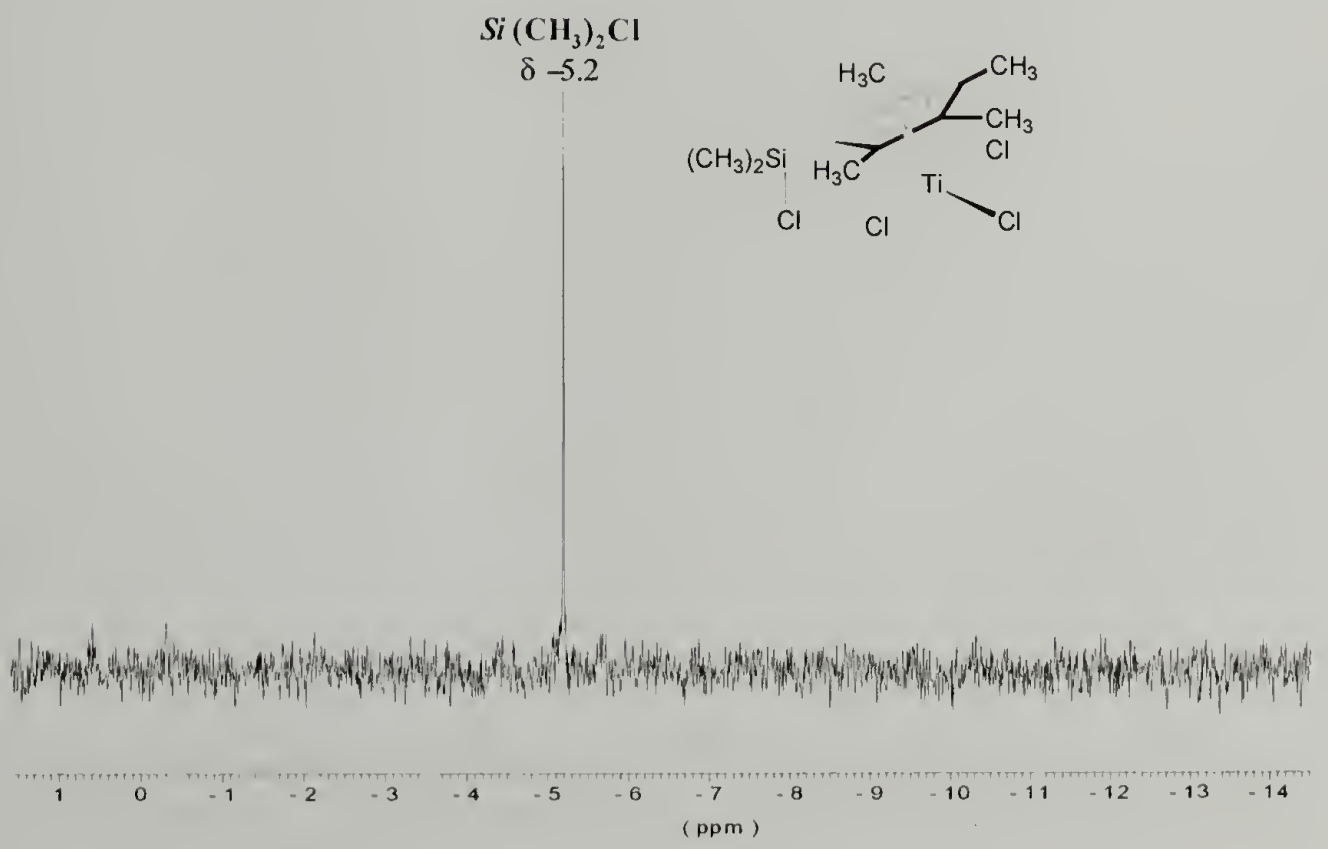

Figure 2.12 Solution ^{29}Si NMR of **6** in CD_2Cl_2

Compound **5** on treatment with $ZrCl_4$ in toluene at 100°C for 3 days resulted in the formation of both the piano-stool complex (**7a**) and the zirconocene (**7b**) in a 60: 40 ratio, as determined from the ^1H NMR resonances for the $Si(CH_3)_2Cl$ units at δ0.71 and δ0.32, respectively (Figure 2.13, Top). The solubility of **7a** and **7b** in toluene, benzene or dichloromethane was poor and consequently ^{13}C NMR could not be performed. Mass spectral data shows the presence of the molecular ion peak of the half sandwich complex (**7a**) at m/z of 407.9038 and the base peak in the isotopic distribution was observed at m/z 409.9038. The experimental and theoretical molecular envelopes match with the appropriate isotopic distributions. The molecular ion peak of **7b** was not observed, andinstead the mass spectrum signal at m/z 187.0095 presumably results from the intramolecular elimination of $Cl(CH_3)_2SiSi(CH_3)_2Cl$ from **7b**.

The chemoselectivity observed in the silyl elimination of **5** with $TiCl_4$ in dichloromethane results in the formation of **6**, and the reaction did not proceed beyond the half sandwich complex even under forcing conditions. The mass spectrum of **6** has a fragmentation pattern similar to that of **ii**, and the most intense fragment in each spectrum is the result of elimination of $TiCl_4$ from the molecular ion. On the other hand, when the reaction of equimolar **5** and $ZrCl_4$ in toluene with heating was performed, the outcome of this reaction was the chemoselective elimination of $(CH_3)_3SiCl$, as confirmed by the ^1H NMR spectrum using the resonance for ($CH_3(\alpha)$) and ($CH_3(\beta)$) as internal standards. However, the reaction does not stop at the formation of the piano stool complex **7a**; rather it undergoes a double insertion to afford the metallocene **7b**. The insertion of the

second mixed silyl cyclopentadienyl congener proceeds at a rate comparable to that of the formation of complex **7a** and results in a 60:40 mixture of **7a** and **7b** respectively.

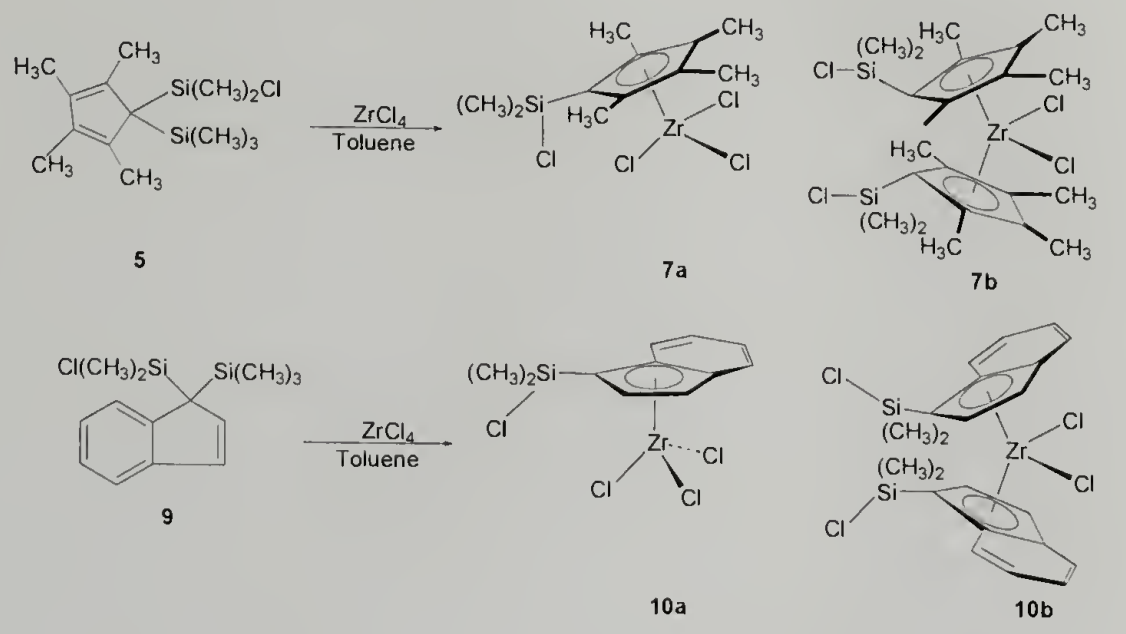

Figure 2.13 Silyl Elimination Chemistry of Mixed Silyl Cyclopentadienyl Congeners with MCl_4: Elimination from **5** with $ZrCl_4$ (Top) and Elimination from **9** with $ZrCl_4$ (Bottom)

Similar to a previous literature report, silyl elimination was not observed in the reaction of **9** with $TiCl_4$ under a range of reaction conditions.[57] On the other hand, **9** undergoes silyl elimination reactions on treatment with $ZrCl_4$ in toluene at 100°C for 3 days. The chemoselectivity in this case also followed the trend of elimination of $(CH_3)_3SiCl$ from **5**, as confirmed from both the ^1H NMR and the mass spectral data. However, double insertion was also observed, which resulted in the formation of both piano stool complex (**10a**) and metallocene (**10b**) as seen by ^1H NMR which displays resonances for the $Si(CH_3)_2Cl$ units of **10a** and **10b** at δ0.56 and at δ0.47, respectively, in a 50:50 ratio. Mass spectral data shows the presence of the molecular ion peak of the half sandwich complex **10a** at m/z of 401.8518, and the base peak in the isotope distribution was observed to be 403.8619 with an appropriate isotopic distribution in the molecular

envelope. The molecular ion peak of the metallocene was not observed, and instead the mass peak at m/z 460.8612, which is attributed to removal of 2 units of $(CH_3)_2Si$ from M^+ of **10b**. The peak at m/z 228.1017 was attributed to the removal of 2 units of $(Me_2Si))ZrCl_4$ from the molecular ion of M^+ of **10b**.

Table 2.1 Characterization Data for Cyclopentadienyl Analogs (Compounds **1**, **2**, and **3**)

Compound (Formula)	NMR	HR-MS
1 ($C_5H_{14}Si$) 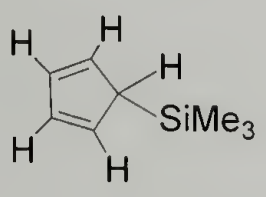	^{1}H NMR: δ0-0.29 (m, 9H, Si(CH_3)$_3$, presence of isomers), 3.0-3.5 (m, 1H, ipso-*H*, presence of isomers), 5.7-6.9 (m, 4H, C_5H_4, presence of isomers).	n.d.
2 ($C_{10}H_{19}Si_2Cl$) 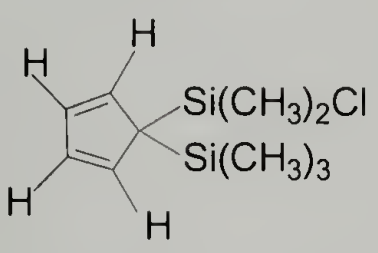	^{1}H NMR: δ0.0(m, 9H, Si(CH_3)$_3$, presence of isomers), 0.3(m, 6H, Si(CH_3)$_2$Cl, presence of isomers), 6.2–6.8(m, 4H, C_5H_4, presence of isomers)	n.d.
3 ($C_7H_{10}SiTiCl_4$) 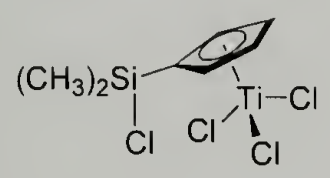	^{1}H NMR: δ0.46 (s, 6H, Si(CH_3)$_2$Cl), 6.0 (m, 2H, Cp-*H*) and 6.3 (m, 2H, Cp-*H*) ^{29}Si NMR (Solution): δ –10.2	Observed (m/z 311.8743)

Table 2.2 Characterization Data for Tetramethylcyclopentadienyl Analogs (Compounds **4**, **5**, **6**, **7a** and **7b**)

Compound (Formula)	NMR	Elemental Analysis	HR-MS
4 ($C_{12}H_{21}Si$) 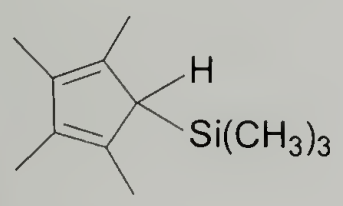	^{1}H NMR: δ0.03 (s, 9 H, $Si(CH_3)_3$,),1.88 (s, 6 H, Cp-$CH_3(\alpha)$) 1.97 (s, 6 H, Cp-$CH_3(\beta)$), 2.75 (Cp–*H*, attached to the ipso carbon)	Calculated ($C_8H_{14}Si$, C(74.0), H(11.3)); Observed (C (74.18), H(11.47))	n.d.
5 ($C_{14}H_{27}Si_2Cl$) 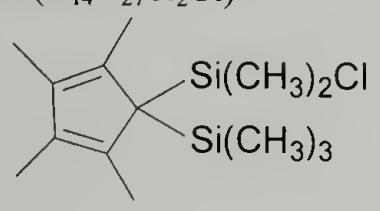	^{1}H NMR: δ0.01 (s, 9 H, $Si(CH_3)_3$), 0.19 (s, 6 H, Si $(CH_3)_2Cl$), 1.82 (s, 6 H, Cp-$CH_3(\alpha)$) and 2.03 (s, 6 H of Cp-$CH_3(\beta)$)	Calculated ((C (58.64), H (9.4)); Observed (C (58.82), H (9.75))	n.d
6 ($C_{11}H_{18}SiTiCl_4$) 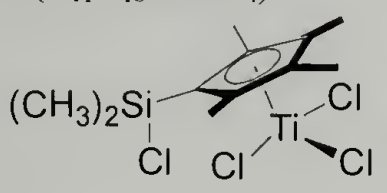	^{1}H NMR: δ0.9 (s, 6 H, Si $(CH_3)_2Cl$), 2.38 (s, 6 H, Cp-$CH_3(\alpha)$) and 2.59 (s, 6 H, Cp-$CH_3(\beta)$) ^{29}Si NMR (Solution): δ -5.0	Calculated (C (35.96), H (4.9); Observed (C(35.83), H (4.65)	Observed (m/z 367.9249)
7a ($C_{11}H_{18}SiZrCl_4$) and **7b** ($C_{22}H_{36}Si_2ZrCl_4$) 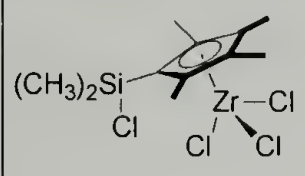 **7a** 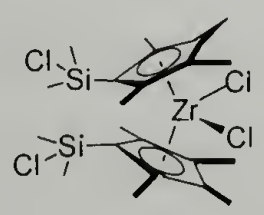 **7b**	^{1}H NMR of **7a**: δ0.71 (s, 6 H, $Si(CH_3)_2Cl$), 1.95 (s, 6 H, Cp-$CH_3(\alpha)$) and 2.11 (s, 6 H, Cp-$CH_3(\beta)$) ^{1}H NMR of **7b**: δ0.32 (s, 12H, $Si(CH_3)_2Cl$), 1.72 (s, 12H, Cp-$CH_3(\alpha)$) and 1.83 (s, 12H, Cp-$CH_3(\beta)$).	n.d.	Observed (m/z 409.9038 (base peak in the isotope distribution of 7a), 281.9047(M^+ of **7b**-ZrCl, 100%), 187.0095 (M^+ of **7b**-(2(Me_4Cp)$ZrCl_2$))

Table 2.3 Characterization Data for Indenyl Analogs (Compounds **8**, **9**, **10a** and **10b**)

Compound (Formula)	NMR	Elemental Analysis	HR-MS
8 ($C_{12}H_{16}Si$) 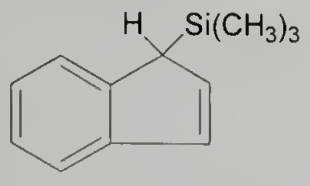	^{1}H NMR: δ-0.01-0.27 (m, 9 H, Si(C*H*$_3$)$_3$), 3.56 (s, 1 H, C-*H*, allylic), 6.70 (d, 1 H, C-*H* olefinic, J=6 Hz), 6.90 (d, 1 H, C-*H* olefinic, J=6 Hz), 7.00- 7.60 (m, 4 H, aromatic, C-*H*).	Calculated (C(76.59), H(8.51)); Observed (C(76.69), H(8.61))	n.d.
9 ($C_{14}H_{21}Si_2Cl$) 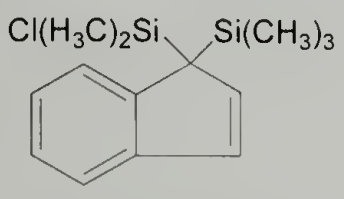	^{1}H NMR: δ0.10-0.16 (m, 9 H, Si(C*H*$_3$)$_3$), 0.19-0.36 (m, 6 H, Si(C*H*$_3$)$_2$Cl), 6.73-6.88 (dd, 1 H, J=1.68, 5.07Hz), 7.09-7.16(dd, 1 H, J=1.50, 5.28), 7.20-7.40 (m, 2 H), 7.30-7.70 (m, 2 H)	n.d	Peak with the m/z of 280.00 and appropriate isotope distribution
10a ($C_{11}H_{12}SiZrCl_4$) + **10b** ($C_{22}H_{24}Si_2ZrCl_4$) 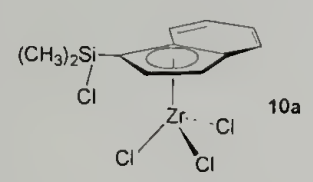 10a 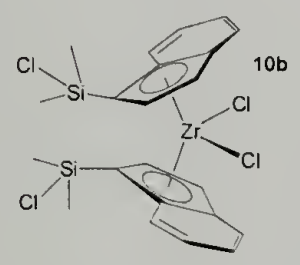 10b	^{1}H NMR: δ0.49 (s, 6 H, Si(C*H*$_3$)$_2$Cl), 10a), 0.38 (s, 12 H, Si(C*H*$_3$)$_2$Cl, **10b**), 7.12-7.52(m, 18 H, aromatic, **10a** and **10b**).	n.d.	Observed (m/z 403.8619(Base peak in the isotope distribution of 10a), 460.8612 (M^+ of **10b**-2(Me_2Si), 10%), 228.1017(M^+ of **10b**-(2(Me_2Si))$ZrCl_4$), 20%))

2.4 Summary

In summary, competitive silyl elimination for the mixed silyl complexes **3**, **5**, and **9** with both $TiCl_4$ and $ZrCl_4$ proceeds with chemoselective elimination of $(CH_3)_3SiCl$ if any reaction occurs at all. Silyl elimination chemistries with $TiCl_4$ proceed cleanly for the exclusive formation of **4** or **6** with the cyclopentadienyl analogs, whereas with the fused aromatic precursors silyl indenes (**9**), no reaction occurs. However, in the silyl elimination reactions of **5**, or **9**, with $ZrCl_4$, the rate of double insertion is comparable to that of piano-stool complex formation, leading to the observed mixture of products. The as prepared samples of silyl substituted zirconium piano stool complexes and metallocenes are soluble in the reaction solvent until the solvent is removed. After which they have much lower solubilities in non-polar solvents due to the formation of oligomeric networks.[65] The reactivity differences between $TiCl_4$ and $ZrCl_4$ may be attributed to the difference in the size of the metal and the Lewis acidity of the metal centers.

Complexes **3** and **6** can be used as precursor catalysts for the assembly of CGCs on amine-functionalized matrices. The catalysts assembly protocols on aminomethylpolystyrene (AMPS) and amine-functionalized silica matrices will be discussed in Chapters 3 and 4, respectively. These supported catalysts have been tested for olefin polymerization.

CHAPTER 3

SUPPORTED CONSTRAINED GEOMETRY CATALYSTS ON CROSSLINKED AMINOMETHYLPOLYSTYRENE: STUDIES OF ETHYLENE AND OCTENE COPOLYMERIZATION

3.1 Introduction

Commercial polymerization processes using soluble SSCs are utilized to synthesize elastomers and low crystallinity polyolefins that remain soluble throughout the polymerization process. In gas phase, slurry, or bulk polymerization, the polyolefin produced is insoluble in the fluidizing gas or reactor diluent or fluid. Therefore, in order to operate in a continuous process, catalyst particles of uniform size and shape need to be fed continually into the reactor, which makes it necessary to support the catalyst on an insoluble solid matrix.[5,53] Metallocenes have been supported on organic, typically polymeric, and inorganic materials. Cyclopentadienyls that contain silyl moieties have been used as anchoring points for metallocene complexes on silica supports. In general, the polymerization activity of these supported metallocenes has not been as high as the corresponding homogeneous systems.[52] Interestingly, polyolefins of ultra-high molecular weight and increased crystallinity have been observed when metallocene supported systems have been utilized.[47,50] In contrast to the large number of studies that correlate the structure of metallocene or CGC to the resulting catalyst performance and resulting polymer properties, the systematic investigation of heterogenized CGCs is not nearly as comprehensive.[66-69]

Adaptation of the assembly protocol of Royo [61] to the use of primary amine functionalized solid supports with precursors catalysts should provide a synthetic route to

CGCs. Towards this goal, (chlorodimethylsilyl)trimethylsilyl derivatives of cyclopentadienes have been synthesized, and the silyl elimination chemistries with $TiCl_4$ or $ZrCl_4$ to provide precursor catalysts have beeninvestigated, as discussed in Chapter 2. The reaction of the precursor catalysts **3** or **6** with aminomethypolystyrene (AMPS) should afford supported CGCs. The immobilized CGC have been investigated for ethylene homopolymerization and ethylene and 1-octene copolymerization (production of LLDPE). The physical properties of ethylene homopolymerization and copolymers are then used to determine the influence of the polystyrene matrix (second sphere of influence) on the reactivity of the cationic metal center and consequently on the properties of the polyolefins produced.

3.2 Experimental Section

3.2.1 Reagents and general techniques

All reactions were performed under nitrogen in Schlenk glassware or in an inert atmosphere dry box. Dry, pure, air-free solvents were obtained from a solvent manifold.[64] Complexes **3** and **6** were synthesized as discussed in Chapter 2. Crosslinked aminomethylpolystyrene (AMPS, 1.29 wt% of N, 0.928 mmol of N/g of support, 1% crosslinking) beads were obtained from Polymer Labratories Inc. Polymerization was performed using an ethylene/propylene manifold and thick-walled reactors.[70] Methylaluminoxane (4.77M, 30 wt% in toluene, MAO), tris(pentafluorophenyl)borane ($(B(C_6F_5)_3$, **I**) , N,N-dimethylanilinium borate ($[(C_6H_5N(CH_3)_2H][B(C_6F_5)]_4$, **III**) and trityl borate ($[(C_6H_5)_3C][B(C_6F_5)]_4$, **II**) were obtained from Albemarle and were used as received.

3.2.2 Instrumentation

Solid State ^{29}Si NMR was recorded at 75 MHz on a Bruker DSX 300 using Magic Angle Spinning (MAS) and Cross Polarization (CP) in a 7mm rotor at a spinning rate of 3000 Hz. Elemental analysis was performed using three Exeter Analytical Inc. 240XA CHN analyzers and a Leeman Labs Inc. Dual View DRE Sequential ICP was used to analyze the Ti and Si content of the samples. Gel Permeation Chromatography of the polyolefins was performed with Polymer Laboratories PL-220 high temperature GPC equipped with a Wyatt MiniDawn (620 nm diode laser) high temperature light scattering detector and refractive index detector at 135°C using 1,2,4-trichlorobenzene as solvent. The dn/dc value for polyethylene used was -0.11. Quantitative solution ^{13}C NMR of the polyolefins were recorded at 150 MHz using AVANCE DPX 600 in continuously proton decoupled mode with a delay time of 8 seconds. Thermal analysis was performed using TA DSC 2910 equipped with a liquid nitrogen cooling accessory unit under a continuous nitrogen purge (50mL/min). Data reported were gathered for the first and second melt with a heating and cooling scan of 10 °C/min.

3.2.3. Synthesis of Complex AMPS-Ti-11

To a slurry of AMPS copolymer (1 g of AMPS, 1.3 wt% of N, 0.928 mmol of N/g of support) in toluene, 74 mg (0.247 mmol) of complex **3** was added and the solution was stirred at 80°C for 3 days. The support was then washed with dichloromethane and toluene mixture (1:4 v:v) numerous times and the supported catalyst was recovered, vacuum dried overnight at 60°C afforded 0.8 g of yellow powder.

Elemental Analyses (observed): C (80.10%), H(7.95%), N(1.79%), Ti (2.10%), Cl

(6.29%), Si (1.4%)

^{29}Si NMR (CP-MAS): δ -10.8, δ -20.5

3.2.4 Synthesis of Complex AMPS-Ti-12

To a slurry of AMPS copolymer (1 g, 1.3 wt% of N, 0.928 mmol of N/g of support) in toluene, 90.82 mg (0.23 mmol) of **6** was added and the solution was stirred at 80°C for 3 days. The supported catalyst was then washed with dichloromethane toluene mixture (1:4 v:v) numerous times and the support was recovered and vacuum dried at 50 °C overnight and afforded 0.9 g of yellow orange powder.

Elemental Analyses (observed): C (82.71%), H (7.38%), N(1.21%), Ti (1.5%), Cl (4.76%), Si (1.0%)

^{29}Si NMR (CP-MAS) : δ -19.6

3.2.5 Representative Polymerization of Ethylene

To a mixture of 10 mL of toluene and 1.0 mL of 30% MAO taken in a polymerization reactor along with a stir bar, 25.3 mg of **AMPS-Ti-11** was added and pressurized with 60 psig of ethylene for 2 hours at room temperature with constant stirring. After 2 hours, the ethylene supply was stopped and the reactor was vented to remove excess ethylene. The reaction mixture was quenched by the addition of 250 mL of 10% by volume of hydrochloric acid in methanol mixture and the polyethylene was filtered out and dried in a vacuum oven overnight to afford 900 mg of polyethylene (Table 3.2, Entry 3).

3.2.6 Representative Copolymerization of Ethylene and 1-Octene

To a mixture of 10.0 mL of toluene and 1.0 mL of MAO in a polymerization reactor, 112.9 mg of **AMPS-Ti-11** was added. To this system was added 1-octene (5 mL) and

ethylene at a pressure of 60 psig was supplied for 2 hours at room temperature with constant stirring. The ethylene supply was stopped and the reactor was vented to remove excess ethylene, the reaction mixture was quenched with 10% by volume hydrochloric acid in methanol, and the polymer was collected by filtration and dried in a vacuum oven overnight to afford 315 mg of product (Table 3.2, Entry 4).

3.3 Results and Discussions

3.3.1 Synthesis of Supported Constrained Geometry Catalysts on Aminomethylpolystyrene

The silyl elimination of **2** and **5** with $TiCl_4$ results in the chemoselective elimination of $(CH_3)_3SiCl$ and exclusive formation of complexes **3** and **6**, respectively as discussed in Chapter 2. However, this not an efficient preparative route to the piano stool complex (chlorodimethylsilyl)tetramethylcyclopentadienyl zirconium trichloride.

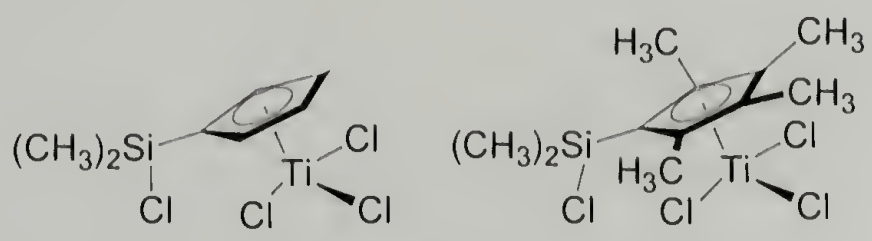

3 **6**

Figure 3.1 Precursor Catalysts **3** and **6**

The titanium precursor catalysts **3** or **6** (Figure 3.1), have been treated with crosslinked amino methyl polystyrene (AMPS, 1% crosslinking, 1.3 wt% N, 0.928 mmol of N/g of support). The mole ratio of amine content of the support to precursor catalysts was selected to be 3:1. The first amine equivalent of AMPS serves as the primary amine for the assembly of the CGC framework, and the other two equivalents serve to scavenge

the two equivalents of HCl generated. The reaction of the precursor catalysts with swollen AMPS resin in hot toluene was allowed to proceed for 3 days, followed by numerous toluene washings to remove soluble by-products and any residual precursor catalyst. The supports were then dried *in vacuo* at room temperature for 12 hours to afford CGC complexes **AMPS-Ti-11**, or **AMPS-Ti- 12**, respectively (Figure 3.2).

^{29}Si NMR of **AMPS-Ti-12** shows the presence of a single silicon resonance at δ -19.6, while the precursor complex has a single silicon resonance at δ -5.2. The presence of the peak at δ -19.7 and this is attributed to the completely assembled CGC, based on literature precedent (Figure 3.3, Trace B).[71] The elemental analyses showed the ratio of Ti:Si:Cl to be 1:1:4, and the ratio of N:Ti to be 3:1, which indicates that the efficiency of precursor loading is quantitative. Moreover, the complete assembly of the CGC framework is indicated by the single ^{29}Si resonance and the absence of partially tethered piano stool complex is also noted from the ^{29}Si NMR spectrum.

On the other hand, ^{29}Si NMR of **11** showed the presence of two silicon resonances. The resonance at δ –20.5 is attributed to the assembled CGC, and the resonance at δ –10.8 can be attributed to a species bearing the chlorodimethylsilyl moiety, which is presumably not the precursor catalyst **3** but rather a titanium amide complex. The elemental analyses showed the ratio of Ti:Si:Cl to be 1:1:4, and the ratio of N:Ti was found to be 3:1. The loading efficiency of the precursor is quantitative based upon both the results from elemental analysis. However, the assembly of the CGC is incomplete as seen, from the ^{29}Si NMR spectrum, which shows resonances that can be attributed to the presence of the CGC and to the partly tethered piano stool complex (Figure 3.4, Trace B).[71]

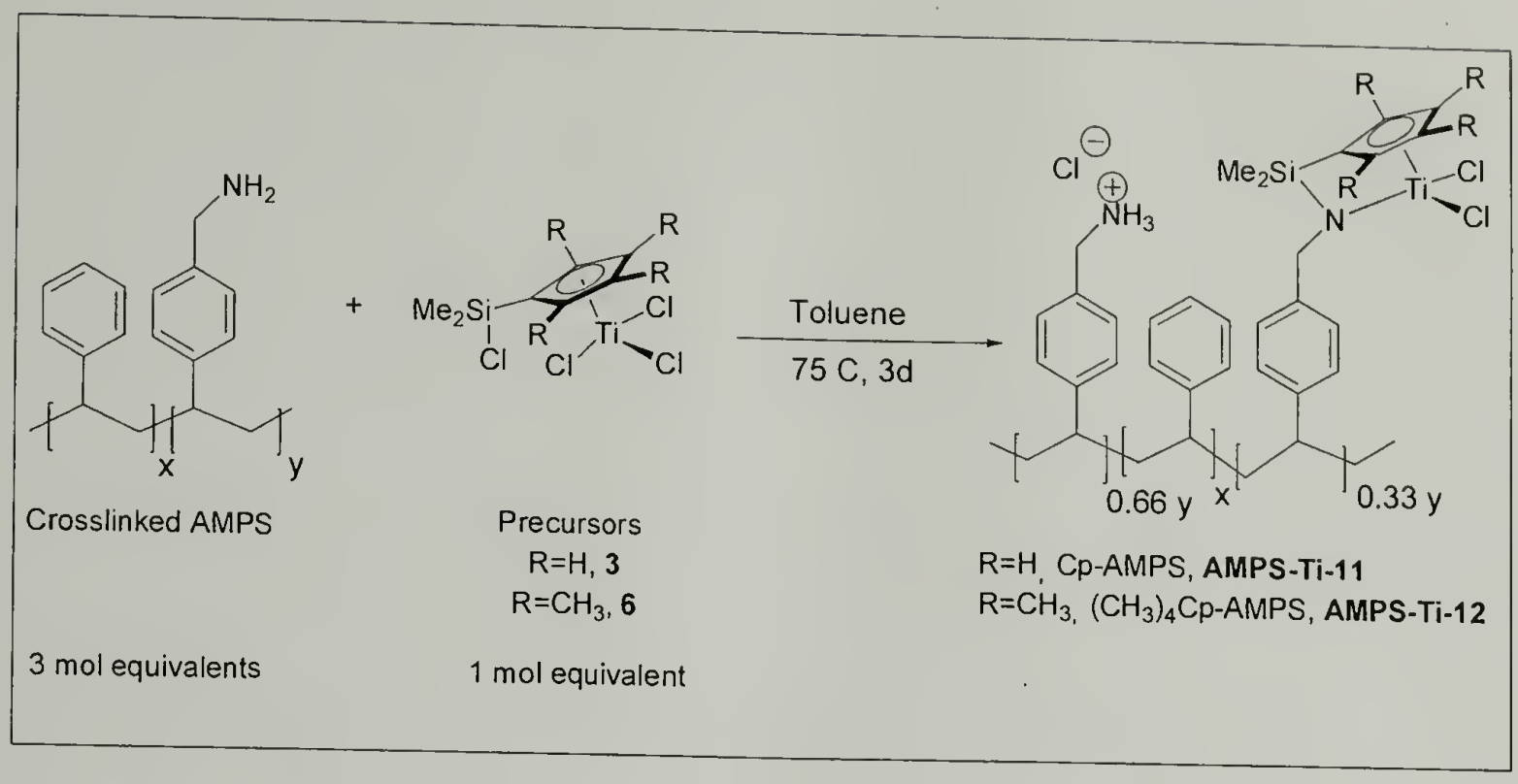

Figure 3.2 Assembly of Constrained Geometry Catalysts (CGCs) on Aminomethylpolystyrene (AMPS)

Table 3.1 Characterization of Supported CGCs (**AMPS-Ti-11** and **AMPS-Ti-12**) Assembled on Aminomethylpolystyrene (AMPS)

Structure of Supported Catalysts	^{29}Si (CP-MAS) NMR 3000Hz	Elemental Analysis (wt%)
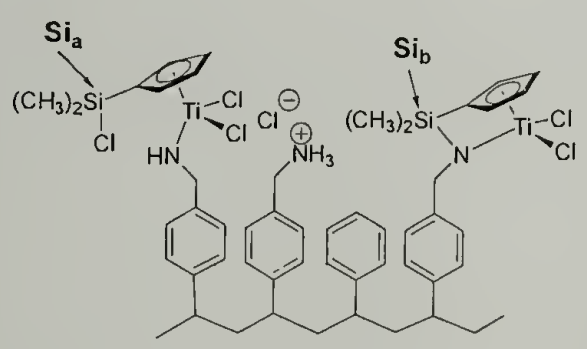 Compound **AMPS-Ti-11**	δ -10.8 (Si_a), δ -20.5 (Si_b)	C (80.10%), H(7.95%), N(1.79%), Ti (2.10%), Cl (6.29%), Si (1.4%)
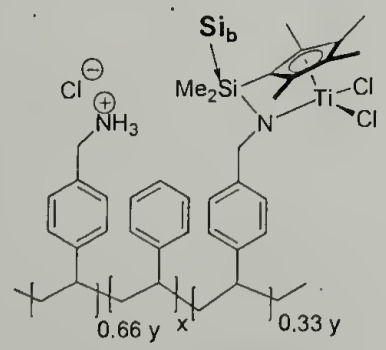 Compound **AMPS-Ti- 12**	δ -19.6 (Si_b)	C (82.71%), H (7.38%), N(1.21%), Ti (1.5%), Cl (4.76%), Si (1.0%)

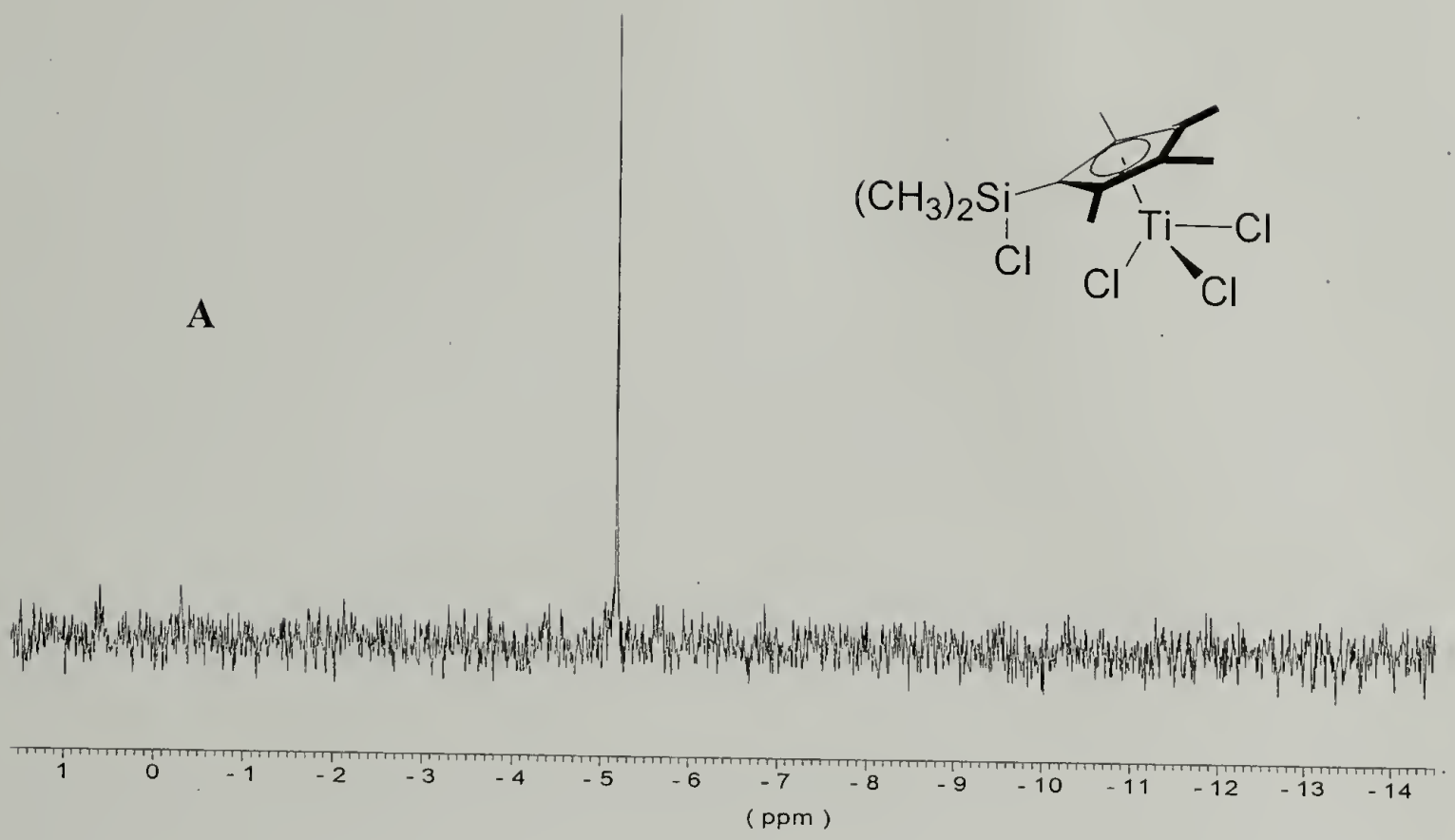

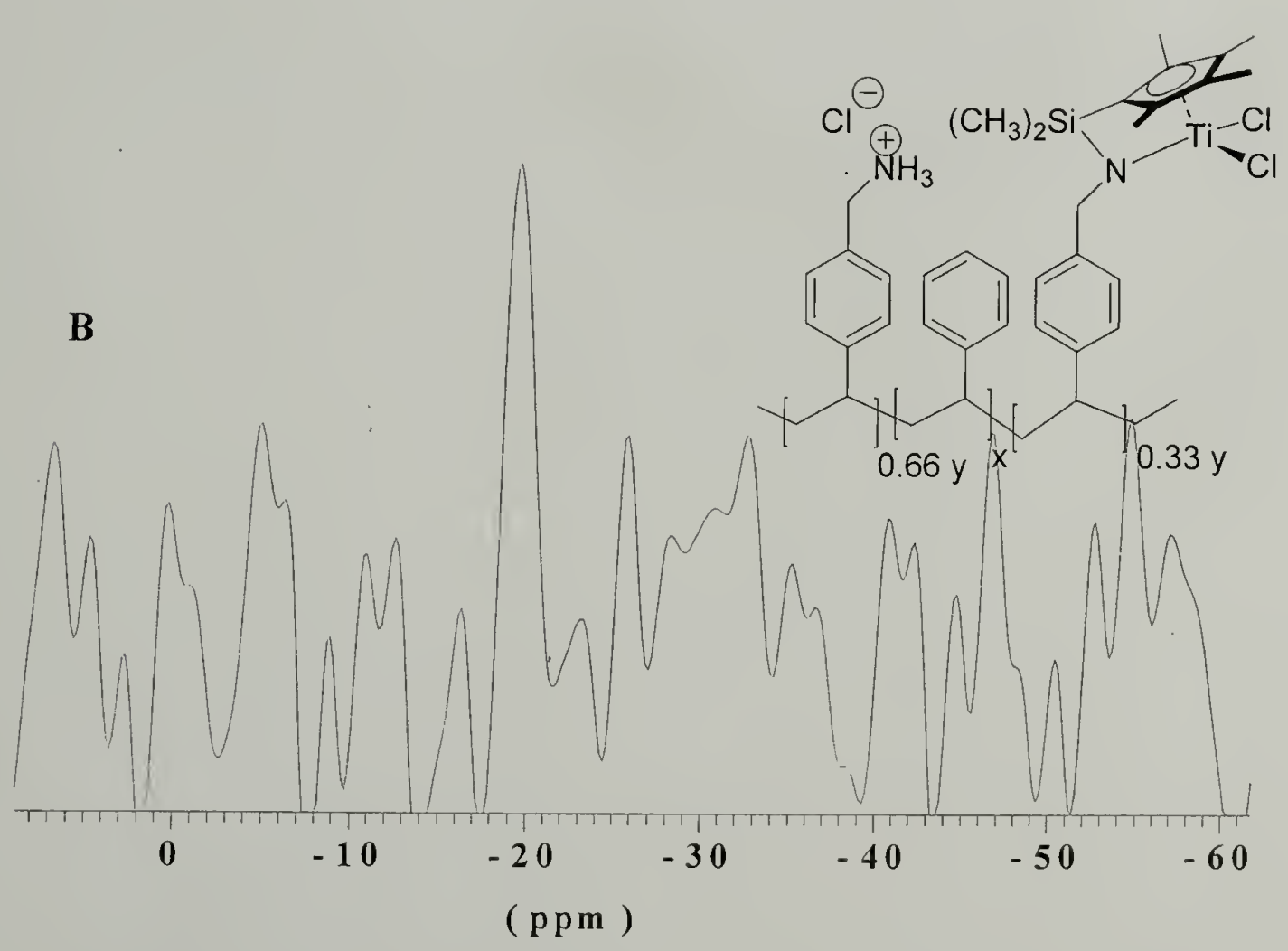

Figure 3.3 ^{29}Si NMR of Precursor Catalyst (**6**, Solution NMR, A) and CGC Assembled on AMPS (**AMPS-Ti-12**, Solid State NMR, CP-MAS, 3000Hz, B)

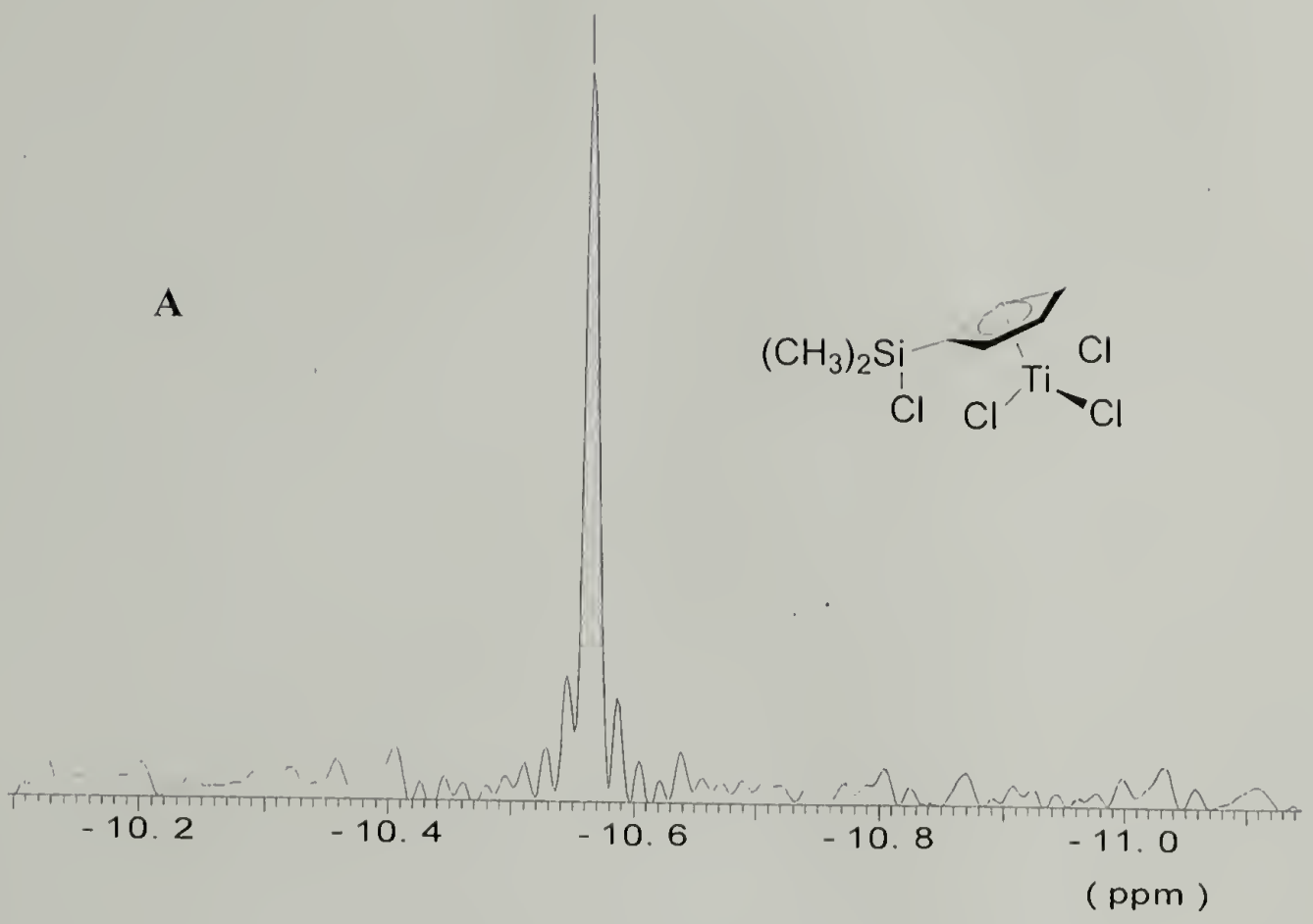

Figure 3.4 ^{29}Si NMR of Precursor Catalyst (**3**, Solution NMR, A) and CGC Assembled on AMPS (**AMPS-Ti-11**, Solid State NMR, CP-MAS, 3000Hz, B)

3.3.2. Ethylene Homo and Copolymerization using Complexes AMPS-Ti-11 and AMPS-Ti-12

The supported catalyst systems **AMPS-Ti-11** and **AMPS-Ti-12** were tested for ethylene and 1-octene polymerization. The cocatalyst used in these polymerization studies was MAO (30 wt % in toluene, 4.77 M). An excess of co-catalyst was used to activate the CGC and as well as to scavenge the ammonium salts formed during the supportation protocol. Olefin polymerizations were conducted by charging a mixture of 10.0 mL of toluene and 1.0 mL of 30% MAO (4.77 M) with a quantity of supported catalyst in a thick walled glass reactor vessel. The system was pressurized with 60 psig of ethylene for a suitable time period with constant stirring. For 1-octene copolymerization studies, the comonomer was added simultaneously with the ethylene by means of an additional cylinder. The ethylene over pressure was delivered into the reactor without the removal of the nitrogen atmosphere. At the end of the polymerization the ethylene supply was stopped and the reactor was vented. The reaction mixture was quenched by the addition of 10% by volume solution of hydrochloric acid in methanol; the polymer was isolated by filtration, and dried in a vacuum oven overnight. Experimental conditions, the yield of polymer, polymerization activity, molecular weights, and melting points of the polymers are listed in Table 3.2.

Table 3.2 Ethylene Homo and Copolymerization Using MAO as the Cocatalyst

Entry	Catalyst (mg)	Activity Kg/mol Ti.hr.atm C_2^-	Tm[c] (°C)	1-Octene in Polymer (mol%)[d]	M_w[e] G/mol	PDI[e]
1	**AMPS-Ti-12** (80.0) [b]	4.1	134.1	0	529200	1.58
2	**AMPS-Ti-12** (110.0)[a]	1.2	119.5, 135.3	2.2	611000	2.94
3	**AMPS-Ti-11** (25.3)[a]	10.1	135.5(PEa) 140.5(PEb)	0	200220 and 409000	2.09, 1.95
4	**AMPS-Ti-11** (112.9)[a]	0.8	125.6	1.9	172900	3.70
5	**3** (2.25)[a]	4.9	133	0	447550	2.67
6	**3** (2.25)[a]	5.1	134.9	0	n.d.	n.d.

C_2^- Ethylene monomer
[a] Ethylene pressure of 60 psig for 120 min
[b] Ethylene pressure of 60 psig for 45 min
[c] First melt of DSC scan
[d] Monomer incorporation calculated by depression in melting point and ^{13}C NMR
[e] Determined by GPC using LS detectors with a 690 nm laser at 135°C in 1,2,4-trichlorobenzene

3.3.3 Ethylene Homo and Copolymerization using AMPS-Ti-12 in Conjunction with MAO as the Cocatalyst

Using **AMPS-Ti-12** in conjunction with MAO in a toluene slurry under 4 atmospheres of ethylene pressure afforded polyethylene (Entry 1, Table 3.2), (Figure 3.5). Thermal analysis of the resulting polymer showed the presence of a unimodal melting peak for HDPE in both the first and second melt scans (DSC) with a final ΔH_f of 56.9 J/g.

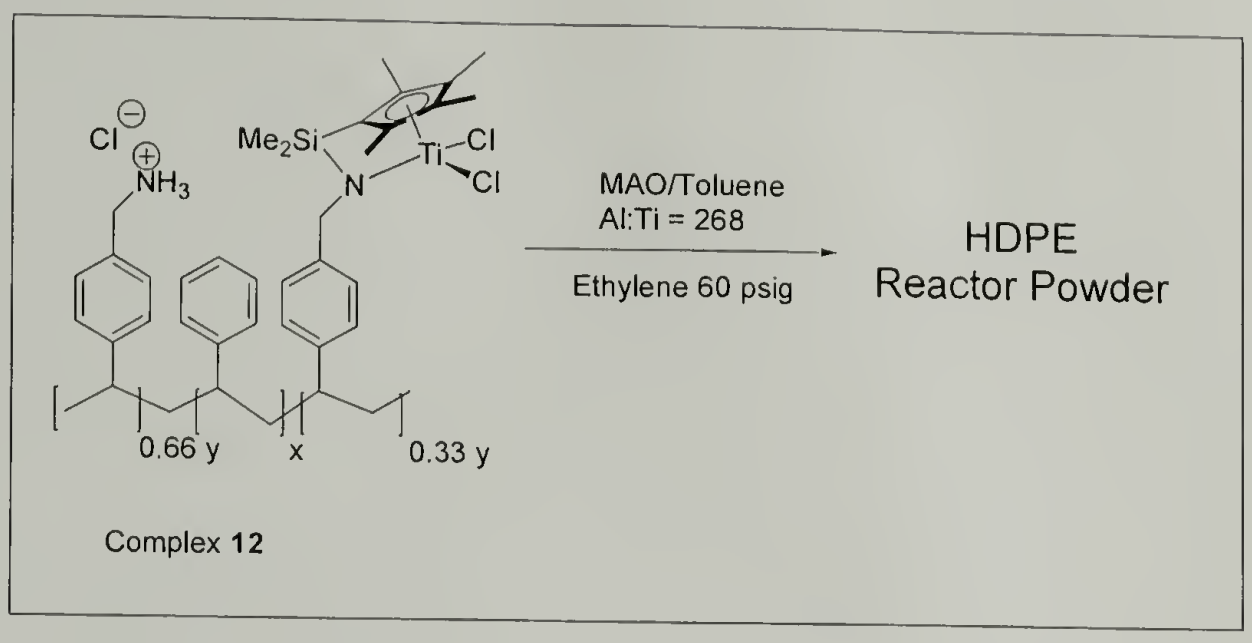

Figure 3.5 Ethylene Homopolymerization using **AMPS-Ti-12** with MAO

The percentage crystallinity of the polymer, which is the ratio of the heat of fusion of the sample to the heat of fusion of a perfect single crystal of polyethylene (293 J/g) was determined to be 20% (Figure 3.6). The degree of crystallinity of this sample is substantially lower than corresponding HDPE samples prepared using soluble CGC. Presumably, the support suppresses the crystallinity of the polymers as the polymer is being synthesized. The extent to which a support may influence the degree of crystallinty for polyolefins prepared via heterogeneous SSC at this moment is not known. Molecular weight analysis using GPC of the polymer gives M_w value of 529,000 g/mol and a PDI of 1.58. The response signals for both light scattering and refractive index detectors were unimodal (Figure 3.7). The physical characteristics of the polyethylene are fully consistent with the formation of HDPE from a SSC, presumably the heterogenized CGC **AMPS-Ti-12**. However, it is possible that during polymerization processes using this

supported catalyst in slurry mode fragmentation of cyclopentadienyl titanium moieties may occur. The resulting solubilized or fragmcnts would polymerize ethylene to HDPE. It is thus difficult to ascertain conclusively the form of the active catalyst, or catalysts, when conducting ethylene polymerization beginning with a heterogeneous SSC.

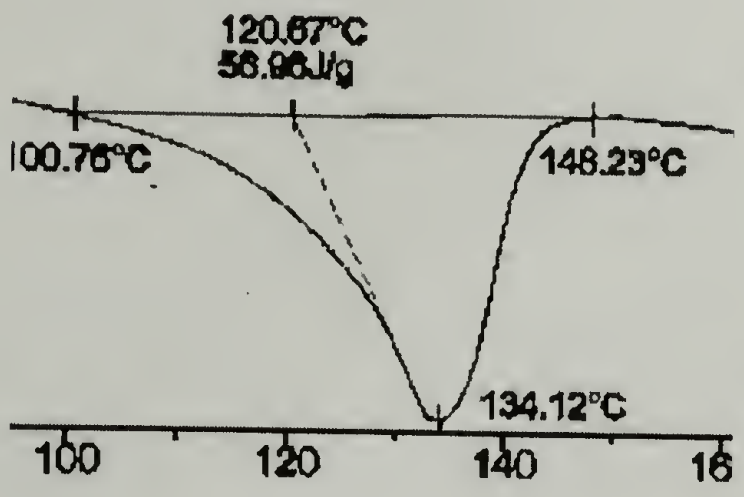

Figure 3.6 DSC Trace of HDPE Synthesized from **AMPS-Ti-12** with MAO

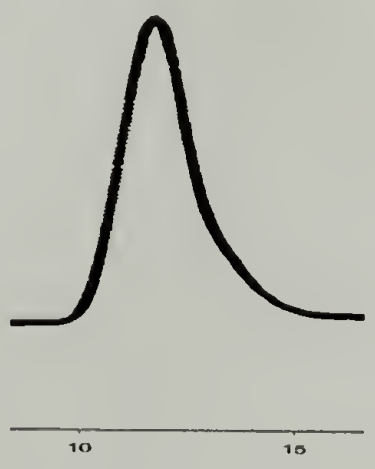

Figure 3.7 GPC Trace of HDPE Synthesized from **AMPS-Ti-12** with MAO

The demonstrated ability of CGCs to incorporate α-olefins during copolymerization with ethylenc provides a method for discerning between heterogenized CGCs and leachcd fragments. Ethylene 1-octene copolymerization was used to verify thc presence of an assembled CGC **AMPS-Ti-12** on the AMPS support (Table 3.2, cntry 2),

(Figures 3.8 and 3.9) and to probe for the presence of leached Ti species. Thermal analysis of the resulting polymer reveals two melting endotherms. The lower melting peak occurs at 119.45 °C and has been attributed to the incorporation of 1-octene units. The copolymer formed due to the incorporation of 1-octene is referred to as LLDPE. It is well documented that a depression in melting point occurs with incorporation of alpha-olefins in a random fashion.[72] The melting point has been correlated to the amount of comonomer incorporated into the HDPE and this was determined to be 2.2 mol% of 1-octene as determined by the depression in melting point of the copolymer through DSC (Figure 3.10) and ^{13}C NMR of the copolymer. A higher melting peak at 135.2 °C has been attributed to the formation of HDPE. This could be a consequence of an ethylene-only polymerization catalyst being formed by the abstraction of a titanium fragment by the action of MAO.

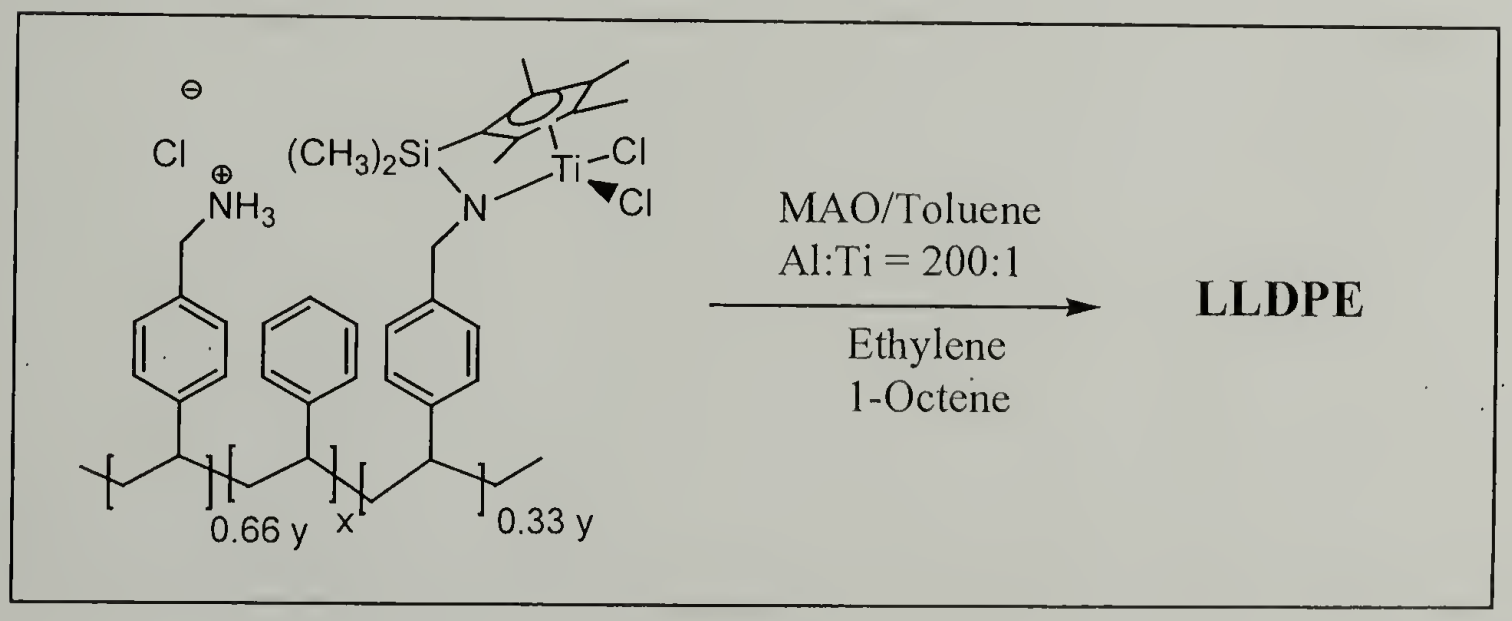

Figure 3.8 Ethylene and 1-Octene Copolymerization using **AMPS-Ti-12** with MAO

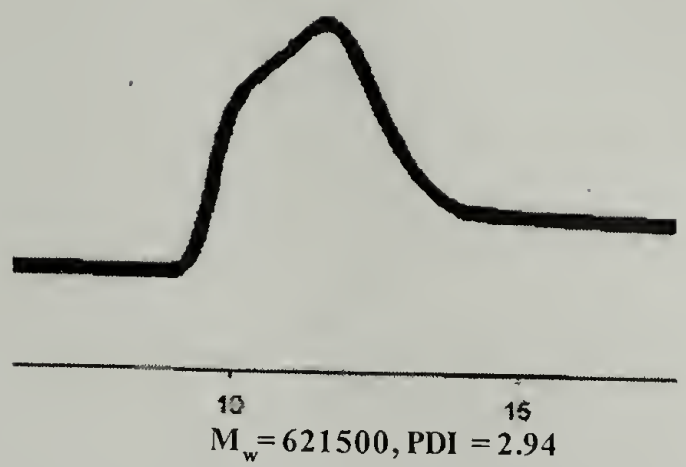

$M_w = 621500$, PDI $= 2.94$

Figure 3.9 GPC Trace of LLDPE Synthesized from **AMPS-Ti-12** with MAO

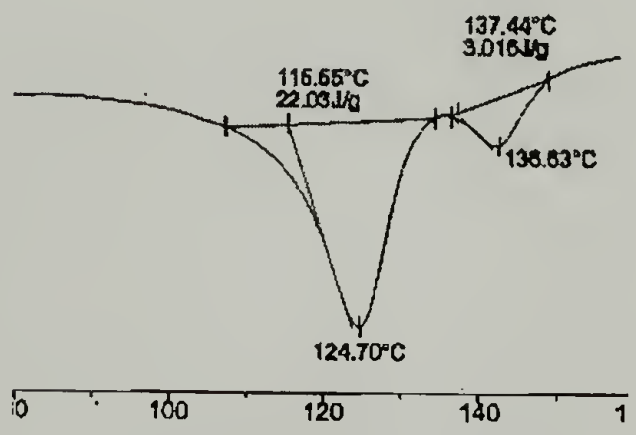

1-Octene incorporated =1.8 mol %

Figure 3.10 DSC Trace of LLDPE Synthesized from **AMPS-Ti-12** with MAO

The observed multi-modality of the DSC endotherms and broadening of GPC peaks that result from the copolymerization of ethylene and 1-octene is indicative of the presence of multiple catalysts being present during the reaction. In order to ascertain that the phenomena of leaching is the primary reason for the production of HDPE during copolymerization reaction with reaction times ranging from 20 min to 2h were performed (Table 3.3, entries 2, 8 and 9). The DSC and GPC analyses of the polymers were performed. The GPC traces show that there is a gradual increase in molecular weight of the polymer with a corresponding increase in the PDIs of the polymers. The increase in

the PDIs at longer reaction times can be attributed to the presence of multiple catalytic sites (Figure 3.11, Traces A, B and C). From DSC, it is observed that the initial formation of LLDPE continues throughout the course of reactions, and the formation of HDPE is observed only at longer reaction times (Figure 3.12, Traces A, B and C). The action of MAO on the supported catalysts presumably leads to a leached Ti, which species that is selective for ethylene homopolymerization. The presence of polyethylene at longer reaction times is seen only after a critical concentration of leached species is present in the solution. On the other hand, precontacting **AMPS-Ti-12** with MAO followed by filtration and the use of the filtrate for ethylene homopolymerization and ethylene-octene copolymerization indicated low activity relative to the activity for the supported catalysts in ethylene polymerization (Figure 3.13, Control 1). Furthermore, the absence of 1-octene incorporation during the ethylene-octene copolymerization experiment using the filtrate is noted (Figure 3.13, Control 1). Another possible origin of the HDPE observed in the copolymerization experiments could be a result of diffusion limitation of 1-octene to a certain CGC sites within the crosslinked polystyrene bead. However, diffusion limitations of the comonomer to catalyst sites dispersed throughout the AMPS were eliminated using a surplus of 1-octene in a well stirred, solvent-comonomer swollen bead.

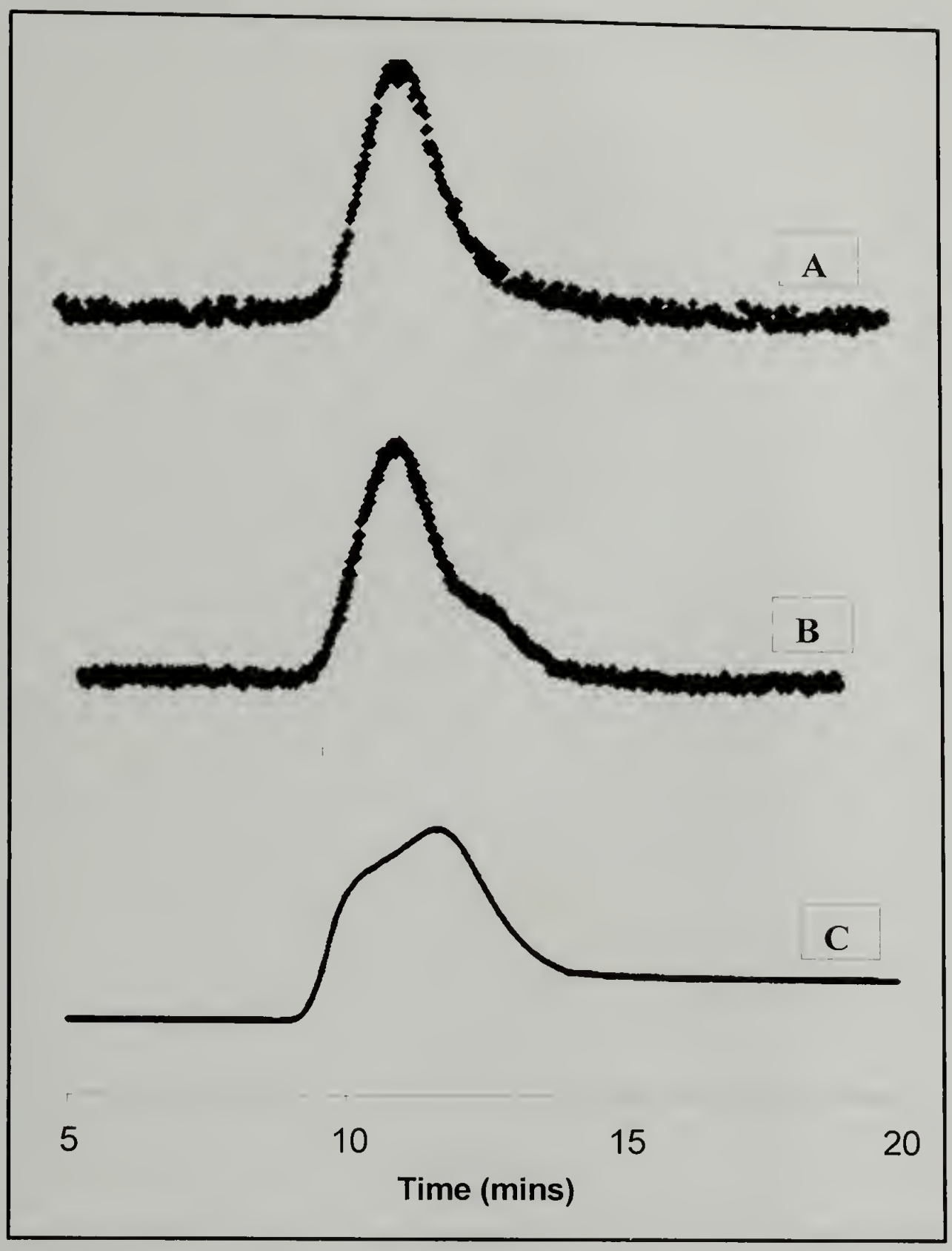

Figure 3.11 Gel Permeation Chromatography Traces for Ethylene-Octene Copolymers Synthesized from **AMPS-Ti-12** for Different Reaction Times: Trace (A, reaction time = 20minutes), Trace B (reaction time = 50 minutes), Trace C (reaction time = 120 minutes)

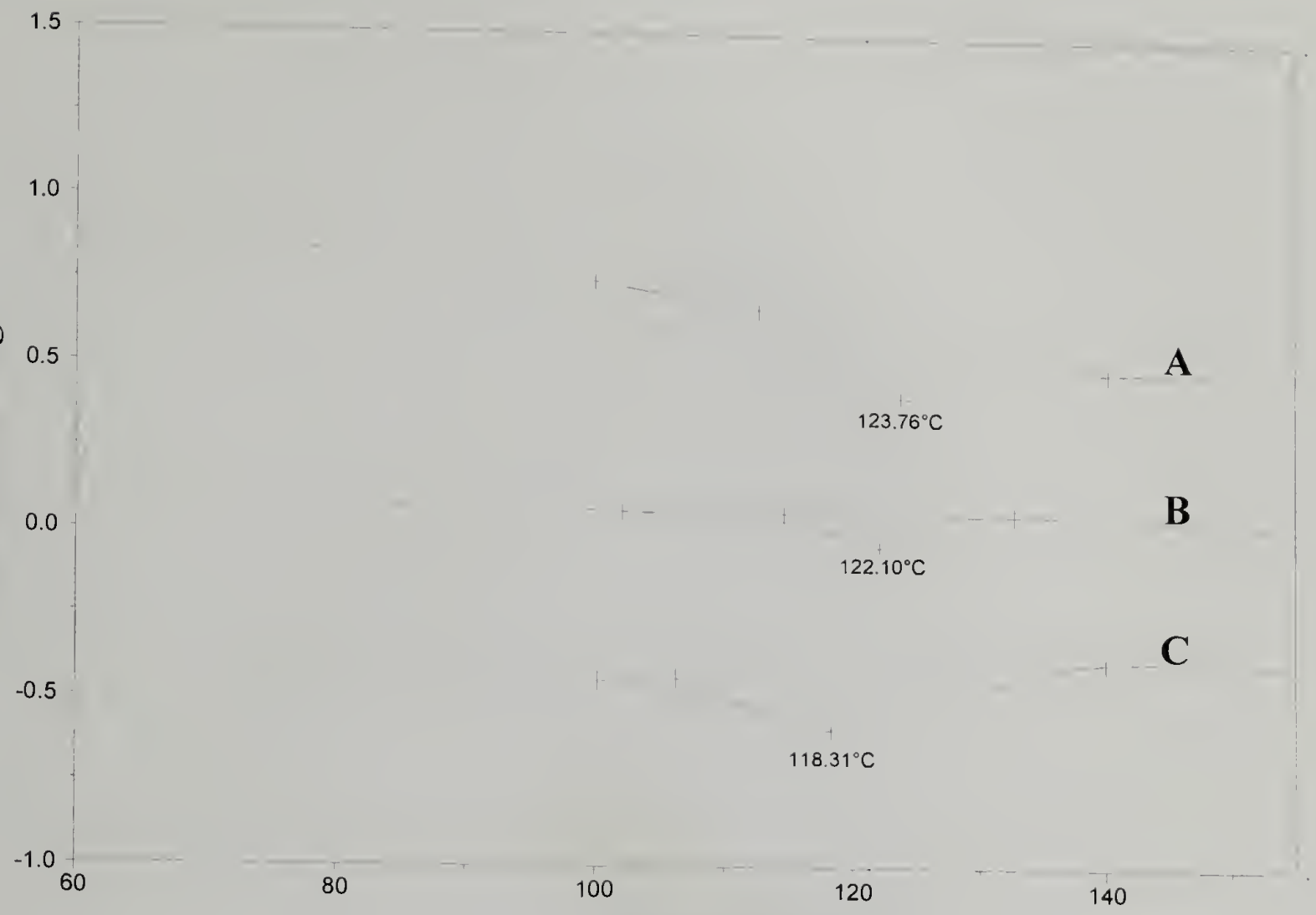

Figure 3.12 DSC Traces for Ethylene-Octene Copolymers Synthesized from AMPS-Ti- 12 for Different Reaction Times: Trace A (reaction time = 20 minutes, ΔH_f = 9.6 J/g), Trace B (reaction time = 50 minutes, ΔH_f = 3.6 J/g), Trace C (reaction time = 120 minutes, ΔH_f = 13.4J/g)

Table 3.3 Ethylene and 1-Octene Copolymerization using **AMPS-Ti-12** in Conjunction with MAO as the Cocatalyst for Different Reaction Times

Entry	Reaction Time (mins)	Catalyst (mg)	Tm[c] (°C)	1-Octene in Polymer (mol%)[d]	M_w [f]	PDI[f]
2	120	**12** (100.0)	119.5, 135.3	2.2	611000 (pepo3)	2.94
7[a]	120	**12** (100.5)	125.5	1.8	n.d	n.d
8	50	**12** (62.2)	122.1	1.9	180400	2.7
9	20	**12** (68.4)	122.5	1.9	65140	2.1

Al:Ti =195-210, 1-Octene =5.0mL, Ethylene Pressure=60 psig
[a] 1-Octene =2.5 mL
[d] Second melt of DSC scan,
[c] Monomer incorporation calculated according to reference
[f] Determined by GPC using LS detectors with a 690 nm laser at 135°C in 1,2,4-trichlorobenzene

3.3.4 Microstructural Analysis of Ethylene-Octene Copolymer Synthesized from AMPS-Ti-12 (Table 3.2, Entry 2)

In order to determine the microstructure of the copolymers synthesized, ^{13}C NMR of the copolymers was performed at 110°C. The ^{13}C resonances of copolymer synthesized from **AMPS-Ti-12** was analyzed and the spectrum is similar to that reported by Cavagna, hence low level of octene incorporations were expected. [7,73] The nomenclature for carbon assignments, monomer sequence distribution and equations relating signal intensity to the sequences in the ^{13}C NMR spectrum of the polyolefins is based on literature precedent.[7,73] The ^{13}C peak resonances were assigned as δ 14.20 (1s+1B_6, CH_3, EOE+EOO+OOE+OOO), 22.89 (2s+2B_6, EOE+EOO+OOE+OOO), 27.20 (βδ+5B_6, EOE), 29.99 (δδ, EEE), 30.06 (δδ+4B_6, EEE), 30.58 (αδ+6B_6, EOE) 32.17

($3s+3B_6$, EOE), 34.42 ($\alpha\delta+6B_6$, EOEE+EEOE), shown in Figure 3.14. Equations that relate signal intensity to monomer sequences were established to quantify the 1-octene incorporated in the copolymer. The octene content is calculated from the ratio of sum of the octene centered sequences to that of all the sequences and was determined to be 1.9 mol %, which in turn correlates well with the depression in melting point of the copolymer observed by Chen and coworkers.[72]

Figure 3.13 Control Experiments for Ethylene-Octene Copolyemrization: Ethylene-Octene Copolymerization using Toluene Filtrate of the Complex **AMPS-Ti-12** activated by MAO (Control 1), Ethylene-Octene Copolymerization using Precursor Catalysts activated by MAO (Control 2), Ethylene Homopolymerization using Commercially available CGC activated by MAO (Control 3)

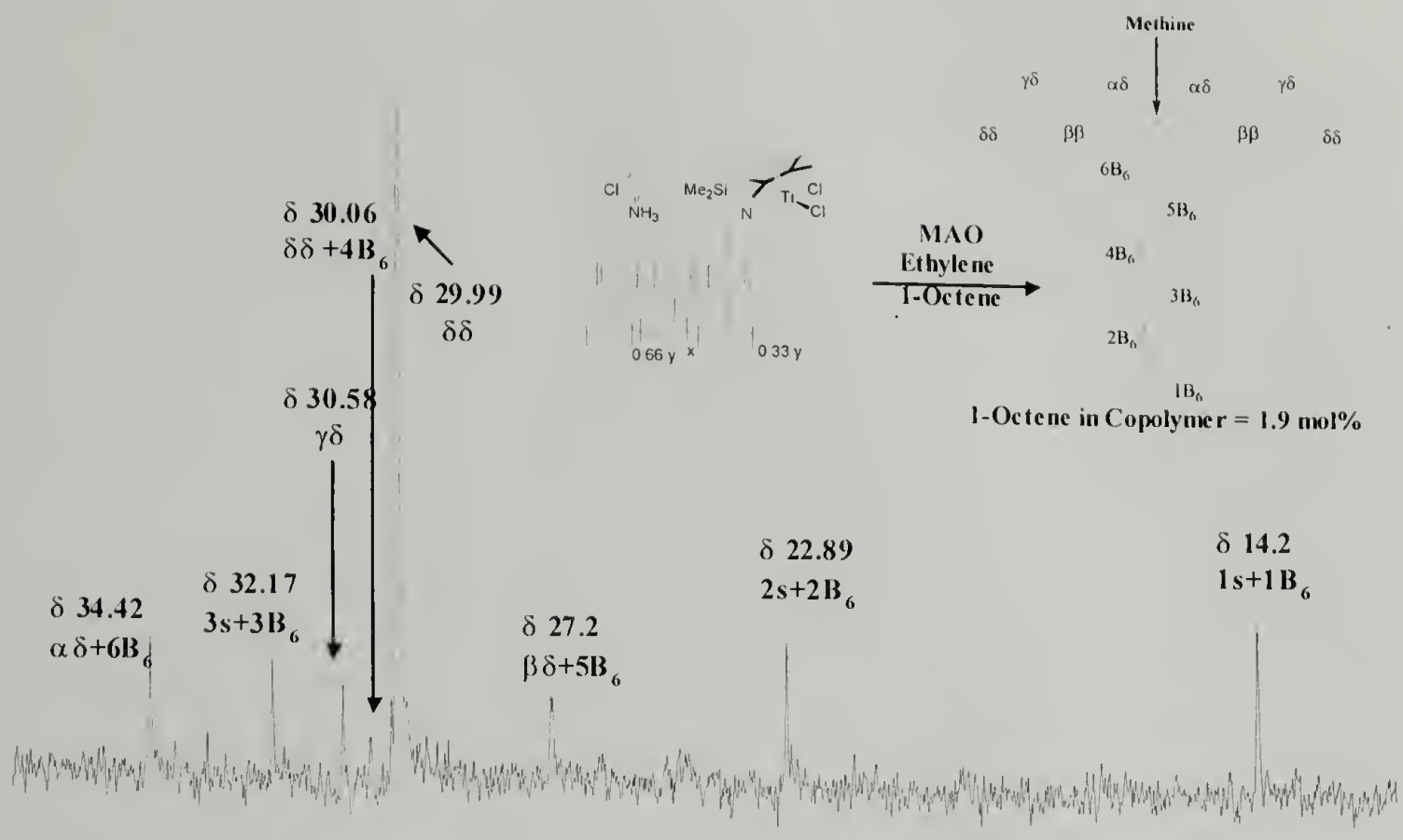

Figure 3.14 ^{13}C NMR (CPD) of Ethylene-Octene Copolymer (LLDPE) Prepared Using **AMPS-Ti-12** in Conjunction with MAO as the Cocatalysts

3.3.5 Ethylene Homo and Copolymerization using AMPS-Ti-11 in Conjunction with MAO as the Cocatalyst

The homopolymerization of ethylene using the mixed catalysts system **AMPS-Ti-11** affords HDPE (Table 3.2, Entry 3). Soxhlet extraction with refluxing toluene afforded two fractions, a lower molecular weight sample of lower crystallinity (PEa) and a higher molecular weight samples with higher crystallinity (PEb). This mixture of PE fractions correlates with the ^{29}Si NMR data, which showed the presence of two silicon moieties.

The copolymerization of ethylene and 1-octene was performed using the mixed catalyst **AMPS-Ti-11**. Analysis of the resulting polymer by DSC reveals the presence of two melting endotherms during the first melt (Table 3.2, entry 4, Figure 3.15). These correspond to a mixture of LLDPE and HDPE fractions. Slow cooling from the melt to ambient temperature followed by a second melting revealed a single endotherm due to the co-crystallization of LLDPE and HDPE. The depression in melting point has been attributed to incorporation of 2.0 mol% of 1-octene. The polymer was extracted from the support using hot trichlorobenzene. Molecular weight analysis by GPC reveals a trace with an overall M_w of 172900 with a PDI of 3.70, and a shoulder of lower molecular weight is observed that correlates well with the two melting endotherms observed in the first melt by DSC (Figure 3.16).

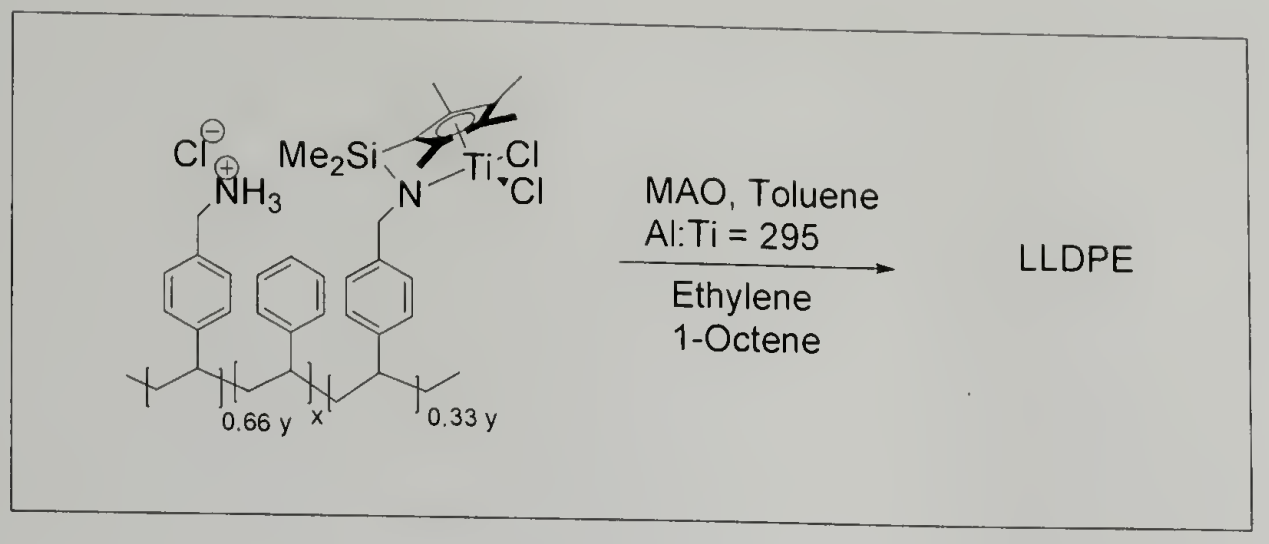

Figure 3.15 Ethylene and 1-Octene Copolymerization using **AMPS-Ti-11** with MAO

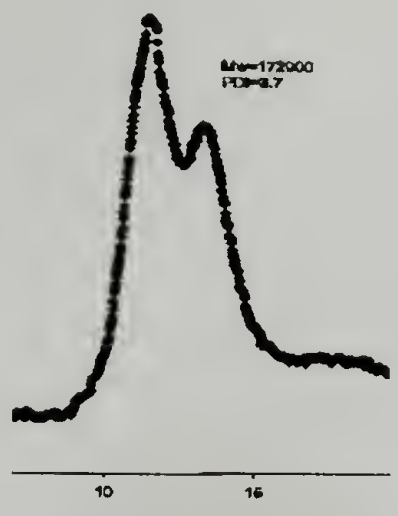

M_w = 172,000; PDI = 2.7

Figure 3.16 GPC Trace of LLDPE Synthesized from **AMPS-Ti-11** with MAO

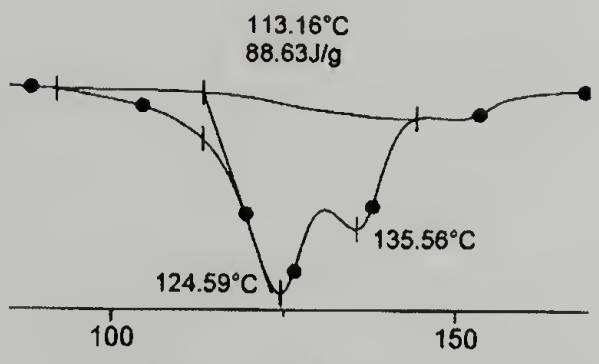

1-Octene incorporated = 2.0 mol %

Figure 3.17 GPC Trace of LLDPE Synthesized from **AMPS-Ti-11** with MAO

3.3.6 Control Polymerization using Precursor Catalyst 3

The polymerization of ethylene and the copolymerization of ethylene 1-octene using precursor catalysts **3** in conjunction with MAO both result in the formation of HDPE (Table 3.2, Entries 5 and 6 respectively). This activated soluble catalyst presumably resembles that of a leached titanium species. The formation of LLDPE in Table 3.2, (entry 4) clearly is the consequence of the formation of CGC architecture as monocyclopentadienyl titanium trichloride complexes did not incorporate α-olefins during copolymerization control experiments (Table 3.2, entry 6; Figure 3.13, Control 2).

3.3.7 Wide Angle X-Ray Diffraction (WAXS) of Polyethylenes

Various SSCs have been supported on organic supports, typically polymeric (soluble polymer or cross-linked polymer bead), and inorganic materials (alumina, silica). Interestingly, polyolefins of ultra high molecular weight and varied degrees of crystallinity have been observed. Polyolefins produced from CGCs supported on cross-linked polystyrene beads have lower crystallinity compared to polyolefins obtained from homogenous analogs. To correlate the influence of the support matrix on the apparent crystal size and the resulting degree of crystallinity of the polyethylene synthesized, Wide Angle X-Ray Diffraction (WAXD) analysis were performed. The reflections used for analysis were (110) and (200), where the broadening of the (110) reflection is affected by distortions of the a and b axes of the polyethylene orthorhombic unit cell. In order to compare the polyethylenes obtained from homogeneous catalysts and the supported catalyst, WAXD analysis of polyethylene produced from analogous homogeneous catalyst (Figure 3.13, control experiment 3) in conjunction with MAO was performed, and the

(110) and (200) reflections were observed to be relatively sharp. The apparent crystal size of the polyethylene was determined using the Scherrer equation to be of 180 Å (Figure 3.18, Trace A).[74] The percentage crystallinity as observed from DSC is about 60%. In contrast, polyethylene produced from **AMPS-Ti-12** (macroligated catalyst, solvent swollen) in conjunction with MAO shows broadened (110) and (200) reflections. The broadening of peaks can be attributed to the reduction in apparent crystal size of the polyethylene and increase in amorphous content of the polymer. The polyethylene produced from **12**/MAO has an apparent crystal size of 113 Å. It was noted that the amorphous halo was much more pronounced for polyethylenes with smaller apparent crystal sizes and lower degrees of crystallinity (Figure 3.18, Trace B). DSC measurements showed that the enthalpy of fusion and the degree of crystallinity of the polyethylenes were considerably reduced, percent crystallinity was calculated to be 20% from DSC measurements. The WAXD data (apparent crystal size, broadening of (110) and (200)) together with the DSC results (lower enthalpy of fusion and lower degree of crystallinity) shows that the supported catalysts results in less ordered polyethylene crystals with a corresponding increase in amorphous and intermediate component content, i.e. the formation of less stable crystalline lamellae. Introduction of 1-octene units leads to further distruption of the crystalline arrangement and an increase in the amorphous content of the polymer. Concomitant decrease in percentage crystallinity (4-6%) and apparent crystal thickness of the polymer (88 Å) is also observed. From the WAXD analysis, the presence of the monocyclic unit cell that can be attributed to the disruption of the orthorhombic unit cell due to the presence of the hexyl branches was noted (Figure 3.18, Trace C).

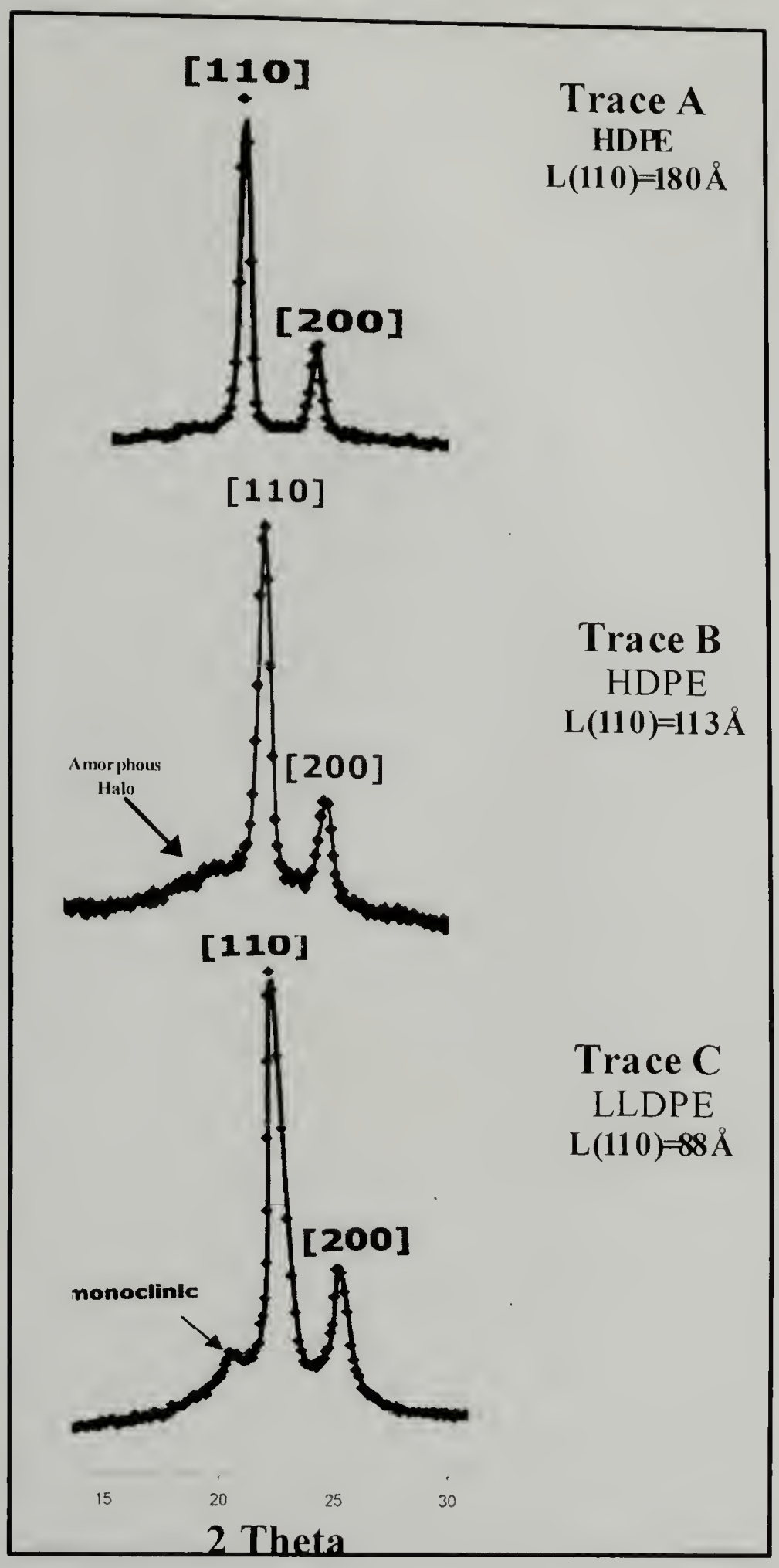

Figure 3.18 Wide Angle X-Ray Diffraction (WAXD) Analysis of Polyolefins, Apparent Crystal Thickness (L) calculated using Scherrer Equation using Diffraction Peak at (110): Trace A (HDPE from Homogeneous CGC), Trace B (HDPE from **AMPS-Ti-12**), Trace C (LLDPE from **AMPS-Ti-12**)

3.3.8 Scanning Electron Microscopy Analysis

The scanning electron micrographs of the **AMPS-Ti-12**, HDPE, and LLDPE prepared from **AMPS-Ti-12**/MAO were recorded (Figures 3.19, 3.20, and 3.21 respectively). The supported catalysts beads were determined to be approximately 100 μm in diameter, whereas the diameter of the HDPE and LLDPE beads were determined to be 1 mm and 0.1 mm, respectively. At higher magnification, it is observed that the supported catalyst beads have a very smooth external surface. By contrast, the polyolefin synthesized from the supported catalysts has fibrous external features that have been attributed to the formation of less stable crystalline structures, although the overall morphology of the supported catalyst has been reproduced. The formation of these fibrillar features on the surface of the polyethylenes correlates with the observation of low crystalline polymers from DSC measurements and of smaller crystalline units from WAXD measurements.

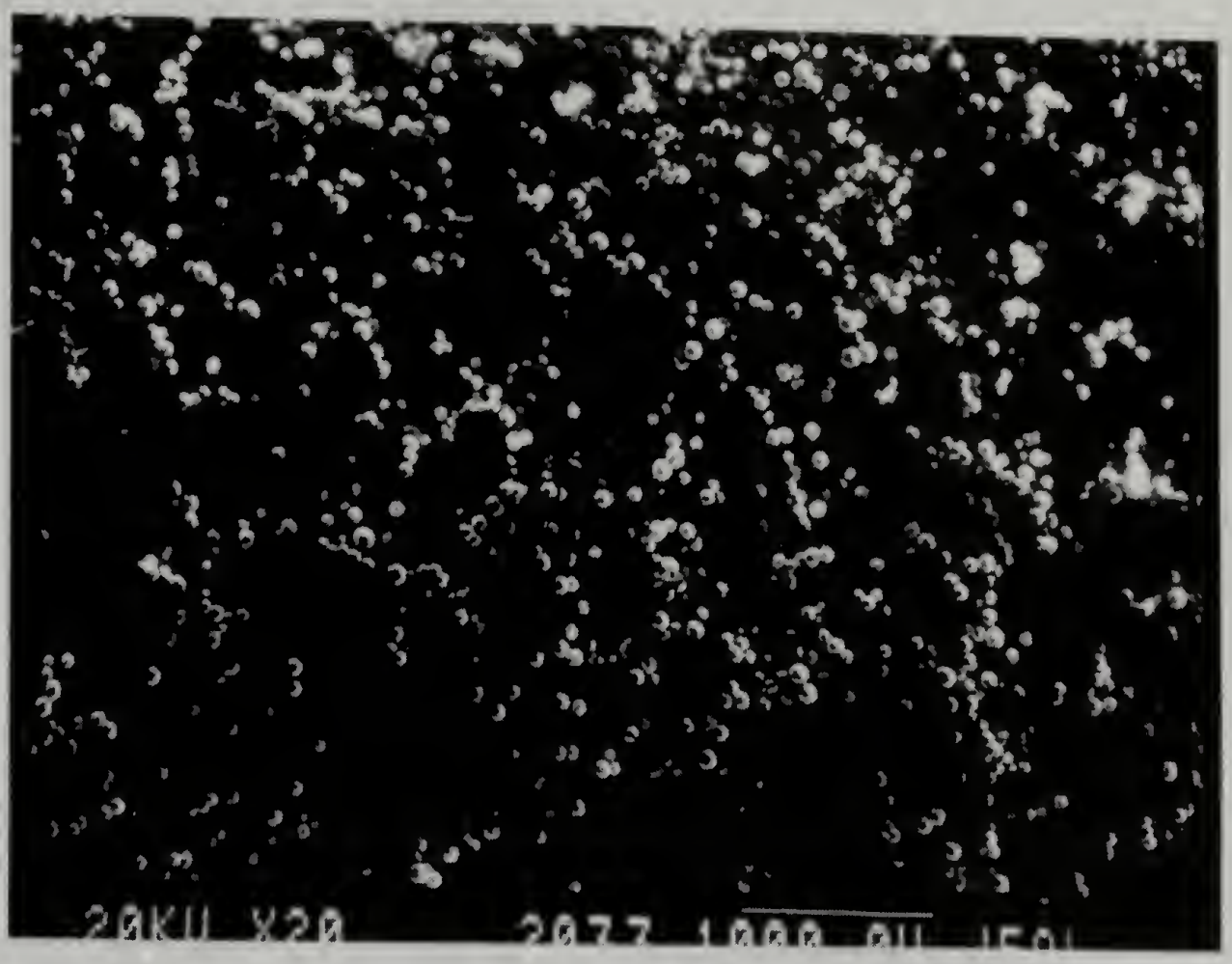

Figure 3.19 Scanning Electron Micrographs: **AMPS-Ti-12** (24x, Top and 200x, Bottom)

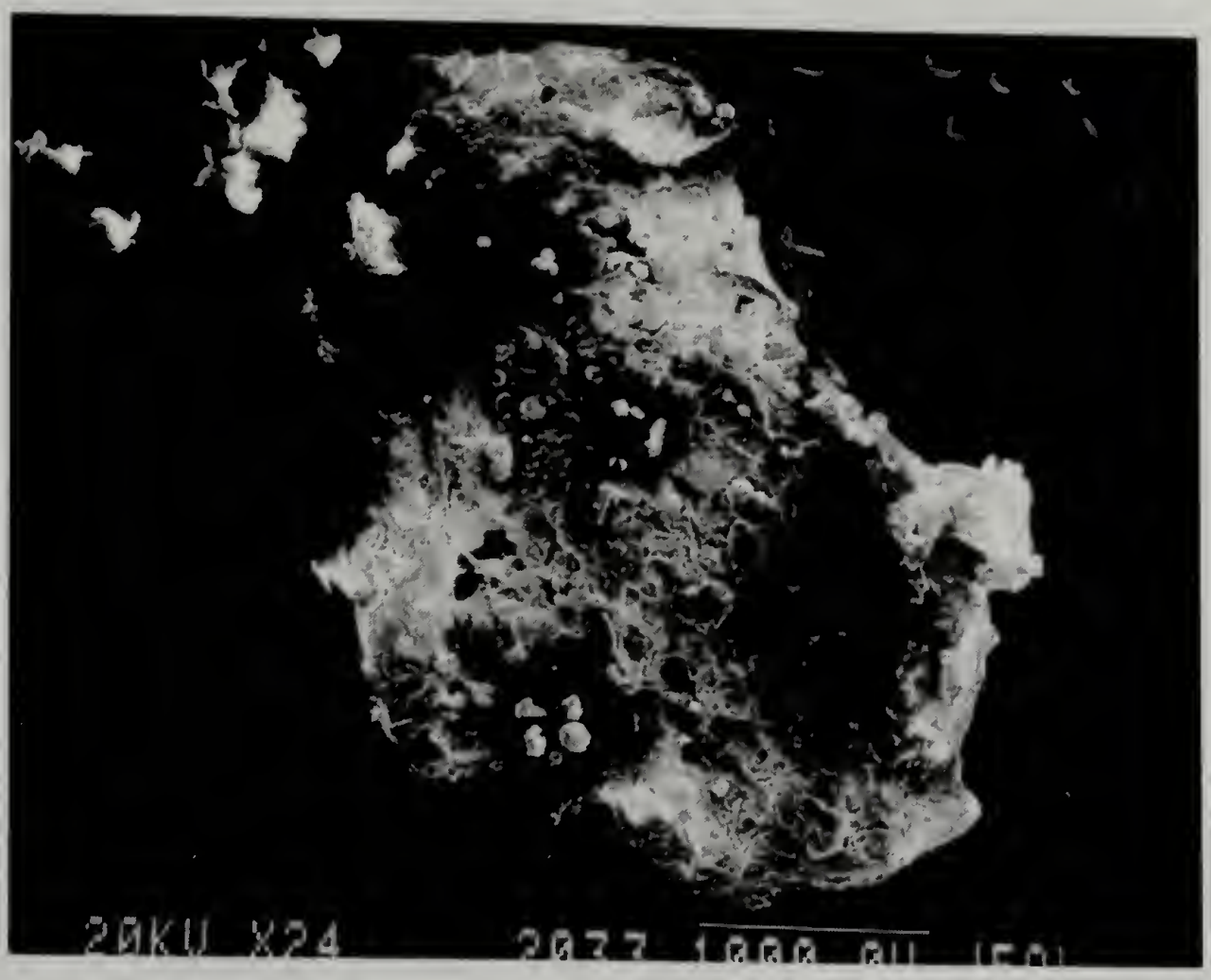

Figure 3.20 Scanning Electron Micrographs of HDPE from **AMPS-CGC-12** (24x, Top and 200x, Bottom)

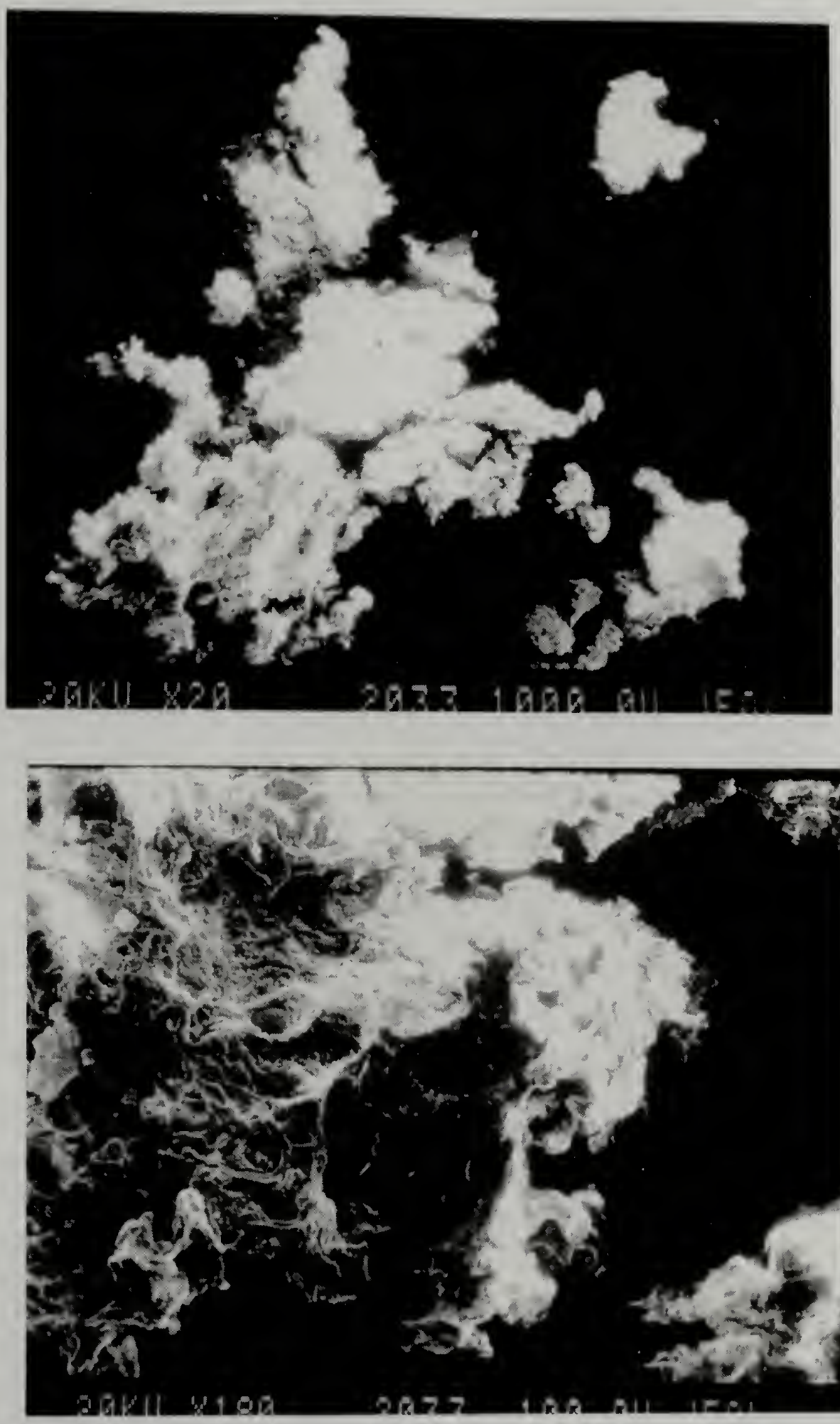

Figure 3.21 Scanning Electron Micrographs of LLDPE from **AMPS-CGC-12** (24x, Top and 200x, Bottom)

3.4 Summary

Protocols for supporting titanium complexes **3** and **6** on an AMPS matrix to produce catalysts **AMPS-Ti-11** and **AMPS-Ti-12**, respectively, have been established. The reaction of **3** with AMPS results in the formation of a mixture of CGC and a titanium amide. However, the reaction of **6** with AMPS exclusively affords the formation of **AMPS-Ti-12** as confirmed by NMR analyses. The presence of the support CGC framework is evident from the formation of LLDPE from the copolymerization studies of ethylene and 1-octene. The molecular weight, molecular weight distribution, melting points, and enthalpy of fusion have been determined for these copolymers. The degree of crystallinity of the polyolefins synthesized from these supported catalysts is substantially reduced relative to that of polymers produced using soluble CGCs. Copolymerization of ethylene and α-olefins provides an easy means for determining the efficiency of supportation of CGCs. The observation of LLDPE formation during ethylene–1-octene copolymerization using **AMPS-Ti-12** is independent confirmation of the structure of the supported CGC. However, an ethylene only polymerization catalyst is apparently being formed by leaching of a titanium fragment from **AMPS-Ti-12** at long reaction times. This is the first example of a supported catalyst system wherein the copolymerization ability of the supported and leached species differ which confirms the presence of a leached species that can be differentiated from the started supporting catalyst by polyolefin product analysis.

CHAPTER 4

SUPPORTED CONSTRAINED GEOMETRY CATAYSTS ON AMINO FUNCTIONALIZED SILICA; STUDIES OF ETHYLENE AND 1-OCTENE POLYMERIZATION

4.1 Introduction

The inorganic matrices to which CGCs have been covalently tethered include silica surfaces and alumina surfaces.[66,67-69] Reaction of the silica surfaces with 4-aminopropyldimethoxysilane (APDMS) results in the production of aminopropyl finctionalized silica surfaces. Pakannen and coworkers have reported functionalization of silica with 4-aminopropyl moieties and subsequently cyclopentadienylsilyl ligands are tethered to the amine units. The CGC framework is assembled on cyclopentadienylsilylamido functionalized silica surfaces by amine elimination between the appropriate homoleptic metal amide and the cyclopentadienylsilylamido ligands. This chemistry affords both the cyclopentadienyl piano stool complexes (formed by incomplete amine elimination) and the completely assembled CGC form on silica (Figure 4.1, Top). Eisen and coworkers have reported an alternative approach to tethered CGCs by synthesis of homogeneous and soluble CGCs containing a pendant trimethyoxysilyl moiety. The soluble CGCs have been synthesized by amine elimination chemistry. The CGCs are tethered onto silica and alumina substrates via reaction of methoxy units as sites that react with the hydroxyl groups of the silica matrices (Figure 4.1, Bottom).[66] However, coordination of the eliminated amines to the metal center and incomplete metal–amine bond activation have been observed, which lead to low activity for polyolefin production.

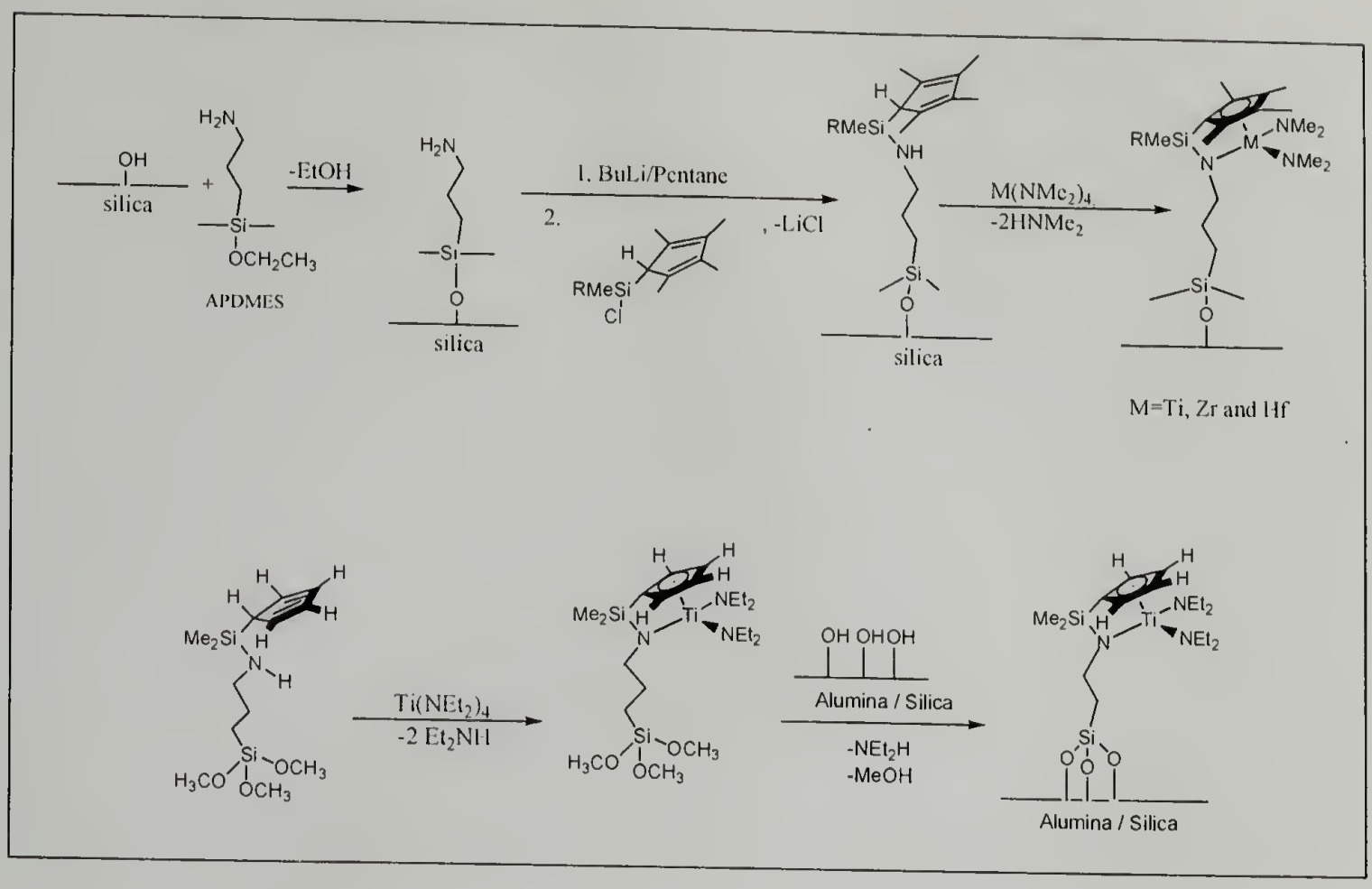

Figure 4.1 Amine Elimination Chemistry as a Route to Prepare Tethered Constrained Geometry Catalysts (CGCs): Reaction on Solid Silica Matrix to Obtain CGC (Top), Converstion of Homogeneous CGCs to Tethered CGCs (Botton)

A few publications dealing with supported CGCs on silica for olefin polymerization have been published in the last few years.[75] However these articles have been mostly focused on the methodologies to synthesize supported CGCs and on initial polymerization results (catalyst activity, polymer molecular weight and polydispersity). Comprehensive studies of synthesis and characterization of silica supported CGCs, and subsequent elucidation of how the silica matrix influences the catalytic performance and the final polyolefin properties have not been reported. In addition the question of how the properties of polyolefins obtained from silica supported CGC and analogous

homogeneous eomplexes needs to be compared.

Methods to adapt the assembly protoeol of Royo to the use of primary amine funetionalized solid supports with preeursors eatalysts as a versatile synthetie route to tether CGCs on polystyrene has been diseussed (Chapter 3). In order to further explore the influence rigid, ordered three-dimensional inorganie matrices on the physical properties of the polyolefins produeed synthetic routes to prepare amine-functionalized mesoporous silica have been designed. This chapter will foeus on the synthesis of aminophenyl-funetionalized mesoporous siliea, assembly of CGCs on these matriees, and polymerization of olefins using these supported eatalysts.

Above their critieal mieelle coneentration, surfaetants (cetyltrimethylammonium bromide, CTAB) form rod-like miseelles in water. These rod-like miseelles are treated with tetraethoxysilane (TEOS) in an alkaline medium to afford rod-like miseelles that are coated with silicate units formed due to the hydrolysis TEOS in the alkaline medium. These silicate exeapsulated mieelles assemble in a hexagonal fashion, which undergoes further condensation to afford hexogonally ordered mesopores. The condensation oecurs between neighboring Si-OH groups, allowing the formation of Si-O-Si bonds, which subsequently results in mesopores materials. The surfaetant, whieh is still trapped in the mesopore, is removed either by solvent extraetion (Soxhlet extraetion) or by heating the sample at 600°C (ealeinations). Removal of the surfactant results in the formation of hexagonally ordered mesoporous silica. The surfaetant used for the production of mesoporous silica determines the pore size of the siliea matrix, while the method of removal of the surfactant determines the surfaee hydroxyl content in the mesopore. For instanee, ealeinations produees mesoporous silica with lower surfaee

hydroxyl content and increased wall thickness due to increased silanol condensation at higher temperatures compared to the Soxhlet method of surfactant removal.[76]

The mesoporous silica support contains uniformly sized, well-ordered pores of sufficient size to accommodate the catalyst, reagent monomer, and nascent polymer chains. The sizes of the hexagonally arrayed cylindrical pores are tailored by the choice of surfactant used as the template in the synthesis (smaller pores (30-40 Å) can be obtained using hexadecyltrimethylammonium, and larger (>70 Å) using Pluronic P123 (polyethylene oxide–polypropylene oxide–polyethylene oxide triblock copolymer). Silanol groups on the pore surfaces permit functionalization with organosiloxanes, which provide a route for introduction of catalyst linkage sites. The silanol content of the pore surfaces is controlled by the method of template removal; calcination results in a low silanol content and hence a small number of isolated silanol groups, whereas solvent extraction yields a high silanol content. A combination of two organosiloxanes is used in this work: *p*-aminophenylsiloxane provides the site for covalent attachment of the catalyst, and either methyl or trimethylsiloxane is used to cap additional silanol groups and to increase the organophilicity of the pores.

4.2 Experimental Section

4.2.1 Materials

Precursor paino stool complex **6**, which was prepared by silyl elimination chemsitry discussed in Chapter 2 and is used to assemble constrained geometry catalysts. Mesoporous silica and amine-functionalized mesoporous silica was prepared by Sandra L. Burkett. These tailored silica matrices have been used as supports for the assembly of CGCs on amine-functionalized silica. Dry, pure, air-free solvents were obtained from a

solvent manifold.[64] Polymerization was performed using an ethylene/propylene manifold and thick-walled reactors.[70] Methylaluminoxane (4.77 M, 30 wt % in toluene), tris(pentafluorophenyl)borane ($(B(C_6F_5)_3$, **I**), trityl borate ($[(C_6H_5)_3C][B(C_6F_5)]_4$, **II** and N,N-dimethylanilinium borate ($[(C_6H_5N(CH_3)_2H][B(C_6F_5)]_4$, **III**) were obtained from Albemarle and used as received, while 1-Octene and tetramethylethylenediammine (TMEDA) were obtained from Aldrich and used after distillation over CaH_2.

4.2.2 Analytical methods

Structural characterization of the mesostructured silica samples was performed by X-ray powder diffraction (XRD) using a Scintag XDS-2000 diffractometer with Cu Kα radiation. Solid State NMR spectra were obtained using a Bruker DSX300 spectrometer, with samples contained in 7 mm zirconia rotors. ^{13}C spectra were recorded at 75.48 MHz using cross polarization (CP) and magic angle spinning (MAS) at a rate of 4–5 kHz, and the chemical shift data is referenced to tetramethylsilane at 0 ppm. ^{29}Si spectra were recorded at 59.63 MHz, with cross polarization, using magic angle spinning at a rate of 2.5–3.0 kHz, and the chemical shift data is referenced to sodium 3-(trimethylsilyl)propionate at 0 ppm. Deconvolution of ^{29}Si MAS NMR spectra was performed using Bruker Xedplot software. Infrared spectra were obtained using a Bruker IFS66 spectrometer, with samples prepared as potassium bromide pellets. Nitrogen adsorption was performed using a Quantachrome Autosorb instrument. Surface area values were obtained by BET analysis. Pore size data, which is reported as the mode of the values for the pore diameter, was obtained by density functional theory (DFT) analysis of the desorption curve.[77]

Elemental analysis of the capped silica samples was performed using Exeter Analytical 240XA CHN analyzers. A Leeman Labs Dual View DRE Sequential ICP was used to analyze the Ti content of the supported CGC samples. The catalysts assembled on amine-functionalized silica were analyzed by Solid State ^{29}Si NMR. Polymer weight average molecular weight (M_w) and polydispersity index (PDI) were determined by gel permeation chromatography (GPC) using a Polymer Laboratories PL-220 high temperature GPC instrument equipped with a Wyatt MiniDawn (620 nm diode laser) high temperature light scattering detector and a refractive index detector. GPC was performed at 135 °C using 1,2,4-trichlorobenzene as the solvent. A dn/dc value of –0.11 was used for polyethylene. Calibration was performed using polystyrene standards. Thermal analysis (differential scanning calorimetry (DSC)) was performed using a TA DSC 2910 instrument equipped with a liquid nitrogen cooling accessory unit under a continuous nitrogen purge (50 mL/min). The melting temperatures for the ethylene/1-octene copolymers were obtained from the second melt using a heating and cooling scan at 10 °C/min. The melting temperatures for polyethylene were obtained from the first melt using a heating and cooling scan at 10 °C/min. The heat of fusion (ΔH_f) for polyethylene was obtained from the first melt using a heating and cooling scan at 10 °C/min. Degree of crystallinity of polyethylenes is defined as the ratio of the heat of fusion observed in the copolymer to the heat of fusion (ΔH_f) of a polyethylene single crystal (ΔH_f=293 J/g). The extent of 1-octene incorporation in the ethylene/1-octene copolymers was determined by the ratio of the integrated intensities of the hexyl branch and the polyethylene backbone. The ^{13}C NMR spectrum obtained at 120 °C using a AVANCE 600 MHz NMR spectrometer with 1,1,2,2-tetrachloroethane as the lock solvent.

4.2.3 Synthesis and Functionalization of Mesoporous Silica Materials

The non-functionalized small pore (HX and HC) and large pore (PC and PX) were synthesized and subsequently, these silica matrices were capped with *p*-aminophenyltrimethoxysilane and other capping units such as methyltrimethoxysilane or trimethylmethoxy silane. The syntheses and characterization of non-functionalized and amine functionalized mesoporous silica was completed by our collaborator, Sandra L. Burkett (Amherst College), based on literature precedent.[78-85] The characterization data of the mesoporous silica materials included in this thesis is needed for subsequent catalysts assembly protocols and structure-property correlations between the supported catalysts and the polyolefins produced.

4.2.4 Assembly of CGC on functionalized mesoporous silica substrates (HXAM-Ti, HCAT-Ti, PXAM-Ti, PCAT-Ti)

Synthesis of supported catalysts was performed under nitrogen in Schlenk glassware or in an inert atmosphere dry box. The mole ratio of the amine content of the support to the titanium catalyst precursor was selected to be 3 to 1. TMEDA was used as a base to scavenge the hydrochloric acid formed as a reaction by-product.

The experimental parameters for the preparation of supported CGCs are specified in Table 4. In a typical reaction, 79.0 mg (0.25 mmol) titanium catalyst precursor was added to slurry of sample **PXAM** (303.0 mg, 1.3 wt % N, 0.928 mmol N per 1 g of silica) in toluene. Following the addition of 0.1 mL (0.5 mmol) TMEDA, the suspension was stirred at 60 °C for 3 d. The support was washed several times with toluene to remove soluble by-products and any residual precursor catalyst, and the supported catalyst was

recovered and dried in vacuo at 60 °C for 12 hours, which afforded 381.0 mg of supported catalyst **PXAM-Ti**.

4.2.5 Representative Ethylene and 1-octene Copolymerization using Silica Supported CGCs in Conjunction with MAO

In a typical reaction, 13.9 mg **PXAM-Ti** was added to a mixture of 10.0 mL toluene and 1.0 mL of 30 wt% MAO (4.77 M) in a thick-walled polymerization reactor; an excess of MAO cocatalyst was used to activate the CGC and to scavenge any ammonium salts remaining from the CGC assembly. 1-Octene (5 mL) was added by means of an additional cylinder, and ethylene was supplied at a pressure of 60 psig (4 atm) for 20 min at room temperature with constant stirring. The ethylene supply was stopped, the reactor was vented to remove excess ethylene, and the reaction mixture was quenched with a 10% by volume of hydrochloric acid in methanol. The polyethylene was filtered and dried *in vacuo* at 60 °C overnight to afford the ethylene/1-octene copolymer.

4.2.6 Representative Ethylene Homopolymerization using Silica Supported CGCs in Conjunction with MAO

In a typical reaction, 13.5 mg **PXAM-Ti** was added to a mixture of 10.0 mL toluene and 1.0 mL 30 wt % MAO (4.77 M) in a thick-walled polymerization reactor; an excess of MAO cocatalyst was used to activate the CGC and to scavenge any ammonium salts remaining from the CGC assembly. The reactor was pressurized with ethylene at a pressure of 60 psig (4 atm) for 10 minutes at room temperature with constant stirring. The ethylene supply was stopped, the reactor was vented to remove excess ethylene, and the reaction mixture was quenched with a 10 % by volume solution of hydrochloric acid in methanol. The polyethylene was filtered and dried *in vacuo* at 60°C overnight.

4.3 Results and Discussion

4.3.1 Substrate Preparation and Characterization

Mesoporous silica was prepared using surfactant templates and tetraethoxysilane (TEOS). The hydroxyl groups within the mesoporous silica have been used to tether various functional moieties that are known as capping agents. Amine functionality is introduced by the addition of the capping agent, 4-aminophenyltrimethoxysilane. The remaining hydroxyl units are capped with either trimethylmethoxysilane or methyltrimethoxysilane (Figure 4.2). The non-functionalized and functionalized mesoporous silica materials are designated by two- or four-letter names, respectively, that are indicative of the template H: hexadecyltrimethylammonium bromide (C_{16}); P: Pluronic P123, the method of surfactant removal X: solvent extraction; C: calcination, the amine source A: *p*-aminophenylsiloxane, and the silanol capping group (M: methylsiloxane; T: trimethylsiloxane (Table 4.1).

Table 4.1 Nomenclature of Mesoporous Silica

Sample	Template	Capping Groups	Pore Diameter Å
HX	C_{16}	None	43
HXAM	C_{16}	AP/M	35
HC	C_{16}	None	32
HCAT	C_{16}	AP/TM	26
PX	P123	None	70
PXAM	P123	AP/M	<70
PC	P123	None	>70
PCAT	P123	AP/TM	<70

C: Calcination, X: Solvent Extraction, AP: Aminophenyl,
TM: Trimethylsilyl, M: Methylsilyl

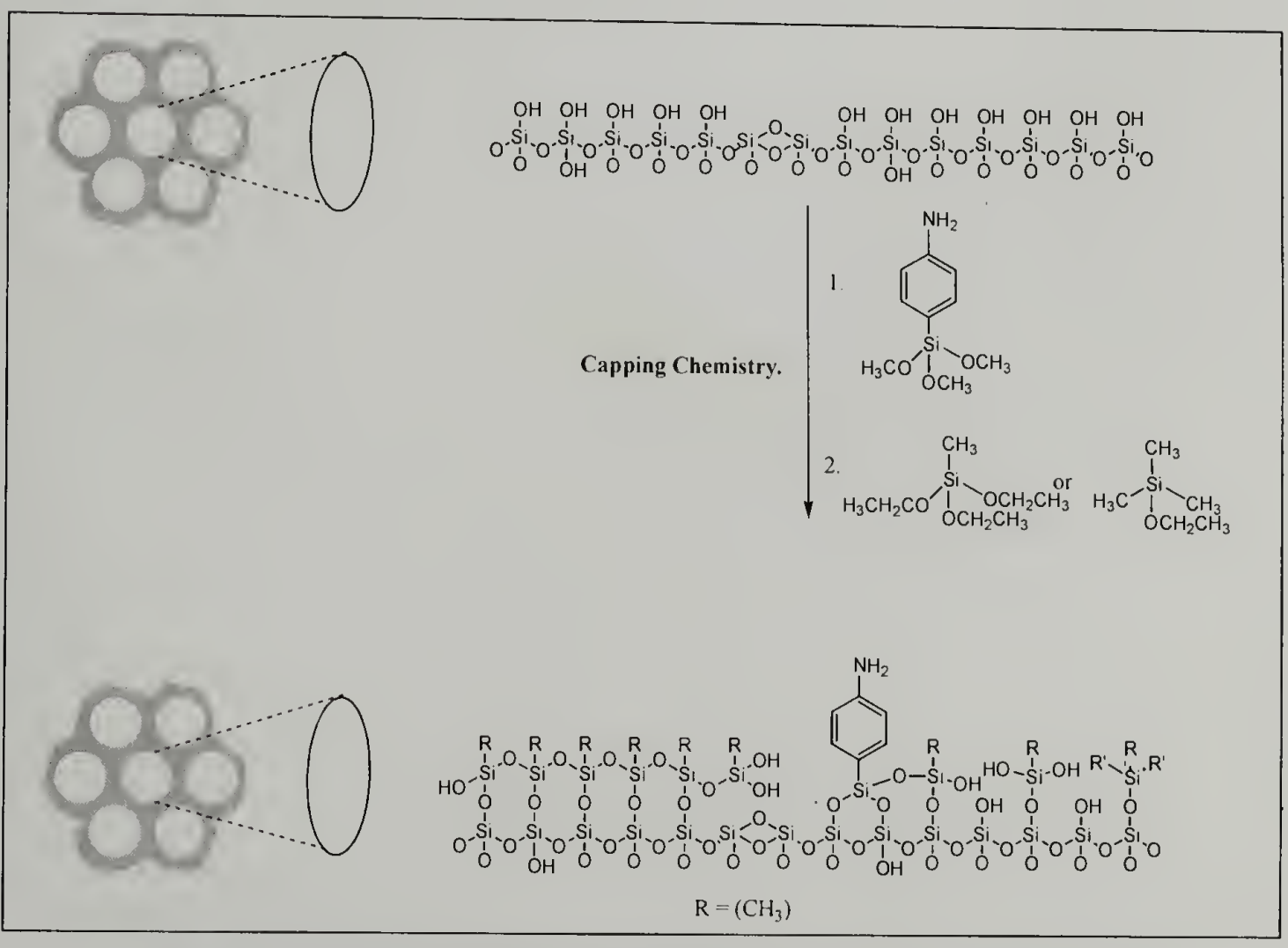

Figure 4.2 Functionalization of Mesoporous Silica: Introduction of 4-Aminophenyltrimethoxy Silane and Trimethylethoxysilane Capping Groups

The characteristic hexagonal symmetry of each of the non-functionalized and functionalized silica materials is apparent from the three peaks in the x-ray powder diffraction pattern, which can be assigned as the (100), (110), and (200) reflections (Table 4.2). The lattice parameter a, which corresponds to the pore-to-pore distance, is calculated from d_{100} ($a = (2/\sqrt{3})\, d_{100}$). The pore-to-pore distances observed for the non-functionalized materials are consistent with published values, based on the template and the method of template removal.[78,79,84] Functionalization of the silica materials does not change the observed pore-to-pore spacing.

Nitrogen adsorption/desorption studies confirm that the non-functionalized and functionalized materials are mesoporous. The BET surface area values reported in Table 4.2 indicate that a decrease in surface area occurs upon introduction of functional groups, which suggests that the organic moieties are attached to the walls of the pores. The pore diameters reported in Table 4.2 represent the mode of the distribution of pore sizes obtained by DFT analysis of the nitrogen desorption curve for each sample.[77] For the samples prepared using the hexadecyltrimethylammonium template (HX, HC, HXAM, HCAT), a narrow distribution of pore diameters is observed, and the mode values for the functionalized materials are observed to be smaller than those of the non-functionalized parent materials. For the samples prepared using the Pluronic P123 template (PX, PC, PXAM, PCAT), broader pore size distributions are observed. A decreased fraction of larger pores and an increased fraction of smaller pores are observed when the functional groups are introduced, consistent with the location of these groups on the pore surfaces. An estimate of the wall thickness of each sample is obtained by comparison of the pore diameter and pore-to-pore distance. The wall thicknesses of the

hexadecyltrimethylammonium templated silica samples increase by approximately 6 Å upon functionalization, which corresponds to the formation of a 3 Å thick monolayer on the pore surface.

Table 4.2. Structural Characterization of Mesoporous Silica Substrates

Sample	d_{100} (Å)	d_{110} (Å)	d_{200} (Å)	a (Å)	Surface Area (m^2/g)	Pore Diameter (Å)	Wall Thickness (Å)
HX	42.6	24.4	21.1	48.9	893	43	6
HXAM	42.1	24.0	20.8	48.2	645	35	13
HC	36.5	20.8	18.0	41.8	826	32	10
HCAT	36.6	20.9	18.0	41.9	535	26	16
PX	99	57.3	49.6	114	571	70	44
PXAM	97	57.1	49.3	113	404	<70	>43
PC	97	55.9	48.2	112	617	>70	<42
PCAT	98	56.1	48.5	112	469	<70	>42

Table 4.3 ^{29}Si MAS NMR Analysis of Mesoporous Silica Substrate Composition

	Integrated area of resonance (ppm in (-)ve)) [a,b]									
Sample	Q^4 109±1 ppm	Q^3 100±1 ppm	Q^2 90±2 ppm	T^3_A 78±3 ppm	T^2_A 68±1 ppm	T^1_A 61±2 ppm	T^3_M 56±3 ppm	T^2_M 51±2 ppm	T^1_M 42±3 ppm	M^1_T 14±1 ppm
HX	49.4	47.6	3.0	0	0	0	0	0	0	0
HXAM	63.9	31.5	4.6	2.1	3.5	3.3	2.4	1.7	1.8	0
HC	61.6	36.6	1.8	0	0	0	0	0	0	0
HCAT	80.5	17.8	1.6	1.2	2.8	5.3	0	0	0	3.7
PX	51.8	40.5	7.7	0	0	0	0	0	0	0
PXAM	60.0	34.5	5.5	5.3	4.2	2.3	1.9	0.8	0.8	0
PC	68.4	29.3	2.3	0	0	0	0	0	0	0
PCAT	78.3	20.8	0.9	0.5	2.5	2.2	0	0	0	3.7

[a] Relative areas are reported such that a constant value of 100 is maintained for the inorganic silica content ($\sum_n Q^n = 100$)

[b] Designation of resonances: $Q^n = \underline{Si}(OSi)_n(OH)_{4-n}$; $T^n_A = \underline{Si}(C_6H_4NH_2)(OSi)_n(OH)_{3-n}$; $T^n_M = \underline{Si}(CH_3)(OSi)_n(OH)_{3-n}$; $M^n_T = \underline{Si}(CH_3)_3(OSi)_n$

Table 4.4 Analysis of Mesoporous Silica Substrate Composition

Sample	Si-OH/Si [a] ^{29}Si NMR	RSi-OH/Si [b,c] ^{29}Si NMR	Si-cap/Si [d] ^{29}Si NMR	Si-amine/Si [e] ^{29}Si NMR	mmol amine/g [f] (Elemental analysis)
HX	0.536	0	0	0	0
HXAM	0.489	0.135	0.051	0.078	0.57
HC	0.402	0	0	0	0
HCAT	0.306	0.119	0.033	0.082	0.77
PX	0.558	0	0	0	0
PXAM	0.493	0.099	0.031	0.103	0.93
PC	0.340	0	0	0	0
PCAT	0.272	0.064	0.034	0.048	0.44

[a] Total silanol content, from Q^n ($n \leq 3$), T^n_A ($n \leq 2$), and T^n_T ($n \leq 2$).
[b] Silanol content within organosiloxane component, from T^n_A ($n \leq 2$) and T^n_T ($n \leq 2$).
[c] R refers to T^n_A ($n \leq 3$), T^n_T ($n \leq 3$), and T^n_M ($n \leq 1$).
[d] Cap refers to T^n_T ($n \leq 3$) and T^n_M ($n \leq 1$)
[e] ^{29}Si NMR
[f] Elemental Analyses

The degree of condensation of the silicate framework and the organosiloxane is determined from ^{29}Si NMR studies. In the ^{29}Si NMR spectra, the resonances for the inorganic silicate units (Q^n = $\underline{Si}(OSi)_n(OH)_{4-n}$) (Representative mesoporous silica ^{29}Si NMR, Figure 4.4) are well resolved from those for the *p*-aminophenylsiloxane groups (T^n_A = $\underline{Si}(C_6H_4NH_2)(OSi)_n(OH)_{3-n}$) and those for the methylsiloxane (T^n_M = $\underline{Si}(CH_3)(OSi)_n(OH)_{3-n}$) and trimethylsiloxane (M^n_T = $\underline{Si}(CH_3)_3(OSi)_n${or simply, M^1_{TM} = $\underline{Si}(CH_3)_3(OSi)$}) moieties.[86] The peak positions and relative integrated areas for each sample are reported in Table 4.3. The ^{29}Si NMR data permit determination of the inorganic (Si_Q-OH/Si), organic ($Si_{T,M}$-OH/Si), and total silanol conten (Si-OH/Si), and of the *p*-aminophenylsiloxane (Si-AP/Si) and methylsiloxane and trimethylsiloxane capping group content (Si-cap/Si) (Table 4.4, Representative ^{29}Si NMR Figure 4.5).

Consistent with previous reports, the silanol content of non-functionalized materials depends on the method used for surfactant removal, with higher silanol contents observed for the non-functionalized extracted materials compared to the non-functionalized calcined materials. The total silanol content (Si-OH/Si) decreases upon functionalization, even though the *p*-aminophenylsiloxane and methylsiloxane groups themselves introduce silanol groups (T^2 and T^1). The observed decrease in inorganic silanol groups (Q^3 and Q^2) suggests that the surface silanol groups have indeed been capped by the organosiloxane moieties. The protocol that uses trimethylsiloxane as the capping group leads to a more substantial decrease in inorganic silanol content and to a smaller organosilanol content in the sample than that in which methylsiloxane is introduced, with the consequence that these samples, prepared using calcined parent materials, have the lowest total silanol contents.

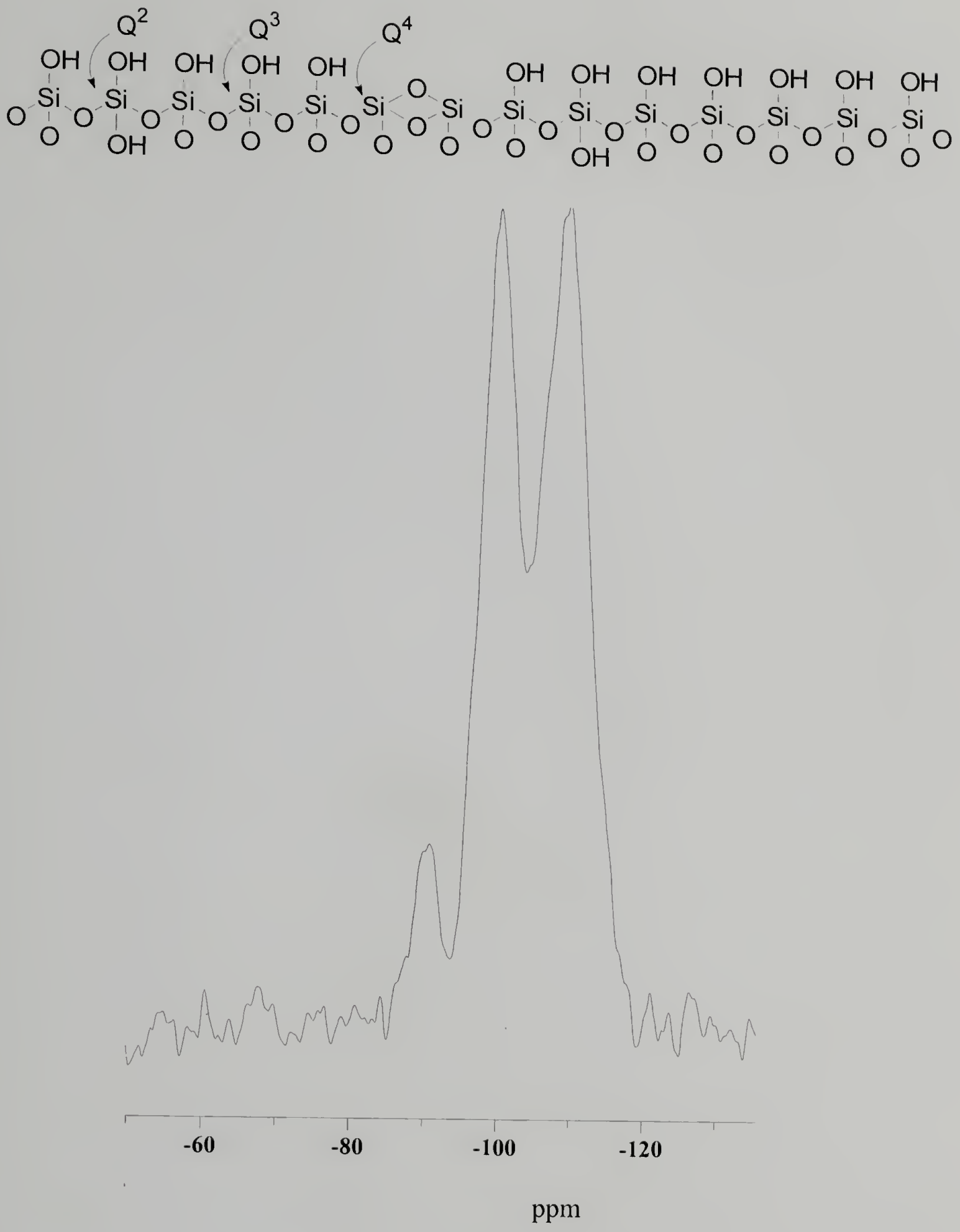

Figure 4.3 ^{29}Si NMR (CP-MAS) of Silica PX, Synthesized using Pluronic 123, and the Surfactant was Removed by Ethanol Extraction: (Q^2, δ –90), (Q^3, δ –100), (Q^4, δ –109)

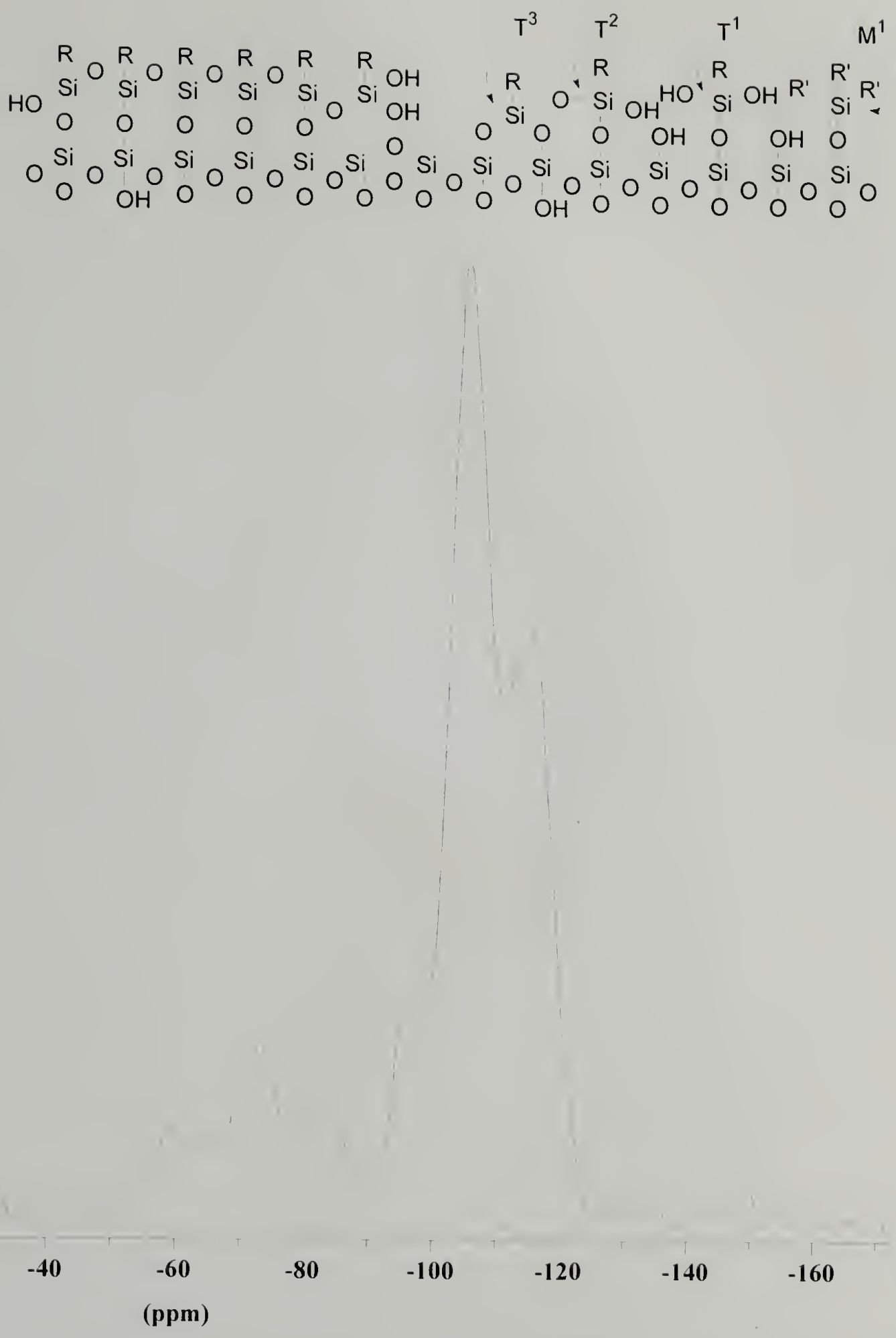

Figure 4.4 ^{29}Si NMR (CP-MAS) of Aminophenyl (AP) and Methyl (M) Functionalized Silica PXAM, Synthesized using Silica PX on treatment with 4-Aminophenyltriethoxysilane and Triethyoxymethylsilane (Q^2, δ –90), (Q^3, δ –100), (Q^4, δ –109), (T^3_{AP}, δ –78), (T^2_{AP}, δ –68), (T^3_M, δ –61), (T^1_{AP}, δ –58), (T^2_M, δ –51)

4.3.2 Catalyst Preparation and Characterization

Several features have gone into the design of the supported CGC system described here. A key consideration in the selection of the catalyst is that the site for covalent attachment to the amine-functionalized silica is remote from the catalytic site (metal-alkyl bond) and will not cleaved during activation and the catalytic cycle. Moreover, the reaction used to provide the linkage of the catalyst to the substrate via a primary amine is directly analogous to a step in the synthesis of the non-supported catalyst,[60] and thus the catalyst can be assembled readily on the substrate as shown in the case of aminomethylpolystyrene matrices. The CGC complex was assembled in a single step by reaction of the precursor titanium piano stool complex (**6**) with the *p*-aminophenyl functionalized silica substrates (**HXAM, HCAT, PXAM,** and **PCAT**, Figure 4.5); the experimental parameters are listed in Table 4.5.

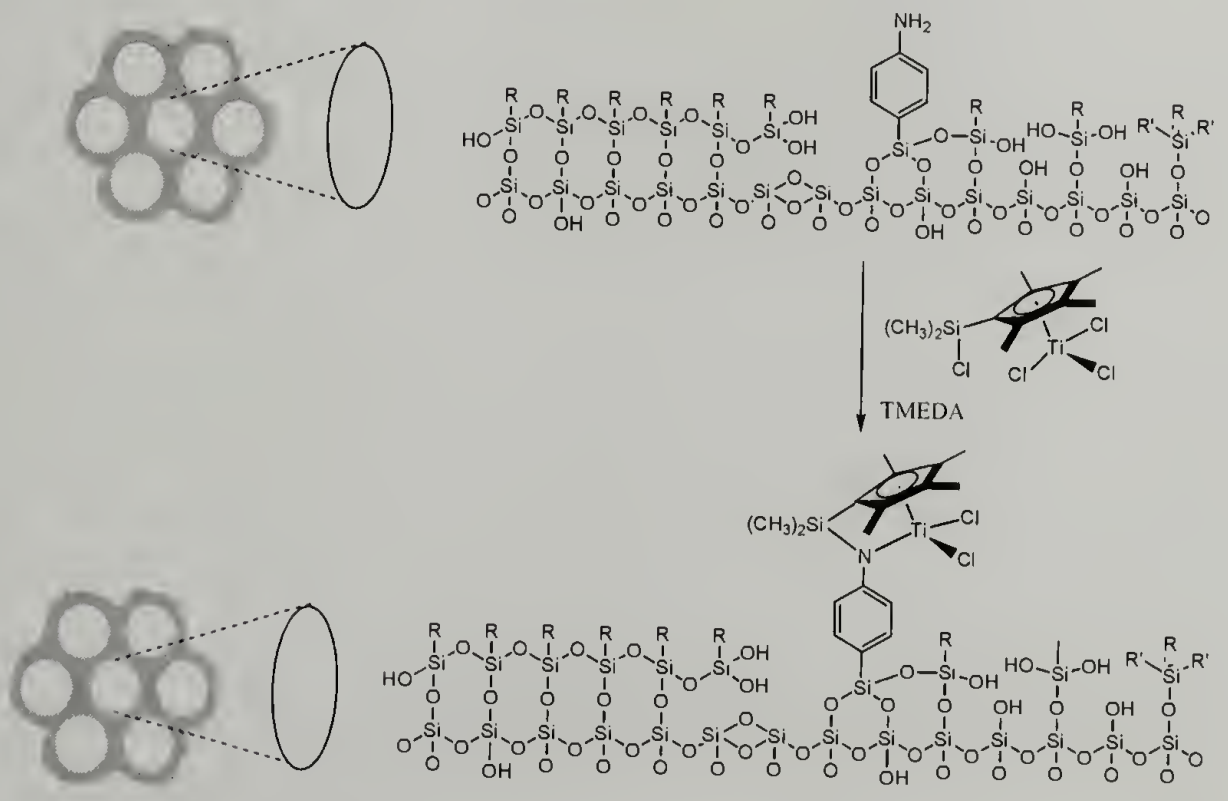

Figure 4.5 Assembly of Constrained Geometry Catalyst Within Mesoporous Silica using TMEDA as the base and Precursor Catalyst **6**

Table 4.5 Preparation of Supported CGCs on Amine Functionalized Mesoporous Silica

Silica Substrate (mg)	Sample	Titanium catalyst Precursor(**6**) (mg) [mmol]	Supported catalyst (mg)	Ti content (mmol/g)
HXAM (506.0)	HXAM-Ti	75.0 [0.20]	571.0	0.35
HC (514.9)	HCAT-Ti	88.7 [0.24]	559.2	0.43
PXAM (303.0	PXAM-Ti	79.0 [0.22]	381.9	0.56
PCAT (465.2)	PCAT-Ti	82.3 [0.22]	584.0	0.37

Formation of the intended CGC product was confirmed in each case by the appearance of a single new resonance at δ -23 to -27 ppm in the ^{29}Si CP MAS NMR spectrum (Example of ^{29}Si CP-MAS, Figure 4.6), which is distinct from the ^{29}Si resonance at -5 ppm observed for the precursor complex in solution. The chemical shift value is consistent with the value reported for the dimethylsilyl moiety of the analogous homogeneous CGC; the chemical shift value does not dramatically vary with different primary amines and cyclopentadienyl, tetramethylcyclopentadienyl, or indenyl ligand framework.[71] From the work of Pakannen and coworkers, it known that the chemical shift for the ^{29}Si NMR of piano stool complex (incompletely assembled CGCs, δ -5 to -12) appear at chemical shifts values that are well resolved from chemical shift of the silicon resonance of the CGC (completely assembled structure, δ -20) complex, when these complexes were assembled on silica surfaces. Hence, from the ^{29}Si NMR analyses of samples, **HXAM-Ti, HCAT-Ti, PXAM-Ti, PCAT-Ti**, complete assembly of the CGCs on mesoporous silica were observed.

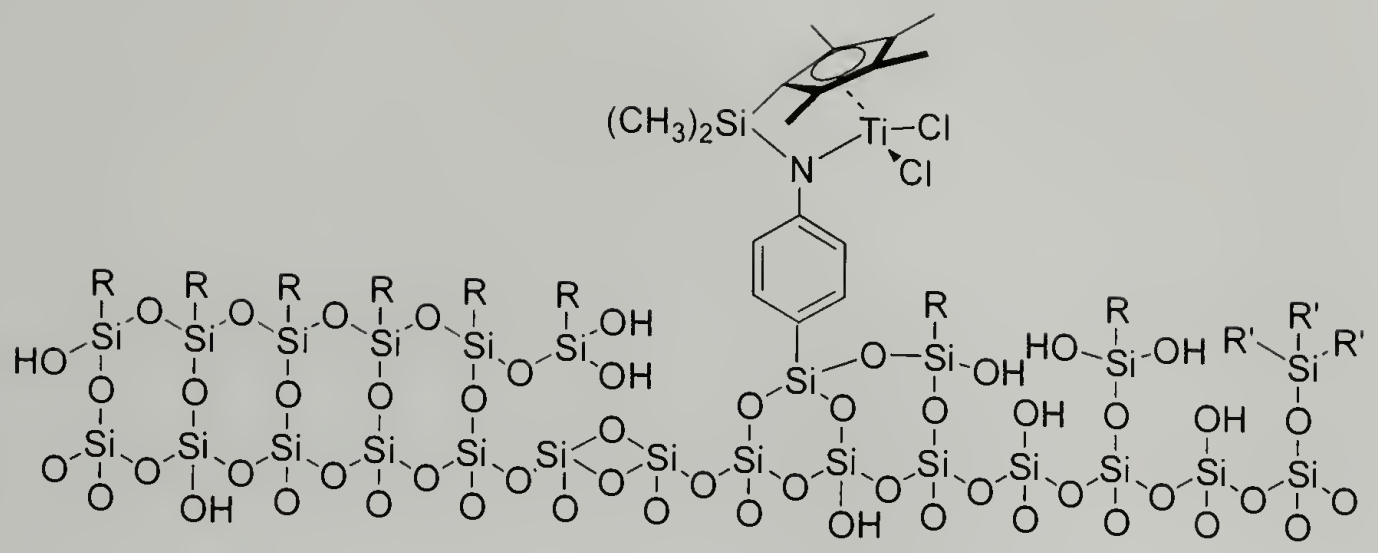

Figure 4.6 ^{29}Si (CP-MAS) of Constrained Geometry Catalyst (PXAM-Ti) within Mesoporous Silica (PXAM): δ –23 ($Si(CH_3)_2$) of CGC structure

4.3.3 Ethylene and 1-Octene Copolymerization Studies

The formation of copolymers of ethylene and 1-octene (LLDPE) can be used as evidence to verify the correct assembly of a CGC complex within mesoporous silica. Homogeneous CGCs incorporate 1-octene during ethylene/1-octene copolymerization[29], whereas the precursor titanium piano stool complex (**6**) or incompletely assembled CGCs (tethered piano stool complex) on amine-functionalized substrates polymerize ethylene but do not incorporate1-octene.

Copolymerization of ethylene and 1-octene was performed using CGCs assembled on aminophenyl grafted mesoporous silica, with MAO as the cocatalyst. Catalyst activity and polymer characterization data for each system are reported in Table 4.6. The catalytic activity of the supported CGCs for the production of polyolefins is 10-12.5 kg/atm.hr.mol Ti and is not dependent on the pore size of the silica matrix, silanol content, method of removal of the surfactant or the presence of different capping groups. The M_w of the copolymer is dependent on the pore size of the supported catalysts. Within a set of CGCs tethered to silica that have similar capping group contents and were prepared by the same surfactant extraction protocol (for instance, **HXAM-Ti** and **PXAM-Ti** or **HCAT-Ti** and **PCAT-Ti**), silica having larger pore sizes (**PXAM-Ti** or **PCAT-Ti**) produces LLDPE of higher molecular weight. The LLDPEs produced have polydispersities of 2.0-3.8 and about 1.5 mol % incorporation of 1-octene.

Table 4.6 Ethylene/1-Octene Copolymerization using Supported CGCs with MAO as the Cocatalyst

Sample	Ti (μmol)	Activity (kg/atm hr.mol Ti)[a]	M_w (x 10^{-5}) (g/mol)[b]	PDI[b]	T_m[c] (°C)	1-Octene incorporation (mol %)[c,d]
HXAM-Ti	4.3	10.1	3.0	2.0	123.0	1.5
HCAT-Ti	7.1	9.8	2.1	2.9	122.0	1.5
PXAM-Ti	7.6	12.3	3.2	3.0	124.0	1.5
PCAT-Ti	4.0	12.5	2.9	3.8	123.0	1.5

[a] Ethylene pressure=60 psig, 1-octene=5.0 mL, Reaction time=15-30 minutes
[b] Determined through GPC at 135 °C in TCB using light scattering detectors calibrated with PS standards
[c] From DSC measurements; second scan with a cooling rate of 10 °C/min
[d] From DSC measurement (depression in melting point) and ^{13}C NMR

From previous studies with CGCs assembled on aminomethylpolystyrene (Chapter 3), it was observed that at long reaction times, ethylene/1-octene copolymerization provides an assay for the presence of leached metal fragments from the supported CGCs since the leached catalytic species homopolymerizes ethylene but does not incorporate 1-octene during copolymerization studies. Hence, ethylene /1-octene copolymerization studies using CGCs assembled within mesoporous silica were run for 20-30 minutes to minimize catalyst leaching. The supported CGCs show lower activity compared to the homogeneous CGCs for ethylene/1-octene copolymerization. The activity of the supported catalyst for the production of ethylene-octene copolymers (LLDPE) is not dependent on the pore size, total silanol content, surface area or the wall thickness of the supported catalysts. On the other hand, the molecular weight of the product copolymers is dependent on the substrate pore size, with larger pore materials affording copolymers of higher molecular weight, likely due to an influence of pore size

on monomer transport to the catalyst sites (Figure 4.7). The copolymers show broad polydispersity indices (PDI=2-4), which are indicative of diffusion limitations of ethylene and 1-octene to a certain CGC sites within the mesoporous silica.

Polyethylene and polyethylene-based copolymers are semicrystalline materials that have well-documented melting endotherms (T_m) and heat of fusion (ΔH_f). HDPE is made of up of linear polyethylene chains that have fewer than four short chain branches per thousand carbon atoms and which has a melting point of greater than 130°C. By contrast, LLDPE, which is a copolymer of ethylene that contains a comonomer such as 1-octene, has a depressed melting point and heat of fusion relative to HDPE. The depression in melting point and heat of fusion is attributed to the disruption of the crystalline polyethylene domains by the hexyl branches from the octene units in the copolymers. Similarly, it is observed that the differential scanning calorimetry (DSC) of the product polymers reveals a melting endotherm (T_m) for each sample at 122–124 °C, which can be attributed to the presence of 1-octene units within the polymer (Table 4.6). A linear correlation exists between the extent of 1-octene incorporation and the observed depression in melting point relative to the melting point of HDPE.[72] For the polymers synthesized using the supported CGCs **HXAM-Ti, HCAT-Ti, PXAM-Ti** and **PCAT-Ti**, the 1-octene content was determined to be 1.5 mol %.

The percent crystallinity of polyethylene was determined from the ratio of the heat of crystallization of the polymer to the heat of crystallization of a single crystal of polyethylene (ΔH = 293 J/g), expressed as a percentage. Incorporation of 1-octene also reduces the degree of crystallinity of the polymer. The low percent crystallinity

(approximately 8–10%) observed for the product copolymers is consistent with the presence of hexyl branches due to incorporation of 1-octene.

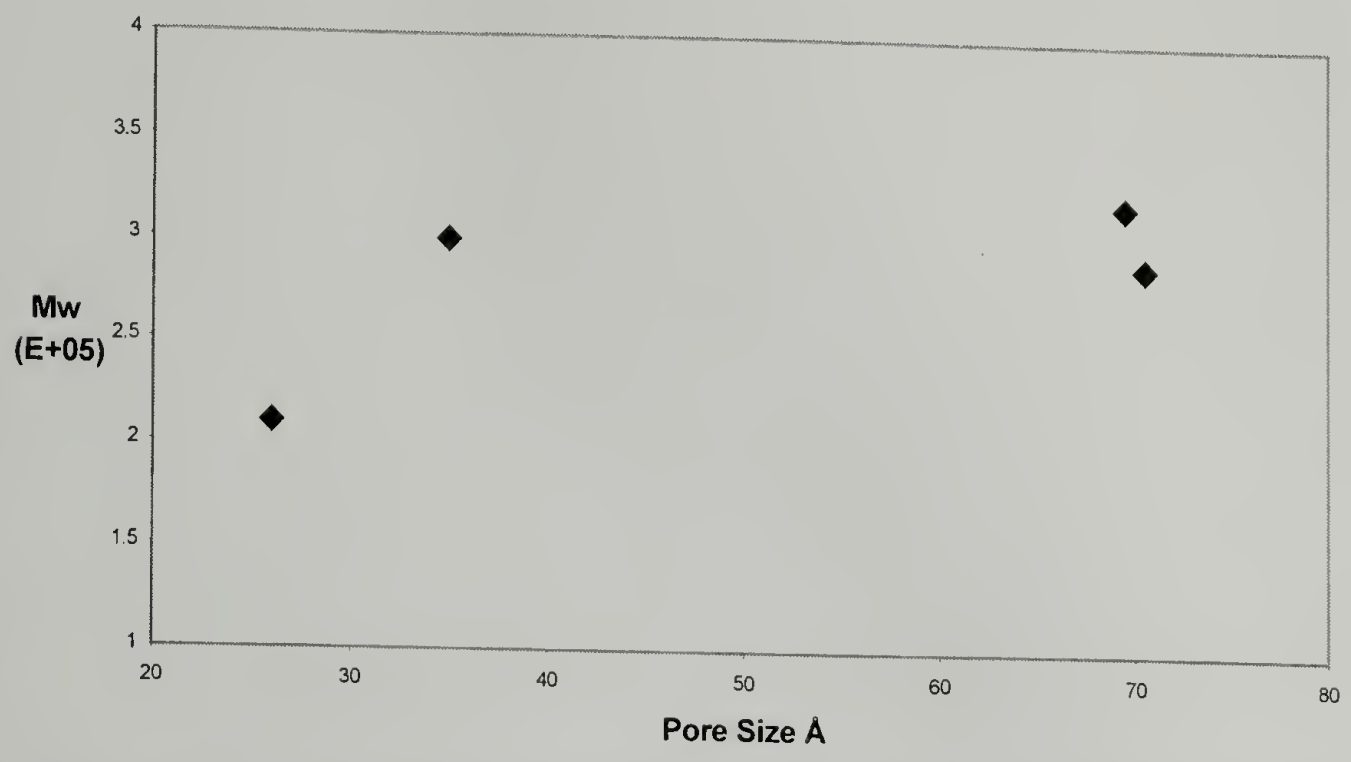

Figure 4.7 Plot of Weight Average Molecular Weight of Ethylene–Octene Copolymer (LLDPE) vs. Pore Size of the Silica Matrix

The extent of 1-octene incorporation was evaluated by solution ^{13}C NMR of the product polymers. The observation of resonances, δ 14.22 (1s+1B_6, CH_3, EOE+EOO+OOE+OOO), 22.89 (2s+2B_6, EOE+EOO+OOE+OOO), 27.21 (βδ+5B_6, EOE), 29.99 (δδ, EEE), 30.08 (δδ+4B_6, EEE), 30.5 (αδ+6B_6, EOE) 32.17 (3s+3B_6, EOE), 34.45 (αδ+6B_6, EOEE+EEOE), confirms the presence of hexyl branches due to 1-octene incorporation.[7] The 1-octene content, which is calculated from the relative integrated intensity of the 1-octene resonances, was determined to be 1.5 mol %, which is consistent with value obtained from the analysis of melting temperature.

To summarize the ethylene/1-octene copolymerization studies, it was determined that only completely assembled CGCs within silica gives rise to the desired polymerization chemistry; namely the formation of LLDPE. This is in contrast to the

leached or incompletely assembled CGCs moieties, which afford only HDPE, which can be distinguished by product analysis. Thus, the copolymerization studies provide a built in assay for the identity of the surface-supported species.

4.3.4 Ethylene Homopolymerization in Conjunction with MAO as the Cocatalyst

The effects of the primary ligand architecture of SSCs on the production of polyethylene of different molecular weights, branch contents, melting points, and degrees of crystallinity are well studied. Polymerization of ethylene was investigated using silica supported CGCs (**HXAM-Ti, HCAT-Ti, PXAM-Ti, PCAT-Ti**) in conjunction with MAO as the cocatalyst in order to evaluate the influence of the substrate (the "second sphere of influence") on the properties of the polymer product; previous ethylene homopolymerization studies using CGCs, metallocenes, and piano stool complexes tethered to inorganic and organic supports have indicated that catalyst activity is lower than that observed for the analogous homogeneous systems.[50] Catalyst activity, polymer molecular weight, polydispersity index, polymer melting point, and percent crystallinity are reported in Table 4.7 for each system investigated here.

Table 4.7 Ethylene Homopolymerization using Supported CGCs with MAO as the Cocatalyst

Sample	Ti (μmol)	Activity (kg/atm. hr. molTi)[a]	M_w (x 10^{-5}) (g/mol)[b]	PDI[b]	T_m[c] (°C)	Percent Crystallinity[d]
HXAM-Ti	3.6	5.5	2.3	1.9	137.9	36.0
HCAT-Ti	7.2	43.7	2.0	2.7	134.8	27.0
PXAM-Ti	7.5	19.7	3.6	2.5	133.1	22.0
PCAT-Ti	3.5	28.8	3.9	2.0	133.7	23.7

[a] Ethylene pressure=60 psig, Reaction time=15-30 minutes

[b] Determined through GPC at 135 °C in TCB using light scattering detectors calibrated with PS standards

[c] From DSC measurements; first scan with a cooling rate of 10 °C/min

[d] ΔH_f obtained from DSC first scan, % crystallinity calculated with respect to a polyethylene single crystal ΔH_f=293 J/g

The catalytic activity of the supported CGCs for the production of polyethylene is not dependent on the pore size of the silica matrix, silanol content, method of removal of the surfactant or the presence of different capping groups. The M_w of the polyethylene is dependent on the pore size of the supported catalysts. Within a set of CGCs tethered to silica having similar capping groups and surfactant extraction protocol (for instance, **HXAM-Ti** and **PXAM-Ti** or **HCAT-Ti** and **PCAT-Ti**), silica having a larger pore size (**PXAM-Ti** or **PCAT-Ti**) produces HDPE of higher molecular weight (Figure 4.10). On the other hand, within a set of CGCs tethered to silica having similar capping groups and surfactant extraction protocol (for instance, **HXAM-Ti** and **PXAM-Ti** or **HCAT-Ti** and **PCAT-Ti**), silica having larger pore sizes (**PXAM-Ti** or **PCAT-Ti**) produces HDPE of lower percent crystallinity Figure 4.9).

Similarly, using the silica supported CGCs, it was observed that the activity for production of polyethylene is lower than observed for analogous homogeneous catalysts. For the current systems, each polyethylene product has a unimodal molecular weight distribution, as detected by GPC. Polyethylene produced from the supported catalyst has polydispersity indices of 1.9-2.5, which is comparable to polyethylenes prepared from analogous homogeneous single site catalysts. The molecular weight of the polyethylene is dependent on the substrate pore size, with larger pore materials affording polymer of higher molecular weight. The lower molecular weights of the polymers formed by the smaller pore systems can be attributed to limitations on diffusion of ethylene to the active sites (Figure 4.8).

The polyethylene products have melting temperatures in the range of 133–137°C and percent crystallinity values of 22–36%, which suggests that the crystallinity of these samples is lower than that of HDPE produced using homogeneous SSCs;[87] a similarly lower degree of crystallinity has been observed for polyethylene synthesized using the CGC supported on aminomethylpolystyrene. In the current system, however, the crystallinity of the polyethylene produced using the CGC supported on porous silica can be tuned by varying the pore size of the substrate, with smaller-pore substrates giving rise to a higher degree of crystallinity than the larger-pore substrates. The growth of the polymer is from a metal–alkyl bond within the pore, and as the polymer grows it is transformed into ordered crystalline components, intermediate component (which is an interface between crystalline and amorphous components) and the disordered amorphous component. The percentage of each of these components influences the crystallinity of the polyolefin synthesized. When polyethylenes are prepared from smaller pore materials, there is less number of confirmations in which the polymer can exist within the pore; hence as the polymer is formed it is pushed into the ordered crystals phase and is kinetically trapped in the more ordered crystalline phase. This contributes to an increase in crystallinity of the polyolefin prepared. On the other hand, polyethylenes produced from supports with larger pore sizes, can exist in more number of confirmation. As the polyethylene is formed, the polymer is pushed into intermediate component affording polyethylenes of lower crystallinity.

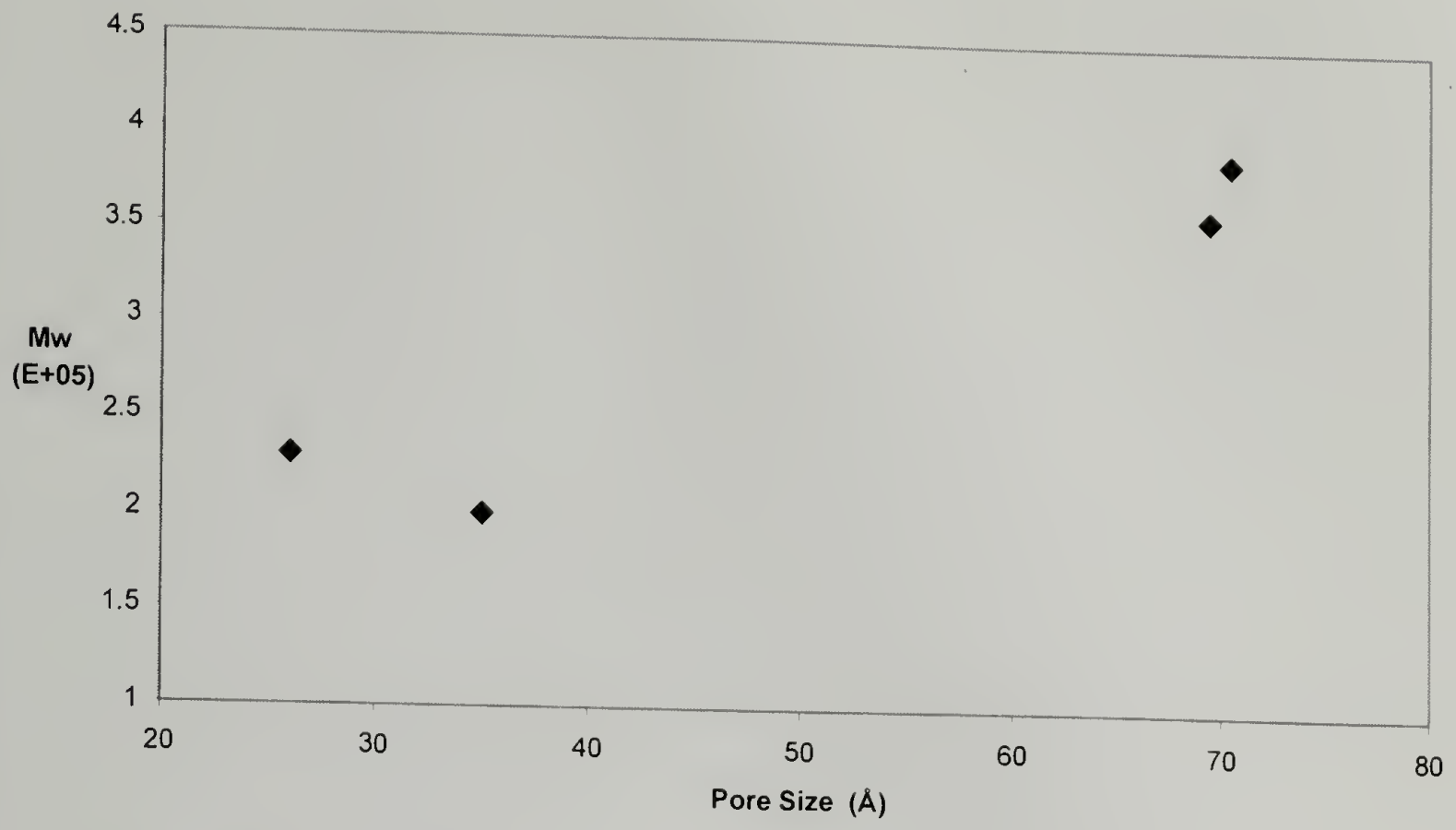

Figure 4.8 Plot of Weight Average Molecular Weight of Ethylene Homopolymer (HDPE) vs. Pore Size of the Silica Matrix Produced in Conjunction with MAO as the Cocatalyst

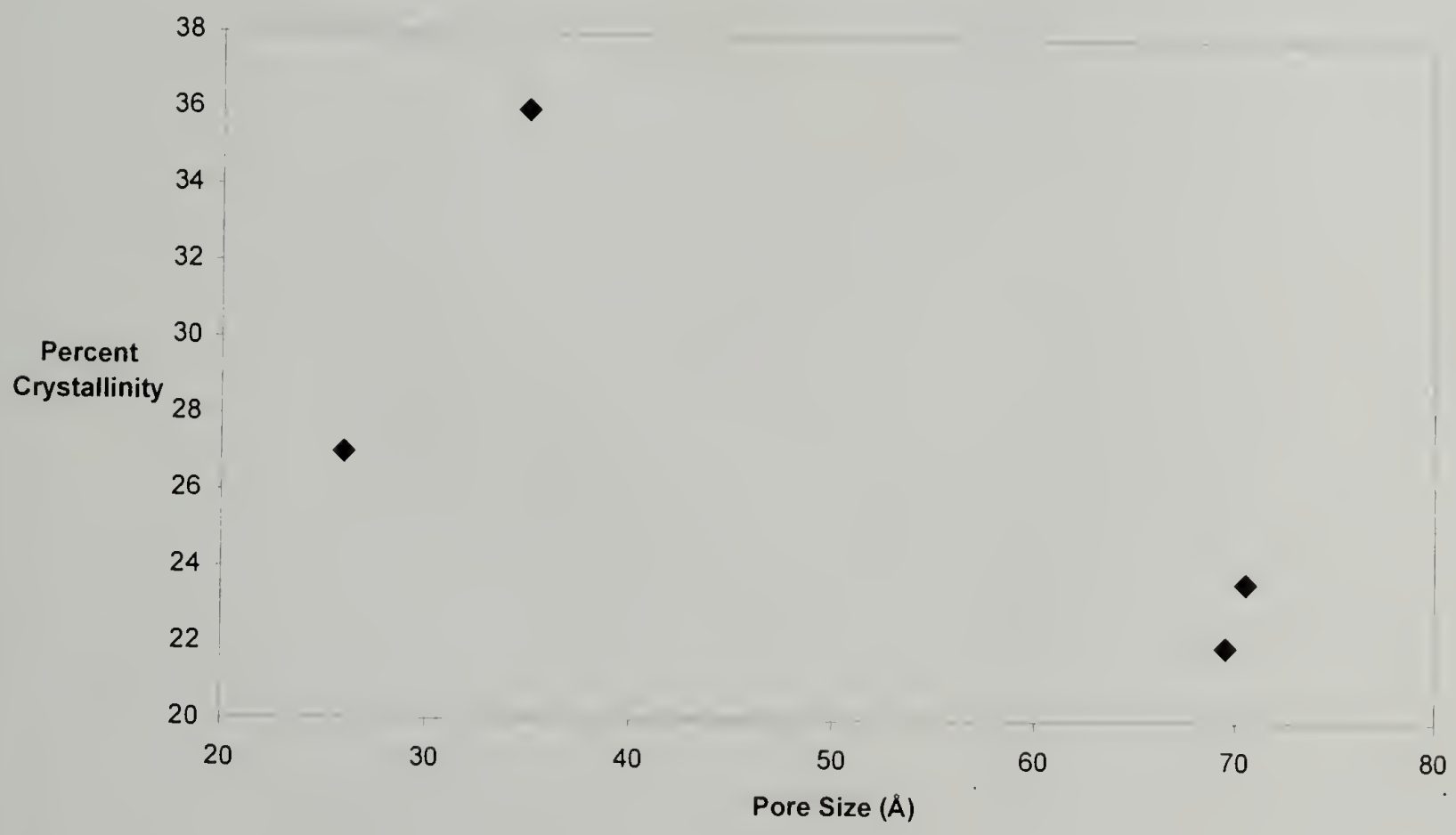

Figure 4.9 Plot of Percent Crystallinity of Ethylene Homopolymer (HDPE) vs. Pore Size of the Silica Matrix Produced in Conjunction with MAO as the Cocatalyst

4.3.5 Ethylene Homopolymerization: Effect of Counterion

During olefin polymerizations involving a group 4 metal catalyst, the activated metal is present as a cation and is balanced by a non-coordinating anion. The interactions between this contact ion pair has a significant influence on the catalytic activity and lifetime of the active species, chain-termination and chain-transfer processes.[11] Consequently there is a need to study the polymerization properties of the silica supported titanium cation and cocatalyst anion.

Ethylene homopolymerization was peformed with CGCs supported within mesoporous silica, in conjunction with MAO as the alkylating agent. Cocatalysts **II** ($[(C_6H_5)_3C][B(C_6F_5)_4]$, Table 4.8) or **III** ($[(C_6H_5)N(CH_3)_2)H][(B(C_6F_5)_4)]$, Table 4.9) was added and the system was pressurized with ethylene. Under comparable conditions, catalytic system containing the metal cation and a borate counterion affords polyethylene with higher activity than polymerizations catalyzed by metal cation and aluminate anion.

Table 4.8 Ethylene Homopolymerization using Supported CGCs with $[C_6H_5)_3C][B(C_6F_5)_4]$ **(II)**

Catalyst	Ti (μmol)	Activity Kg/atm.hr. mol Ti [a]	T_m [b]	Percent Crystallinity[c]	M_w [d] $*10^5$
PXAM-Ti	8.1	31.48	133.8	21.0	3.1
PCAT-Ti	7.0	27.3	134.8	24.0	3.3
HXAM-Ti	8.1	35.8	136.8	31.9	2.9
HCAT-Ti	7.9	98.7	139.8	36.9	2.1

[a] Ethylene pressure 60 psig (4 atm), Reaction time=10-15 mins
[b] Determined by DSC (first melt) with heating and cooling cycles at 10°C/min, under nitrogen purge
[c] ΔH_f obtained from DSC first scan, % crystallinity calculated with respect to a polyethylene single crystal ΔH_f=293 J/g
[d] Determined by GPC at 135°C using light scattering detector and calibrated using polystyrene standards, PDI=1.8-2.4

Table 4.9 Ethylene Homopolymerization using Supported CGCs with $[C_6H_5)N(CH_3)_2H][B(C_6F_5)_4]$ (**III**)

Catalyst	Ti (μmol)	Activity Kg/atm.hr.mol Ti [a]	T_m [b] °C	Percent Crystallinity[c]	M_w [d] $*10^5$
PXAM-Ti	8.0	30.1	134.6	23.8	1.85
PCAT-Ti	7.1	30.4	135.9	31.4	1.8
HXAM-Ti	8.2	25.6	138.4	49.1	1.6
HCAT-Ti	8.1	60.6	137.0	34.8	1.65

[a]Ethylene pressure 60 psig (4 atm), Reaction time=10-15 mins
[b]Determined by DSC (first melt) with heating and cooling cycles at 10°C/min, under nitrogen purge
[c]ΔH_f obtained from DSC first scan, % crystallinity calculated with respect to a polyethylene single crystal ΔH_f=293 J/g
[d] Determined by GPC at 135°C using light scattering detector and calibrated using polystyrene standards, PDI=1.7-2.5

The effect of the counterion on the percent crystallinity and molecular weight of the polyolefin was analyzed. Similar to the MAO cocatalyzed polymerizations, larger pore silica supported CGCs/MAO/**II** or silica supported CGCs/MAO/**III** (Figure 4.10 and Figure 4.12) afford polyethylene with higher molecular weight but lower crystallinity. The trends in molecular weight of polyethylene are in keeping with the expectation that larger pores offer no diffusion problems to the monomer, affording higher molecular weight polyethylene. On the other hand, CGCs within smaller pore silica face monomer transport problems to the active sites, leading to polyethylenes of lower molecular weight.

The characteristics of metal cation and the cocatalyst anion play an important role in the production of polyethylene with a range of molecular weight. For instance, CGCs supported on silica with cocatalyst **II** (Table 4.8) affords polyethylenes produced with comparable activity and percent crystallinity compared to the use of cocatalyst **III** (Table 4.11, Figure 4.13) under similar reaction conditions. However, the molecular weight of

polyethylene produced from CGC-silica/**II** is higher than polyethylene produced from CGC silica/**III.** The observed depression in the molecular weight of polyethylene produced from CGC silica/**III** can be can be attributed to the coordination of the dimethylaniline co-product to the cationic titanium center. On the other hand, 1,1,2-triphenylethane is formed during the metal activation protocol from CGC-silica/**II** (Table 4.8), this presumably does not interact with the metal center.

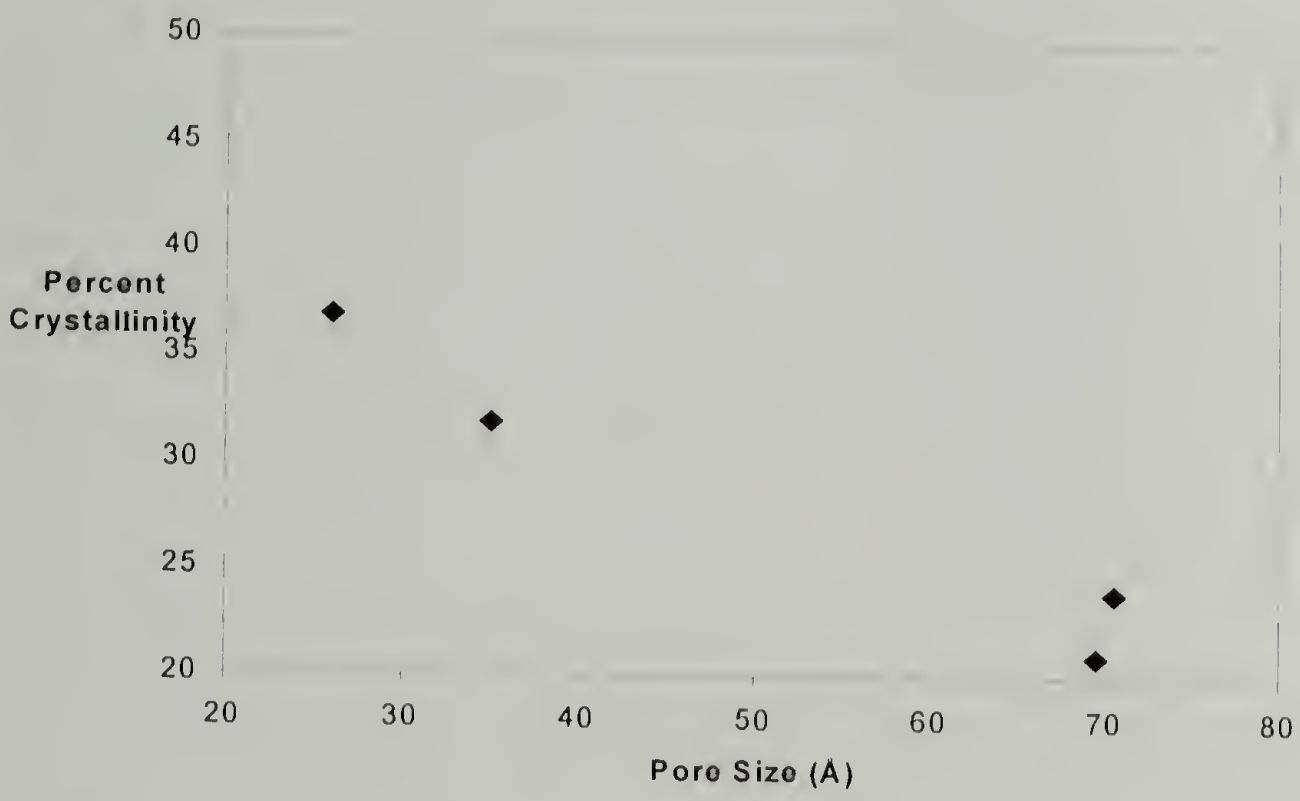

Figure 4.10 Plot of Weight Average Molecular Weight of Ethylene Homopolymer (HDPE) vs Pore Size of the Silica Matrix Produced in Conjunction with Trityl Borate (**II**) as the Cocatalyst

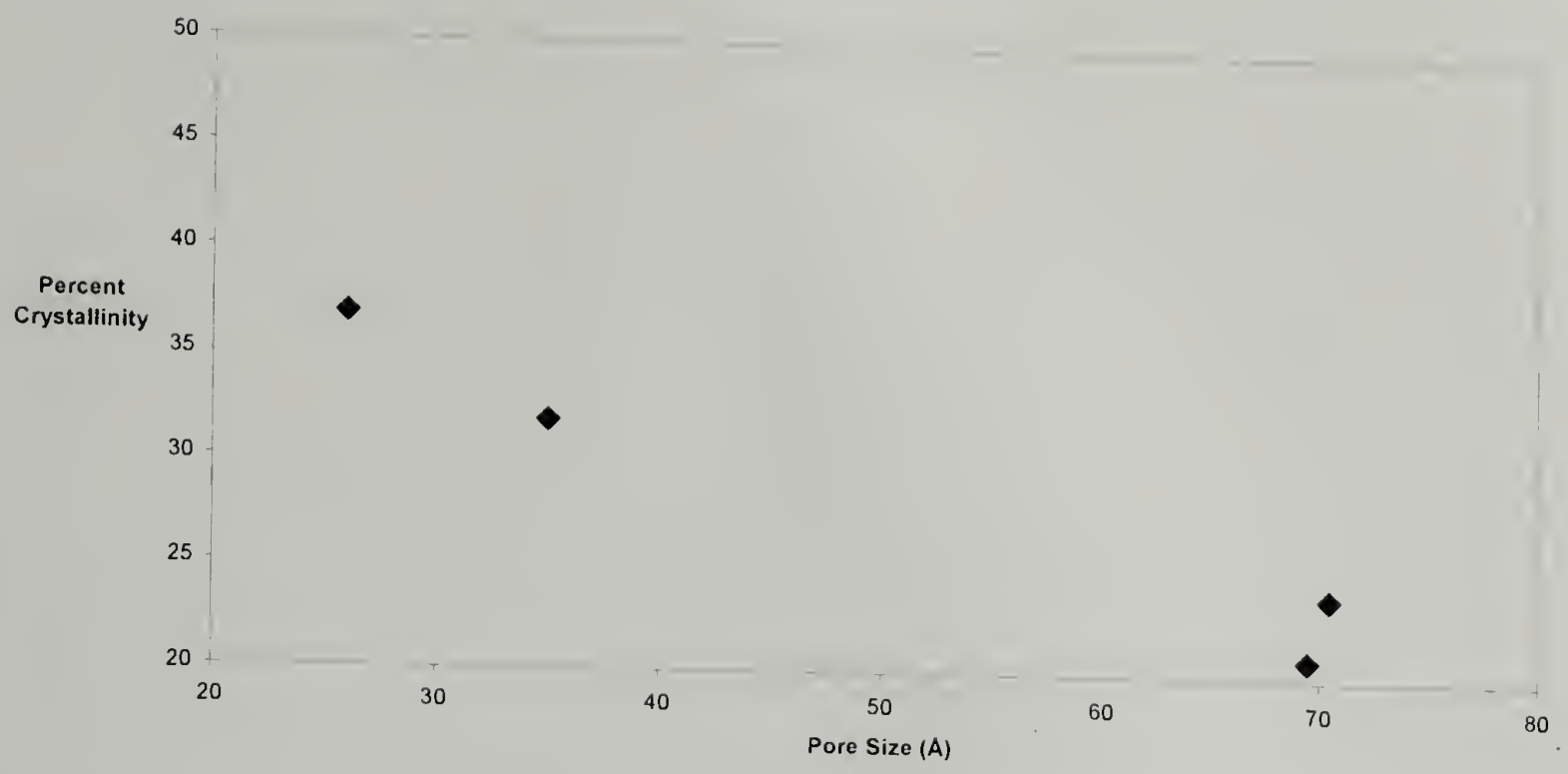

Figure 4.11 Plot of Percent Crystallinity of Ethylene Homopolymer (HDPE) vs Pore Size of the Silica Matrix Produced in Conjunction with Trityl Borate (**II**) as the Cocatalyst

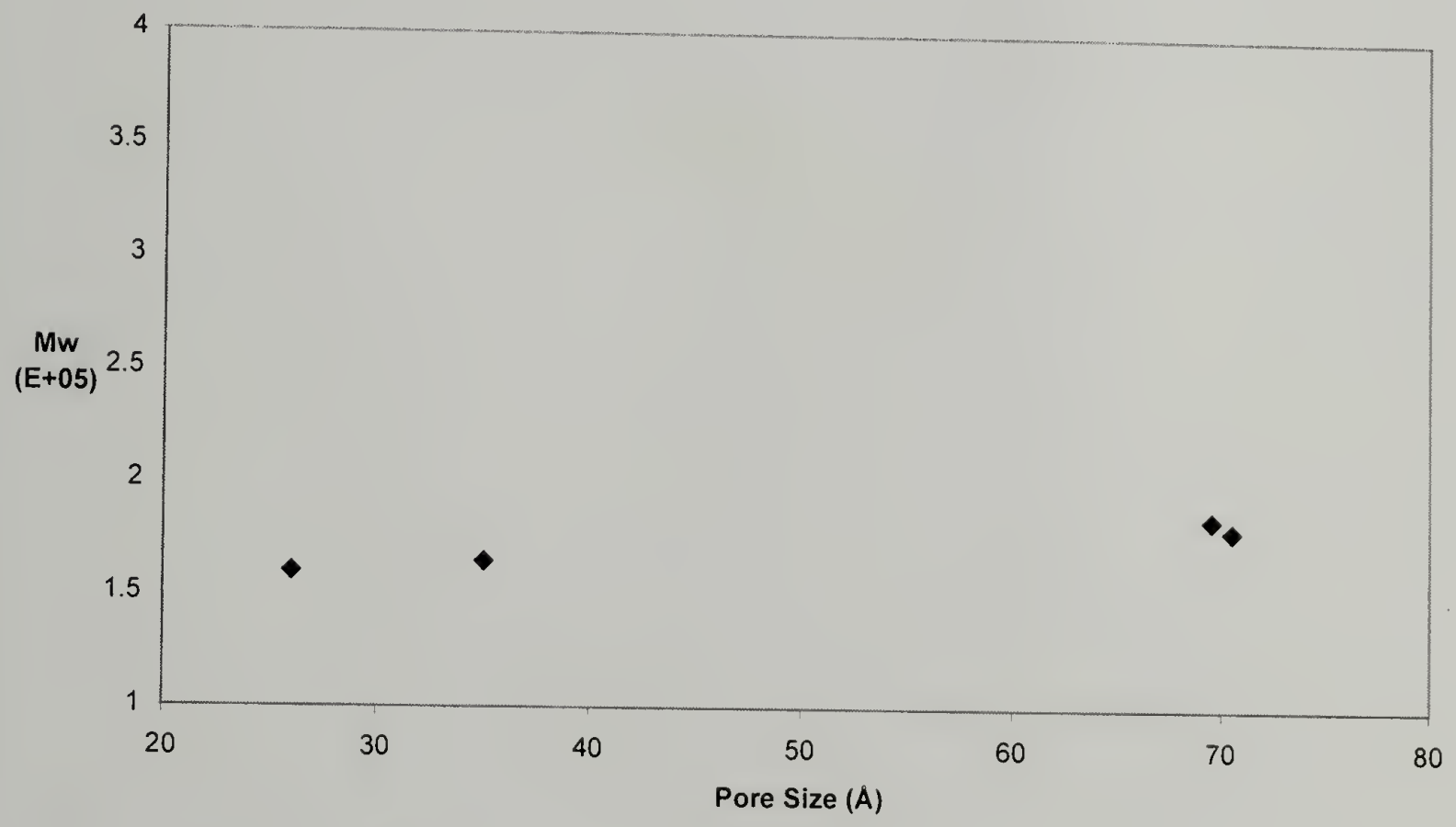

Figure 4.12 Plot of Weight Average Molecular Weight of Ethylene Homopolymer (HDPE) vs Pore Size of the Silica Matrix Produced in Conjunction with Anilinum Borate (III) as the Cocatalyst

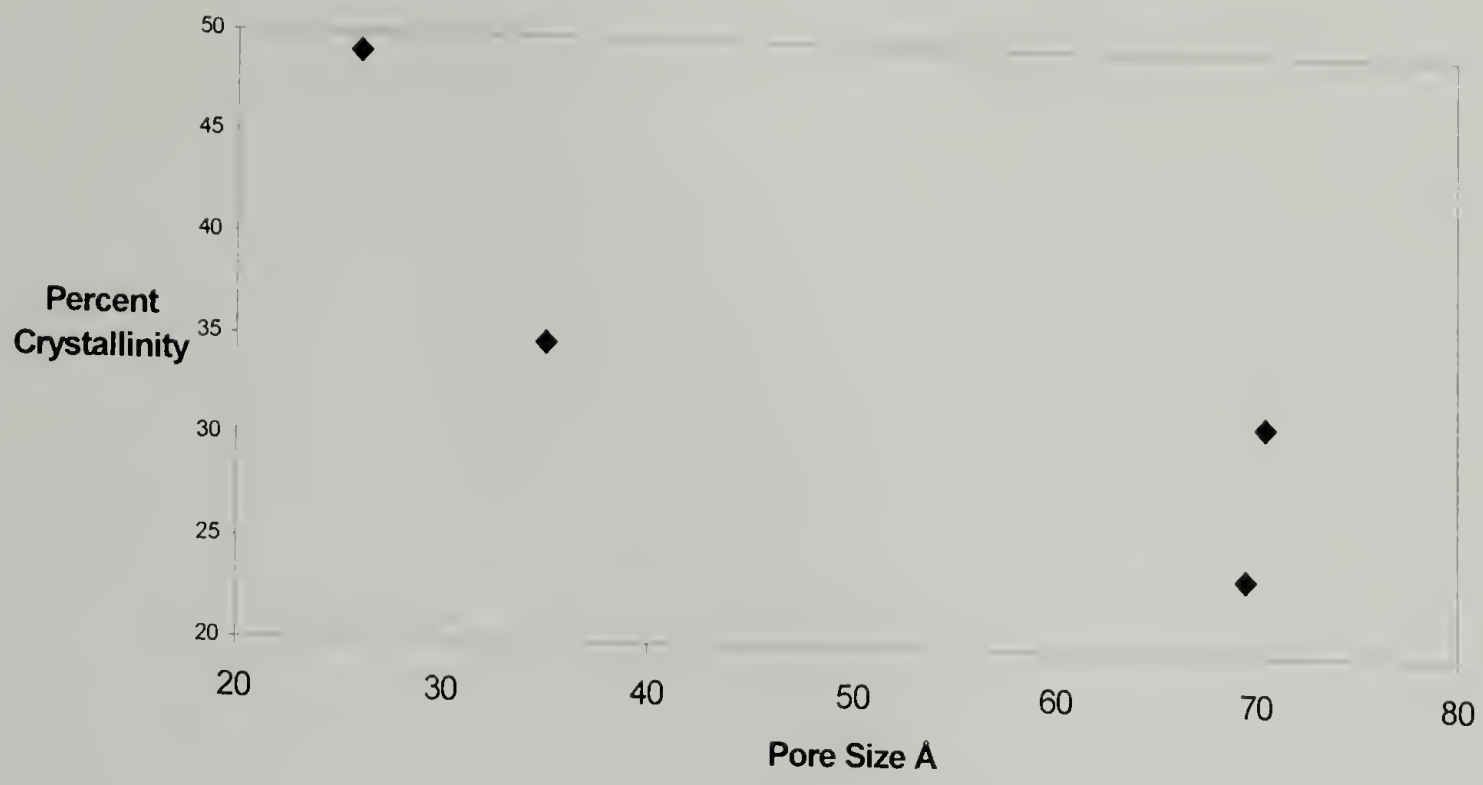

Figure 4.13 Plot of Percent Crystallinity of Ethylene Homopolymer (HDPE) vs Pore Size of the Silica Matrix Produced in Conjunction with Anilinium Borate (**III**) as the Cocatalyst

4.4 Summary

Mesoporous silica with different pore sizes, silanol content, and surface area has been synthesized. Amine groups are introduced when silica is treated with 4-aminophenyltrimethoxysilane. The remaining silanol groups are capped with either methyltrimethoxysilane or triemethylmethoxy silane. Subsequently, protocols for supporting titanium complexes **6** on amine functionalized mesoporous silica matrix affording constrained geometry catalysts have been established. Verification of the presence of the support CGC framework is evident by the formation of LLDPE from the copolymerization studies of ethylene and 1-octene. Characterization of the molecular

weight, molecular weight distribution, melting points, and enthalpy of fusion have been determined for these copolymers. The degree of crystallinity of the polyolefins synthesized from these supported catalysts is substantially reduced relative to polymers produced using soluble CGCs. However, the effect of the support is seen in the production of polyethylenes with a range molecular weights and percent crystallinity. Catalysts within smaller pore materials afford polyethylenes of lower molecular weights but higher percent crystallinity, irrespective of the cocatalyst used. The plausible reasons for the dependence of the properties of polyethylene on the pore sizes of the silica matrices have been discussed.

CHAPTER 5

COMPARISON OF POLYMER PROPERTIES PREPARED USING CONSTRAINED GEOMETRY CATALYSTS (CGCs) TETHERED TO SILICA OR POLYSTYENE SUPPORTS

5.1 Introduction

The influence of metal-ligand architecture on the performance single site catalyst for the production of polyolefins has been well established.[21,22,37] Single site catalysts need to be adapted in order that they can be used in large-scale commercial polyolefin production. The catalyst needs to be attached either by covalent or ionic interaction onto solid supports such as silica, alumina, polystyrene or polysiloxanes. Once attached, these catalysts can be used in gas phase or slurry processes for polyolefin production.[53] An important question must first be addressed: does the support influence the physical properties of polyolefins produced? In the investigation of the support influence on polyolefin production, the first step was to identify a class of single site catalysts and support matrices that could be used. Subsequently, methods to tether SSC to the support matrices had to be designed. These supported SSCs were then be used as model systems to explore the question of support influence.

The single site catalysts that have been used in this study are Constrained Geometry Catalysts (CGCs). There are two synthetic routes by which CGCs can be assembled on amine-functionalized supports. These include amine elimination chemistry and adaptation of the precursor piano stool complexes prepared by a silyl elimination route to amine functionalized solid supports.[66-69,75,88] In the amine elimination route, coordination of the eliminated amine to the metal center in the CGC can be problematic.

The presence of the coordinated amine reduces the activity of the metal center. The active catalystic sites from metal-amide complexes are obtained by activation of these complexes with MAO. However, complete activation of metal-amide bond is difficult to achieve and results in a mixture of partially activated and completely activated complexes. The multi-site catalytic system affords polymers with broad molecular weight distribution. To overcome the problems associated with amine elimination chemistry, synthetic routes to prepare precursor piano stool complexes by silyl elimination chemistry have been developed (Chapter 2). Adapting the work of Royo to amine fuctionalized supports, precursor catalyst **6** was treated with support matrices containing primary amine units. By this route, complete assembly of CGC is thus possible in a single step. The site of activation of the metal-halide moieites and the site of polymcrization are isolated from the site of attachment of the CGC to the support matrix. Methods for assembly of CGC on aminomethylpolystyrene (Chapter 3) and amine-functionalized silica (Chapter 4) have been developed. The assembled CGCs were identified by solid-state ^{29}Si CP-MAS NMR. The CGCs are known to produce ethylene and 1-octene copolymers (LLDPE), while the precursor piano stool complex affords high-density polyethylene from attempts to ethylene and 1-octene. This observation affords direct proof of the correct assembly of the CGC framework on the support matrices.

The ethylene homopolymers and copolymers snthesized from these supported catalysts have been characterized. In this chapter, the properties of the polyolefins synthesized from CGCs within two very different support matrices will be compared.

5.2 Support Characteristics

Recognizing that the AMPS and silica matrices are different in their structural components; we have chosen the material properties shown in Table 5.1 to compare and contrast the features of the supports. The AMPS matrix is less-ordered, amorphous, semiflexible with irregular micropores, and has a broad distribution of the pore sizes (500-1000Å). On the other hand, the silica matrices are ordered, amorphous, rigid with hexagonally arranged mesopores and have tunable pore sizes (Figure 5.1). The supports have tethered primary amines onto which CGCs can be assembled. In this comparison study, the properties of the matrices namely, including order, rigidity ,and pore sizes, have been used to compare between the observed polyolefin properties and the supported single site catalysts.

Table 5.1 Material Properties of AMPS and Silica Matrices

Material Property	**AMPS**	**Silica**
Order/Crystallinity	Less-ordered, Amorphous	Highly ordered, Amorphous
Rigidity	Semiflexible	Rigid
Regularity of pore	Irregular	Regular, cylindrical, hexagonally arranged pore
Pore dimensions	Microporous (> 500μm)	Single pore size in a given sample, tunable (30-80Å)
Polarity	Completely hydrophobic interior	Hydrophobic/hydrophilic tunable depending on the capping groups

5.3 CGC Assembly Protocol

Piano stool complexes that are the precursor to CGCs have been synthesized by silyl elimination chemistry as shown in Chapter 2. It was noted that CGC assembly using precursor piano stool complex **3** and the support matrix (AMPS and amine-functionalized silica) afforded a mixture of the completely assembled CGC form as well as tethered piano stool complexes. However, optimization of reaction conditions using precursor catalyst **6** has yielded completely assembled CGC on AMPS and amine-functionalized silica.

The CGC covalently bound to AMPS used for the comparison study is **AMPS-Ti-12**; the assembly protocol and polymerization results have been presented in Chapter 3. The CGCs tethered to amine-functionalized silica have also been prepared (Chapter 4). Silica supported CGCs used for the comparison study include **HXAM-Ti, HCAT-Ti, PXAM-Ti** and **PCAT-Ti**, where **H** refers to the small pore materials and **P** refers to the large pore materials, **X** and **C** refer to the surfactant removal protocol, namely, solvent extraction or calcinations, respectively. Finally, **A** and **M** or **T** refer to the capping units which are aminophenyl and trimethylsilyl or aminophenyl and methylsilyl units (Figure 5.1 and 5.2)

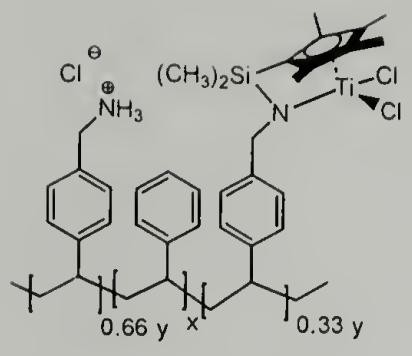

AMPS-Ti-12

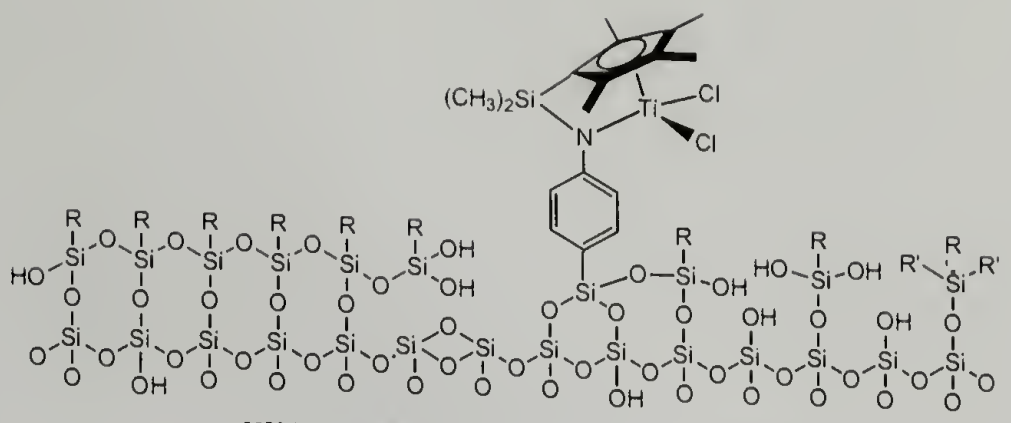

HXAM-Ti, HCAT-Ti, PXAM-Ti and PCAT-Ti

Figure 5.1 Constrained Geometry Catalysts Confined Within AMPS and Amine-Functionalized Silica

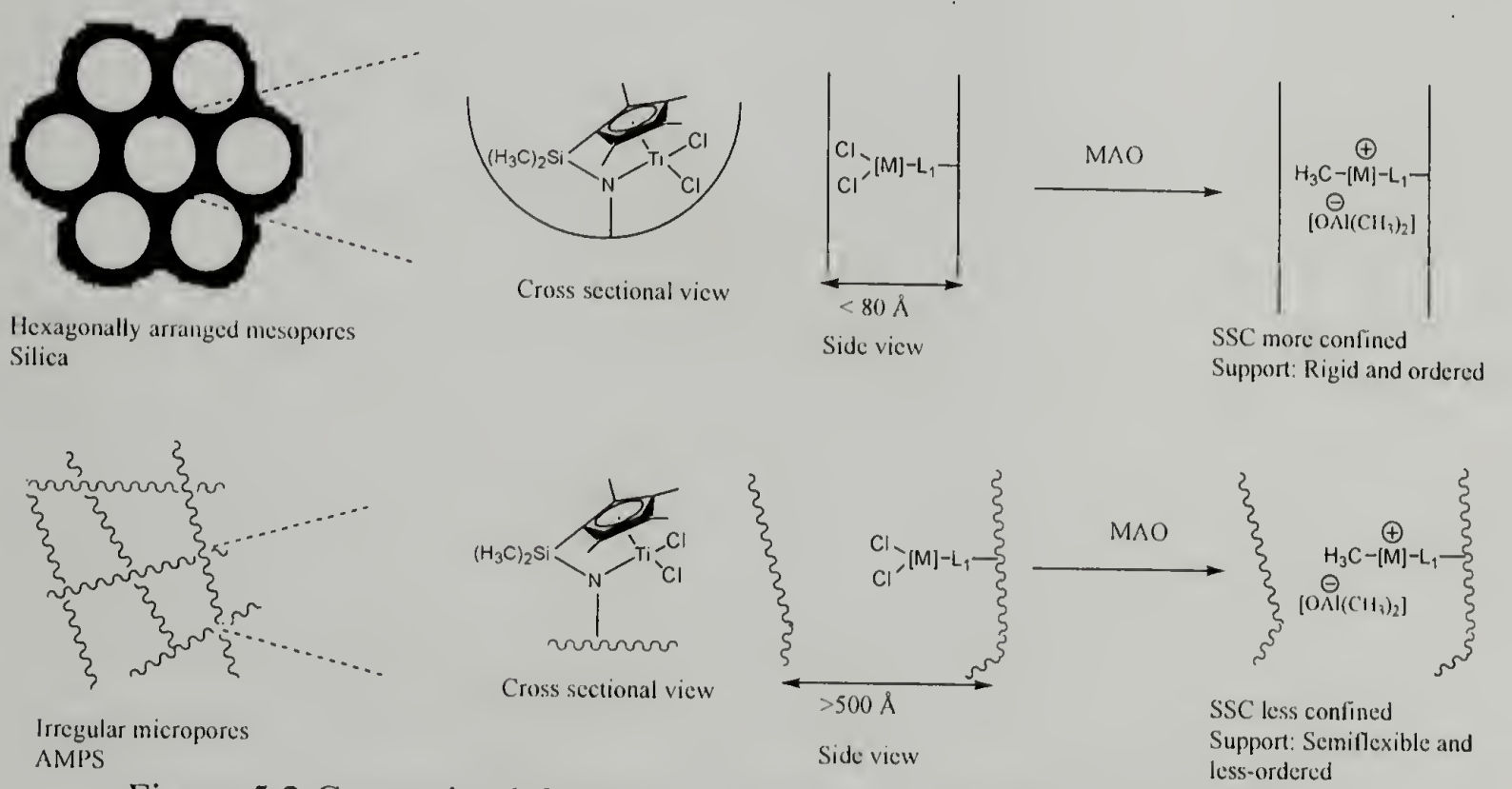

Figure 5.2 Constrained Geometry Catalysts Confined Within AMPS and Amine-Functionalized Silica: Cross sectional and Side View

5.4 Ethylene and 1-Octene Copolymerization using Supported CGCs in Conjunction with MAO as the Cocatalysts

Ethylene homo and copolymers have been prepared from supported catalysts and their physical properties were compared in order to investigate the support influence. The impact of the support matrix on the weight average molecular weight (M_w), PDI, and comonomer incorporation of LLDPE was studied. The molecular weight (M_w) of LLDPE obtained from **AMPS-Ti-12** was found to be higher than the analogous silica based CGCs. The trend in molecular weight of LLDPE produced as a function of the supported catalyst is shown in Figure 5.3. The M_w of the copolymers prepared from **AMPS-Ti-12** is higher than that of the copolymers prepared from the silica based CGCs (**HXAM-Ti** and **PXAM-Ti**). The formation of higher molecular weight polyethylene from CGCs within polystyrene supports has been attributed to the active titanium catalyst being more accessible in a semiflexible, solvent swollen, microporous polystyrene matrix than in the rigid, more ordered, mesoporous silica matrices. The copolymers prepared from a set of silica matrices with similar surfactant removal and capping chemistry but different pore sizes (30 and 70 Å), **HXAM-Ti** and **PXAM-Ti** respectively, were compared. The larger pore material afforded LLDPE of higher M_w. This observation is in keeping with diffusion limitations of the monomers to the active site in smaller pore silica matrices being responsible for the decrease in M_w. Similarly, supported catalysts (**HCAT-Ti** and **PCAT-Ti**) with pore size of 30 and 70 Å, respectively, show that larger pore materials

afforded LLDPE of higher M_w. Within a set of silica supported CGCs, the pore size of the supported catalyst is the only factor that influences the M_w of LLDPE prepared.

During the activation of supported catalysts with MAO abstraction of metal fragments from the supported catalysts can occur. This phenomenon is known as leaching and the metal components formed are soluble in the polymerization solvent. Extensive leaching of metal catalysts from inorganic matrices has been previously reported.[53] The effect of leaching was seen in the broadening of the molecular weight distribution (PDI) of the copolymers due to the formation of polymer from multiple active sites. Leaching of titanium fragments from the supported catalysts was noticed in both the silica and AMPS supported CGCs (Chapters 3 and 4, respectively). However, the extent of leaching was less pronounced in the case of CGCs tethered to AMPS than from CGCs assembled on silica. The copolymers synthesized from **AMPS-Ti-12** showed lower PDI compared to copolymers from silica-based supports under similar experimental conditions.

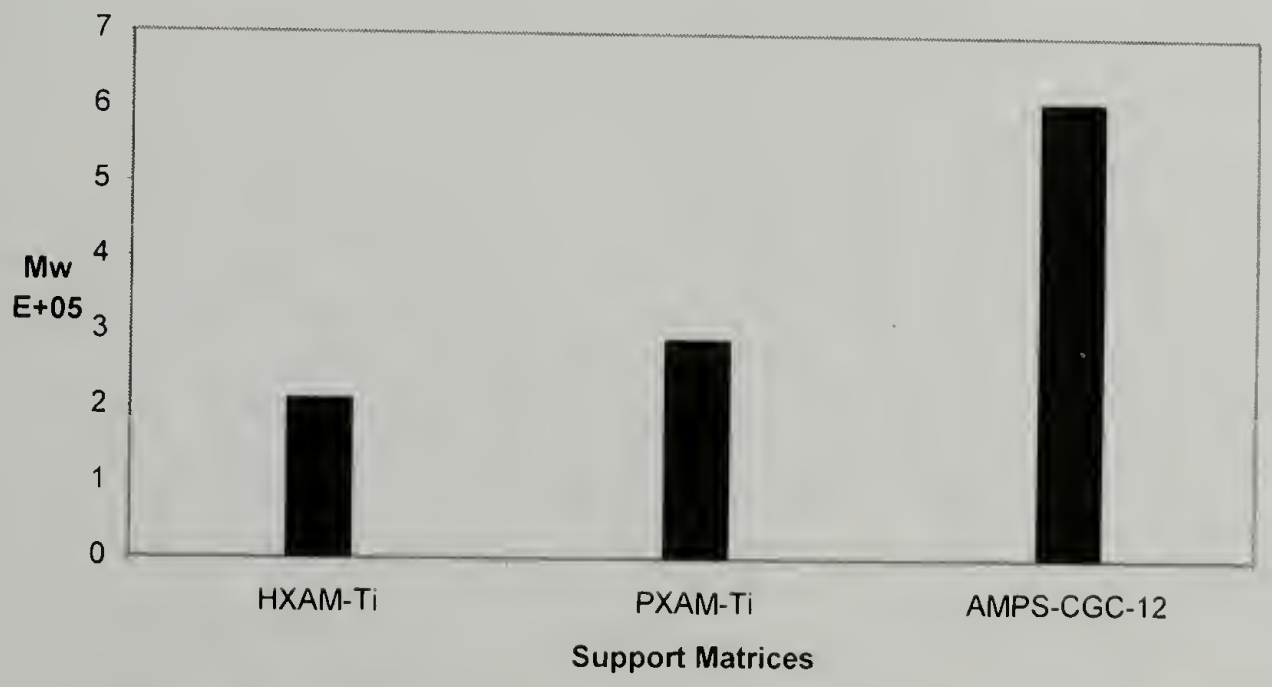

Figure 5.3 Molecular weight of LLDPE as a Function of the Supported Cataly

The CGCs tethered to polystyrene or silica matrices produced LLDPEs with 1.5-2.0 mol % of 1-octene incorporation. The support matrix does not influence the extent of comonomer incorporation. The hexyl branch within the copolymer samples disrupts the overall crystallinity of the polyolefins, leading to low percent crystallinity (4-8%).

5.5 Ethylene Homopolymerization Using Supported CGCs

In order to study the influence of the support matrix, the properties of polyethylenes (M_w and percent crystallinity (% X)) prepared from tethered CGCs in conjunction with MAO as the cocatalyst were compared.

5.5.1 Effect of Supported CGCs on Molecular Weight of Polyethylene

The local environment of the supported catalyst can be discussed in terms of its pore volume or size, rigidity and presence of ordered components present in the matrix. Each of these parameters can influence the properties of the polyolefin synthesized. The CGCs within mesoporous silica are more confined due to the rigid, well-ordered, crystalline support with smaller pore sizes in comparison to CGCs within AMPS. These supported CGCs in conjunction with MAO and ethylene afforded high-density polyethylene. In Figure 5.4, the trend in M_w of polyethylene produced from CGCs within small pore silica (**HXAM-Ti**), large pore silica (**PXAM-Ti**) and polystyrene (**AMPS-Ti-12**) supports is shown. The **AMPS-Ti-12** affords polyethylene of higher molecular weight ($M_w > 500{,}000$ g/mol) compared to the silica matrices ($M_w < 400{,}000$ g/mol). The formation of higher molecular weight polyethylene from the polystyrene supports is attributed to the active titanium cationic center being more accessible within solvent-swollen, semiflexible polystyrene matrix compared to the silica matrices. Within a set of

silica-supported CGCs, the method of surfactant removal (calcination or extraction), presence of different capping groups (AP/T or AP/M), and silanol content do not affect the molecular weight of HDPE. The pore size of the CGC silica is the sole influence on the molecular weight of HDPE, with larger pores affording higher molecular weight.

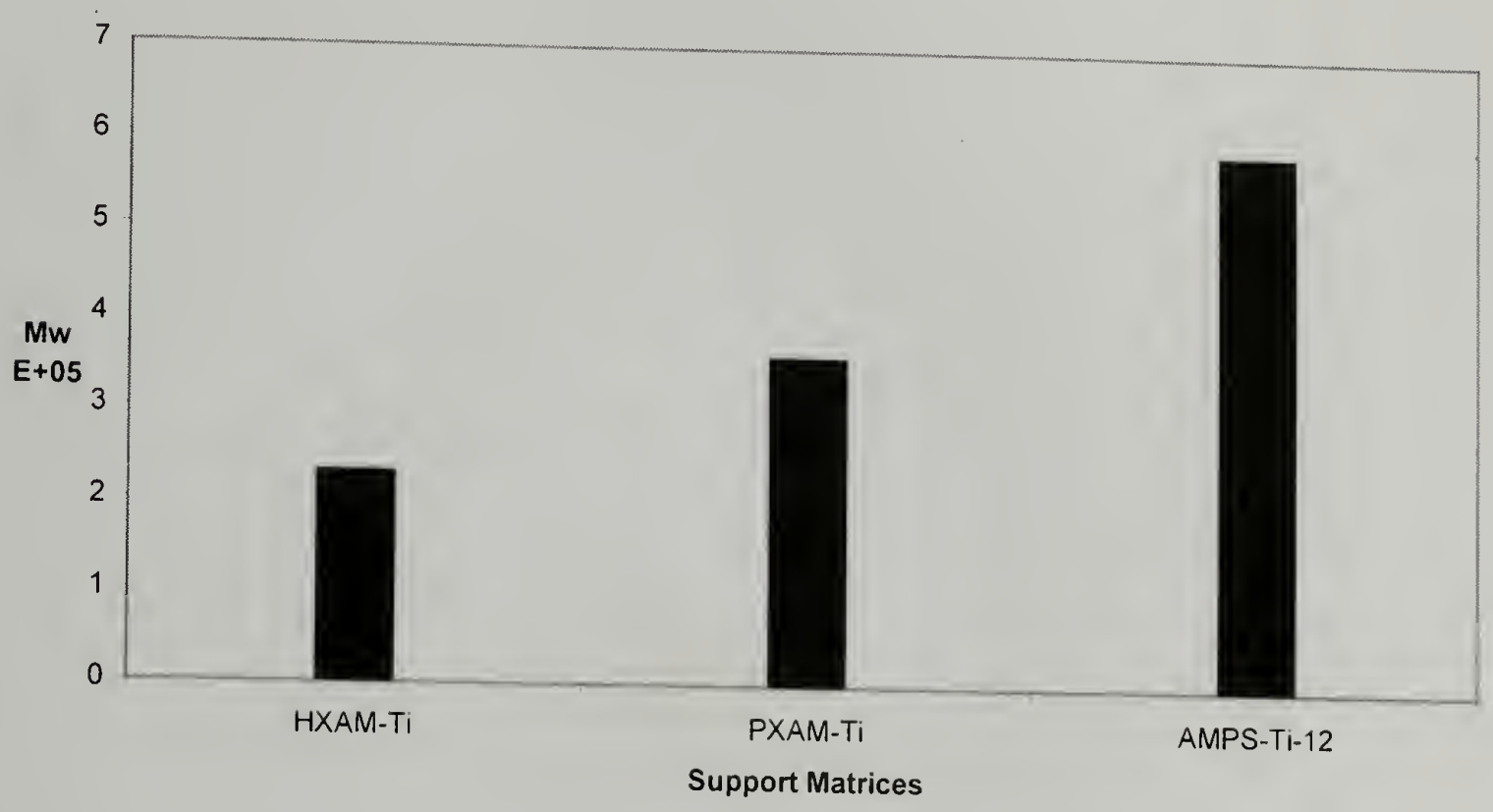

Figure 5.4 Molecular weight of HDPE as a Function of the Supported Catalyst/MAO

5.5.2 Effect of Supported CGCs on Crystallinity of Polyethylene

Crystalline polymers show organization at various length scales, starting from interatomic spacing to macroscopic levels. This organization of the crystalline polymer is important for subsequent understanding of related polymer properties, which include morphology, deformation behavior, mechanical properties and crystallization phenomena. Analysis of a polyethylene sample reveals three different components (Figure 5.5).

Lamellar segments that consist of individual crystals are highly ordered with apparent lamellae thickness of at least 100 Å. A less-ordered region that is devoid of crystalline units is referred to as the amorphous component. The juxtaposition of the crystalline and amorphous regions results in interface, which is also referred to as the intermediate component of the polymer. Polyethylenes are semicrystalline due to the presence of ordered crystalline, less ordered amorphous and the intermediate component.

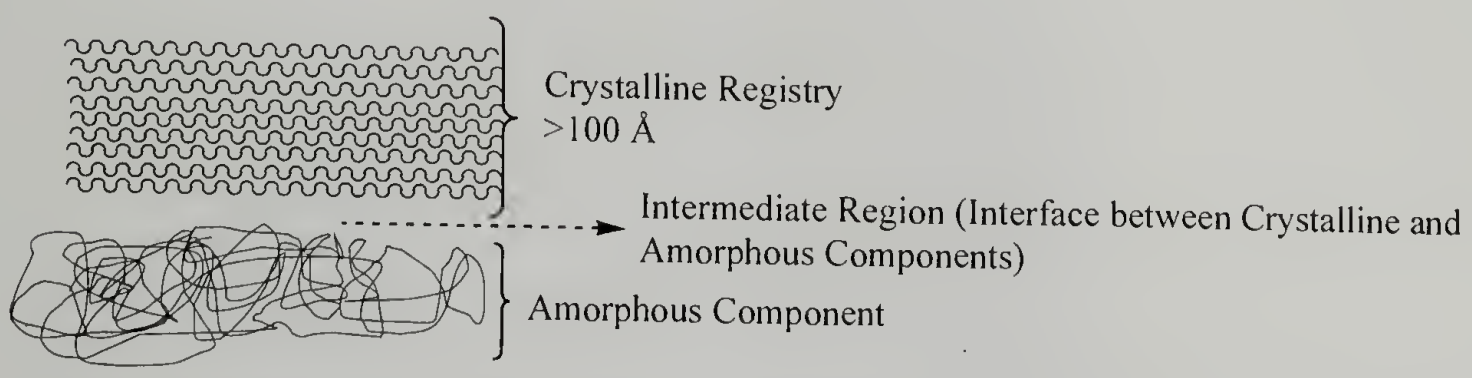

Figure 5.5 Representative Cartoon of the Components of Semicrystalline Polyethylene

Using supported CGCs, HDPE prepared have percent crystallinities comparable to that of polyolefins with short chain branches (butyl or hexyl) has been discussed in the Chapters 3 and 4. The apparent crystal size of polyethylene lamellae is 100-150 Å as determined from WAXD studies. The apparent crystal thickness of polyethylene is greater than the pore diameter of silica (30-70 Å) supports and which suggested that crystallization of the polyethylene occurs outside the pores of the support matrix. However, in order to determine whether the percent crystallinity of polyethylene is dependent on the structural characteristics of the supported catalyst; pore size, pore volume, presence or absence of ordered pores, rigidity of the support, representative Figure 5.2. The trend in percent crystallinity of polyethylene as a function of the support

matrix is shown in Figure 5.6. Polyethylene produced from matrices with smaller pore sizes (**HXAM-Ti** and **PXAM-Ti**) have higher percent crystallinity compared to the polyethylenes prepared from larger pore silica or AMPS.

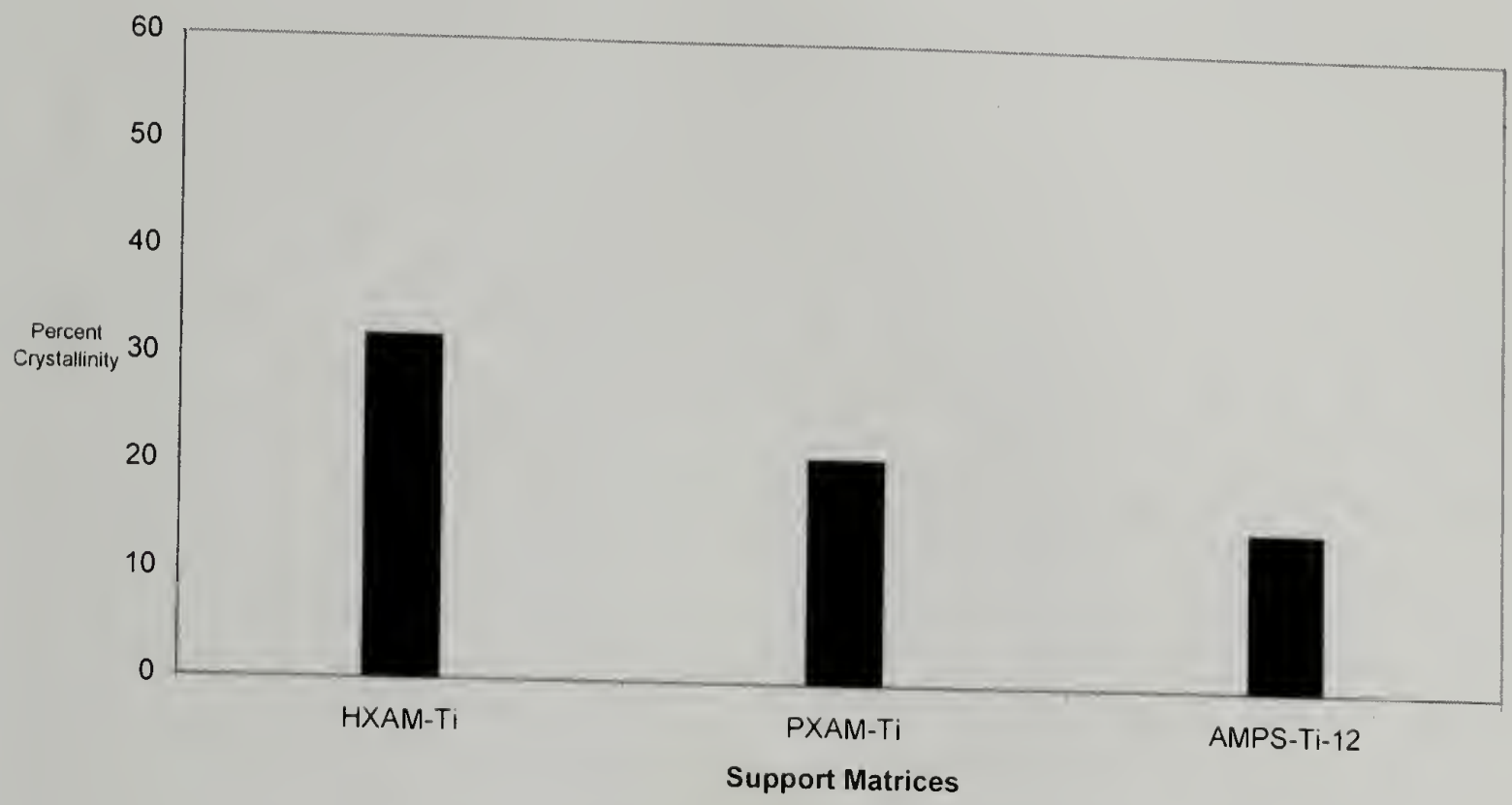

Figure 5.6 Percent Crystallinity of HDPE as a Function of the Supported Catalyst/MAO

When polyethylene is prepared from smaller pore materials, there are fewer possible conformations that the polymer can adopt prior to exiting from the pore. The polymer exiting out of the pore can order with other polymer chains coming out of adjacent pores. These ordered polymer chains can lock into registry and organize themselves into the crystalline polyethylene phase, which contributes to an increase in crystallinity of the polyolefin prepared. On the other hand, polyethylene produced from

larger pore, less-ordered supports (AMPS), can exist in more number of conformations. This greater degree of polymer chain freedom contributes more to the intermediate and amorphous components, which yields polyethylene of lower crystallinity (Figure 5.7). Another observation was that within a set of silica matrices (**HXAM-Ti** and **PXAM-Ti**, or **HCAT-Ti** and **PCAT-Ti**) polyethylenes prepared from silica with smaller pore sizes have higher percent crystallinity (Figure 5.7).

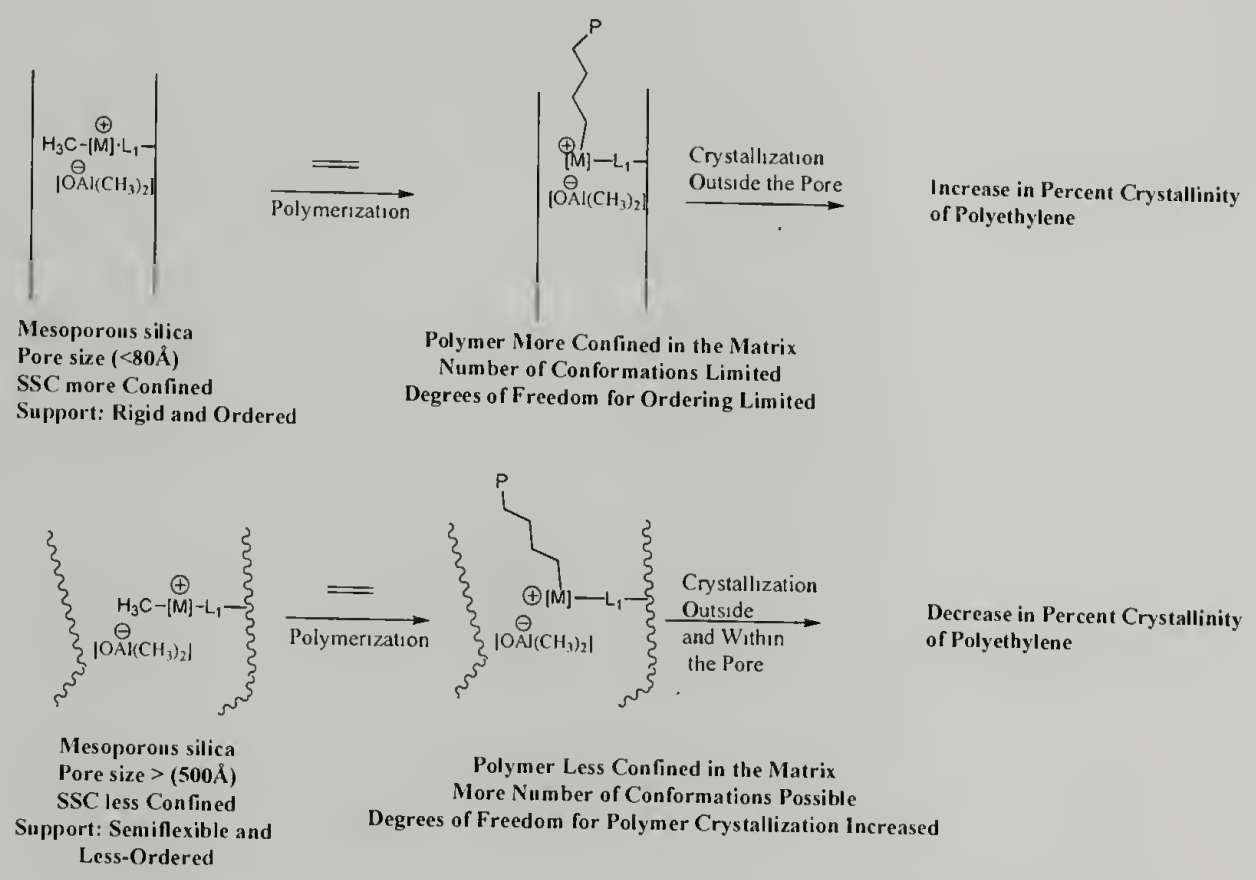

Figure 5.7 Representative Cartoon of the Formation of Semicrystalline Polyethylene with Tunable Crystallinite Content from CGCs within Silica (Top) and AMPS (Bottom)

Preliminary results from Solid State ^{13}C NMR of two polyethylene samples prepared from less-ordered and ordered supported catalysts shows the presence of the crystalline, intermediate and amorphous components in each of the sample. The polyethylenes formed within less ordered systems contribute more to the intermediate component in the crystalline hierarchy than the crystalline region and therefore have

lower percent crystallinity. By contrast, polyethylene prepared from a smaller pore matrix that is more ordered contributes more to the crystalline region and therefore has higher percent crystallinity. Thus rigidity, presence of ordered units and pore sizes of the support matrix are variables by which percent crystallinity of the polyethylenes can be altered.

5.5.3 Influence of Borate Counterions

The influence of the cocatalyst on the properties of polyolefins produced from single site catalysts is well documented.[11] The influence of the counterion on the properties of polyethylenes produced from CGCs tethered to silica and polystyrene matrices has been investigated. The supported constrained geometry catalysts (**AMPS-Ti-12, HXAM-Ti** and **PXAM-Ti**) were alkylated with MAO, followed by the addition of N,N-dimethylanilinium borate (**III**) or trityl borate (**II**) and subsequently pressurized with ethylene. The polyethylenes formed were analyzed for their molecular weights and percent crystallinity. The trends in molecular weight of polyethylene formed from CGCs in conjunction with **II** or **III** are shown in Figures 5.8 and 5.9, respectively. It is observed that contrary to the use of MAO as the cocatalysts, silica matrices (**HXAM-Ti** and **PXAM-Ti**) in conjunction with borates afford polyethylene of higher molecular weight compared to polystyrene matrices. The formation of lower molecular weight of the polyethylene is more an influence of the nature and interaction of the metal cation-borate anion rather than the influence of the structure and composition of the support. Within a set of silica matrices (**HXAM-Ti, HCAT-Ti, PCAT-Ti** and **PXAM-Ti**), the method of surfactant removal (calcinations or extraction) and presence of different capping units does not influence the M_w of the polyethylene. The molecular weight of polyethylene is

once again a function of the pore size of silica; mass transport limitation of smaller-pore silica (≈30 Å) results in lower M_w compared to polyethylene of higher M_w from larger-pore materials (≈70 Å).

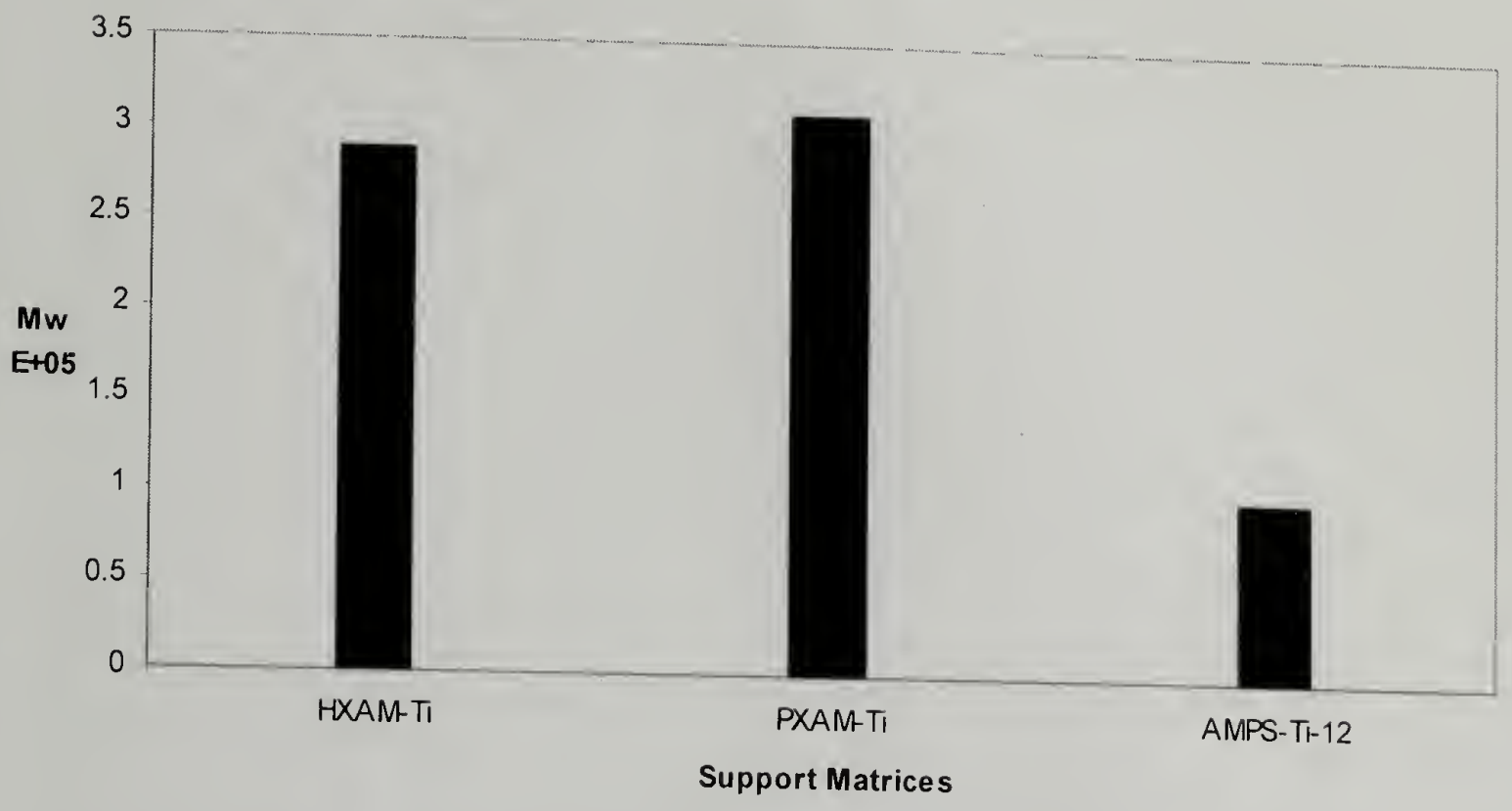

Figure 5.8 Molecular weight of HDPE as a Function of the Supported Catalyst: Effect of Trityl Borate (**II**)

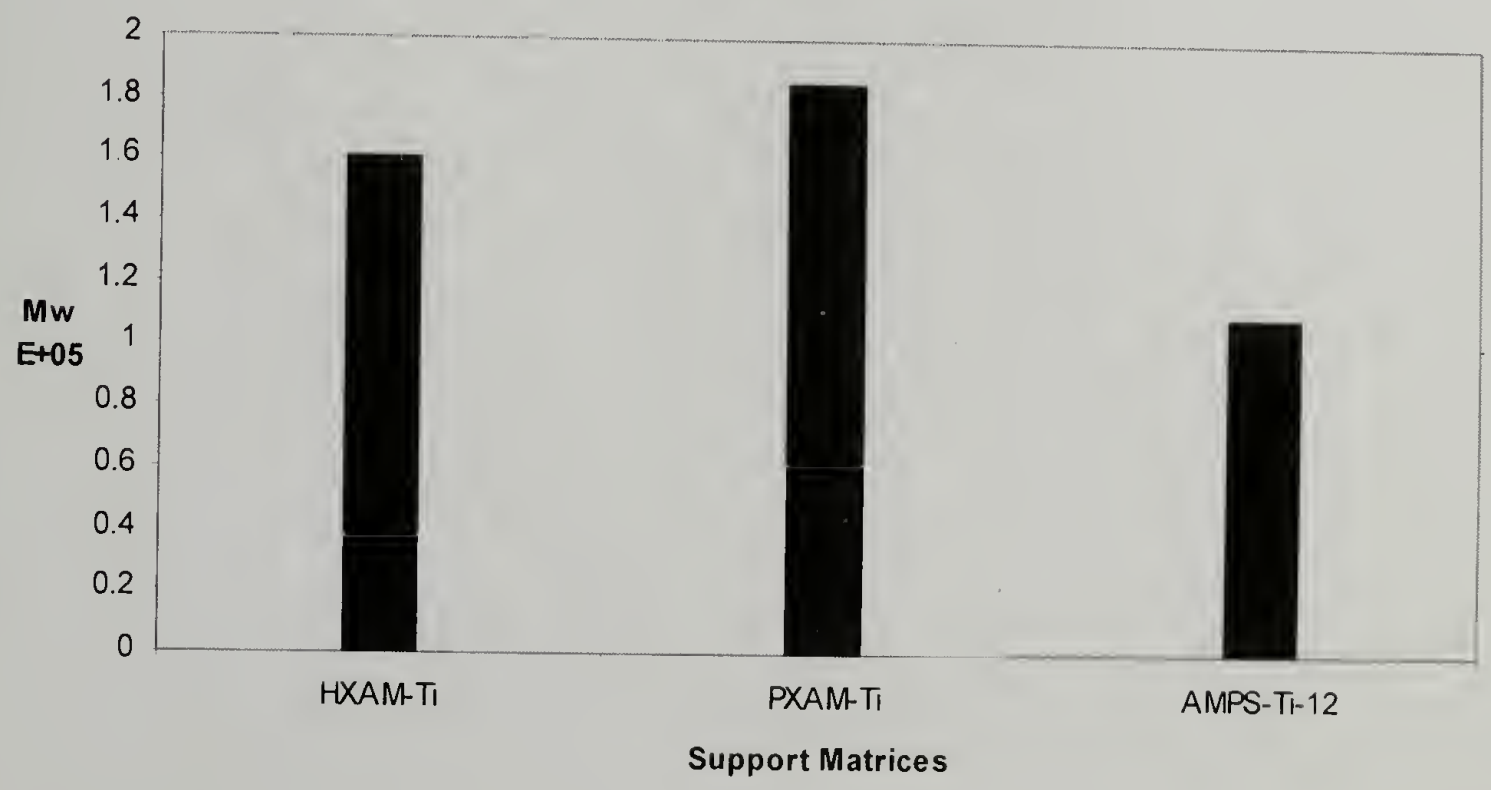

Figure 5.9 Molecular weight of HDPE as a Function of the Supported Catalyst: Effect of Anilinium Borate (**III**)

The effect of counterions on the percent crystallinity of polyethylene was investigated. The CGCs within AMPS or silica matrices in conjunction with anilinium borate or trityl borate cocatalysts during ethylene polymerization afforded polyethylene of higher crystallinity compared to the use of MAO as the cocatalyst. The percent crystallinity of polyethylene is increased when prepared from silica support matrices that have ordered units, rigidity, structural integrity and smaller pore dimension compared to less ordered, semiflexible polystyrene matrices. Irrespective of the cocatalysts and counterion, CGCs within mesoporous silica matrices afford polyethylenes of higher crystallinity compared to the microporous polystyrene matrices (Figure 5.10 and 5.11). Within the set of CGCs tethered to silica, regardless of the method of surfactant removal or the type of capping group, the pore size of the silica matrix influences the percent crystallinity of polyethylene; smaller pore materials afford polyethylenes of higher crystallinity compared to the larger pore silica.

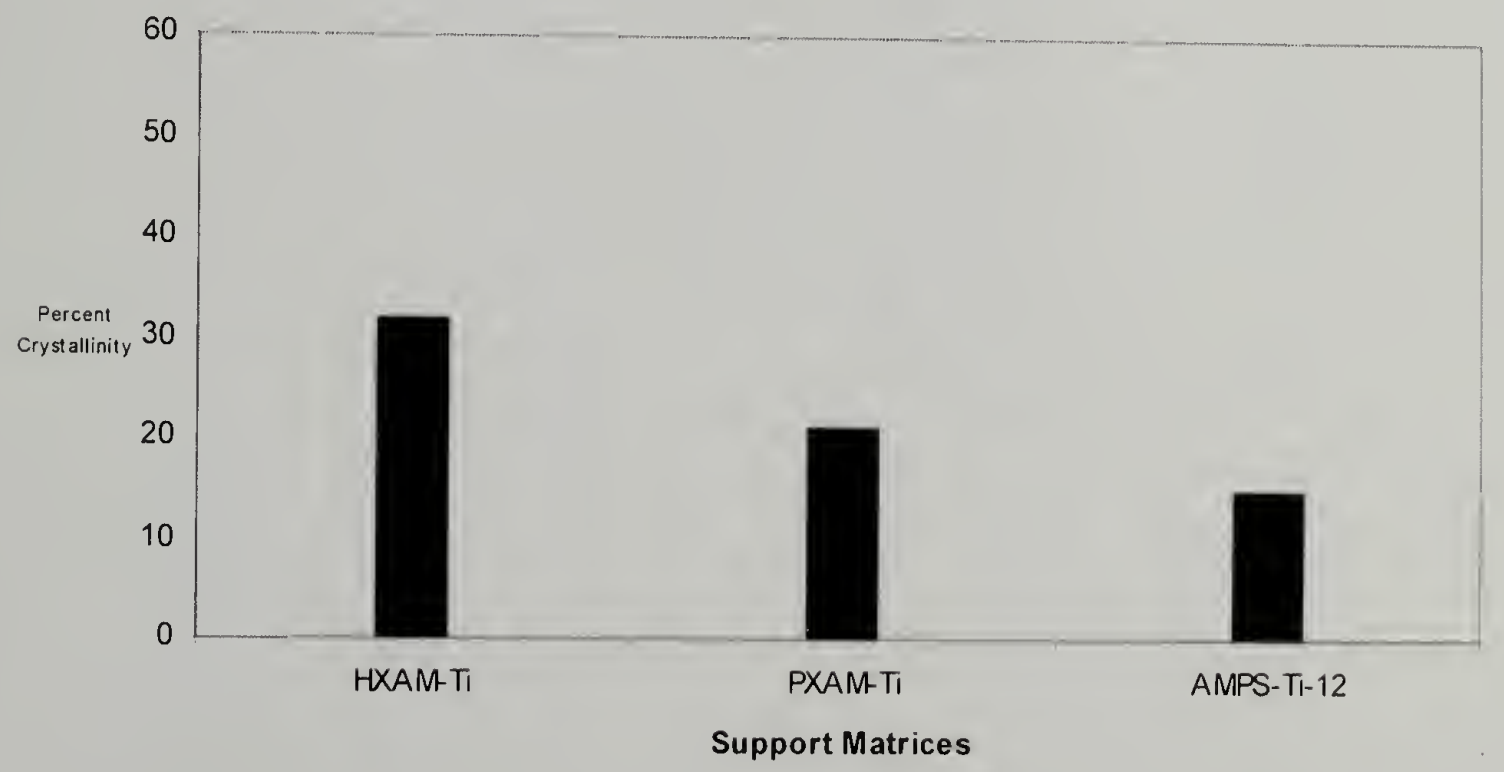

Figure 5.10 Percent Crystallinity of HDPE as a Function of the Supported Catalyst: Effect of Trityl Borate (**II**)

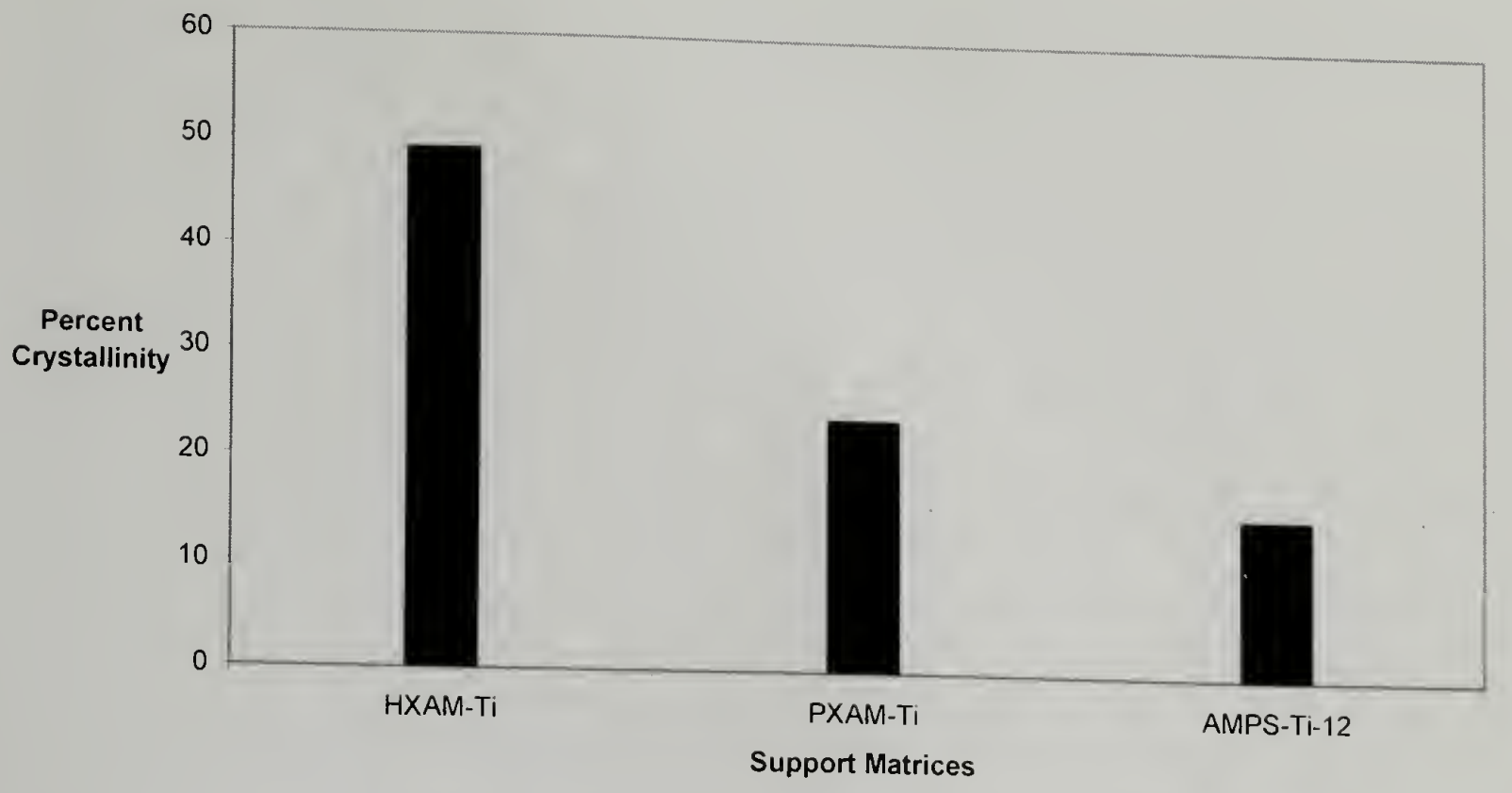

Figure 5.11 Percent Crystallinity of HDPE as a Function of the Supported Catalyst: Effect of Anilinium borate (**III**)

5.6 Summary

In order to answer the question of how a support can influence the properties of polyolefins prepared from supported catalysts, a detailed experimental investigation was performe. The experimental investigation included strategies to prepare precursor catalysts for CGCs (Chapter 2), methods to tether CGCs on amine functionalized polystyrene (Chapter 3)and amine-functionalized silica were developed (Chapter 4). Using these supported catalysts in conjunction with MAO and ethylene monomer, polyethylenes were prepared and the properties of polyethylene evaluated. It was observed that M_w and percent crystallinity of polyethylene is dependent on the pore size matrix from which it is prepared. Diffusion limitation of the monomer to more constrained active sites leads to the formation of lower M_w polymers. Matrices that are semiflexible, less ordered and amorphous with larger pore volumes (AMPS) afford

polyethylenes lower crystallinity. By contrast, rigid ordered silica matrices that have tunable pore volumes afford polyethylenes with lower molecular weight but higher crystallinity. The plausible reasons for the observed correlation in the properties of the polyolefins and the supported catalysts used have been discussed.

Other possible reasons to the formation of lower crystalline polyethylenes from less-ordered AMPS supports cannot be ruled out. The AMPS supported catalysts could afford polyethylene with more alkyl branches than silica based CGCs. The alkyl branches can act as defects that lower the crystallinity of polyethylene. The type and number of molecular branch defects could not be observed in the ^{13}C and ^{1}H NMR of HDPE produced from these supported catalyst. The conventional NMR techniques are not sensitive enough to observe these branch-based defects. Other reasons for the observed depression in percent crystallinity of polyethylenes from AMPS compared to silica based matrices is that during the CGC activation process, MAO or any other cocatalysts can partition to different extents in these supports. This effect of cocatalysts partitioning in various can impact the properties of polyolefin produced.

CHAPTER 6

POLYOLEFINS FROM METHYLALUMINOXANE SUPPORTED MOIETIES IN CONJUNCTION WITH CONSTRAINED GEOMETRY CATALYSTS

6.1 Introduction

There are two important aspects that are being addressed in literature for polymerization of olefins. The first is manipulation of the ligand architecture to provide pathways to generate various forms of polyolefins (primary ligand influence). The second important aspect of polymerization is the nature of the cocatalyst used in the polymerization mixture. Methylaluminoxane (MAO) is a cocatalyst that is most commonly used in olefin polymerization. These cocatalysts are typically used in large excess relative to the concentration of the metal complex.[11] A challenge is to reduce the excessive amount of MAO needed for olefin polymerization. The amount of MAO used can be substantially reduced by adsorbing or covalently tethering MAO to a heterogeneous support (silica or alumina). SSCs activated by aluminoxanes supported on heterogeneous matrices form the majority of olefin polymerization catalysts. [5,52,53] Boron based Lewis acid have been used as efficient cocatalysts instead of MAO for olefin polymerization.[11]

There are three main methods for supporting aluminoxanes. A common technique used to affix aluminoxanes to support surfaces is by reaction of the support matrix and aluminoxanes in toluene at 80-90°C in a closed vessel (incipient wetness technique). Alternatively physisorption of MAO on the support matrix can also afford aluminoxanes fixed to the support. This mehod requires longer reaction time.[92] An other method was to support aluminoxane is *in situ* hydrolysis of the aluminoxane with the support matrix

(silica) in hydrocarbon suspension or with reactive components in the gas phase.[51,89-91] In contrast, synthetic routes to tether boron-based cocatalysts need to be individually designed.

Aluminoxanes tethered to supports have been used for the homopolymerization and copolymerization of ethylene and propylene. The supported cocatalysts have been synthesized by incipient wetness technique or by *in situ* hydrolysis of the alkyl aluminum and the support.[90]

In keeping with the general thrust of this thesis, the use of supported cocatalysts with appropriate constrained geometry catalysts needs to be explored in order to address the issue of the support influence on the properties of polyolefins synthesized. Synthetic strategies to tether single site CGCs on polystyrene and mesoporous silica have been developed. These supported catalysts have been used for ethylene polymerization studies (Chapters 2, 3 and 4). Whereas the tethered CGCs show decent activity for ethylene homo and copolymerization, these supported catalysts show negligible activity for propylene polymerization. Synthetic routes to tether cocatalysts to supports need to be developed and ethylene and propylene polymerization using commercially available CGCs has to be explored. The polyethylene properties from tethered cocatalysts system have been compared with polyethylenes obtained from tethered CGCs and homogeneous polymerization using CGC.

6.2 Experimental Section

6.2.1 Methods and Materials

All reactions were performed under nitrogen in Schlenk glassware or in an inert atmosphere dry box. All air-free and dry solvents used were obtained from a solvent

purification manifold.[64] Aminomethylpolystyrene (AMPS) was obtained from Polymer Laboratories Inc., the constrained geometry catalysts (**CGC 1**, Figure 1) was obtained from Boulder Scientific, Tris(pentafluorophenyl)borane ($B(C_6F_5)_3$, **I**), trityl borate ($[(C_6H_5)_3C][B(C_6F_5)_4]$, **II**), N,N-dimethylanilinium borate ($[(C_6H_5)N(CH_3)_2H][B(C_6F_5)_4]$, **III**) and MAO (4.77 M, 30 wt % in toluene) were obtained from Albermarle and used as received. The syntheses of mesoporous silica matrices are discussed in Chapter 4. Ethylene and propylene polymerization was performed using a gaseous monomer manifold and heavy glass walled reactors.[70]

6.2.2 Instrumentation

Elemental analysis was performed using three Exeter Analytical Inc.240XA CHN analyzers and a Leeman Labs Inc. Dual View DRE Sequential ICP was used to analyze the aluminum loadings in the samples. ^{13}C NMR spectra of the polyolefins were recorded at 150 MHz on an Avance DPX 600 using a quantitative pulse program for solution NMR at 135 °C. Gel Permeation Chromatography was performed with a Polymer Laboratories PL-220 high temperature GPC equipped with a Wyatt MiniDawn (620 nm diode laser) high temperature light scattering detector and refractive index detector at 135 °C using 1,2,4-trichlorobenzene as solvent and calibrated using polystyrene standards. The dn/dc value for polypropylene used was -0.105. Thermal analyses was performed using TA DSC 2910 equipped with liquid nitrogen cooling accessory unit under a continuous nitrogen purge (50mL/min) with a heating and cooling scan rate of 10 °C/min.

6.2.3 Syntheses of MAO Tethered Matrices

6.2.3.1 Synthesis of MAO Tethered to AMPS (AMPS-Al-1)

Dried aminomethylpolystyrene (AMPS; 0.501g, 1.0 mmol of N/g of support) was swollen in 5mL of dry toluene. To the solvent-swollen AMPS, 10.0 mL of MAO (30 wt% in toluene, 4.47 M) was added and the reaction was allowed to proceed for 2 days. The MAO supported AMPS was washed with toluene several times to remove non-adsorbed MAO and trimethylaluminum. The dried supported cocatalyst was obtained by drying under vacuum at 60°C to yield 1.8 g of MAO supported on AMPS (Compound **AMPS-Al-1**)

Elemental Analysis (wt %/g of sample): C (44.67), H (6.66), N (0.31), Al (25.1)

6.2.3.2 Synthesis of MAO Tethered to AMPS (AMPS-Al-2)

Dried aminomethylpolystyrene (AMPS; 1.009 g, 1.0 mmol of N/g of support) was swollen in 5mL of dry toluene. To solvent-swollen AMPS, 10.0 mL of MAO (30 wt % in toluene, 4.47 M) was added and the reaction was allowed to proceed for 2 days. The MAO supported AMPS was washed with toluene several times to remove non-adsorbed MAO and trimethylaluminum. The dried supported cocatalyst was obtained by drying under vacuum at 60°C to yield 2.305 g of MAO supported on AMPS (Compound **AMPS-Al-2**)

Elemental Analysis (wt %/g of sample): C (54.39), H (6.87), N (0.51), Al (20.9)

6.2.3.3 Representative Synthesis of MAO Tethered to Mesoporous Silica

Dry mesoporous silica (**HX**, **HC**, **PX,** or **PC**) was slurried in 5 mL of dry toluene to which a predetermined amount of MAO (30 wt % in toluene, 4.47 M) was added and

the reaction was allowed to proceed for 2 days. The MAO adsorbed silica was washed with toluene several times to remove non-adsorbed MAO and trimethylaluminum. Toluene was removed *in vacuo* at 60°C and afforded dry powder MAO-silica mixture (Table 6.1).

6.2.3.4 Representative Ethylene Polymerization

To slurry of 106.0 mg of supported cocatalyst **AMPS-Al-1** in 10.0 mL of toluene taken in a polymerization reactor equipped with a stir bar, 7.86 μmol of **CGC1** was added and pressurized with 60 psig of ethylene. The polymerization mixture was stirred at room temperature. After 10 minutes, the ethylene supply was stopped and the reactor was vented to remove excess ethylene, the reaction mixture was quenched with 10% volume of hydrochloric acid in methanol. The polyethylene was collected by filtration and dried in a vacuum oven overnight to afforded polyethylene (Table 6.2, Entry 1).

6.2.3.5 Representative Propylene Polymerization

To 50.8 mg of supported cocatalyst **AMPS-Al-1** taken in a polymerization reactor equipped with a stir bar, 1 mL toluene containing 7.86 μmol of **CGC1** was added and pressurized with 40 psig of propylene with constant stirring. After 1 hour, the propylene supply was stopped and the reactor was vented to remove excess ethylene, the reaction mixture was quenched with solution of 10 % by volume of hydrochloric acid in methanol. The polypropylene was collected by filtration and dried in a vacuum oven overnight to afford 1.4 g of polypropylene (Table 6.4, Entry 6).

6.3 Results and Discussions

6.3.1 Synthesis of MAO Tethered to Supports

The aminomethylpolystyrene (AMPS) resins are crosslinked (1% crosslink density) with amine loading of 1.0 mmoles and can be swollen in toluene. Reaction of AMPS with MAO in toluene afforded aluminoxane tethered to AMPS. Polystyrene supports with different MAO amounts in the reaction mixture resulted in the production of **AMPS-Al-1** and **AMPS-Al-2**. The aluminum loading of samples **AMPS-Al-1** and **AMPS-Al-2** were determined by ICP analysis. From these analyses, it was observed that both the producted supported cocatalysts have different loading of aluminum (Table 6.1, Figure 6.1).

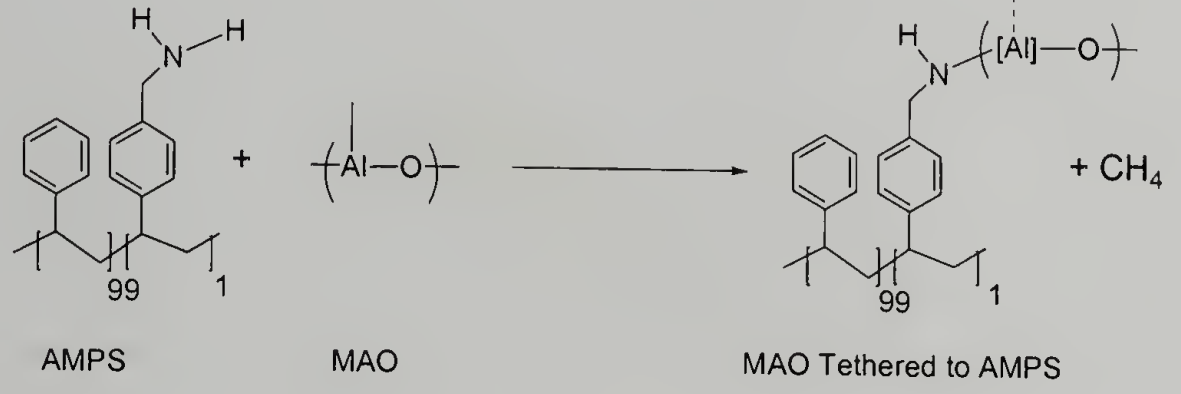

Figure 6.1 Syntheses of MAO Tethered to Aminomethylpolystyrene (AMPS)

The syntheses of mesoporous silica matrices that have been used as supports to adsorb MAO have been discussed in Chapter 4. The non-functionalized and functionalized mesoporous silica materials are designated by two- or four-letter names, respectively, that are indicative of the template (H: hexadecyltrimethylammonium bromide; P: Pluronic P123), the method of surfactant removal (X: solvent extraction; C: calcination). Four mesoporous silica samples (HX, HC, PX, PC) that have been used to

tether MAO have the following parameters; pore diameter of 30-70Å, total silanolcontent (Si-OH/Si as determined from Solid State ^{29}Si NMR) of 0.34-0.56 and surface area of 570-900 $m^2\ g^{-1}$. These mesoporous silica samples were treated with MAO to obtain MAO tethered mesoporous silica (**HX-Al**, **HC-Al**, **PX-Al**, **PC-Al**, respectively, Figure 6.2). The aluminoxane loading on the silica sample is dependent on the amount of MAO that has been pretreated with silica and the number of silanol units present in the silica sample.

Table 6.1 Synthesis of MAO Tethered to Various Support Matrices

Aluminoxane Tethered to Support	Supports (mg)	MAO Added	MAO Tethered to Support (Mg)	Al Loading in 50 mg of Support (mmol)
AMPS-Al-1	AMPS (501.9)	5.0 mL	1810.9	2.2E-4
AMPS-2	AMPS (1009.2)	10.0 mL	2311.6	1.8E-4
PX-Al	PX (201.0)	5.0 mL	609.1	5.7E-4
HX-Al	HX (261.5)	5.0 mL	946.5	6.3E-4
PC-Al-1	PC (252.7)	5.0 mL	620.1	5.1E-4
PC-Al-2	PC (124.4)	5.0 mL	1040.9	7.6E-4
PC-Al-3	PC (125.5)	7.5 mL	1657.7	8.0E-4
HC-Al	HC (253.9)	5.0 mL	640.9	5.2E-4

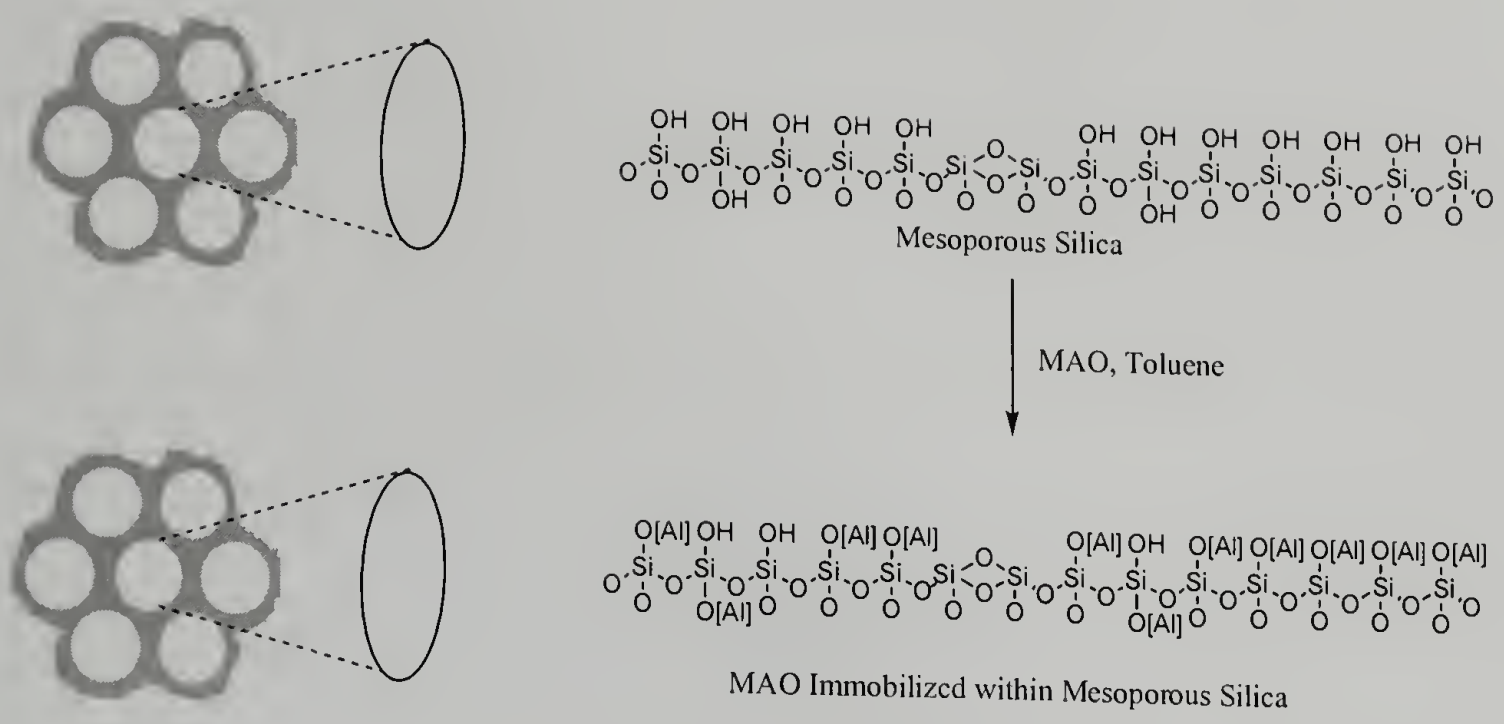

Figure 6.2 Syntheses of MAO Tethered to Mesoporous Silica

6.3.2 Ethylene Homopolymerization using MAO Tethered to Aminomethylpolystyrene

Ethylene homopolymerization was performed using supported cocatalysts **AMPS-Al-1** in conjunction with constrained geometry catalyst (**CGC1**) in toluene as the polymerization solvent, and the reaction afforded polyethylene with good activity (Figure 6.3). The polyethylene obtained has a melting point greater than 130 °C , which is indicative of the presence of HDPE. The weight average molecular weight (M_w) of the polyethylene was determined to be 800,000. The heat of fusion (ΔH_f) was determined by DSC measurements and the percent crystallinity relative to a polyethylene single crystal was calculated to be 37.5% (Table 6.2, entry 1). In order to evaluate the influence of the supported cocatalyst on the properties of polyethylene produced, other polymerization control experiments were performed. In the first control experiment performed, the catalyst **CGC1** was pretreated with MAO and the activated catalysts was treated with the

aminomethylpolystyrene support and the pressurized with ethylene. High-density polyethylene was obtained from this reaction with a higher catalyst activity, melting point and percent crystallinity but lower molecular weight (Table 6.2, entry 2) compared to the polyethylene produced from supported cocatalyst (**AMPS-Al-1**). It is well documented that the presence of trimethylaluminum present in MAO induces chain transfer processes occurring during olefin polymerization, which results in lower molecular weight polyethylene.[92] The formation of lower molecular weight polyethylene in Table 6.2, entry 2 can be attributed to chain transfer to the trimethylaluminum units. On the other hand, **CGC 1** and MAO in toluene were pressurized with ethylene in the absence of AMPS afforded high density polyethylene with M_w of 75,000 (Table 6.2, entry 3), which is comparable to the molecular weight of polyethylene obtained from the pretreatment of **CGC 1** with MAO and further reaction with aminomethylpolystyrene and ethylene. The percent crystallinity of polyethylene obtained is higher in homogeneous experiments (Table 6.2, entry 3) compared to polymes obtained from supported cocatalysts or supported SSCs.

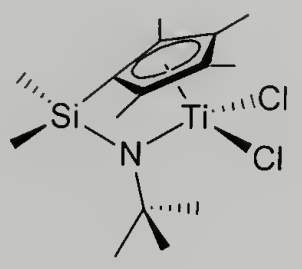

Figure 6.3 Constrained Geometry Catalysts (**CGC 1**)

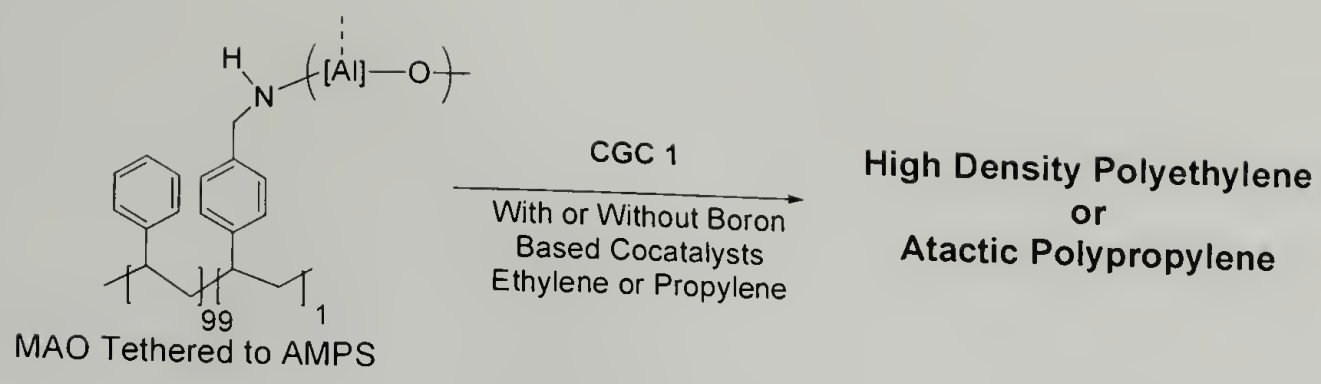

Figure 6.4 Preparation of Polyolefins using MAO Tethered to Aminomethylpolystyrene in Conjunction with **CGC 1**

Table 6.2 Ethylene Polymerization using **CGC 1**

Entry	Support	Al:Ti [a, b]	Activity Kg/molTi.hr.atm [c]	M_w [d]	PDI [d]	T_m [e]	% Crystallinity[f]
1	AMPS-Al-1 [g]	325	76.6	800,000	2.6	136.2	37.5
2	AMPS [h]	1195	227	77,000	2.5	138.0	51.2
3	None [I]	1195	403	74,000	1.6	139.0	64.8

[a] Aluminum loadings determined by ICP
[b] Using Constrained Geometry Catalyst **CGC1** (7.86 μmol)
[c] Ethylene pressure 60 psig (4 atm), Reaction time=15-30 minutes
[d] Determined by GPC at 135°C using light scattering detector and calibrated using polystyrene standards
e Determined by DSC (first melt), heating and cooling rates of 10 C/min under nitrogen
[f] Percentage Crystallinity = Observed (ΔH_f)/293 *100
[I] Cocatalyst (MAO) tethered to AMPS matrix, supported cocatalyst, (106.0mg of MAO-AMPS-1)
[2] Cocoatalyst and catalysts mixture treated with the support matrix swollen in toluene (102.5mg of AMPS)
[3]Homogeneous Polymerization

Ethylene homopolymerization was performed using supported cocatalysts **AMPS-Al-1** in conjunction with **CGC 1** in toluene as the polymerization solvent. The reaction afforded polyethylene with good activity (Figure 6.3). The polyethylene obtained has a melting point greater than 130 °C indicative of the presence of high-density polyethylene. The weight average molecular weight (M_w) of the polyethylene was determined to be

800,000. The heat of fusion (ΔH_f) was determined by DSC measurements and the percent crystallinity relative to a polyethylene single crystal was calculated to be 37.5% (Table 6.2, entry 1). In order to evaluate the influence of the supported cocatalyst on the properties of polyethylenes produced. In the first control experiment performed, the catalyst **CGC1** was pretreated with MAO and the activated catalysts was treated with AMPS and the pressurized with ethylene. High-density polyethylene was obtained from this reaction with a higher catalyst activity, melting point and percent crstyallinity but lower molecular weight (Table 6.2, entry 2) compared to the polyethylene produced from supported cocatalyst (**AMPS-Al-1**). It is well documented that the presence of trimethylaluminum present in MAO is responsible for chain transfer processes occurring during olefin polymerization, which results in lower molecular weight polyethylene.[92] The formation of lower molecular weight polyethylene in Table 6.2, entry 2 can be attributed to the chain transfer to trimethylaluminum units. On the other hand, **CGC 1** and MAO in toluene were pressurized with ethylene in the absence of AMPS afforded high density polyethylene with M_w of 75,000 (Table 6.2, entry 3), that is comparable to the molecular weight of polyethylene obtained from the pretreatment of **CGC 1** with MAO and further reaction with aminomethylpolystyrene and ethylene. The percent crystallinity of polyethylene obtained is higher in homogeneous experiments (Table 6.2, entry 3) compared to polymerizations in the presence of supported cocatalysts or supported single site catalyst.

Polyethylenes synthesized from heterogeneous matrices to which either the single site catalyst or cocatalyst is attached has lower percent crystallinity compared to polyethylene synthesized from a homogeneous catalyst and cocatalyst mixture (Table

6.3). The growth of the polymer is from a metal-alkyl bond within the pore, as the polymer grows it is transformed into ordered crystalline components, intermediate component and the disordered amorphous component. The percentage of each of these components influences the crystallinity of the polyolefin synthesized. In the presence of support matrix, intermediate component and the amorphous content increases affording polyethylenes with lower crystallinity. However, the molecular weight of the polyethylene produced from single site catalyst or catalyst tethered to support matrix is higher than polyethylene synthesized from homogeneous single site catalyst.

Table 6.3 Comparison of Polyethylene Properties Obtained by Tethering SSCs or Cocatalysts

Reaction Coordinates	M_w	T_m	% Crystallinity
CGC tethered to AMPS + MAO	590,000	134.1	19.6
MAO tethered to AMPS + **CGCb1**	800,000	136.2	37.5
CGC1+ MAO, further reaction with MAO	77,000	138.0	51.2
Homogeneous Polymerization (No AMPS)	74,000	139.0	64.8

6.3.3 Propylene Homopolymerization using MAO Tethered to Aminomethylpolystyrene (AMPS)

In order to determine the influence of the supported cocatalyst for propylene polymerization, two supported cocatalysts with different aluminum content were synthesized as discussed previously (**AMPS-Al-1** and **AMPS-Al-2**). Using supported cocatalyst **AMPS-Al-2** with **CGC 1** in toluene and propylene as the monomer (Table 6.4,

entry 4), polypropylene was prepared (Figure 6.3). With an Al:Ti ratio of 60, polypropylene was synthesized from this reaction with low activity and M_w of 230,000.

Table 6.4 Propylene polymerization using MAO Tethered to Aminomethylpolystyrene with **CGC 1**

Entry	AMPS-Al (mg)	Al loading (10^{-4} Moles) [e]	Al: Ti [f]	Activity [g] (Kg/molTi.atm.hr)	Mw [h]	% rr [i]
4[c]	**2** (100.9)	3.6	59:1	2	230,000	37.0
5[a]	**2** (50.9)	1.8	500:1	43	22000	38.0
6[a]	**1** (50.8)	2.2	502:1	60	15,000	39.0
7[b]	51.2	-	485:1	55	24,000	38.0
8[d]	Homogeneous	-	485:1	35	25,000	39.0

[a] Additional MAO added during activation protocol, $3.81*10^{-3}$ moles
[b] Cocatalyst and catalyst mixture treated with the support matrix swollen in toluene
[c] No excess MAO added
[d] No support added, homogeneous polymerization
[e] Aluminum loadings determined by ICP
[f] Using **CGC 1** (7.86 μmol)
[g] Propylene pressure 40 psig (2.8 atm), Reaction time=1 hour
[h] Determined by GPC at 135°C using light scattering detector and calibrated using polystyrene standards, PDI of Polypropylene=1.9-2.3
[i] Determined by NMR at 100°C with 1,1,2,2 tetrachloroethane-d_2 as the lock solvent

From microstructural analysis of the polypropylene by ^{13}C NMR, which will be discussed later in this chapter, the polypropylene formed was determined to be mostly syndio enriched with percent rr (% rr) in the range of 35-40. The percent rr is a measure of the syndiotactic components in the polypropylenes produced and is determined by triad analyses of ^{13}C NMR of polypropulene. Propylene polymerization was performed with supported catalysts **AMPS-Al-2** with additional amount of toluene swollen MAO in order to study the effect of the aluminum content on the activity and molecular weight of

polypropylene produced (Table 6.3, entry 5). The total Al:Ti ratio was determined to be 500:1, affording the production of polypropylene with higher activity but lower molecular weight (M_w 22,000). The lower molecular weight can be attributed to chain transfer to the trimethylaluminum species present in the excess MAO that was added. In yet another propylene polymerization with supported catalyst **AMPS-Al-1** and **CGC1**, addition of more MAO led to an overall Al:Ti ratio of 502:1, afforded polypropylene of higher activity and lower molecular weight compared to the use of supported catalyst **2** under similar reaction conditions. Two control propylene polymerizations were performed to study the effect of the amount of aluminum and the presence of the support on the activity and molecular weight of polypropylene produced. In one experiment, **CGC1** was activated with MAO in toluene and the catalyst/cocatalyst mixture was pretreated with the support, followed by the addition of propylene monomer, affording polypropylene of M_w 24,000 (Table 6.4, entry 7). In another control experiment, **CGC1** was activated with MAO in toluene, followed by the addition of the propylene, resulting in polypropylene with M_w of 25,000 but with activity lower than that of entry 7.

From these observations, we presume that a critical concentration of aluminoxane on the support is necessary to produce polypropylene with fairly good activity (Table 6.4, entries 5,6, and 7). However, the presence of trimethylaluminum species due to the addition of excess MAO affords polypropylene of molecular weights comparable to homogeneous propylene polymerizations (M_w 15,000-25,000). The reduction in the molecular weight of polypropylene is attributed to the competitive chain transfer reaction of the growing polymer chain to trialkylaluminum that is known to occur in these systems. However, the loading of aluminoxane on the support or the addition of more

MAO to the reaction mixture does not affect the overall tacticity of the polypropylene synthesized.

6.3.4 Propylene Homopolymerization using MAO Tethered to Aminomethylpolystyrene (AMPS): Effect of Counterions

The use of tethered MAO units to polystyrene for production of polypropylenes with a range of molecular weights has been discussed in the previous section. The other aspect that needs to be addressed is the influence of counterions in propylene polymerizations. In each of these polymerizations, supported cocatalyst is used to activate **CGC1**; to this mixture boron-based cocatalysts **I**, **II,** or **III** have been added and the effect of titanium cation with the cocatalyst anion on the polypropylene properties has been evaluated (Table 6.5, entries 9-11)

Table 6.5 Propylene Homopolymerization using MAO Tethered to AMPS (**AMPS-Al-2**) in Conjunction with **CGC 1**: Effect of the Counterion

Entry	Support Cocatalyst	Al loading[b] (10^{-4} moles)	Al:Ti	B:Ti [c]	Activity [d]	Mw [e]	% rr [f]
5[a]	50.9	1.8	277:1	-	43	22,000	38.0
9[a]	50.1	1.8	277:1	1:1 (**I**)	50	25,000	40.0
10[a]	50.5	1.8	277:1	1:1 (**III**)	66	34000	39.0
11[a]	50.6	1.8	277:1	1:1 (**II**)	68	26000	38.0

[a] Excess MAO added ($3.81*10^{-3}$ moles)
[b] Al loading from ICP
[c] Boron based cocatalyst, tris(pentafluorophenyl)borane (**I**), trityl borate (**II**) or N,N-dimethylanilinium borate (**III**)
[d] Propylene pressure 40 psig (2.8 atm), reaction time=1 hour, CGC **1** (7.6μm)
[e] Determined by GPC at 135°C using light scattering detector and calibrated using polystyrene standards, PDIs of polypropylene determined to be 1.9-2.4
[f] Determined by NMR at 100°C with 1,1,2,2 tetrachloroethane as the lock solvent

Propylene polymerization was performed with supported catalysts **AMPS-Al-2** (Table 6.4, entry 5) affording polypropylene of M_w 22,000. In order to study the effect of counterions, to a mixture of supported cocatalyst **AMPS-Al-2** and **CGC 1** and pressured with propylene, **I** was added (Table 6.5, entry 9). Polypropylene obtained through the use of titanium cation and borate anion shows slightly higher activity and molecular weight (Table 6.5, entry 9) compared to the use of titanium cation counterbalanced by aluminate anion (Table 6.5, entry 5). Similarly, the addition of **II** or **III** to supported cocatalyst **AMPS-Al-2** and **CGC 1** with propylene affords polypropylene of higher molecular weight and activity compared to the use of aluminate counterions. Although the presence of borate counterions affords polypropylene with higher activity and molecular weight compared to the aluminate counterions, the nature of the counter anion does not alter the percent tacticity of the polypropylene (% rr = 35-39).

6.3.5 Propylene Homopolymerization using MAO Tethered to Mesoporous Silica

As discussed in Chapter 4, four different silica samples with different pore sizes, hydroxyl content and wall thickness were synthesized (HX, HC, PX and PC). These silica matrices have been used as supports to tether MAO and mesoporous silica supported cocatalysts have been prepared. The supported cocatalysts have been treated with more MAO and **CGC 1** in toluene and then pressured with propylene; the activity, M_w, and percent tacticity of the formed polypropylene is shown in Table 6.6)entries 12-17), Figure 6.4. The activity, molecular weight (M_w 9,000-18,000) and percentage tacticity (% rr = 36-39) of polypropylene prepared from silica supported cocatalysts with **CGC1** were found to be independent of the physical parameters of the silica matrix,

namely, the pore size, the hydroxyl content on the surface or the amount of aluminoxane loading.

Propylene polymerizations using supported silica matrices with **CGC1** and various boron based cocatalysts afforded polypropylene of similar molecular weight and percentage tacticity; the counter anion does not affect the properties of polyolefins prepared using silica supports. Polypropylene produced using silica-supported cocatalysts affords polypropylene of slightly lower molecular weight and activity compared to polystyrene supported cocatalysts. This can be attributed to catalytic deactivation sites (Si-O units)present on the more chemically interactive silica surface, which reduce the overall activity for production of polypropylene. Also, compared to polystyrene matrices, the aluminoxane loading in each of the silica samples is higher. This could plausibly be the reason for preparation of lower molecular weight polypropylene.

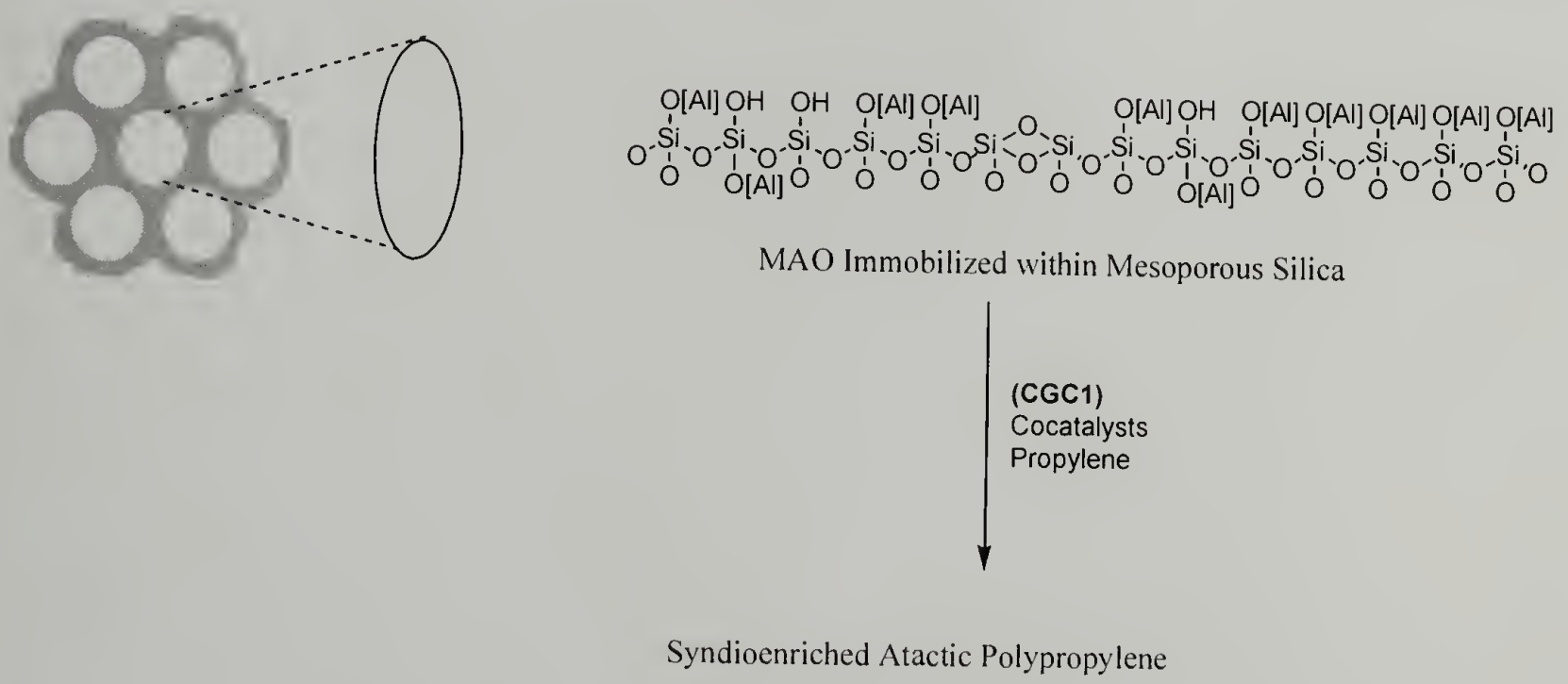

Figure 6.5 Preparation of Polyolefins using MAO Tethered to Mesoporous Silica in Conjunction with **CGC 1**

Table 6.6 Propylene Homopolymerization using MAO Tethered to Mesoporous Silica in Conjunction with **CGC 1**

Entry	MAO-Silica (mg)	Al loading (10^{-4} Moles) [a]	Al: Ti [b]	Activity [c] (Kg/molTi.atm.hr)	Mw [d]	% rr [e]
12	**PX-Al**	5.7	500:1	46	19,000	39.0
13	**HX-Al**	6.3	625:1	43	12000	38.0
14	**PC-Al-1**	5.1	619:1	31	14,000	
15	**PC-Al-2**	7.6	334:1	55	11,000	38.0
16	**PC-Al-3**	8.0	328:1	34	9,000	39.0
17	**HC-Al**	5.2	619:1	31	10,000	
3	Homogeneous	.38	485:1	35	25,000	40.0

Additional MAO added during activation protocol ($3.81*10^{-3}$ moles)
[a] Aluminum loadings determined
[b] Using Constrained Geometry Catalyst **1** (7.86 μmol)
[c] Propylene pressure 40 psig (2.8 atm), Reaction time=1 hour
[d] Determined by GPC at 135°C using light scattering detector and calibrated using polystyrene standards, PDI of Polypropylene=1.9-2.3
[e] Determined by NMR at 100°C with 1,1,2,2 tetrachloroethane as the lock solvent

6.3.6 Microstructural Analysis of Polypropylene

Propylene is a prochiral monomer that have two enantiofaces (*Re* and *Si*). The constrained geometry catalyst is regiospecific and the propylene monomer adds in a (2,1) fashion into the metal-alkyl bond.[93] However, CGCs are known to synthesize polypropylene in which random incorporation of *Re* and *Si* face into the metal-alkyl bond during propagation is observed, resulting in predominantly syndio enriched atactic polypropylenes.

Using ^{13}C NMR, the presence of tactic components of polypropylene can be determined. The chemical shift of the various carbons in a polymer chain are sensitive to the relative stereoconfigurations of the neighbouring monomer units. The chemical shift of the methyl group is especially useful to identify the stereoconfiguration of the monomer units. In the modified Fischer projection, the polymer backbone can be represented as a horizontal line and the relative orientations of the pendant methyl groups are shown as vertical lines. The lower case letter *m* represents the meso form and *r* represents the racemo dyad between adjacent chiral methine carbon units. Each dyad is given a single letter representation, a triad is given a two-letter representation and a pentad is given a four-letter representation. (Figure 1.5, Chapter 1) The percent syndiotacticity was determined from triad analysis of the methyl region ^{13}C carbon resonance of the polymer.[8]

Two different propylene samples were analyzed for the percent syndiotacticity. Polypropylene synthesized from analogous homogeneous CGCs in conjunction with MAO as the catalyst (Figure 6.6). In the ^{13}C NMR, 3 sets of multiplets were observed at δ (19.8-21.2) attributed to methyl carbon, the singlet at δ 28.4 was attributed to the methine carbon and finally the multiplets at δ (45.4-47.8) were attributed to the methylene carbon. In the region of δ (19.8-21.2), multiplets attributed to rr, mr + rm and mm were integrated to obtain corresponding intensity of each of these resonance. Finally the percent syndiotacticity was obtained as a ratio of the rr content to the total rr+mr+rm+mm triad content in the polymer. For the polypropylene synthesized from homogeneous polymerization (Table 6.4, entry 8), the percent rr was determined to be 39.

Similarly, polypropylene synthesized from MAO tethered system in conjunction with **CGC1** (Table 6.4, entry 4) was analyzed by ^{13}C NMR (Figure 6.7). Thr precent syndiotacticity was determined to be 37%. Tacticity of polypropylene is not dependent on the mode of polypropylene production, namely, homogeneous or supported cocatalyst. The production of various forms of polypropylene is dependent on the group symmetry and the primary ligand influence of the activated single site catalyst.

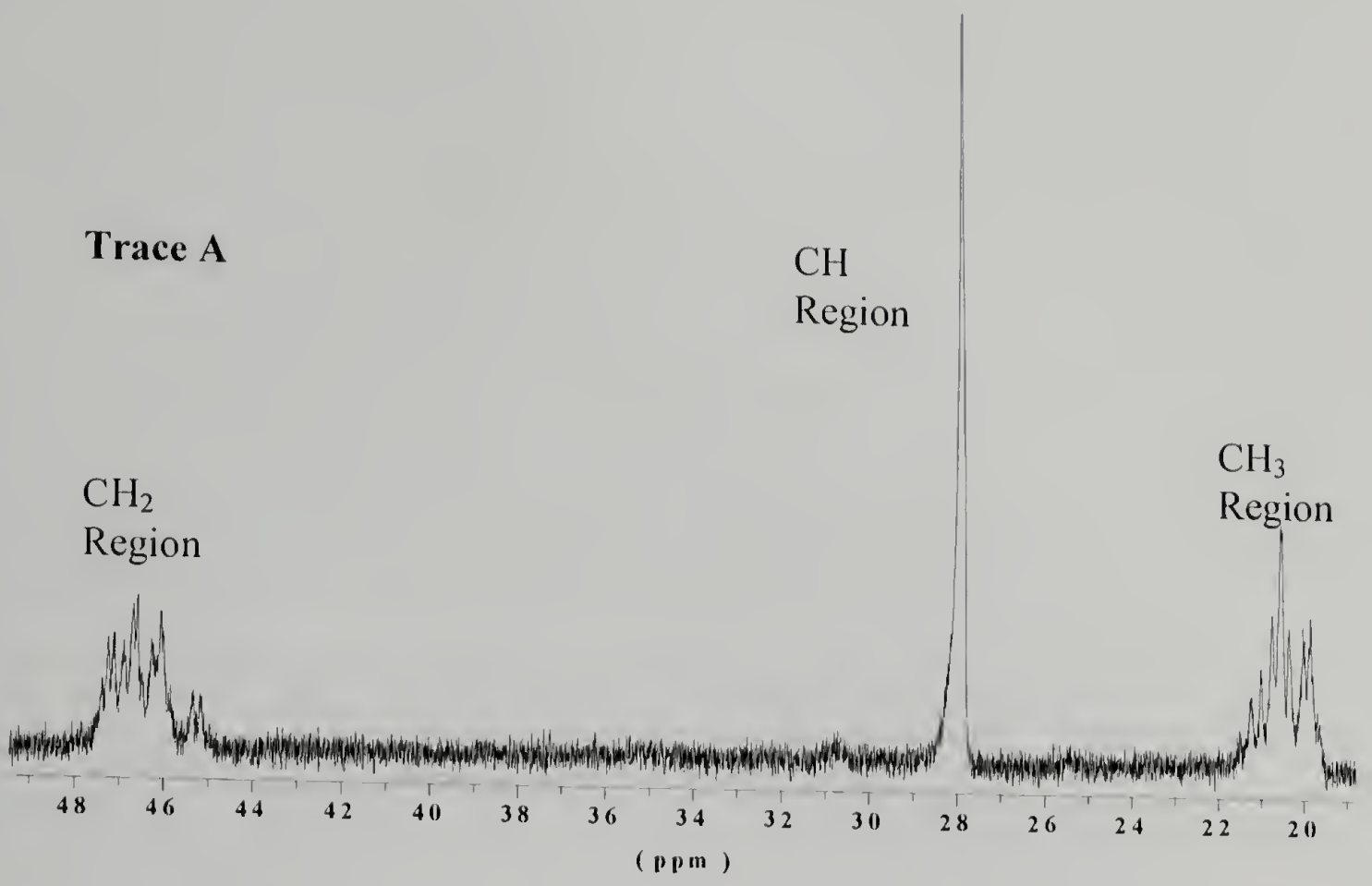

Figure 6.6 ^{13}C NMR Analyses of Polypropylene Sythesized from **CGC 1** and MAO in Toluene (Homogeneous Polymerization): Trace A (CH_2, CH, and CH_3 Regions), Trace B (Expanded CH_3 Region)

Trace A

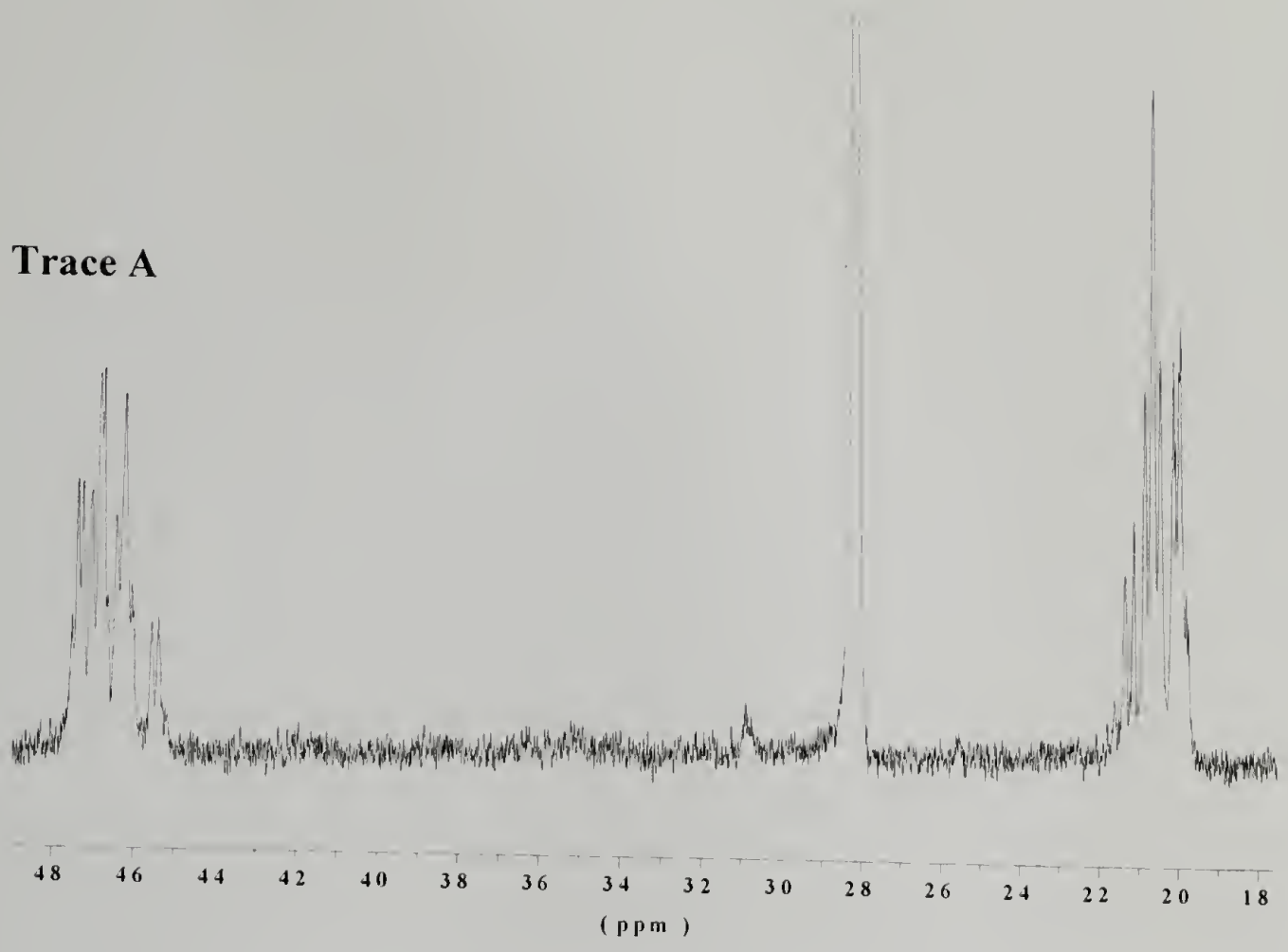

Trace B

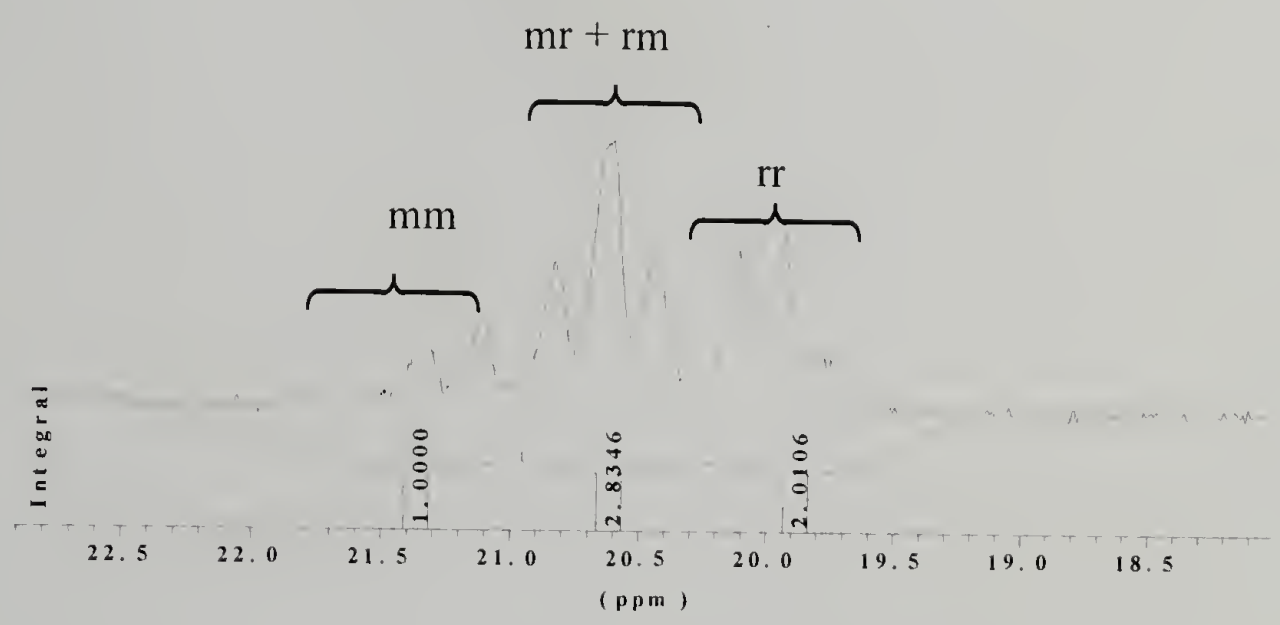

Figure 6.7 ^{13}C NMR Analyses of Polypropylene Sythesized from MAO Supported Aminomethylpolystyrene (**AMPS-Al-2**) with **CGC 1**: Trace A (CH_2, CH and CH_3 Regions), Trace B (CH_3 Region)

6.4 Summary

In this chapter, synthetic protocols to tether methylaluminoxane to aminomethylpolystyrene or mesoporous silica have been developed in order to study the effect of supported cocatalyst on the polymerization of olefins. Using MAO tethered to aminomethylpolystyrene in conjunction with **CGC 1**, ethylene homopolymerization was performed. The molecular weight (M_w) of the polyethylene formed was higher than that prepared with tethered single site catalyst or homogeneous single site catalysts. On the other hand, the percent crystallinity of the formed HDPE was higher than supported SSCs but lower than HDPE produced from homogeneous polymerization reactions. The presence of lower crystalline fractions can be attributed to the influence of the support.

Using MAO tethered to aminomethylpolystyrene and mesoporous silica, propylene polymerization were performed in conjunction with **CGC1** as the metal catalyst component. The aluminoxanes tethered to polystyrenes in the absence of excess soluble aluminoxanes and trimethylaluminum affords polypropylenes of higher molecular weight compared to homogeneous polymerizations and this observation can be attributed to the decrease in chain transfer to alkyl aluminum species. The activity and the molecular weight for the production of polypropylene is a function of the type of support to which the aluminoxane is attached, loading of aluminoxane, amount of trimethylaluminum and presence of borate counterions. However, the tacticity of the polypropylene is dependent on the primary ligand influence of the constrained geometry catalyst and is not influenced by the presence of supported catalyst/cocatalyst matrices.

CHAPTER 7

LINEAR OR BRANCHED POLYETHYLENES SYNTHESIZED FROM SUPPORTED ARYLOXY TITANIUM (IV) CYCLOPENTADIENYL COMPLEXES

7.1 Introduction

Numerous efforts are being directed towards the synthesis of Single Site Catalysts (SSCs) for the polymerization of olefins to produce branched polyethylenes. There are now several known SSCs that copolymerize ethylene and α-olefins to produce branched copolymers with uniform comonomer distributions across the entire molecular weight range, and have tunable levels of commoner incorporation. [24,37,38] An alternative method for the production of branched polyethylenes utilizing only ethylene as monomer can be achieved by judicious choice of catalyst(s) and reaction conditions (Figure 7.1). The use of Ni or Pd based cationic or neutral complexes afford polyethylenes with tunable branch content via a chain isomerization mechanism.[54] Multi-component catalyst systems can be utilized where one catalyst oligomerizes ethylene to α-olefins (or vinyl macromers) and a second catalyst is employed to copolymerize ethylene with the α-olefin formed *in situ* to prepare branched polyethylenes. Recently, there have been reports of branched polyethylene synthesis by the use of Ti and/or Zr catalysts in conjunction with an aluminum or boron cocatalyst.[94-97]

Polyethylene with significant number of ethyl branches has also been observed with MAO as the cocatalysts for certain zirconocenes, and this has been attributed to

the formation of 1-butene in the product feed and subsequent copolymerization with ethylene.[98] During ethylene homopolymerization the interaction between the metal cation (Ti or Zr) and the co-catalyst anion (borates) has been tuned to afford α–olefins *in situ*, which are subsequently copolymerized with ethylene. Branched polyethylene having exclusively butyl branches can be prepared using monocyclopentadienyl titanium trimethyl/$B(C_6F_5)_3$. This catalyst combination apparently produces 1-hexene *in situ*, by an ethylene trimerization reaction, which is then copolymerized with ethylene to afford branched polyethylene.[99]

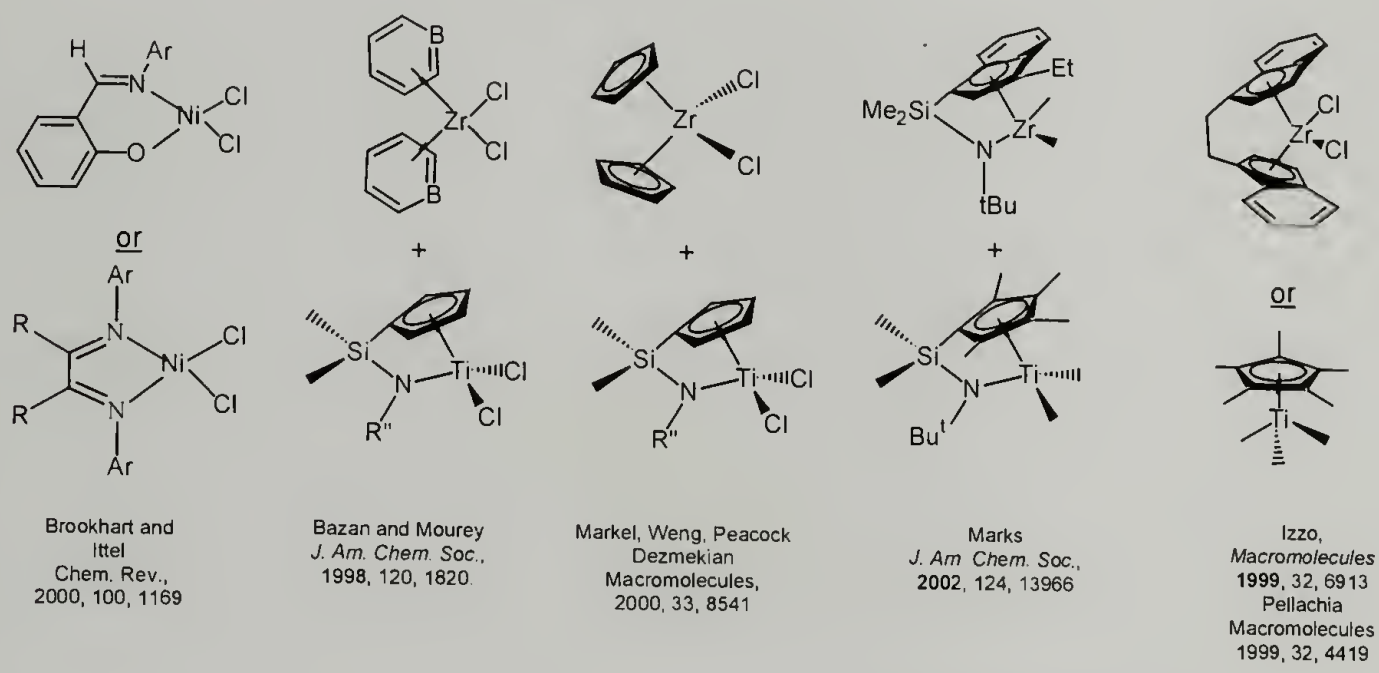

Figure 7.1 State of the Art in Homogeneous Single Site Catalysts for the Production of Branched Polyethylenes

For single site eatalysts that are covalently bound to a support questions arise as to what influenee the support will have on catalyst performance and the properties of the resulting polymer. In this chapter, we have dcsigned synthetie sehemes to tether piano stool eomplexes (**13-16**) on hydroxy -funetionalized polystyrene supports (**HPS**) in order to study the influenee of the support matrix on the eatalyst performanee and the properties of the resulting polyolefin.

7.2 Experimental Section

7.2.1 Methods and Materials

All reaetions werc performed under nitrogen in Schlcnk glassware or in an inert atmosphcre dry box. All solvents used were obtained from a solvent purifieation manifold.[64] Titanium tetrachloride, bis(trimethylsilyl)eyelopentadiene,

2,5,5-tris(trimethylsilyl)-1,3-eyelopentadicnc, cyclopentadicnyltitanium triehloride (**13**) , pentamethyleyeloepentadienyltitanium trichloride (**14**), AIBN, and hydrazine hydrate were obtained from Aldrieh and used as rceeivcd. Styrene and 4-aeetoxystyrenc werc obtained from Aldrich and used after distillation from CaH_2. Methylaluminoxanes, tris(pentafluorophenyl)borane ($(B(C_6F_5)_3$, **I**), trityl borate ($[(C_6H_5)_3C][B(C_6F_5)]_4$, **II**) and N,N-dimethylanilinium borate ($[(C_6H_5N(CH_3)_2H][B(C_6F_5)]_4$, **III**) werc obtained from Albemarle and used as reccivcd. The complcxes trimcthylsilylcyclopentadienyltitanium triehloride (**15**) and bis(trimethylsilyl)cyelopentadienyltitanium triehloride (**16**) were synthesizcd aecording to published procedurcs.[65,100] Polymerization was performed using an cthylene/propylcne manifold and thiek-walled reactors.[70]

7.2.2 Instrumentation

^{1}H NMR spectra were obtained at 300 MHz using a Bruker DPX 300. ^{13}C NMR were recorded at 75 MHz using a Bruker DPX 300 in the continuously proton decoupled (CPD) or DEPT 90 mode in solutions of $CDCl_3$ or CD_2Cl_2. ^{13}C NMR spectra of the polyolefins in tetrachlorethylene- d_2 were recorded at 150 MHz on an Avance DPX 600 using a quantitative pulse program for solution NMR at 135 °C. Elemental analysis was performed using three Exeter Analytical Inc.240XA CHN analyzers and a Leeman Labs Inc. Dual ViewDRE Sequential ICP was used to analyze the Ti and Si loadings in the samples. Gel Permeation Chromatography (GPC) of the polyolefins was performed with a Polymer Laboratories PL-220 high temperature GPC equipped with a Wyatt MiniDawn (620 nm diode laser) high temperature light scattering detector and refractive index detector at 135 °C using 1,2,4-trichlorobenzene as solvent and calibrated using polystyrene standards. The dn/dc value for polyethylene used was -0.11. Thermal analyses was performed using TA DSC 2910 equipped with liquid nitrogen cooling accessory unit under a continuous nitrogen purge (50mL/min) with a heating and cooling scan rate of 10 °C/min. Infrared analyses were performed using a Perkin Elmer 2000 FTIR on samples prepared as KBr pellets. Wide Angle X-Ray (WAXD) diffractograms of the polymer powder in a capillary tube was performed using Cu Kα radiation (wavelength of 1.54 Å) with a nickel filter. The X-Rays were collimated into a fine beam of circular cross section using a pinhole collimator; a HDPE standard was used to calibrate the d (110) and d (200) peak positions.

7.2.3 Support Preparation

7.2.3.1 Synthesis of Poly (styrene-*r*-4-acetoxystyrene) (APS)

Styrene (24.5 mL, 0.24 mol) and 4-acetoxystyrene (5.0 mL, 0.03 mol) was combined with AIBN (500 mg, 0.003 mol) in a round-bottomed flask. The reaction mixture was flushed with nitrogen for 5 minutes, and the flask was placed in an oil bath at 70°C for approximately three hours. The resulting polymer was precipitated into a litre of methanol, filtered, and dried *in vacuo* at 120 °C overnight. The resulting dry weight of the polymer (APS) was 12.0 grams. ^{1}H NMR analysis reveled 16 mol % 4-acetoxy styrene incorporation in the copolymer.

^{1}H NMR ($CDCl_3$): δ 1.1-2.2 (C-*H* aliphatic main chain, CH_2 and CH), δ2.3 ($OCOCH_3$), δ 6.5-7.2 (C-*H* aromatic)

^{13}C NMR ($CDCl_3$, CPD): δ21.7, 40.8, 42.8, 44.5, 46.4 (aliphatic *C*H and CH_2), 121.3, 126.1, 128.1, 128.4 (C_6H_4 and C_6H_5), 145.6 (*para* carbon in phenyl unit), 169.7 (OCO)

FTIR (ν cm^{-1}): s 697, 756, 847, 909, 940, 1017, 1166, 1200, 1382, 1452, 1493, 1505, 1601(C=C), 1766(COO stretch), 2924 (aliphatic C-H), 3026(aromatic C-H), 3060 (aromatic C-H), 3082 (aromatic C-H)

7.2.3.2 Synthesis of Poly(styrene-*r*-4-hydroxystyrene) (HPS)

The 12.0 g of **APS** were dissolved in a solution of 250 mL of THF to which 4.08 mL of hydrazine hydrate was added with vigorous stirring. After four days of reaction at room temperature, the resulting **HPS** copolymer was precipitated into excess methanol and dried *in vacuo* at 115 °C overnight (yield =75%).

FTIR (ν cm^{-1}): 696, 755, 872, 888, 1027, 1121, 1170, 1255, 1452, 1493, 1512, 1601(C=C), 2850, 2917 (aliphatic C-H), 3060 (aromatic C-H), 3082 (aromatic C-H), 3510 (OH stretch)

Elemental Analyses: Observed C (87.84), H (7.44), O (4.72, 0.3mol %)

Gel permeation chromatography: M_w (70,000), PDI=1.9

7.2.4 General Procedure for Supported Catalyst Preparation

Assembly of the aryloxy piano stool complex on **HPS** was carried out in the glovebox. The precursor catalysts (**13-16**) and **HPS** were dissolved in toluene in a 50 mL Schlenk flask, sealed and removed from the glovebox and placed in an oil bath at 70 °C with vigorous stirring for two days. Subsequently, the toluene was removed *in vacuo*, leaving behind the solid supported catalyst. The supported catalysts were analyzed via ^{13}C NMR, and elemental analyses. Table 7.1 lists the supported catalysts with the respective precursor and support amounts used, along with the effective molar ratio OH: to catalyst.

7.2.5 General Synthesis of (Cyclopentadienyl)-(aryloxy)Titanium (IV) Complex

Synthesis of (Monophenoxy)(Cyclopentadienyl)Titanium (IV) Dichloride (17)

To a solution of 10.0 mL of dichoromethane and cyclopentadienyltitanium trichloride (**13**, 100 mg, 0.45 mmol), phenol (34 mg, 0.38 mmol) was added slowly with constant stirring. The reaction was allowed to proceed at room temperature for a period of 12 hours. The solvent was removed *in vacuo* to afford an orange solid (**17**, 90 mg, 90% yield).

^1H NMR ($CDCl_3$): 6.6 (s, 5H, C_5H_4), 7.0-7.6 (m, 5H, C_6H_5)

^{13}C NMR ($CDCl_3$, CPD): 118.8, 121.3,123.9, 124.9, 129.9, 168.3

Elemental analysis ($C_{11}H_{10}Cl_2OTi$): Calculated C (47.4); H (3.27); Observed C (47.8), H (3.6)

HR-MS Calculated (275.9764), Observed (275.9595)

Synthesis of Bis(Phenoxy) (Cyclopentadienyl) Titanium (IV) Chloride (18)

To a solution of 10.0 mL of toluene and cyclopentadienyltitaniumtrichloride (**13**, 108 mg, 0.4 mmol), phenol (81 mg, 0.88 mmol) was added slowly with constant stirring and refluxed for a period of 12 hours. The solvent was removed *in vacuo* to afford a red solid (**18**, 110 mg, 85% yield).

^{1}H NMR ($CDCl_3$): 6.8(s, 4H, C_5H_4), 6.6-7.4 (m, 10H, C_6H_5)

Elemental analysis ($C_{17}H_{15}ClOTi$): Calculated C (42.35), H (2.83); Observed C (42.76), H (2.94)

HR-MS Calculated (406.0638), Observed (406.0890)

Synthesis of Mono(phenoxy)(trimethylsilylcyclopentadienyl) Titanium (IV) Dichloride (19)

To a mixture of 10.0 mL of dichoromethane and (trimethylsilyl)cyclopentadienyltitanium trichloride (**15**, 102 mg, 0.34 mmol), phenol (32 mg, 0.35 mmol) was added slowly with constant stirring and the reaction was allowed to proceed at room temperature for a period of 12 hours. The solvent was removed *in vacuo* to prepare an orange solid (**19**, 110 mg, 82% yield).

^{1}H NMR ($CDCl_3$):0.4 (s, 9H, $Si(CH_3)_3$) 6.8 (t, 2H), 7.1 (t, 2H) 7.0-7.4 (m, 5H, C_6H_5)

^{13}C NMR ($CDCl_3$, CPD): -0.2, 118.8, 124.6,123.9, 126.9, 128.6, 129.8, 137.5, 168.3

Elemental analysis ($C_{14}H_{18}Cl_2OSiTi$): Calculated C (47.1), H (5.14); Observed C (46.9), H (5.16)

HR-MS Calculated (347.9986), Observed (347.9954)

Synthesis of (Bis(phenoxy)(Trimethylsilyl(Cyclopentadienyl))-Titanium(IV) Chloride (20)

To a solution of 10.0 mL of toluene and eomplex (**15**, 102 mg, 0.34 mmol), phenol (75 mg, 0.7 mmol) was added slowly with constant stirring and the reaetion mixture was refluxed for a period of 1 day. The solvent was removed *in vacuo* and affords a red solid in 90 % yield (**20**).

^{1}H NMR ($CDCl_3$):0.3 (s, 9H, $Si(CH_3)_3$) 6.6-7.4 (m,14H, C_6H_5, C_5H_4)

^{13}C NMR ($CDCl_3$, CPD): 0, 115.7, 118.9, 121.5, 123.2, 126.3, 130.1, 133.7, 167.6

Elemental analysis: ($C_{20}H_{23}ClO_2SiTi$): Calculated C (59.06), H (5.66); C (59.29), H (5.81)

7.2.6 Representative Ethylene Polymerization

To a mixture of 10 mL of toluene and 1.7 mL of 30 wt % of MAO (4.77M) taken in a polymerization reaetor equipped with a stir bar, 31.1 mg of complex **HPS-Ti-1** was added and pressurized with 60 psig of ethylene with constant stirring. After 27 minutes, the ethylene supply was stopped and the reaetor was vented to remove exeess ethylene, the reaction mixture was quenched with 10% volume of hydrochloric aeid in methanol mixture. The polyethylene was eolleeted by filteration and dried *in vacuo* overnight to afford 350 mg of polyethylene (Table 7.2, Entry 1).

7.2.7 Representative Copolymerization of Ethylene and Octene:

To a mixture of 10.0 mL of toluene and 1.7 mL of 30 wt% of MAO in toluene (4.77M) in a polymerization reactor, 38.2 mg of **HPS-Ti-1** was added. To this system was added 1-octene (5 mL) and ethylene at a pressure of 60 psig was supplied for 15 mintues with stirring. The ethylene supply was stopped and the reactor was vented to remove excess ethylene, the reaction mixture was quenched with 10% hydrochloric acid-methanol mixture and the polymer was collected by filtration and dried *in vacuo* overnight to afford 730 mg of product (Table 7.5, Entry 18).

7.3 Results and Discussion

7.3.1 Preparation and Characterization of HPS

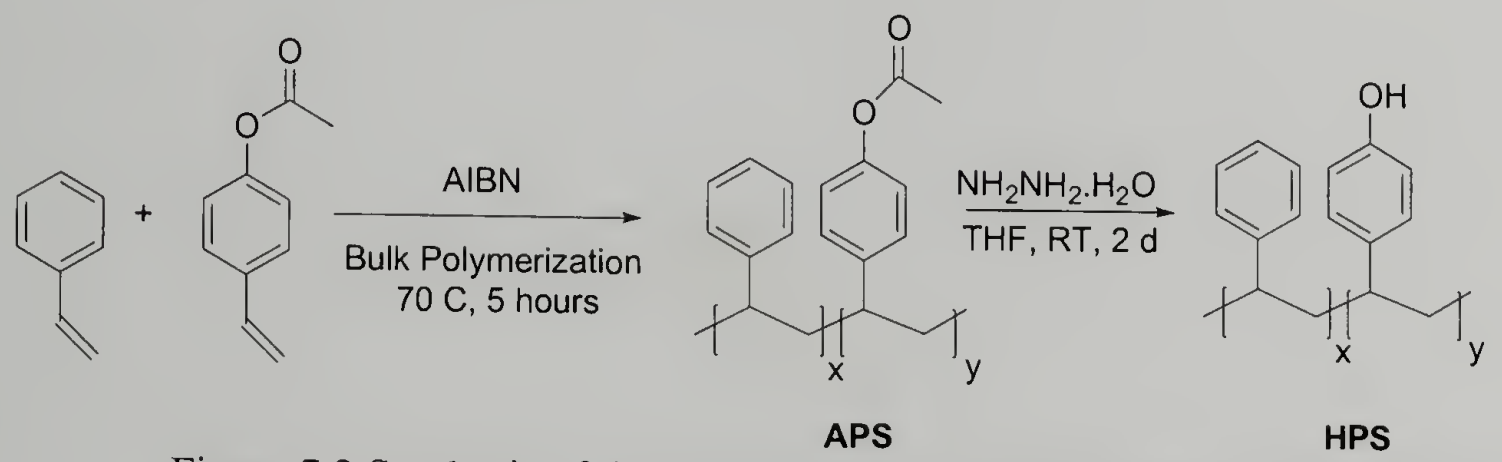

Figure 7.2 Synthesis of the Support Matrix: Poly(Styrene-*r*-HydroxyStyrene) (**HPS**)

In order to synthesize supported aryloxy based piano stool complexes, a soluble hydroxypolystyrene matrix was prepared by the random copolymerization of 4-acetoxystyrene and styrene with AIBN as the radical initiator. Poly(styrene-*r*-4-hydroxystyrene) (**HPS**), was subsequently prepared by the reaction of poly(styrene-*r*-4-acetoxystyrene) with hydrazine hydrate (Figure 7.2).[101] The complete conversion of the acetoxy groups to hydroxyl groups was confirmed by IR spectroscopy. In the resulting product **HPS**, complete absence of the C=O stretching mode at 1766 cm^{-1}

and appereance of the OH stretch at 3510 cm^{-1} was noted. The molecular weight and the hydroxyl content of the soluble HPS support (macroligand) was determined to be 70,000 M_w with 0.3 mol % hydroxyl groups.

7.3.2 Preparation and Characterization of Macroligated Aryloxy Cyclopentadienyl Complexes

The piano stool complexes (**13-16**) used to assemble aryloxy complexes on the macroligand are shown in Figure 7.3. The reaction of complexes **13-16**, with HPS in toluene at 60 °C for 2 days (Figure 7.4, Table 7.1) affords a viscous reaction mixture that ultimately results in a polymeric gel having low solubility in toluene.

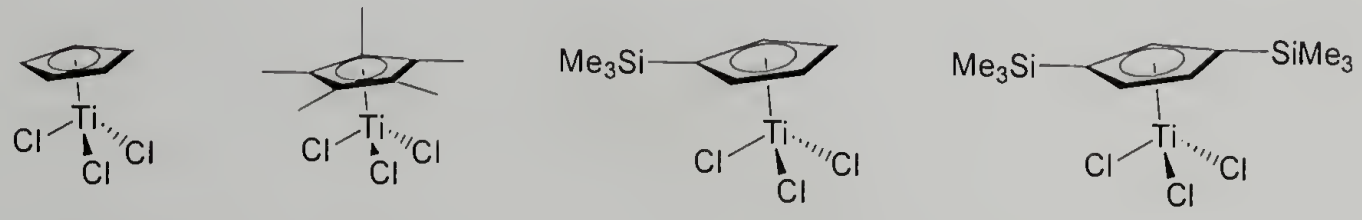

13 **14** **15** **16**

Figure 7.3 Precursor Piano Stool Catalysts (**13-16**) used to Assemble Aryloxy Complexes of **HPS**

The initial reaction of **13-16** with HPS affords the aryloxycyclopentadienyltitanium(IV) dichloride, (form **A**). The hydrochloric acid formed as the by-product of the reaction of the Ti-Cl with the hydroxyl groups on the HPS was removed *in vacuo*. The low solubility observed is indicative of the formation bis(aryloxy)cyclopentadienyltitanium(IV) chloride, (form **B**), which crosslinks the polymer. The net result of the reaction is formation of macroligated catalysts

immobilized on polystyrene (Figure 7.4). Elemental analyses of the Ti:Cl mole ratio of macroligated complex was performed, the experimentally determined values were in the range of 1:1.5-1.7 (Table 7.1). These values are intermediate between those expected for forms **A** and B in a 60:40 mixture and are indicative of the presence of both forms. The probability of formation of a tris(aryloxy)cyclopentadienyltitanium(IV) species is considered to be quite low based on steric factors. Analyses by NMR on the macroligated complexes swollen with C_6D_6 were performed to further quantify the formations of forms **A** and **B**. There are not sufficient chemical shift differences in the ^{1}H NMR and ^{13}C NMR spectra for **HPS-Ti-1, HPS-Ti-2**, and **HPS-Ti-3** to differentiate between the two forms. However, the ^{13}C NMR of **HPS-Ti-4** has two resonances for $Si(CH_3)_3$ at δ -0.2 and δ1.5 which are attributed to the formation of form **A** and form **B** respectively (Figure 7.10). The ratio of **HPS-Ti-4 A** to **HPS-Ti-4 B** determined by elemental analysis and ^{13}C NMR are in good agreement.

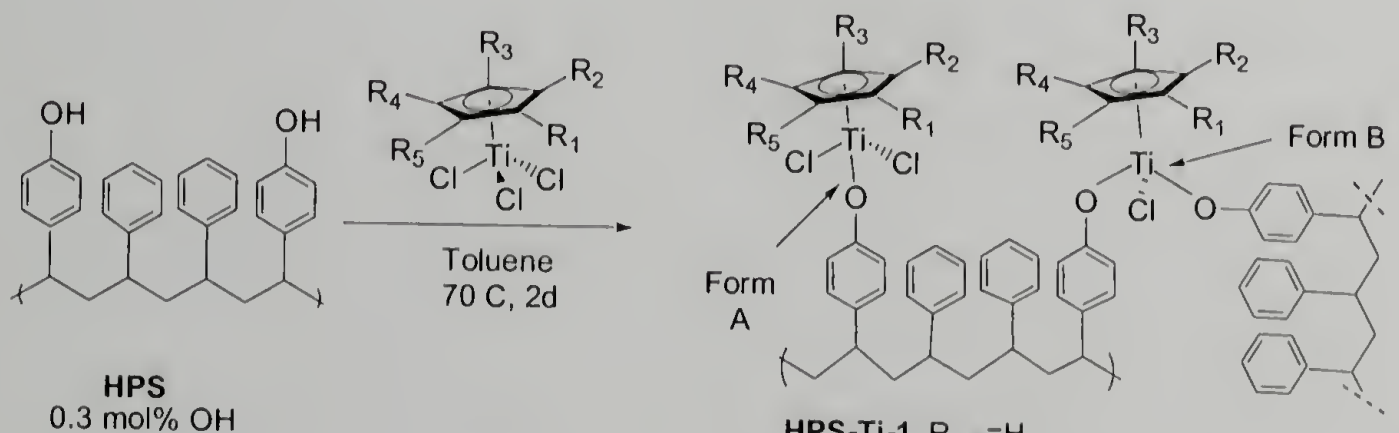

Figure 7.4 Syntheses of Aryloxy Cyclopentadienyl Tianium Based Macroligated Catalysts

Related observations have been made by Xu *et al.* for $CpTiCl_3$ supported on hydroxyl containing styrene terpolymers.[102] Following activation by MAO, electron spin

resonance (ESR) spectra were recorded for Ti(III) species that were then assigned to the presence of mono-aryloxy and bis-aryloxy, (both inter- and intra-chain ligation) macroligated catalyst centers during styrene polymerization

Table 7.1 Elemental Compositions of the Aryloxy Cyclopentadienyl Titanium Based Macroligated Catalysts

Precursor Catalyst (mmol)	Macroligand (OH mmol)	Supported Catalysts	Elemental Analysis (Found) Ti:Cl:Si
13 (0.5)	3.0	**HPS-Ti-1**	1:1.5:n.d.
14 (0.4)	3.1	**HPS-Ti-2**	1:1.3:n.d.
15 (0.3)	3.0	**HPS-Ti-3**	1:1.7:1
16 (0.3)	3.0	**HPS-Ti-4**	1:1.8:2

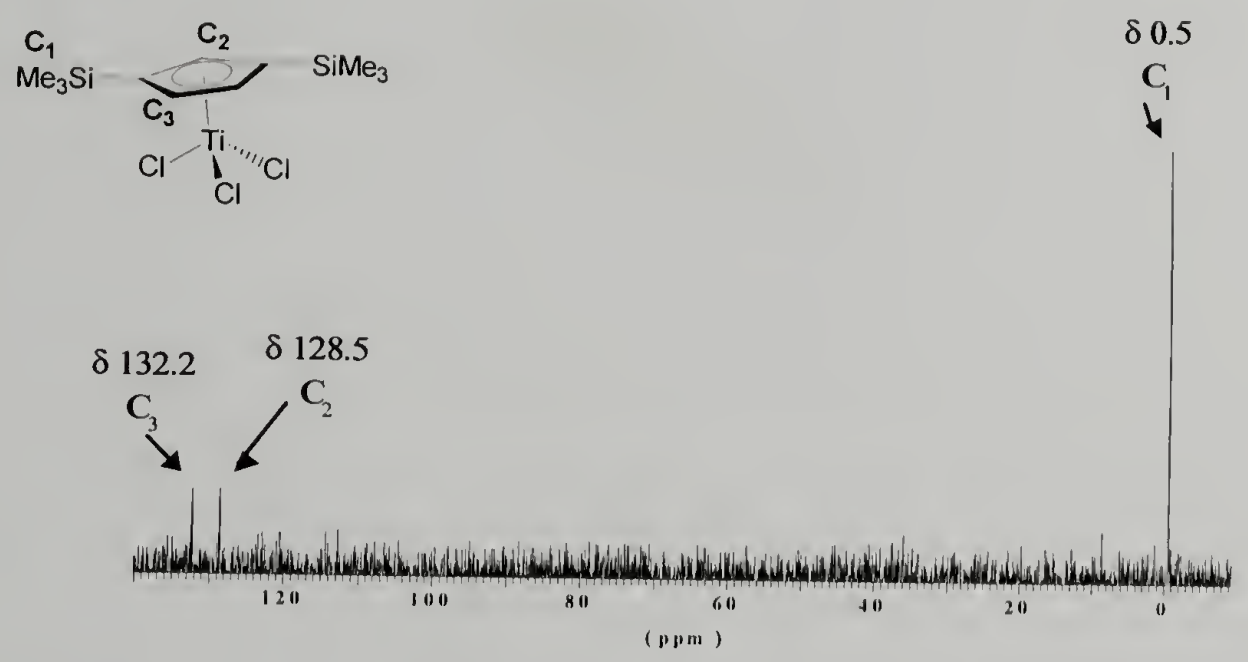

Figure 7.5 ^{13}C DEPT Spectrum of Bis(trimethylsilyl)CyclopentadienylTitanium (IV) Chloride (**16**)

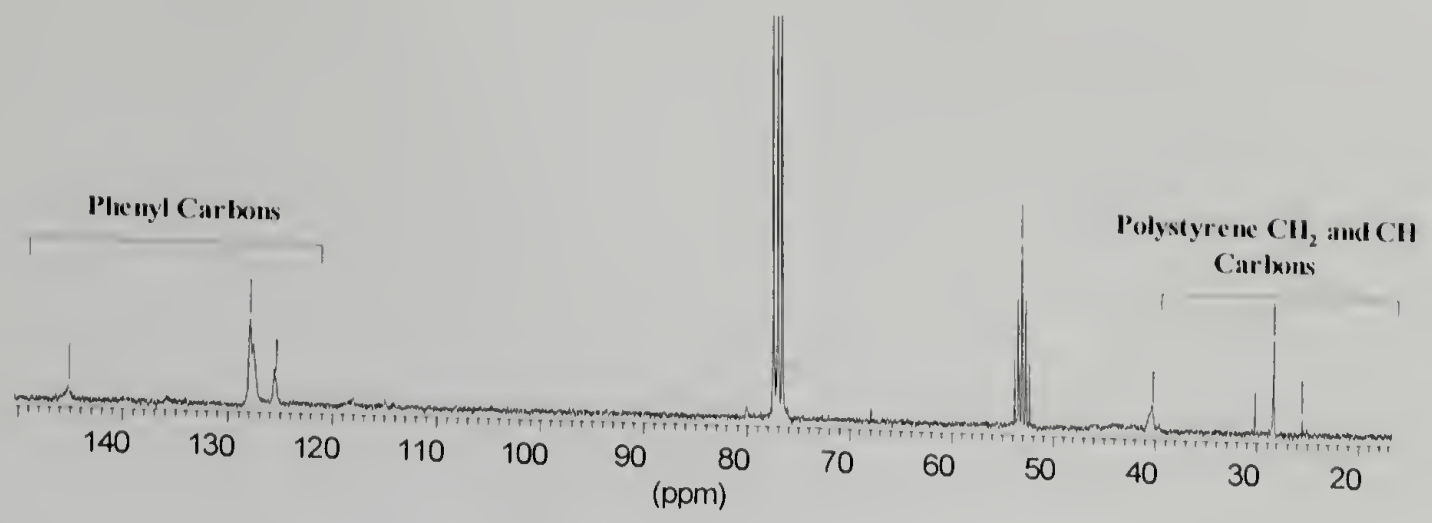

Figure 7.6 ^{13}C DEPT Spectrum of Poly (Styrene-r-4-hydroxylstyrene) Copolymer (**HPS**)

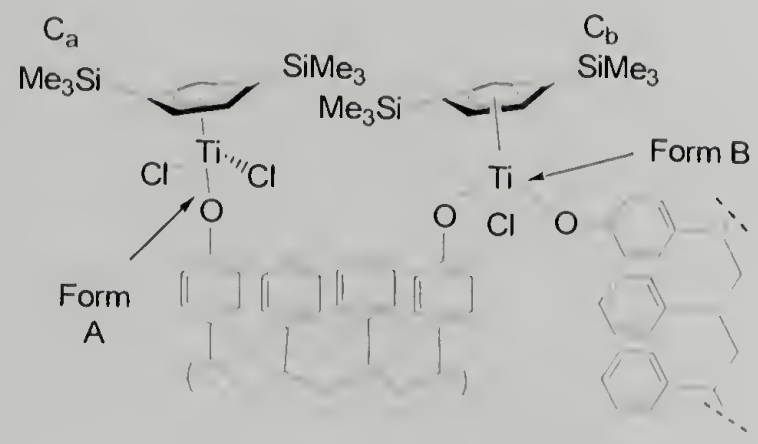

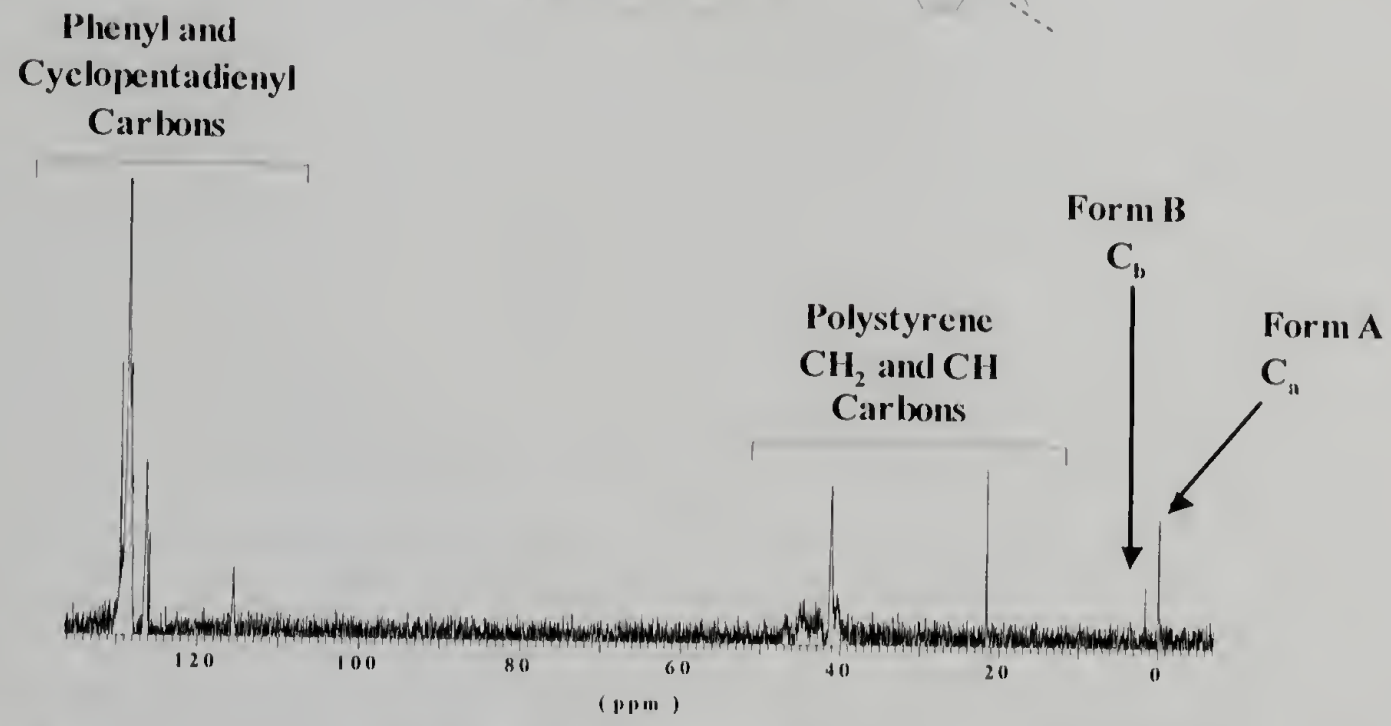

Figure 7.7 ^{13}C DEPT Spectrum of C_6D_6 Swollen Gel Containing Macroligated Complex HPS-Ti-4

7.3.3 Ethylene Homopolymerization using Macroligated Complexes in Conjunction with MAO as the Cocatalyts and Corresponding Control Polymerizations

Ethylene polymerization was performed using macroligated complexes in conjunction with MAO as the cocatalyst in toluene at room temperature. Experimental conditions, polymerization yield, molecular weights (M_w), melting points (T_m), enthalpy of fusion (ΔH_f), degree of crystallinity of the polymers are shown in Table 7.2, entries 1-4. Under comparable Al:Ti ratios, **HPS-Ti-2** and **HPS-Ti-3** showed similar activities for the production of polyethylene and these catalysts are more active than **HPS-Ti-1**, with **HPS-Ti-4** being the least active. The molecular weights of the polyethylenes produced range from high for those prepared using **HPS-Ti-3** and **HPS-Ti-4** ($M_w > 200,000$) to moderate for those prepared by **HPS-Ti-1** and **HPS-Ti-2** ($M_w < 100,000$).

Table 7.2 Ethylene Homopolymerization using Macroligated Catalysts in Conjunction with MAO as the Cocatalysts and Ethylene Control Polymerizations

Entry	Catalyst	Activity Kg/mol Ti.hr.atm[a]	T_m[b] (°C)	% Crystallinity[c]	M_w[d]	PDI[d]
1	**5**	16	121.5	14.8	52050	1.7
2	**6**	45	130.1	27.2	33390	2.3
3	**7**	43	134.0	29.5	498750	1.6
4	**8**	8	129.1	15.5	204500	1.8
5	**17**	64	131.0	12.2	570000	1.8
6	**18**	17	130.8	26.5	550000	1.5

[a] Al:Ti=600-1600, Ethylene pressure 60psig, room temperature, 10-25 minutes reaction
[b] DSC **second** scan,
[c] Ratio of heat of fusion of polyethylene sample to theoretical heat of fusion of polyethylene single crystal ΔH=293 J/g,
[d] Determined through GPC at 135 °C in TCB using light scattering detectors calibrated with PS standard

Complex **HPS-Ti-1** afforded polyethylene of unimodal molecular weight distribution as observed from the GPC with a PDI of 1.7. The thermal analysis of the polymer showed a melting point of 121.5°C in the first and the second melt cycles. The physical characteristics of the polyethylene are fully consistent with the formation of a polyolefin from a SSC, and the depression in melting point is indicative of short chain branches. The ^{13}C NMR resonances were assigned as 14.27 ($1B_4$, CH_3, EHE), 22.92 ($2B_4$), 23.41 (δδ), 27.21 (βδ, EHEE+EEHE), 29.58 ($3B_4$, EHE), 29.98 (δδ, EEE), 30.45 (γδ, HEEE+EEEH), 34.10 ($4B_4$, EHE), 34.41 (αδ, EHEE+EEHE), 38.04 (CH, methine) as shown in Figure 7.8.[7] From ^{13}C NMR, exclusive butyl branches were observed at an incorporation level of 1.5 mol%. An explanation for the exclusive formation of butyl branches is the *in situ* formation of 1-hexene by a selective trimerization of ethylene. The catalytic trimerization of ethylene is promoted by the presence of Ti(II) which is known to result from the reduction of Ti(IV) precursors by reaction with MAO (Figure 7.9).[103] The Ti(II) species coordinates to two moles of ethylene (Figure 7.9, step 2) and under further oxidative addition (Figure 7.9, step 3) to form a Ti(IV) cationic metallacyclopentane. The metallacyclopentane undergoes further addition of an ethylene molecule (step 4) and results in a Ti(IV) metallacycloheptane. The metallacycloheptane undergoes β-H elimination and reductive elimination to produced both 1-hexene and Ti(II) species (step 5). The formed Ti(II) species reenters the trimerization catalytic cycle while the generated 1-hexene is then subsequently copolymerized with ethylene to prepare short chain butyl branches (SCB) in these resulting polyethylene copolymer (Figure 7.10).[99]

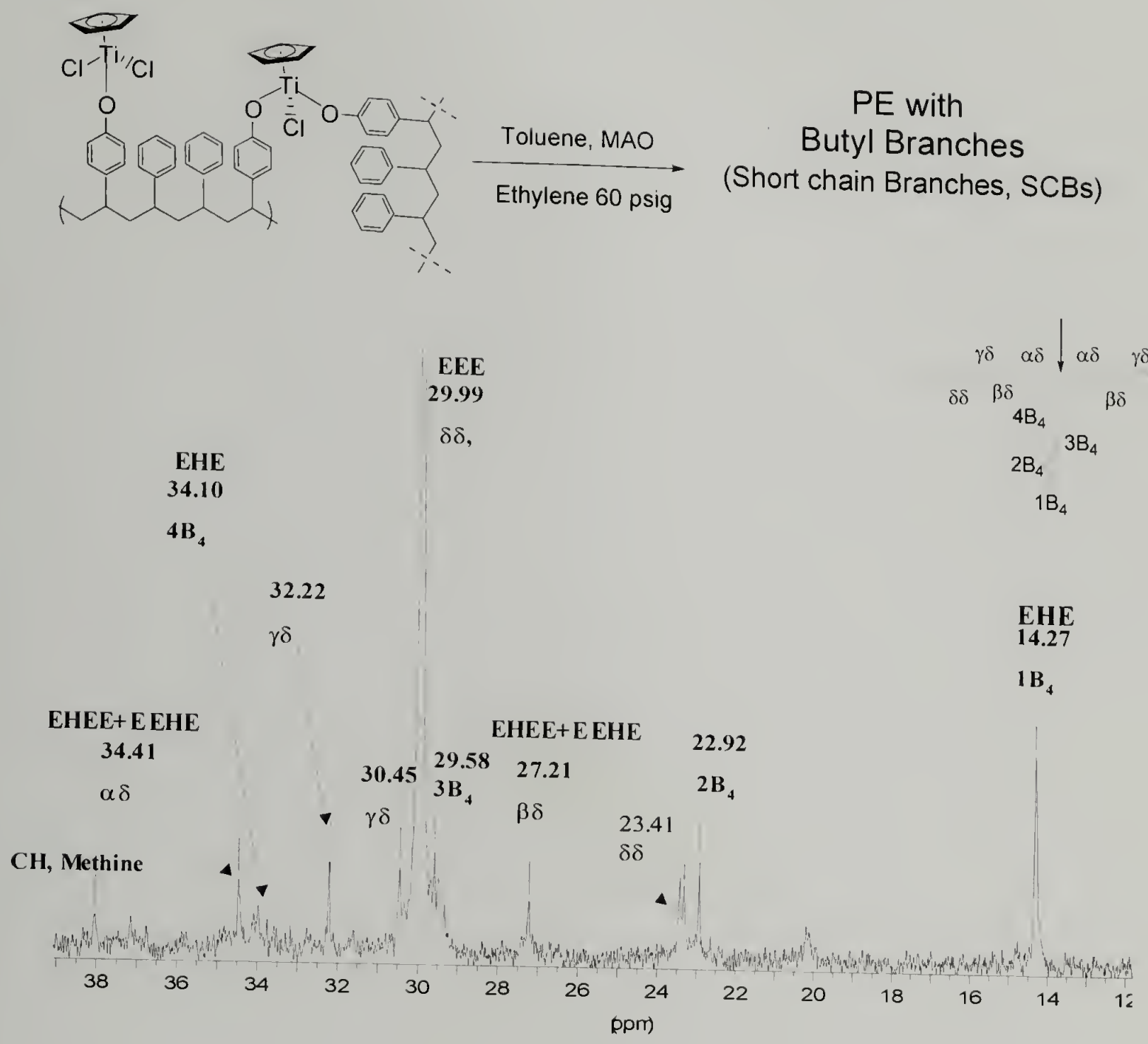

Figure 7.8 ^{13}C CPD Spectrum of Polyethylene with Butyl Short Chain Branches Synthesized from Complex **HPS-Ti-1** in Conjunction with MAO as the Cocatalysts

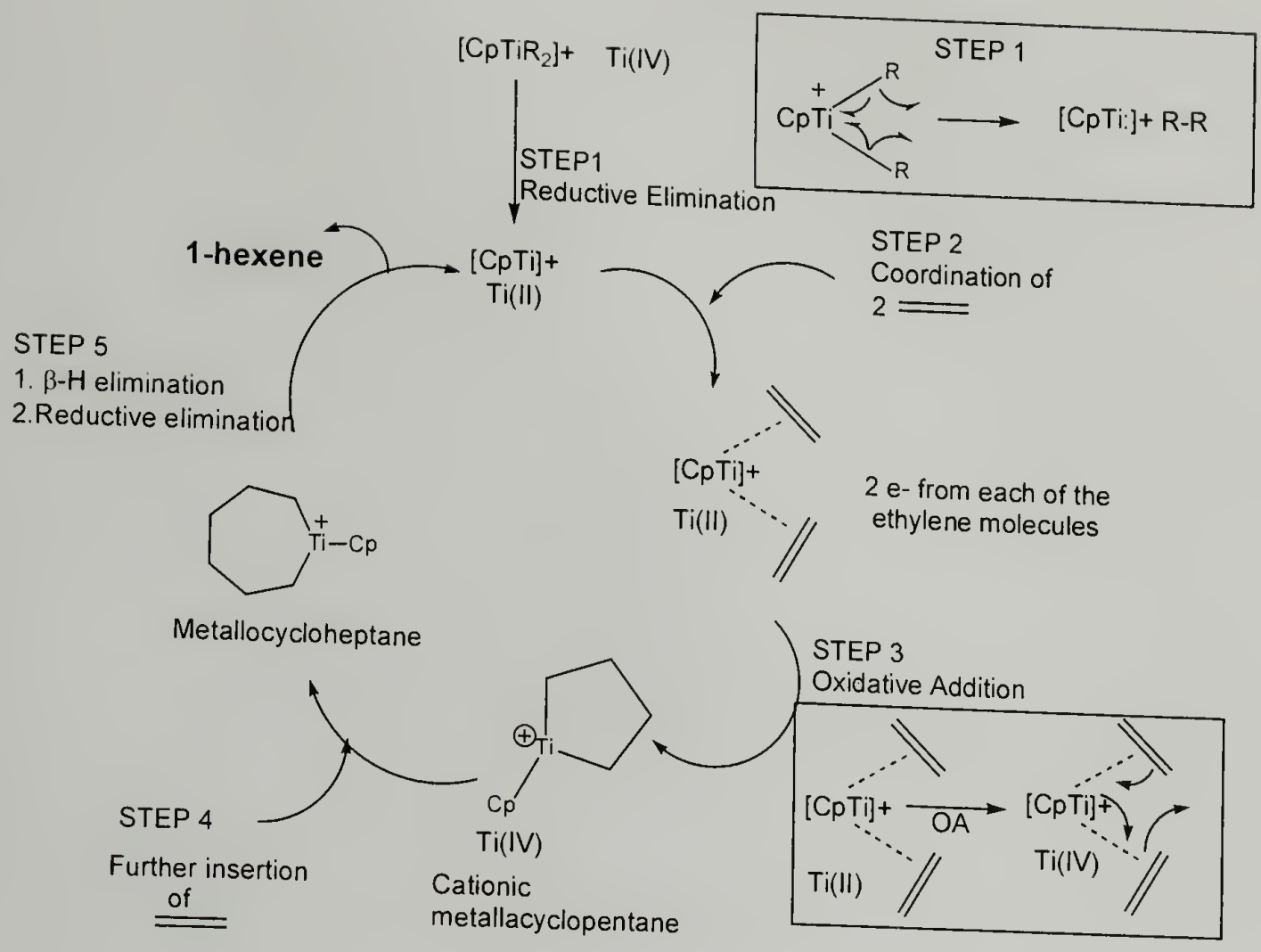

Figure 7.9 Synthesis of 1-Hexene by Ethylene Trimerization Process

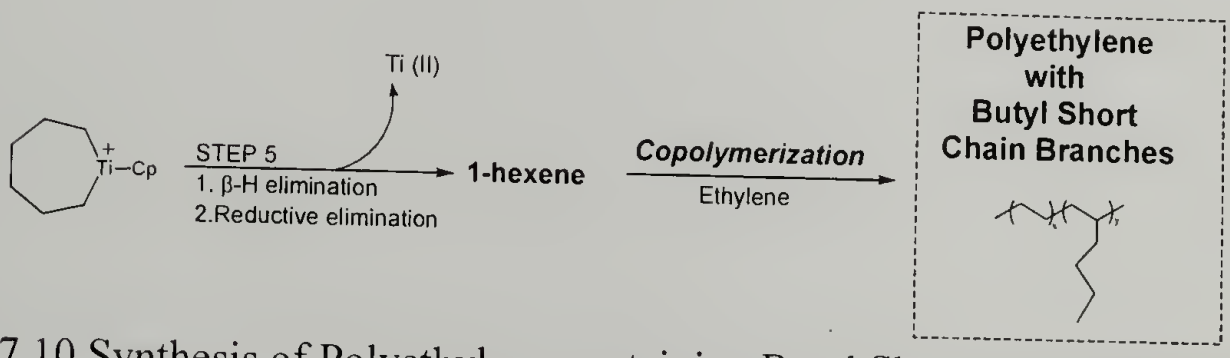

Figure 7.10 Synthesis of Polyethylene containing Butyl Short Chain Branches Produced by Ethylene Trimerization Process

In order to further investigate the importance of the macroligand -supported catalysts in generating SCB in ethylene polymerizations, a series of control experiments were performed. Pretreatment of **HPS** with an excess of MAO results in formation of aluminum aryloxides. The subsequent addition of **13** results in a cationic piano stool complex with aluminate counterions, which on treatment with ethylene results in the formation of polyethylene with a T_m of 132.0°C, and fewer than 4 short chain branches per 1000 C atoms as determined by ^{13}C NMR. From both ^{13}C NMR and DSC analysis, polyethylene obtained by this reaction is referred to as HDPE. Homogeneous solution polymerization of **13** with MAO and ethylene as the monomer also affords HDPE. Hence, ethylene polymerization using either MAO activated homogeneous catalysts **13** in solution or ethylene slurry polymerization using **HPS** treated with MAO and subsequent reaction with **13** affords HDPE from ethylene polymerization. But tethering **13** onto **HPS** and activation with MAO affords polyethylene with butyl short chain branches. Hence, the polystyrene matrix must perturb the ligand environment of the titanium complex and the influence of the support manifest itself by producing branched polyethylene having lower melting points and better flow properties. These control experiments also show that the attachment of titanium to the macroligand in **HPS-Ti-1** is retained after activation with the MAO co-catalysts during polymerization of ethylene.

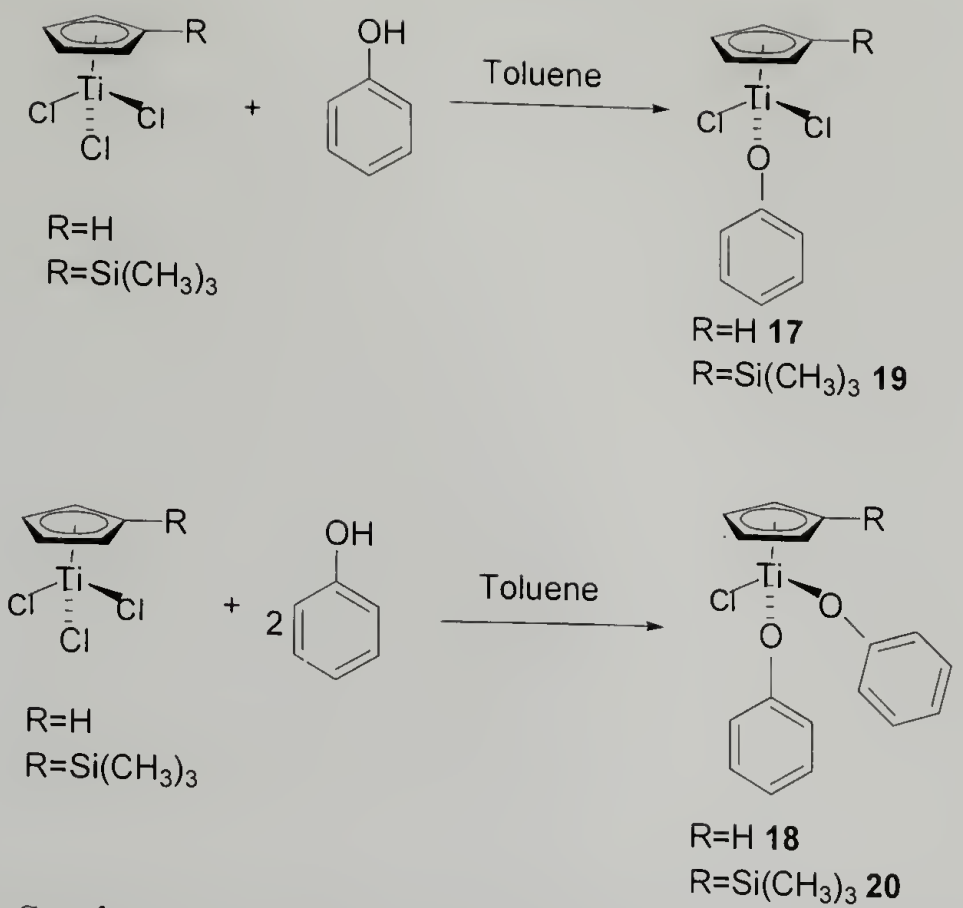

Figure 7.11 Syntheses of Analogous Homogeneous Aryloxy Cyclopentadienyl Piano Stool Complexes (**17-20**)

In order to further probe the influence excerted by the macroligand, control small molecular analogs of mono and bisaryloxy cyclopentadienyl titanium complexes, **17** and **18** respectively, were synthesized as shown in Figure 7.11, NMR characterizations Figure 7.12-7.15. These non-bridged complexes **17** and **18** activated by MAO afforded HDPE from ethylene homopolymerization (Table 7.2, entries 5 and 6). These results are consistent with those reported by Nomura and coworkers for structurally similar catalyst structures.[104,105] The characterization reported for the polyethylenes produced by Nomura are limited to molecular weight analysis. No determination of the presence, or absence, of short chain branches was described. For catalyst **HPS-Ti-1**, the presence of the macroligand is apparently necessary for the production of SCBs during ethylene homopolymerization.

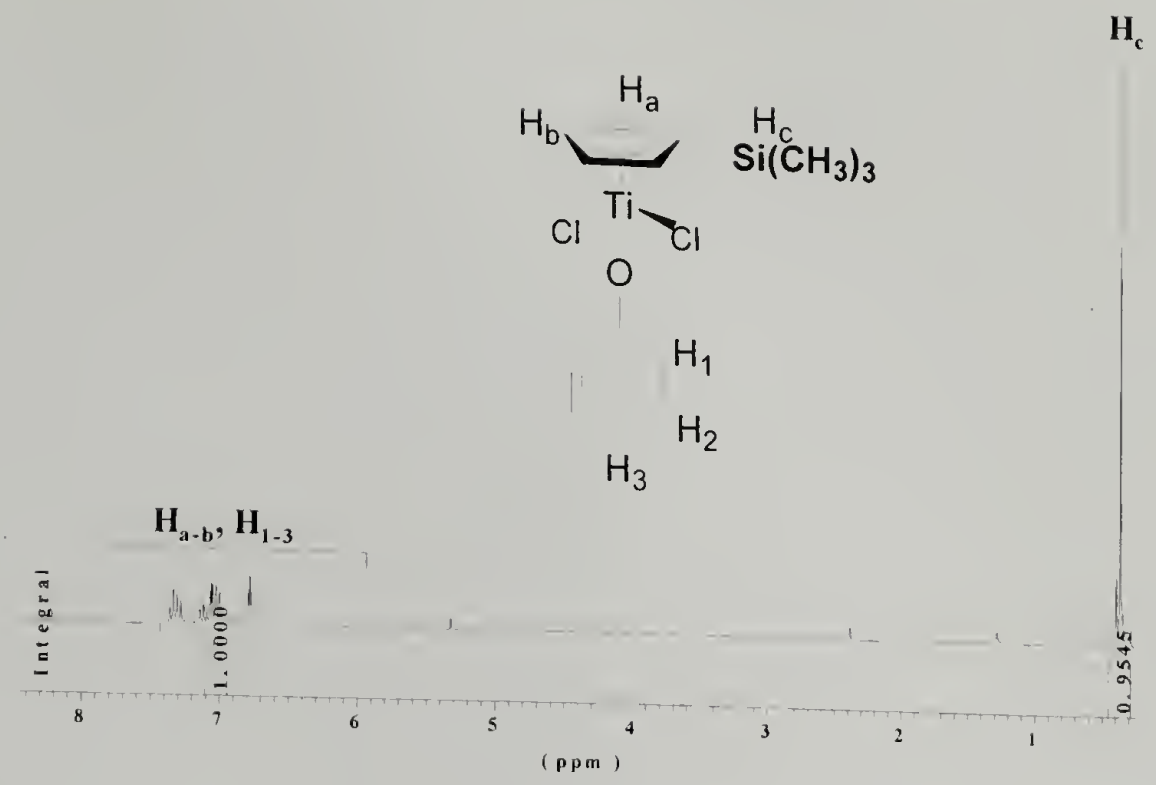

Figure 7.12 ^{1}H NMR Spectrum of Complex **19** in CD_2Cl_2

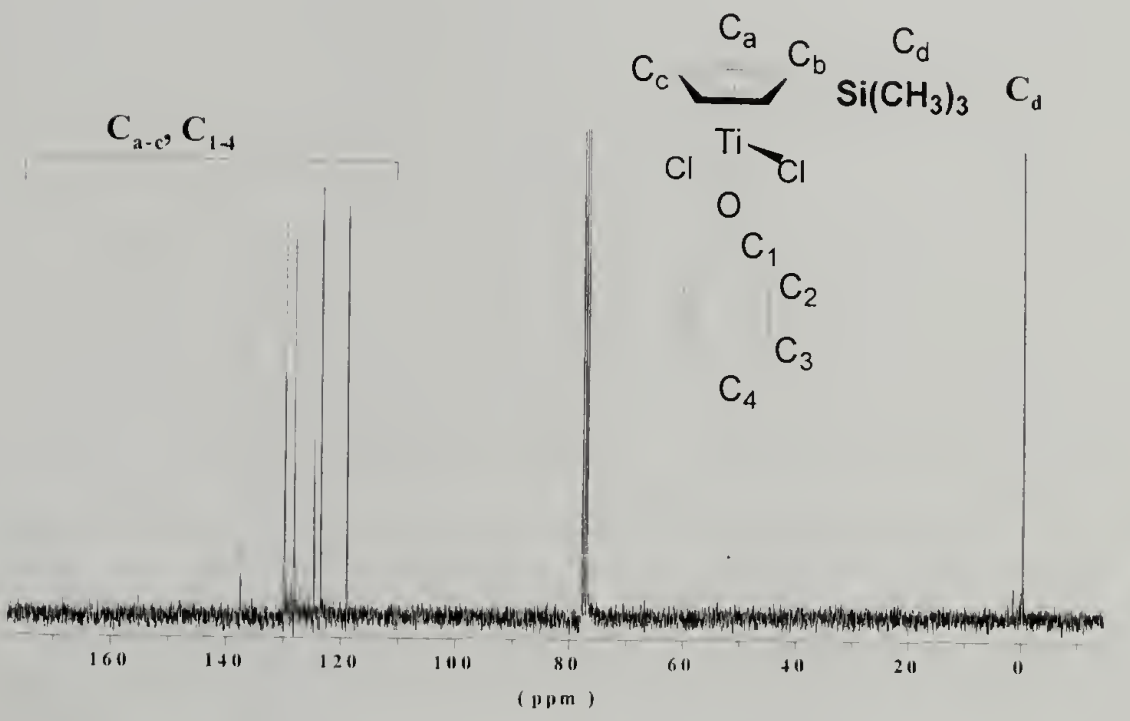

Figure 7.13 ^{13}C NMR (CPD) Spectrum of Complex **19** in $CDCl_3$

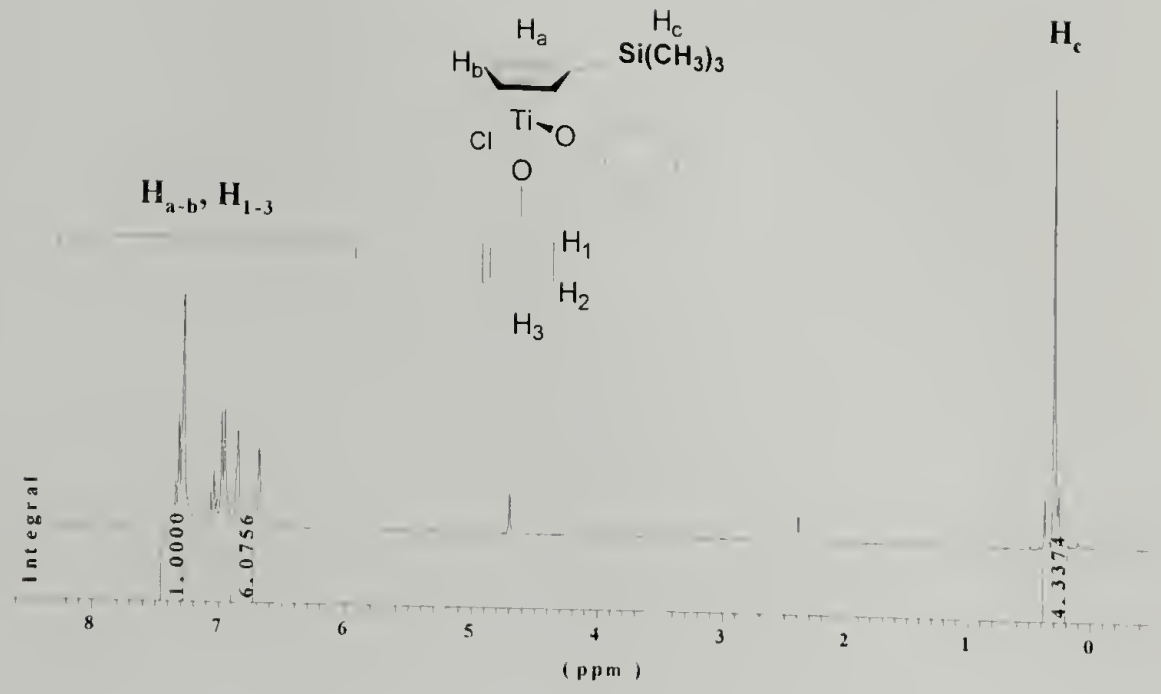

Figure 7.14 ^{1}H NMR Spectrum of Complex **20** in $CDCl_3$

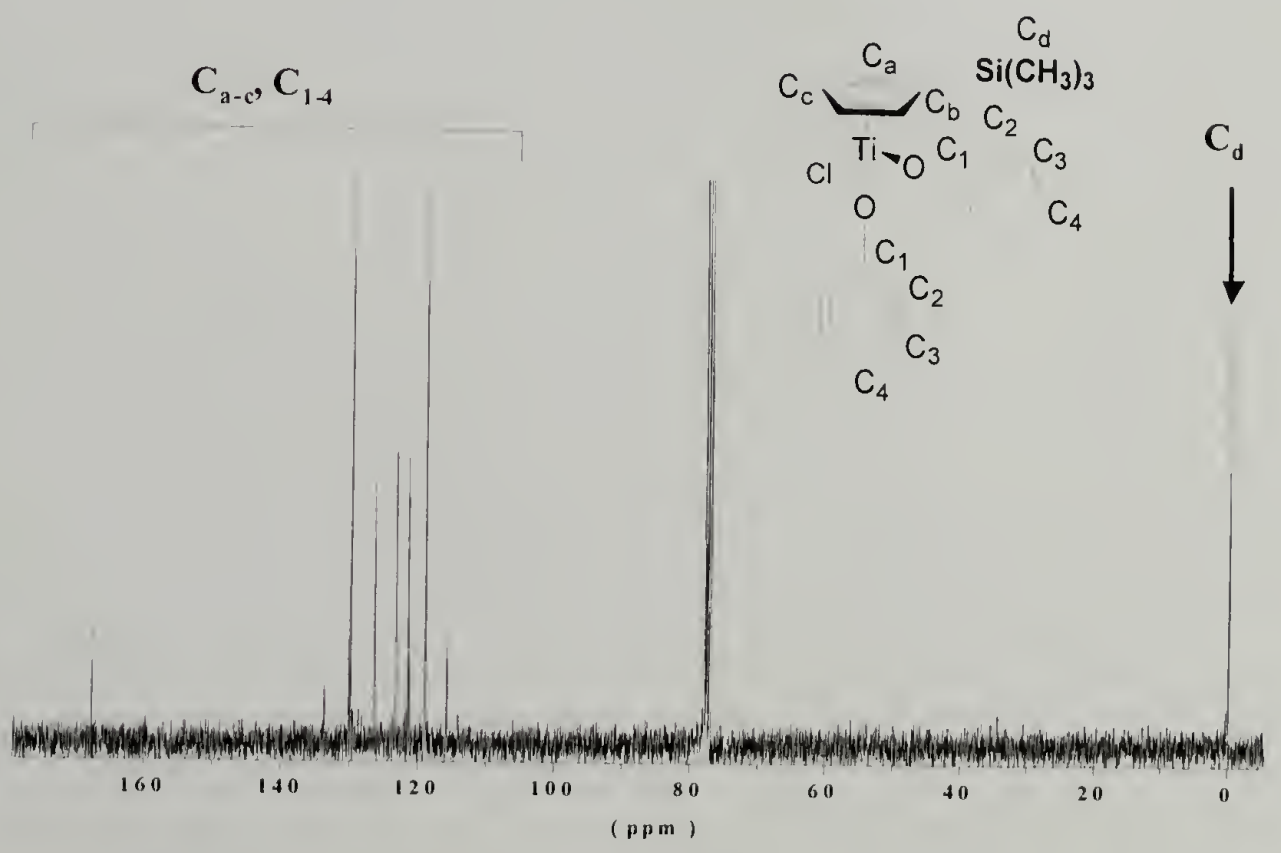

Figure 7.15 ^{13}C CPD Spectrum of Complex **20** in $CDCl_3$

7.3.4 Effect of the Cocatalysts in Ethylene Homopolymerization and Corresponding Control Experiments

During olefin polymerizations involving a group 4 metal catalyst, the activated metal is present as a cation and is counter-balanced by a non-coordinating anion. The interactions between this contact ion pair has asubstantial influence on the catalytic activity, lifetime of the active species, chain-termination and chain–transfer processes.[11] Hence, there is a need to study the polymerization properties of the macroligated metal cation-anion pair. In order to explore the effect of the counterion, ethylene polymerizations were performed using macroligated catalysts with MAO as the alkylating agent and $B(C_6F_5)_3$ (**I**) as the cocatalyst (Table 7.3, entries 7-9).

Table 7.3 Ethylene Polymerization using Macroligated Complexes with MAO as the Alkylating Agent in Conjunction with $B(C_6F_5)_3$`(**I**) as the Cocatalysts

Entry	Catalysts	B:Ti	Activity Kg/mol Ti.hr.atm	Tm[a] (°C)	% Crystallinity[b]	Mw [c]	PDI[c]
7	**5**	1.2:1	62	130.0	2.0	65230	bimodal
8	**6**	1.19:1	121	132.7	6.6	75600	Bimodal
9	**8**	1.37:1	61	129.9	5.4	82320	1.5

[a] DSC **first** scan,
[b] Calculated with respect to a polyethylene single crystal ΔH_f=293 J/g
[c] Determined through GPC at 135 °C in TCB using light scattering detectors calibrated with PS standards

For a comparable Ti:B ratio, **HPS-Ti-2** and **HPS-Ti-3** showed similar activities for the production of polyethylene and these catalysts are more active than **HPS-Ti-1**, with **HPS-Ti-4** being the least active. The molecular weights of the polyethylenes produced range from high for those prepared using **HPS-Ti-3** ($M_w > 200,000$) to moderate for those prepared by **HPS-Ti-1**, **HPS-Ti-2**, and **HPS-Ti-4** ($M_w < 100,000$). Under the experimental conditions **HPS-Ti-1**, **HPS-Ti-2** and **HPS-Ti-4** afforded HDPE as determined by the polymer melting point (Table 7.3, entries 7-9). However, **HPS-Ti-3** (Table 7.4, entries 10 and 11) afforded polyethylene with a melting point of 121.4°C and were attributed to the presence of short chain branches. To establish the type of branches formed, ^{13}C NMR of the polymer was performed. The observed resonances were attributed to presence of butyl branches and were assigned as 14.17 ($1B_4$, CH_3, EHE), 23.48 ($2B_4$), 27.17 (βδ, EHEE+EEHE), 29.40 ($3B_4$, EHE), 29.99 (δδ, EEE), 30.47 (γδ, HEEE+EEEH), 32.22 (γδ), 34.10 ($4B_4$, EHE), 34.41(αδ, EHEE+EEHE), 38.00 (methine, EHE) as shown in Figure 7.16. The presence of butyl branches is attributed to the coproduction of 1-hexene during polymerization of ethylene as shown in Figure 7.12. From ^{13}C NMR, 1-hexene incorporated was determined to be 1.5 mol%. The absence of ethyl and hexyl branches was also noted. The molecular weight and extent of branching in PE does not change with an increase in the B:Ti ratio.

Table 7.4 Ethylene Homopolymerization using Macroligated Catalyst (**HPS-Ti-3**) with MAO Alkylating Agent and Boron based Cocatalysts

Entry	Catalyst 7 [a]	Activity Kg/mol Ti.hr.atm [e]	T_m [f] (°C)	% Crystallinity [g]	Crystal Size [h] (Å)	Mw [i]	PDI [i]
10	5.5 **I** [b]	64	124.4	2.4	126	216200	Bimodal
11	8.0 **I** [c]	60	121.4	2.1	120	242300	Bimodal
12	6.0 **III** [b]	146	118.4	2.4	116	217900	2.6
13	8.2 **III** [c]	301	123.5	3.9	120	227200	Bimodal
14	5.0 **II** [b]	275	130.4	9.8	138	97600	2.05
15	7.5 **II** [c]	108	131.4	12.5	140	84600	1.87
16	[d] 5.7 **III** [b]	4.6	123	132.9	590000	1.7	2
17	[d] 6.1 **III** [b]	4.9	126	123.1	140000	3.0	3

[a f (I)] $B(C_6F_5)_3$, [(II)] $(C_6H_5)C(B(C_6F_5)_4$, [(III)] $(C_6H_5)N(CH_3)_2H(B(C_6F_5)_4)$; Ti:B ratio =1:1 [b] and 1:10 [c]
[d] Control catalysts **19** and **20**, Ti:B=1:1
[e] Ethylene pressure of 4 atm, reaction for 5-10 minutes
[f] DSC **first** scan,
[g] Calculated with respect to polyethylene single crystal ΔH_f=293 J/g,
[h] Determined from WAXS using Scherrer Equation
[i] Determined through GPC at 135 °C in TCB using light scattering detectors calibrated with PS standards

In branched polyolefins, the content and the identity of the branch can be a function of proximity between the cationic metal center and anionic (borate) counterion.[11] In order to further explore the interactions between the metal cation and other borate

counter-ions for the production of SCBs were investigated. Ethylene polymerizations was performed using **HPS-Ti-3** with MAO as the alkylating agent with two different borate cocatalysts $[(C_6H_5)N(CH_3)_2)H][(B(C_6F_5)_4)]$ (**III**) and $[(C_6H_5)_3C][B(C_6F_5)_4]$ (**II**). Interestingly, ethylene polymerization using **HPS-Ti-3**/MAO with **III** affords polyethylene with SCBs as seen from DSC and ^{13}C NMR studies (Table 7.5, entries 12 and 13). In contrast, ethylene polymerization using **HPS-Ti-3**/MAO with **II** affords HDPE. With cocatalysts **II** and **III**, the metal cation is counter balanched by the $B(C_6F_5)_4^-$. The SCBs observed using complex **HPS-Ti-3**/MAO/ **III** can be attributed to the coordination of the dimethylaniline co-product to the cationic titanium center. On the other hand, 1,1,2-triphenylethane is formed during the metal activation protocol **HPS-Ti-3**/MAO/**II** (Entries 14 and 15, Table 7.5), this presumably does not interact with the metal center.

In order to determine the influence of the cocatalysts, small molecular analogs of mono and bisaryloxy trimethylsilylcyclopentadienyl titanium complexes, **19** and **20** respectively, were synthesized as shown in Figure 7.5. MAO activation of these non-bridged complexes with various boranes and borates as cocatalysts was used for ethylene homopolymerization. For example, **19** alkylated with MAO and subsequent treatment with **III** afforded HDPE, while **20**/MAO/**III**/ethylene afforded polyethylene with butyl short chain branch (Table 7.5, entries 16 and 17, respectively). The formation short chain branches using macroligated complex **HPS-Ti-3**/ MAO/**III** could be attributed to the 1-hexene production from Form **B** in **HPS-Ti-3** counter balanced by borate anion.

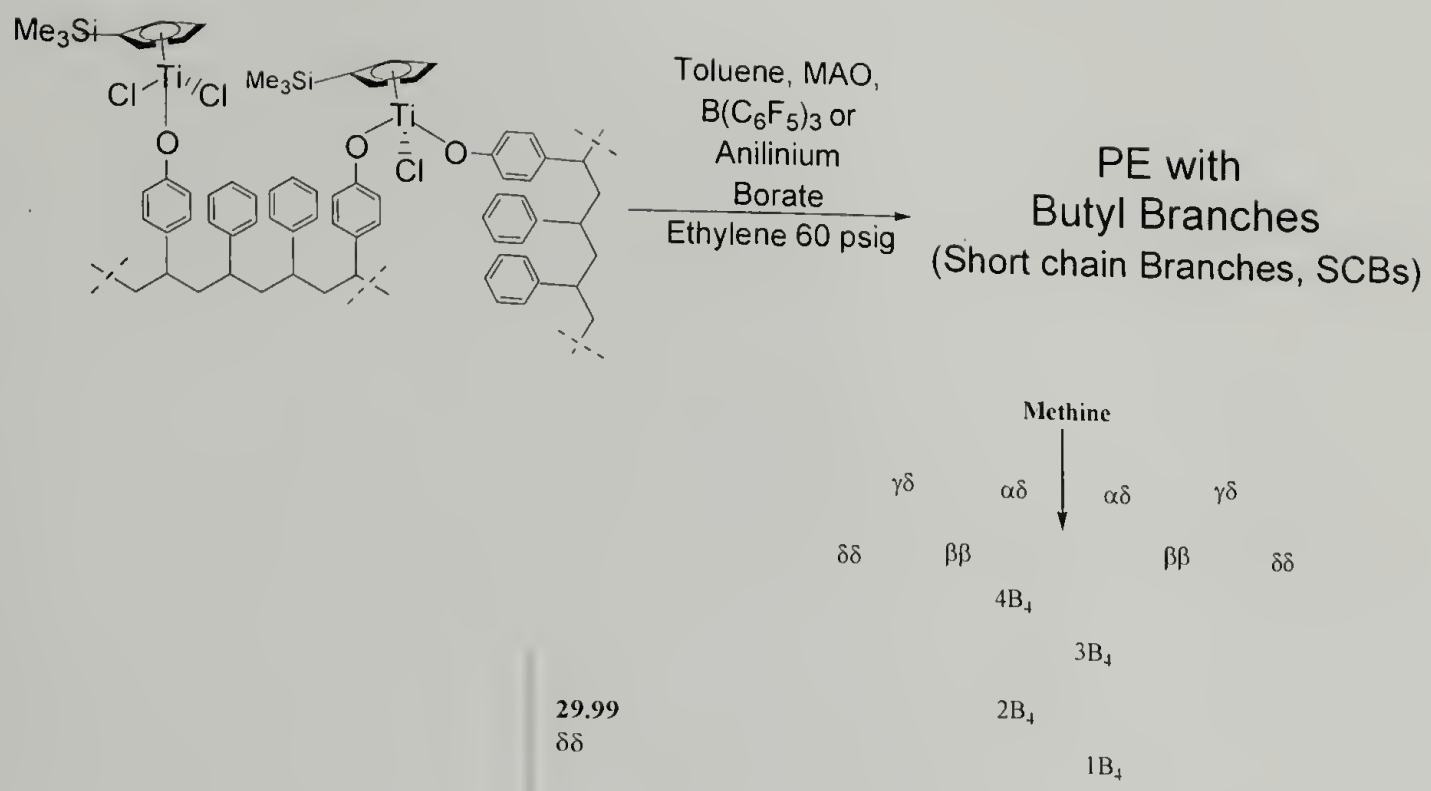

Figure 7.16 ^{13}C CPD Spectrum of Polyethylene with Butyl Short Chain Branches Synthesized from Complex **HPS-Ti-3** in Conjunction with MAO as theAkylating Agent and **I** as the Cocatalysts

7.3.5 Polyethylenes Characterized by Wide Angle X-Ray Diffraction (WAXD)

Various SSCs have been supported on organic, typically polymeric (soluble polymer or cross-linked bead) and inorganic materials (alumina, silica). Interestingly, polyolefins of ultra high molecular weight and varied degrees of crystallinity have been observed. Polyolefins produced from CGCs supported on cross-linked polystyrene beads have lower crystallinity compared to polyolefins obtained from their homogenous analogs. To correlate the influence of the macroligand on the apparent crystal size and the resulting degree of crystallinity of the polyethylene synthesized, WAXD)analyses were performed. The reflections used for analysis were (110) and (200), where the broadening of the (110) is affected by distortions of the a and b axes of the polyethylene orthorhombic unit cell. In order to compare the polyethylenes obtained from homogeneous catalysts and the macroligated catalysts, WAXD analysis of polyethylene produced from **15** (homogeneous catalyst) in conjunction with MAO was performed and the (110) and (200) reflections were observed to be relatively sharp. The apparent crystal size of the polyethylene was determined to be of 180 Å using Scherrer equation. In contrast, polyethylene produced from **HPS-Ti-3** (macroligated catalyst, solvent swollen) in conjunction with MAO shows broadened (110) and (200) reflections. The broadening of peaks can be attributed to the reduction in apparent crystal size of the polyethylene and increase in amorphous content of the polymer. The polyethylene produced from **15**/MAO has an apparent crystal size of 150 Å. It was noted that the amorphous halo was much more pronounced in polyethylenes with smaller apparent crystal sizes and lower degree of crystallinity. DSC measurements showed that the enthalpy of fusion and degree of

crystallinity of the polyethylenes were considerably reduced. The WAXD data (apparent crystal size, broadening of (110) and (200)) together with the DSC results (lower enthalpy of fusion, lower degree of crystallinity) shows that the macroligated catalysts results in less well-ordered polyethylene crystals with a corresponding increase in amorphous and intermediate component content, i.e. ,the formation of less stable crystalline lamellae.

7.3.6 Ethylene-Octene Copolymerizations using Macroligated Catalysts in Conjunction with MAO as the Cocatalysts and Control Experiments

The production of branched polyetylenes from an ethylene-only feed using supported aryloxy titanium- based catalysts in conjunction with various cocatalyts has been discussed early in this chapter. The other aspect that needs to be addressed is the preparation of branched polyethylenes by using a mixed monomer feed containing both ethylene and 1-octene. The effect of the macroligated catalysts in conjunction with MAO as the cocatalyst for ethylene and 1-octene copolymerization (Table 7.5, entries 18-21) should be examined. The substituents on the cyclopentadienyl ring affect the amount of comonomer incorporated into the copolymer. It has been shown in the case of nonbridged cyclopentadienyl aryloxy titanium species such as ^{t}BuCp, $(CH_3)_5$Cp, and $(^{t}Bu)_2$Cp that the Cp-Ti-O bond angle changes from 117.6°, 120.5° and 119.3°.[106] Under comparable polymerization conditions, the activity of the ligands has been shown to be $(CH_3)_5Cp > {}^{t}Bu\ Cp > (^{t}Bu)_2Cp$. However ,for 1-hexene incorporation, the activity of the substituents has been shown to ^{t}Bu Cp > $(CH_3)_5$Cp > $(^{t}Bu)_2$Cp. On the other hand, the molecular weight for the copolymer is highest for $(^{t}Bu)_2$Cp followed by ^{t}Bu and then the $(CH_3)_5$Cp analogue. Rotational flexibility of the substituted Cp group affects the activity

and amount of 1-octene incorporated into the ethylene chain. Correlating the results obtained by Nomura, it was observed that for ethylene-octene copolymer, **HPS-Ti-3** and **HPS-Ti-1** shows the higher activity than **HPS-Ti-2** and **HPS-Ti-4**. Also, **HPS-Ti-3** affords higher-level 1-octene incorporation compared to the other three macroligated catalsyts. The copolymers synthesized from these supported catalysts are of moderately high molecular weights.

Table 7.5 Ethylene-1-Octene Copolymerization using Macroligated Catalysts in Conjunction with MAO

Entry	Catalysts	Al:Ti	Activity Kg/mol Ti.hr.atm	Tm[a] (°C)	Octene incorporation in copolymer[a,b]	Mw[c]	PDI[c]
18	**HPS-Ti-1**	511	48	116.4	3	268100	bimodal
19	**HPS-Ti-2**	665	17	119.8	2.8	177200	2.4
20	**HPS-Ti-3**	1710	42	105.1	4	407000	2.2
21	**HPS-Ti-4**	1613	10	123.3	2	501400	bimodal
22	**15**	660	5.1	134.9	-	n.d	n.d.
23	**19**	780	60	114.1	3	400,000	2.0
24	**20**	765	71	115.3	3	110,000	1.9

[a] DSC **first** scan,
[b] Calculated from depression in melting point and ^{13}C NMR measurements
[c] Determined through GPC at 135 °C in TCB using light scattering detectors calibrated with PS standards

The formation of ethylene-octene based copolymers using supported aryloxy based cyclopentadienyl complexes can also be used as additional evidence for the

presence of the tethered aryloxy moiety. Previous control polymerization performed with complex **HPS-Ti-3** in conjunction with MAO as the cocatalysts and ethylene and 1-octene in the monomer feed afford HDPE (Table 7.5, entry 22). On the other hand, the use of small molecular analogs **19** (monoaryloxy) and **20** (bisaryloxy) complexes with MAO afford the formation of ethylene-octene copolymers (LLDPE) from ethylene and 1-octene copolymerization (Table 7.5, entries 23 and 24).

7.3.7 Copolymer Microstructure Analysis of Ethylene-Octene Copolymers obtained from Macroligated Catalysts

In order to determine the microstructure of the copolymers synthesized, ^{13}C NMR of the copolymers was performed at 110°C. The ^{13}C resonances of copolymer synthesized from complex **HPS-Ti-1** was analyzed and the spectrum is similar to that reported by Cavagna, hence low level of octene incorporations were expected. [7,73] The nomenclature for carbon assignments, monomer sequence distribution and equations relating signal intensity to the sequences as reported by Randall is used to identify the branches in ^{13}C NMR of polyolefin.[7] The ^{13}C peak resonances were assigned as δ 14.19 (1s+1B_6, CH_3, EOE+EOO+OOE+OOO), 22.85 (2s+2B_6, EOE+EOO+OOE+OOO), 27.10 (βδ, OOEE+EEOO), 27.20 (βδ+5B_6, EOE), 29.99 (δδ, EEE), 30.01 (δδ+4B_6, EEE), 32.12 (3s+3B_6, EOE), 34.04 (4B_4, EHE) 34.42 (αδ+6B_6, EOEE+EEOE), 38.01(CH, EOO+OOE, methine) shown in figure 7.17. A quantitative relationship between signal intensity to monomer sequences were established to quantify the 1-octene incorporated in the copolymer.[7] The octene content is calculated from the ratio of the sum of the octene centered sequences to that of all the sequences and was determined to be 1.5 mol %. The presence of 4B_4 branch (butyl branch) was also observed. This can be attributed to the 1-

hexene formed by ethylene trimerization and further incorporation of 1-hexene into the copolymer. The resonances $4B_4$ and ($\alpha\delta$+$6B_6$) were used to roughly quantify the ratio of hexane (1.0 mol%) and octene (1.5 mol%) incorporated into the ethylene chain.

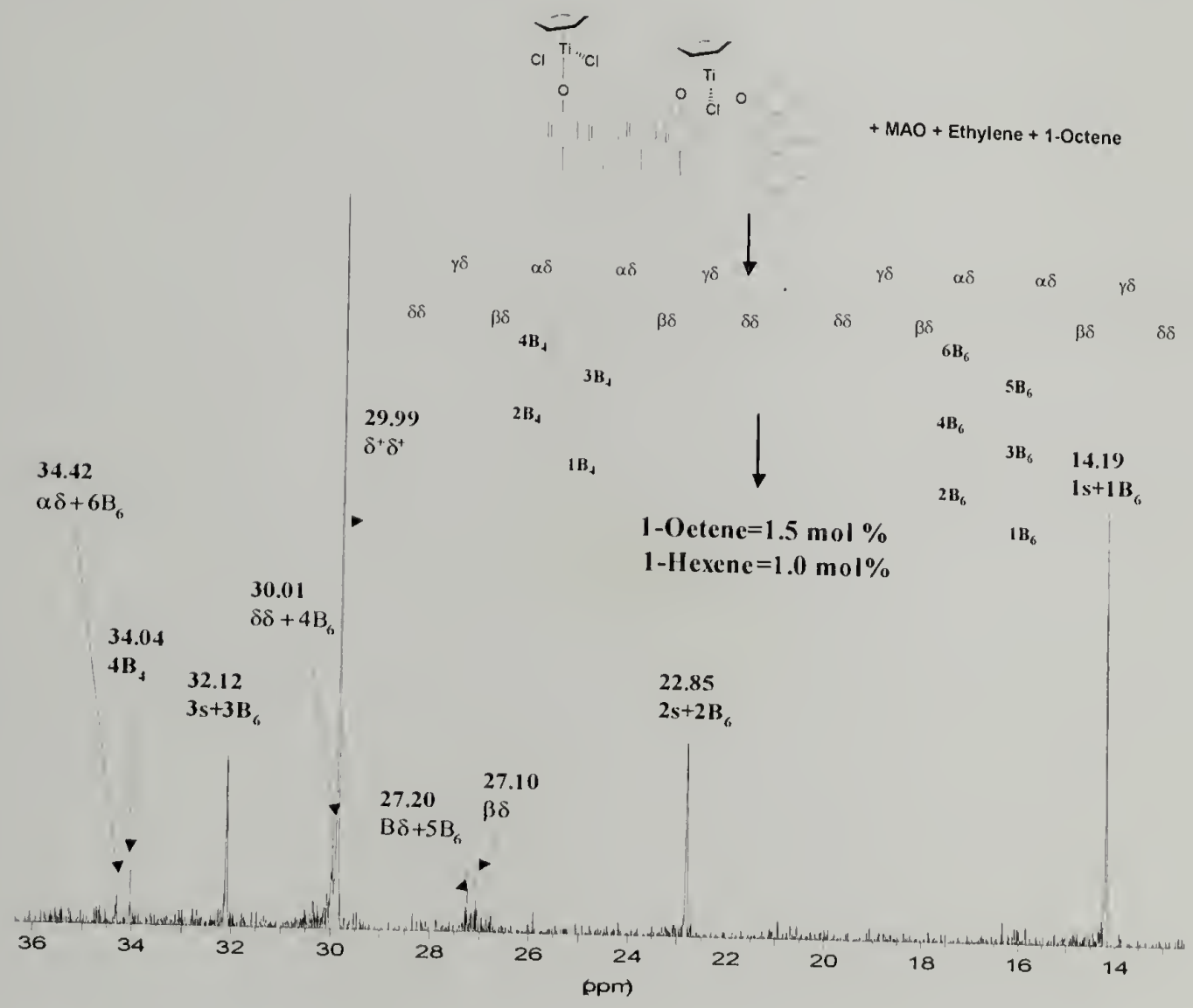

Figure 7.17 ^{13}C CPD Spectrum of Ethylene Octene Copolymer Synthesized from Complex **HPS-Ti-2** in Conjunction with MAO as the Cocatalysts

The microstructure of ethylene-octene copolymer obtained from complex **HPS-Ti-2** was also analyzed and assigned as δ 14.22 (1s+1B_6, EOE+EOO+OOE+OOO), 22.87 (2s+2B_6, EOE+EOO+OOE+OOO), 26.95 (βδ, OOEE+EEOO), 27.05 (βδ + 5B_6, EOE), 29.97 (δδ, EEE), 32.21 (3s+3B_6, EOE), 34.51 (αδ+6B_6, EOEE+EEOE), 38.04 (CH, methine). The α-olefin incorporation in the copolymer was roughly estimated to be 2.5 mol % established both by ^{13}C NMR and depression in melting point as determined from DSC measurements.

The microstructure of ethylene-octene copolymer obtained from complex **HPS-Ti-3** was assigned as δ 14.22 (1s+1B6, CH_3), 22.87 (2s+2B6, CH_2(2)), 26.97 (βδ + 3B6, CH_2(5)), 27.27 (βδ + 5B_6, EOE), 29.96 (δδ+4B6, CH_2(4)), 32.11 (3s+3B_6, CH_2(3)), 34.50 (αδ + 6B_6), 38.01 (CH, methine). The 1-octene incorporated into the copolymer was determined to be about 3.8 mol% and this value is corroborated by the observed depression in melting point.

7.4 Summary

In this chapter, two synthetic routes to prepare branched polyethylenes using immobilized Cyclopentadienyl(aryloxy)titanium(IV) precursor complexes on hydroxypolystyrene (macroligand) is discussed. One method to make branched polyethylene is to prepare α-olefins *in situ*, which are then copolymerized with ethylene. Hence, the immobilized complex acts both as as oligomerization and a copolymerization catalysts. For example, ethylene polymerization using **HPS-Ti-1**/MAO affords polyethylene with butyl short chain branches. The formation of the butyl short chain

branched polyethylene has been attributed to the production of 1-hexene by ethylene trimerization process and subsequent copolymerization with ethylene. The presence of butyl short chain branches has been confirmed by ^{13}C NMR studies and depression of melting point relative to HDPE. Non-bridged complexes (cyclopentadienyl) (phenoxy)titanium(IV) and ((cyclopentadienyl)bis(phenoxy)titanium(IV) activated by MAO for ethylene homopolymerization affords HDPE. Treatment of hydroxy support matrix with MAO and subsequent addition of **13** and ethylene monomer affords HDPE. Hence, the presence of macroligated catalyst is vital for the production of butyl branches in polyethylene.

The catalyst-cocatalyst mixtures afford smetal cation and cocatalyst anion and the characteristics of the cation-anion formed plays an important role in the production of butyl SCBs during ethylene homopolymerization. Complex **HPS-Ti-3** activated by MAO with cocatalysts **I** or **II** affords polyethylene with butyl SCBs. On the other hand, **HPS-Ti-3** activated by MAO in conjunction with **III** affords HDPE. The formation of SCBs was found to be dependent on the cyclopentadienyl substituents, the influence exerted by the polystyrene macroligand as well as the nature of the cocatalysts. We have demonstrated a novel method for the production of SCBs in polyethylene by the use of macroligated catalysts in conjunction with various cocatalysts during ethylene homopolymerization.

BIBLIOGRAPHY

(1) Ziegler, K.; Holzkamp, E.; Breil, H.; Martin, H. *Angew. Chem.* **1955**, *67*, 541.

(2) Natta, G.; Pino, P.; Mazzananti, G. *Gazz. Chem. Ital.* **1957**, *87*, 852.

(3) Cossee, P. *J. Catal.* **1964**, *3*, 80.

(4) Arlman, E. J. *J. Catal.* **1964**, *3*, 99.

(5) Jenny, C.; Maddox, P. *Current Opinion in Solid State and Material Science* **1998**, *3*, 94-103.

(6) Reding, W. *Jounal of Polymer Science* **1956**, *21*, 561.

(7) Randall, J. C. *J. Macromol. Sci.-Rev. Macromol. Chem. Phys.* **1989**, *C29*, 201-317.

(8) Resconi, L.; Cavallo, L.; Fait, A.; Piemontesi, F. *Chem. Rev.* **2000**, *100*, 1253.

(9) Breslow, D. S.; Newbury, N. R. *J. Am. Chem. Soc.* **1957**, *79*, 5072.

(10) Anderson, A.; Cordes, H. G.; Herwig, J.; Kaminsky, W.; Merck, A.; Mottweiler, R.; Pein, J.; Sinn, H.; Vollmer, H. J. *Angew. Chem.* **1976**, *15*, 630.

(11) Chen, E. Y. X.; Marks, T. J. *Chem. Rev.* **2000**, *100*, 1391.

(12) Bochmann, M.; Wilson, L. M. *J. Chem. Soc., Chem. Comm.* **1986**, 1610.

(13) Eshius, J. J. W.; Tan, Y. Y.; Teuben, J. H.; Renkema, J. *J. Mo.l Catal.* **1990**, *62*, 277.

(14) Jordan, R. F. *Adv. Organomet. Chem.* **1991**, *32*, 325.

(15) Hlatky, G. G.; Turner, H. W.; Eckman, R. R. *J. Am. Chem. Soc.* **1989**, *111*, 2728.

(16) Yang, X.; Stern, C. L.; Marks, T. J. *Organometallics* **1991**, *10*, 840.

(17) Chein, J. C. W.; Tsai, W.-M.; Rausch, M. D. *J. Am. Chem. Soc.* **1991**, *113*, 8570.

(18) Coates, G. W. *Chem. Rev.* **2000**, *100*, 1223.

(19) Coates, G. W. *J. Chem. Soc. , Dalton Trans.* **2002**, 467.

(20) Alt, H. G.; Koppl, A. *Chem. Rev.* **2000**, *100*, 1205.

(21) Angermund, K.; Fink, G.; Jensen, V. R.; Kleinschmidt, R. *Chem. Rev.* **2000**, *100*, 1457.

(22) Brintzinger, H. H.; Fischer, D.; Mulhaupt, R.; Rieger, B.; Waymouth, R. M. *Angew. Chem.-Int. Edit. Engl.* **1995**, *34*, 1143.

(23) Coates, G. W.; Waymouth, R. M. *Science* **1995**, *267*, 217.

(24) McKnight, A. L.; Waymouth, R. M. *Chem. Rev.* **1998**, *98*, 2587.

(25) Shapiro, P. J.; Bunel, E.; Schaefer, W. P.; Bercaw, J. E. *Organometallics* **1990**, *9*, 867.

(26) Shapiro, P. J.; Cotter, W. D.; Schaefer, W. P.; Labinger, J. A.; Bercaw, J. E. *J. Am. Chem. Soc.* **1994**, *116*, 4623.

(27) Okuda, J. *Chem. Berichte* **1990**, *123*, 1649.

(28) Okuda, J.; Schattenmann, F. J.; Wocadlo, S.; Massa, W. *Organometallics* **1995**, *14*, 789.

(29) Chum, P. S.; Kruper, W. J.; Guest, M. J. *Adv. Mater.* **2000**, *12*, 1759.

(30) Dekmezian, A. H.; Soares, J. B. P.; Jiang, P. J.; Garcia-Franco, C. A.; Weng, W. Q.; Fruitwala, H.; Sun, T.; Sarzotti, D. M. *Macromolecules* **2002**, *35*, 9586.

(31) Llinas, G. H.; Mena, M.; Palacios, F.; Royo, P.; Serrano, R. *J. Organomet. Chem.* **1988**, *340*, 37.

(32) Jutzi, P. *Chem. Rev.* **1986**, *86*, 983.

(33) Mena, M.; Pellinghelli, M. A.; Royo, P.; Serrano, R.; Tiripicchio, A. *J. Chem. Soc.-Chem. Commun.* **1986**, 1118.

(34) Nomura, K.; Naga, N.; Miki, M.; Yanagi, K.; Imai, A. *Organometallics* **1998**, *17*, 2152.

(35) Nomura, K.; Naofumi, N.; Takaoki, K.; Imai, A. *J. Mol. Catal. A-Chem.* **1998**, *130*, L209.

(36) Nomura, K.; Komatsu, T.; Imanishi, Y. *Macromolecules* **2000**, *33*, 8122.

(37) Britovsek, G. J. P.; Gibson, V. C.; Wass, D. F. *Angew. Chem.-Int. Edit.* **1999**, *38*, 428.

(38) Gibson, V. C.; Spitzmesser, S. K. *Chem. Rev.* **2003**, *103*, 283.

(39) Jayaratne, K. C.; Keaton, R. J.; Henningsen, D. A.; Sita, L. R. *J. Am. Chem. Soc.* **2000**, *122*, 10490.

(40) Jayaratne, K. C.; Sita, L. R. *J. Am. Chem. Soc.* **2000**, *122*, 958.

(41) Schollard, J. D.; McConville, D. H. *J. Am. Chem. Soc.* **1996**, *118*, 10008.

(42) Schollard, J. D.; McConville, D. H.; Rettig, S. J. *Organometallics* **1997**, *16*, 958.

(43) Naik, S. D.; Ray, W. H. *J. Appl. Polym. Sci.* **2001**, *79*, 2565.

(44) Roscoe, S. B.; Frechet, J. M. J.; Walzer, J. F.; Dias, A. J. *Science* **1998**, *280*, 270.

(45) Roscoe, S. B.; Gong, C. G.; Frechet, J. M. J.; Walzer, J. F. *J. Polym. Sci.: Pt. A Polym. Chem.* **2000**, *38*, 2979.

(46) Preishuber-Pflugl, P.; Brookhart, M. *Macromolecules* **2002**, *35*, 6074.

(47) Tian, J.; Soo-Ko, Y.; Metcalfe, R.; Feng, Y. D.; Collins, S. *Macromolecules* **2001**, *34*, 3120.

(48) Tajima, K.; Aida, T. *Chem. Commun.* **2000**, 2399.

(49) Tajima, K.; Ogawa, G.; Aida, T. *J. Polym. Sci.: Pt. A Polym. Chem.* **2000**, *38*, 4821.

(50) Kageyama, K.; Tamazawa, J.; Aida, T. *Science* **1999**, *285*, 2113.

(51) Van Looveren, L. K.; De Vos, D. E.; Vercruysse, K. A.; Geysen, D. F.; Janssen, B.; Jacobs, P. A. *Catal. Lett.* **1998**, *56*, 53.

(52) Ribeiro, M. R.; Deffieux, A.; Portela, M. F. *Ind. Emg. Chem. Res.* **1997**, *36*, 1224.

(53) Hlatky, G. G. *Chem. Rev.* **2000**, *100*, 1347.

(54) Ittel, S. D.; Johnson, L. K.; Brookhart, M. *Chem. Rev.* **2000**, *100*, 1169.

(55) Spence, R.; Piers, W. E. *Organometallics* **1995**, *14*, 4617.

(56) Bohme, U.; Thiele, K. H. *J. Organomet. Chem.* **1994**, *472*, 39.

(57) Amor, F.; Okuda, J. *J. Organomet. Chem.* **1996**, *520*, 245.

(58) Carpenetti, D. W.; Kloppenburg, L.; Kupec, J. T.; Petersen, J. L. *Organometallics* **1996**, *15*, 1572.

(59) Hughes, A. K.; Meetsma, A.; Teuben, J. H. *Organometallics* **1993**, *12*, 1936.

(60) Ciruelos, S.; Cuenca, T.; Gomez, R.; GomezSal, P.; Manzanero, A.; Royo, P. *Organometallics* **1996**, *15*, 5577.

(61) Royo, B.; Royo, P.; Cadenas, L. M. *J. Organomet. Chem.* **1998**, *551*, 293.

(62) Mohring, P. C.; Coville, N. J. *J. Organomet. Chem.* **1994**, *479*, 1.

(63) Mohring, P. C.; Vlachakis, N.; Grimmer, N. E.; Coville, N. J. *J. Organomet. Chem.* **1994**, *483*, 159.

(64) Pangborn, A. B.; Giardello, M. A.; Grubbs, R. H.; Rosen, R. K.; Timmers, F. J. *Organometallics* **1996**, *15*, 1518.

(65) Winter, C. H.; Zhou, X. X.; Dobbs, D. A.; Heeg, M. J. *Organometallics* **1991**, *10*, 210.

(66) Galan-Fereres, M.; Koch, T.; Hey-Hawkins, E.; Eisen, M. S. *J. Organomet. Chem.* **1999**, *580*, 145.

(67) Juvaste, H.; Pakkanen, T. T.; Iiskola, E. I. *Organometallics* **2000**, *19*, 4834.

(68) Juvaste, H.; Pakkanen, T. T.; Iiskola, E. I. *Organometallics* **2000**, *19*, 1729.

(69) Juvaste, H.; Pakkanen, T. T.; Iiskola, E. I. *J. Organomet. Chem.* **2000**, *606*, 169.

(70) Constable, G. S.; Gonzalez-Ruiz, R. A.; Kasi, R. M.; Coughlin, E. B. *Macromolecules* **2002**, *35*, 9613.

(71) Alt, H. G.; Reb, A.; Milius, W.; Weis, A. *J. Organomet. Chem.* **2001**, *628*, 169.

(72) Chen, H. Y.; Chum, S. P.; Hiltner, A.; Baer, E. *J. Polym. Sci. Pt. B-Polym. Phys.* **2001**, *39*, 1578.

(73) Cavagna, F. *Macromolecules* **1981**, *14*, 215.

(74) Krimm, S.; Tobolsky, A. V. *Journal of Polymer Science* **1951**, *7*.

(75) McKittrick, M. W.; Jones, C. W. *J. Am. Chem. Soc.* **2004**, *126*, 3052.

(76) Anwander, R. *Chem. Mater.* **2001**, *13*, 4419.

(77) Thommes, M.; Köhn, R.; Fröba, M. *Appl. Surf. Sci.* **2002**, *196*, 239.

(78) Lim, M. H.; Stein, A. *Chem. Mater.* **1999**, *11*, 3285.

(79) Zhao, D.; Feng, J.; Huo, Q.; Melosh, N.; Fredrickson, G. H.; Chmelka, B. F.; Stucky, G. D. *Science* **1998**, *279*, 548.

(80) Feng, X.; Fryxell, G. E.; Wang, L.-Q.; Kim, A. Y.; Liu, J.; Kemmerr, K. M. *Science* **1997**, *276*, 923.

(81) Liu, J.; Feng, X. D.; Fryxell, G. E.; Wang, L. Q.; Kim, A. Y.; Gong, M. L. *Adv. Mater.* **1998**, *10*, 161.

(82) Fryxell, G. E.; Liu, J.; hauser, T. A.; Nie, Z.; Ferris, K. F.; Mattigod, S.; Gong, M.; Hallen, R. T. *Chem. Mater.* **1999**, *11*, 2148.

(83) Vecera, M.; Gasparic, J. *Detection and Identification of Organic Compounds*; Plenum: New York, 1971.

(84) Zhao, X. S.; Lu, G. Q.; Hu, X. *Microporous Mesoporous Mat.* **2000**, *41*, 37.

(85) Socrates, G. *Infrared Characteristic Group Frequencies*; Wiley: New York, 1980.

(86) Liepins, E.; Zicmane, I.; Lukevics, E. *J. Organomet. Chem.* **1986**, *306*, 167.

(87) Musikabhumma, K.; Spaniol, T. P.; Okuda, J. *Macromol. Chem. Phy.* **2002**, *203*, 115.

(88) Kasi, R. M.; Coughlin, E. B. *Organometallics* **2003**, *22*, 1534.

(89) Van Looveren, L. K.; Geysen, D. F.; Vercruysse, K. A.; Wouters, B. H.; Grobet, P. J.; Jacobs, P. A. *Mesoporous Molecular Sieves 1998* **1998**, *117*, 477.

(90) Van Looveren, L. K.; Geysen, D. F.; Vercruysse, K. A.; Wouters, B. H.; Grobet, P. J.; Jacobs, P. A. *Angew. Chem.-Int. Edit.* **1998**, *37*, 517.

(91) Van Looveren, L. K. M.; Vankelecom, I. F. J.; De Vos, D. E.; Wouters, B. H. J.; Grobet, P. J.; Jacobs, P. A. *Applied Catalysis a-General* **1999**, *180*, L5.

(92) Fink, G.; Steinmetz, B.; Zechlin, J.; Przybyla, C.; Tesche, B. *Chem. Rev.* **2000**, *100*, 1377.

(93) Resconi, L.; Camurati, I.; Grandini, C.; Rinaldi, M.; Mascellani, N.; Traverso, O. *J. Organomet. Chem.* **2002**, *664*, 5.

(94) Abramo, G. P.; Li, L. T.; Marks, T. J. *J. Am. Chem. Soc.* **2002**, *124*, 13966.

(95) Barnhart, R. W.; Bazan, G. C.; Mourey, T. *J. Am. Chem. Soc.* **1998**, *120*, 1082.

(96) Li, L. T.; Metz, M. V.; Li, H. B.; Chen, M. C.; Marks, T. J.; Liable-Sands, L.; Rheingold, A. L. *J. Am. Chem. Soc.* **2002**, *124*, 12725.

(97) Markel, E. J.; Weng, W. Q.; Peacock, A. J.; Dekmezian, A. H. *Macromolecules* **2000**, *33*, 8541.

(98) Izzo, L.; Caporaso, L.; Senatore, G.; Oliva, L. *Macromolecules* **1999**, *32*, 6913.

(99) Pellecchia, C.; Pappalardo, D.; Gruter, G. J. *Macromolecules* **1999**, *32*, 4491.

(100) Lund, E. C.; Livinghouse, T. *Organometallics* **1990**, *9*, 2426.

(101) Nasrullah, J. M.; Raja, S.; Vijayakumaran, K.; Dhamodharan, R. *J. Polym. Sci. Pt.-A, Pol. Chem.* **2000**, *38*, 453.

(102) Xu, J. T.; Zhao, J.; Fan, Z. Q.; Feng, L. X. *Macromol. Rapid Comm.* **1997**, *18*, 875.

(103) Chien, J. C. W.; Salajka, Z.; Dong, S. *Macromolecules* **1992**, *25*, 3199.

(104) Nomura, K.; Komatsu, T.; Imanishi, Y. *J. Mol. Catal. A-Chem.* **2000**, *152*, 249.

(105) Nomura, K.; Komatsu, T.; Nakamura, M.; Imanishi, Y. *J. Mol. Catal. A-Chem.* **2000**, *164*, 131.

(106) Nomura, K.; Naga, N.; Miki, M.; Yanagi, K. *Macromolecules* **1998**, *31*, 7588.